Basic Considerations in Electrical Generating Capacity Adequacy Evaluation

A Thesis Submitted to the College of

Graduate Students and Research

in Partial Fulfillment of the Requirement

for the Degree of Master of Science

in the Department of Electrical Engineering

University of Saskatchewan

Saskatoon

By

Dange Huang

PERMISSION TO USE

In presenting this thesis in partial fulfillment of the requirements for a Master of Science degree from the University of Saskatchewan, the author has agreed that the Libraries of this University may make it freely available for inspection. The author has further agreed that permission for copying of this thesis in any manner, in whole or in part, for scholarly purposes may be granted by the professor or professors who supervised the thesis work recorded here or, in their absence, by the Head of the Department or the Dean of the College in which the thesis work was done. It is understood that any copying or publication or use of this thesis or parts thereof for financial gain shall not be allowed without the author's written permission. It is also understood that due recognition shall be given to the author and to the University of Saskatchewan in any scholarly use which may be made of any material in this thesis.

Requests for permission to copy or to make other use of material in this thesis in whole or part should be addressed to:

Head of the Department of Electrical Engineering
University of Saskatchewan
Saskatoon, Saskatchewan
Canada S7N 5A9

ABSTRACT

The primary function of a power system is to supply its customers with electrical energy as economically as possible and with acceptable reliability and quality. Generating capacity adequacy evaluation is the oldest and most extensively studied aspect of power system reliability assessment. A wide range of methods have been developed to perform this evaluation. Two computer programs were developed based on the analytical and simulation techniques and used as tools in this research work. A number of basic considerations in generating capacity adequacy evaluation are investigated. Generating unit residence time distributions and peaking load units are incorporated in the analysis.

Two commonly encountered misconceptions regarding the basic system reliability indices are examined by applying the two programs to two reliability test systems. Reliability index probability distributions can be used to supplement the information provided by the expected index values. The concept of creating distributions and the additional information that can be obtained is illustrated in this thesis.

Generating unit residence time distributions are generally categorized as being either exponential or non-exponential in form. The exponential distribution is utilized, however, in virtually all practical system studies. The impacts on the system reliability of non-exponential unit state residence time distributions are examined in this research.

Peaking load units and base load units have different operating characteristics. The functions of peaking load units vary with changes in the system operating conditions.This is examined in this research.

The conclusions and techniques presented in this thesis should prove valuable in power system planning and operation.

ACKNOWLEDGEMENTS

I would like to express my sincere gratitude and appreciation to my supervisor, Dr. Roy Billinton, for his guidance, support and encouragement during my graduate study. I would also like to acknowledge Dr Billinton's time, effort, patience and helpful suggestions in the preparation of this thesis.

I would like to thank my parents, Pinlan Zhan and Jinsheng Huang, my best friend Bingxian Shi, for their love and consistent encouragement. Appreciation also goes to all my friends, both inside and outside the Electrical Engineering department.

Financial assistance provided by Dr. Roy Billinton in the form of research support from the Natural Sciences and Engineering Research Council (NSERC) of Canada is thankfully acknowledged.

CONTENTS

LIST OF TABLES

LIST OF FIGURES

LIST OF ABBREVIATIONS

A	Availability
CEA	Canadian Electricity Association
COPT	Capacity Outage Probability Table
DAUFOP	Derated Adjusted Utilization Forced Outage Probability
DOI	Duration of Interruption
DPLVC	Daily Peak Load Variation Curve
EIR	Energy Index of Reliability
ENS	Energy Not Supplied
ENSI	Energy Not Supplied per Interruption
FD	Forced Derated Time
FO	Forced Outage Time
FOR	Forced Outage Rate
FOT	Forced Outage Time
HLI	Hierarchical Level I
HLII	Hierarchical Level II
HLIII	Hierarchical Level III
hr	hour
IEAR	Interrupted Energy Assessment Rate
IEEE	Institute of Electrical and Electronic Engineers
IEEE-RTS	IEEE Reliability Test System
Int	Interruption
LCI	Load Curtailed per Interruption
LDC	Load Duration Curve
LLD	Loss of Load Duration
LLO	Loss of Load Occurrence
LOE	Loss of Energy
LOEE	Loss of Energy Expectation
LOL	Loss of Load
LOLE	Loss of Load Expectation
LOLF	Loss of Load Frequency
LOLP	Loss of Load Probability
MCS	Monte Carlo Simulation
MTTF	Mean Time to Failure
MTTR	Mean Time to Repair
MW	Megawatt
MWh	Megawatt hour

O	Operating Time
O(FD)	Operating Time under forced derated state
O(FD)adj	Adjusted outage time
occ/yr	occurrences per year
RBTS	Reliability Test System
ST	Service Time
U	Unavailability
UFOP	Utilization Forced Outage Probability
Wkdy	Week day
Wknd	Weekend
yr	year

1. INTRODUCTION

1.1 Power System Reliability

Electrical power systems are very complex and highly integrated. Failures in any part of the system can cause interruptions of supply to end users. The primary function of a power system is to supply its customers with electrical energy as economically as possible with acceptable reliability and quality. Power system reliability is defined as the ability of the system to satisfy the customer demand [1-3]. System reliability can be improved by increased investment in the system. The associated costs however, may be unacceptable. The economic and the reliability constraints are often in conflict and can lead to difficult managerial decisions [2-4].

Demands for electric power with high reliability and quality have increased tremendously in the past few decades due to the digital revolution. It is expected that the requirements for high quality, reliable power supply will continue to increase in the immediate future. Customers such as commercial, industrial and residential users have come to expect a highly reliable supply with relatively low rates. The electric power industry throughout the world is undergoing considerable change with respect to structure, operation and regulation. Many individual parties including generating companies, network owners, network operators, energy suppliers, regulators, together with the end users are all involved in a power system. They are often in conflict and new concerns regarding system reliability have arisen [2, 5-8]. In the new competitive environment, electric utilities face the challenging task of minimizing capital investments and operating and maintenance expenditures in order to hold down electricity rates while maintain the reliability at an acceptable level.

Reliability is an important consideration during the planning, design and operating phases of an electric power system. Criteria and techniques have been developed and utilized by utilities and systems over many years [2,3,8,10]. Deterministic criteria were first used in virtually all practical applications and some of them are still in use today. The essential weakness of deterministic criteria is that they do not respond to the stochastic nature of system behavior, customer demands or component failures. Since a power system behaves stochastically, it is necessary to consider probabilistic methods that are able to respond to the actual factors that influence the reliability of the system. The unavailability of applicable data, limited computational resources and the lack of evaluation techniques have limited the use of probability methods in the past. This is now no longer the case and there are many examples of practical applications.

1.2 Power System Reliability Evaluation

Considerable activity has occurred in the development and application of probabilistic techniques for power system reliability evaluation and there is a wide range of related publications [11-18].

Today, most utilities have valid and applicable reliability data and most engineers have a working understanding of probability theory. The availability of highly developed reliability evaluation techniques and computer technologies have made the use of probabilistic techniques highly practical. Many utilities utilize probabilistic techniques in addition to deterministic techniques as probabilistic methods can provide quantitative input to the decision making process. Probabilistic techniques are employed extensively in system planning and operation, in both single and interconnected systems. This utilization is expected to continue to increase in the future.

1.2.1 Basic Aspects of Power System Reliability Evaluation

Two basic aspects of power system reliability are system adequacy and system security [1-3,10]. This division is shown in Figure 1.1.

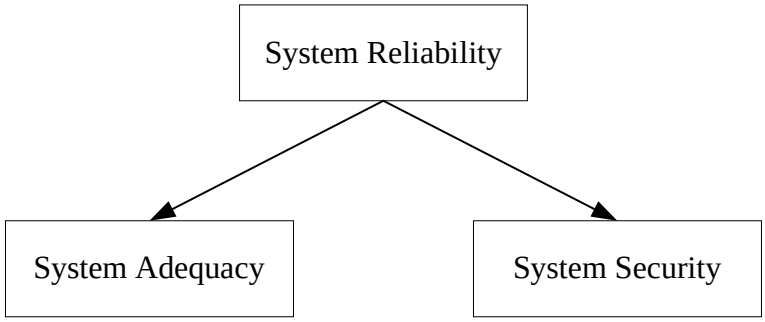

Figure 1.1: Basic aspects of system reliability

System adequacy involves the existence of sufficient facilities in the system to satisfy the customer demand. These facilities include the generating capacity required to generate enough energy and the transmission and distribution elements needed to transfer the generated energy to the customer load points. Adequacy involves static system conditions rather than system disturbances and is affected by many factors such as the installed capacity, unit sizes, unit availabilities, maintenance requirements, interconnections and so on. System security, however, concerns the ability of the system to respond to disturbances. Power systems have to maintain certain levels of static and spinning reserves in order to achieve a required level of adequacy and security.

Considerable work has been done in the domain of adequacy assessment. Some work has been done on the security problem, such as quantifying spinning reserves, operating capacity requirements or transient stability margins. This thesis is focused on system adequacy assessment.

1.2.2 Hierarchical Levels

A power system consists of the three basic functional zones of generation, transmission and distribution [1-2,10] shown in Figure 1.2.

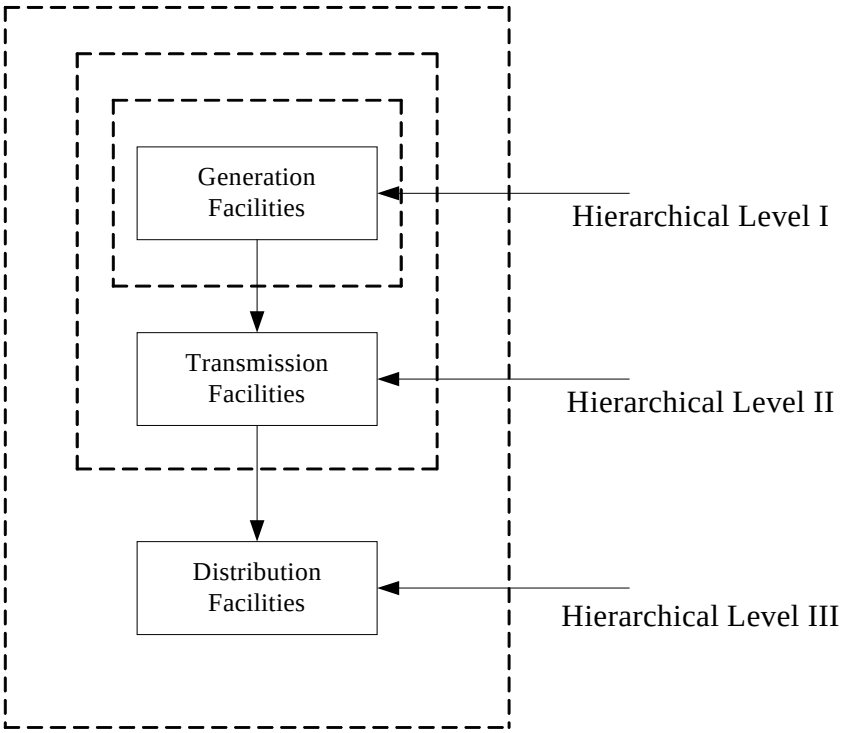

Figure 1.2: Hierarchical levels

The three functional zones shown in Figure 1.2 can be combined to form hierarchical levels. Hierarchical Level I (HLI) is concerned with only the generation facilities, while Hierarchical Level II (HLII) includes both the generation and transmission facilities, Hierarchical Level III (HLIII) includes all the three functional zones to provide a complete system. Studies at HLI and HLII are performed regularly. It is difficult to perform HLIII studies in an actual system due to the scale of the problem. Functional zone studies are usually performed without including the zones above them.

This thesis is focused on HLI evaluation. Adequacy evaluation at HLI involves the determination of the total system generation required to satisfy the total load requirement. Adequacy evaluation in this area is the oldest and most extensively studied aspect of power system reliability assessment. In these studies, the reliability of the transmission and distribution zones and their ability to move the generated energy to the customer load points are not included. The basic model at HLI is shown in Figure 1.3.

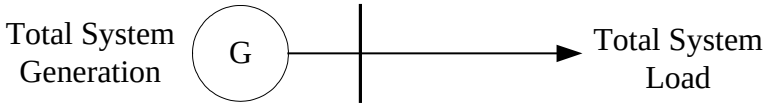

Figure 1.3: System model for adequacy evaluation at HLI

The simple model shown in Figure 1.3 is used to decide how much additional capacity to install and when. Generating capacity adequacy evaluation is an important area of power system reliability evaluation [10-18]. Extensions, modifications and new algorithms are being continuously published.

1.2.3 Methods of Adequacy Assessment at HLI

The basic approach to perform adequacy evaluation at HLI consists of the three segments shown in Figure 1.4 [1,2,3].

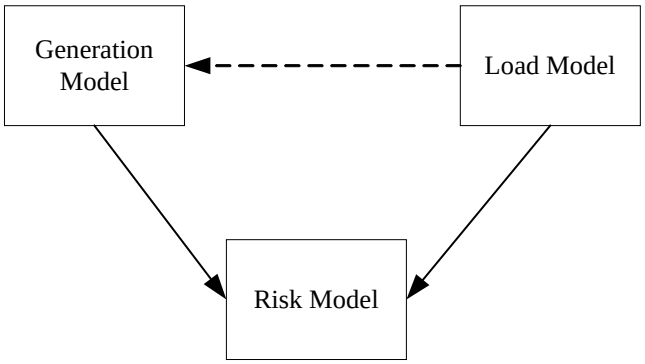

Figure 1.4: Conceptual model in adequacy assessment at HLI

The generation model and the load model shown in Figure 1.4 are combined to form the risk model. The risk indices obtained are overall system adequacy indices and do not include transmission constraints and transmission reliabilities.

A wide range of methods has been developed to perform generating capacity reliability evaluation. These techniques can be categorized into two types, analytical methods and simulation methods. Analytical methods represent the system by mathematical models and evaluate the reliability indices using direct numerical solutions. Simulation methods estimate the reliability indices by simulating the actual process and random behavior of the system. The most widely used analytical technique

in HLI evaluation is the loss of load approach. This process has been extended to include the loss of energy.

Both the analytical methods and the simulation methods have their own merits and demerits [2, 20,21]. Analytical techniques can provide the expected index values in a relative short computation time. Assumptions are sometimes needed to simplify the problem, particularly when the system and the operating procedures are complex. Simulation methods generally require longer computing times and more computational resources, but theoretically, can include all aspects and contingencies in the power system. There is increasing interest in modeling the system behavior more comprehensively and in producing a more informative set of reliability indices. The development of increased computing power has made the use of simulation methods a practical and viable tool for large system reliability assessment.

1.2.4 Basic Reliability Indices

There is a number of basic reliability indices used to assess generating capacity adequacy. The most common indices are as follows [1,3].

The loss of load expectation (LOLE) is the expected number of days (hours) in a specified period in which the daily peak load (hourly load) exceeds the available generating capacity.

The loss of energy expectation (LOEE) is the expected unsupplied energy due to generating inadequacy. The LOEE incorporates the severity of the deficiencies.

The loss of load frequency (LOLF) is the expected frequency of encountering a generation deficiency in a given period.

These three indices are utilized in this research.

1.3 Two Reliability Test Systems

The analytical and simulation programs developed in this research are applied to two test systems designated as the RBTS [22] and the IEEE-RTS [23].

The RBTS is a basic reliability test system developed at the University of Saskatchewan for educational and research purposes. It contains 11 generating units and has an installed generating capacity of 240 MW. The annual system peak load is 185 MW. The RBTS provides the opportunity to conduct a large number of reliability studies with reasonable solution times.

The IEEE-RTS was developed by the Reliability Test System Task Force of the Application of Probability Methods Subcommittee. The IEEE-RTS provides a reasonably comprehensive test system containing generation, transmission and load data. It can be used to provide a consistent and generally acceptable set of data and to compare different techniques. It contains 32 generating units and has an installed generating capacity of 3405 MW. The annual peak load of the IEEE-RTS is 2850 MW.

The detailed reliability data required at HLI for the two test systems are given in Appendix A.

1.4 Research Objectives

As noted above, this thesis is focused on adequacy evaluation at HLI. The objectives of this research are divided into five parts.

1.4.1 Computer Programs

The first part of the research objectives involves the development of two digital computer programs based on the analytical and simulation methods. Three types of load data are considered in each program. They are constant load, daily peak and hourly load values. A range of reliability indices can be obtained using the two programs. The developed softwares are used as platforms to perform generating capacity adequacy evaluation.

1.4.2 Basic Considerations

The work involves the examination of some basic considerations in HLI adequacy evaluation. Although the basic indices noted in Section 1.2.4 have been in use for some time, there are still misconceptions that need to be examined and discussed. The misconceptions are illustrated numerically using the two test systems and the two developed programs.

The simulation program provides the opportunity to extend the basic indices normally calculated using the analytical method to include index probability distributions. This thesis briefly illustrates the concept of creating distributions and the additional information that can be obtained and utilized in generating capacity risk assessment.

1.4.3 Generating Unit State Residence Time Distributions

This part of the thesis involves an examination of the effect of generating units residence time distributions on the system reliability. Various Weibull distributions are considered and results obtained from the simulation program are compared and analyzed.

1.4.4 Considering Peaking Load Units in HLI Adequacy Evaluation

This thesis examines some of the basic assumptions used in modeling peaking load units in an HLI adequacy evaluation. The basic generating unit unavailability parameter in an HLI study is the unit Forced Outage Rate (FOR) [2]. The FOR is the ratio of the forced outage hours to the sum of the forced outage hours plus the service hours. The FOR provides an adequate estimate for base load units. The FOR does not, however, provide an adequate estimate for peaking load units which have fewer operating hours and many more start-ups and shut-downs than base load units. The four-state model proposed in [24] provides a better representation for a peaking load unit and forms the basis for the Utilization Forced Outage Probability (UFOP) statistic

used by Canadian electric power utilities [25]. The UFOP is the probability of a generating unit not being available when needed. The Derated Adjusted Utilization Forced Outage Probability (DAUFOP) is the probability of a generating unit with derated states not being available when needed [25]. The UFOP and DAUFOP can be used to calculate system reliability indices and provide a better reliability representation of peaking load units than the conventional FOR. The UFOP is dependent on the demand placed upon the unit and therefore varies with changes in the operating conditions and load levels. How the UFOP change with changes in the system operating conditions is examined. The peaking load unit state residence time distributions are usually considered to be exponential. The simulated distributions for the peaking load units are illustrated in this thesis.

1.4.5 The UFOP and the DAUFOP

The UFOP is usually calculated for a certain operating condition and then used in many situations where the operating conditions are different. Using a fixed UFOP to evaluate system reliability introduces some error. The differences in the results when a fixed UFOP or the simulated UFOP are used is compared and analyzed.

Peaking load units can also have derated states which impact the system reliability. This effect should be considered. The DAUFOP of these peaking units can be used to calculate the reliability indices. The results produced using the DAUFOP are more accurate than those obtained using the UFOP, but require more unit data. The differences in the reliability indices produced using the UFOP and the DAUFOP are examined to see if the DAUFOP is necessary in the reliability evaluation of a specific system.

1.5 Outline of the thesis

This thesis contains seven chapters. The contents of each chapter are briefly outlined as follows.

Chapter 1 Introduction

This chapter introduces some basic concepts on the function of a power system and on power system reliability. The categories and the hierarchical levels associated with power system reliability evaluation are presented. The focus of the research described in this thesis, the basic reliability indices used in HLI adequacy evaluation and the methods used to perform the evaluation are briefly introduced. The two reliability test systems used in this research are introduced. The objectives of the research described in this thesis are also presented.

Chapter 2 Programs

The analytical and simulation methods that the two developed computer programs are based on are introduced. A recursive algorithm is used in the analytical program to form the capacity outage probability table used as the generation model. The sequential Monte Carlo Simulation method is employed in the simulation program. The state duration sampling method is used to simulate the behavior of the generating units. The structures of the two programs and the assumptions made are presented. The data inputs and system configurations are illustrated together with the graphical user interfaces. The outputs of the two programs are also described.

Chapter 3 Basic Considerations in Reliability Evaluation at HLI

Some misconceptions regarding the basic reliability indices are introduced in this chapter. These misconceptions are illustrated by applying the analytical and simulation programs to both the RBTS and the IEEE-RTS. The index probability distributions using the simulation program are shown in this chapter. The concept of creating and utilizing additional information from the index probability distributions is introduced.

Chapter 4 The Effect of Generating Unit State Residence Time Distributions on System Reliability

The RBTS and the IEEE-RTS generating unit data are modified to contain units with Weibull distributed state residence time distributions and the reliability indices are obtained from the simulation program. The test systems are modified to incorporate units with derated states having Weibull distributions. The results when the shape parameters change are compared to show the effect of the residence time distributions on the system reliability.

Chapter 5 Reliability Evaluation at HLI Considering Peaking Load Units

The simulation of peaking load units using the four-state model is described in detail in this chapter. The calculation of the UFOP and DAUFOP is also introduced. The RBTS and the IEEE-RTS are modified to contain peaking load units. The changes in the UFOP with required reserve, system peak load and unit residence time distributions are examined. The peaking load unit state residence time distributions are also examined in this chapter.

Chapter 6 The UFOP and the DAUFOP

The obtained UFOP is used to modify the generation data in the analytical program. The reliability indices produced by the analytical program using different sets of UFOP are compared and the errors introduced by using a fixed UFOP are illustrated.

The two test systems are further modified to contain peaking load units with derated states. The results from the simulation program show the effect of the derated states on system reliability. The obtained DAUFOP is used in the analytical program. The reliability indices are compared with those obtained when the UFOP is used. The differences in the two sets of reliability indices can be used to determine if a DAUFOP is necessary for a specific system.

Chapter 7 Summary and Conclusions

This chapter summarizes the research described in this thesis and presents some conclusions regarding this research.

2. PROGRAMS

2.1 Introduction

Analytical and simulation methods for generating capacity adequacy evaluation have been in use for some time. Developments in Monte Carlo simulation occurred later than comparable analytical methods. Both methods have their own advantages and disadvantages [2, 3, 26]. They complement each other and it's not valid to say that one method is superior to the other. The choice of the most suitable method depends on the problem and the solution requirements.

Most analytical methods are based on the Calabrese approach [27] in which the generation model is represented by a Capacity Outage Probability Table (COPT). This is normally constructed using an enumeration method, e.g., the recursive algorithm [2,8]. The Calabrese approach forms the basis for the loss of load method [27]. Another significant technique is the frequency and duration method [8, 28-31].

Simulation is a more sophisticated procedure that treats the problem as a series of experiments [2, 3, 19, 21, 26,32]. There are different types of simulation processes and are loosely referred to as Monte Carlo simulation (MCS). Simulation processes can be generally categorized as being either random or sequential. The random approach simulates the basic intervals of the system lifetime by randomly chosen intervals, while the sequential approach simulates the basic intervals in chronological order.

Two programs based on the analytical and simulation methods have been developed in this research and the results obtained using the two methods under different conditions have been compared. Selected factors that affect system reliability are incorporated in the generation model. Three types of load data are considered in each

program. They are constant load, daily peak and hourly load values. A range of reliability indices can be obtained using the two programs.

The analytical program uses the recursive algorithm to form the COPT and uses the loss of load approach to calculate the adequacy indices. The frequency and duration method is not used in the analytical program. Generating unit derated states and load forecast uncertainty can be incorporated in the calculation. The load can be a straight line, or expressed by discrete points, for example, 8760 points for a year. It can also be in the form of multiple steps.

The simulation program is based on the sequential Monte Carlo approach. The state duration sampling method is used to simulate the behavior of the generating units. The derated states, state residence time distributions and peaking unit loading orders are considered during the simulation process. The load is expressed in the form of chronologically discrete load points.

The methods applied in the two programs are described in detail in the following sections. The two programs are used as a platform for research in generating capacity reliability evaluation. The structures of the two programs, and the inputs and outputs are described later in this chapter.

2.2 Methods

2.2.1 Analytical Method

The method [2] used in the analytical program is introduced here.

Generating Unit Models and Parameters

The two-state model for a generation unit is shown in Figure 2.1.

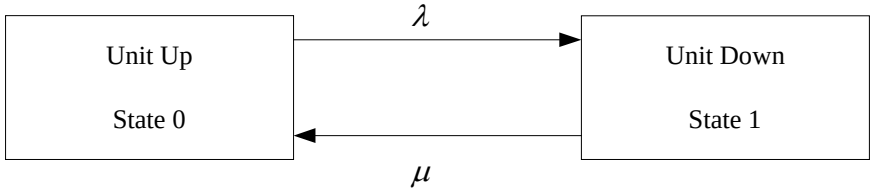

Figure 2.1: Two-state model for a base load unit

where λ = expected failure rate

μ = expected repair rate

The basic generating unit parameter used in adequacy evaluation is the unavailability, also known as the forced outage rate (FOR). The availability (A) and unavailability (U) are given by Equations (2.1) and (2.2) respectively.

$$Unavailability(FOR) = U = \frac{\lambda}{\lambda + \mu} = \frac{r}{r + m} = \frac{\sum[DownTime]}{\sum[DownTime] + \sum[UpTime]} \qquad (2.1)$$

$$Availability = A = \frac{\mu}{\lambda + \mu} = \frac{m}{r + m} = \frac{\sum[UpTime]}{\sum[DownTime] + \sum[UpTime]} \qquad (2.2)$$

where m = mean time to failure = MTTF = $1/\mu$

r = mean time to repair = MTTR = $1/\lambda$

The model for a base load unit that has one derated or partial output state is shown in Figure 2.2. This model can be expanded to include more derated states.

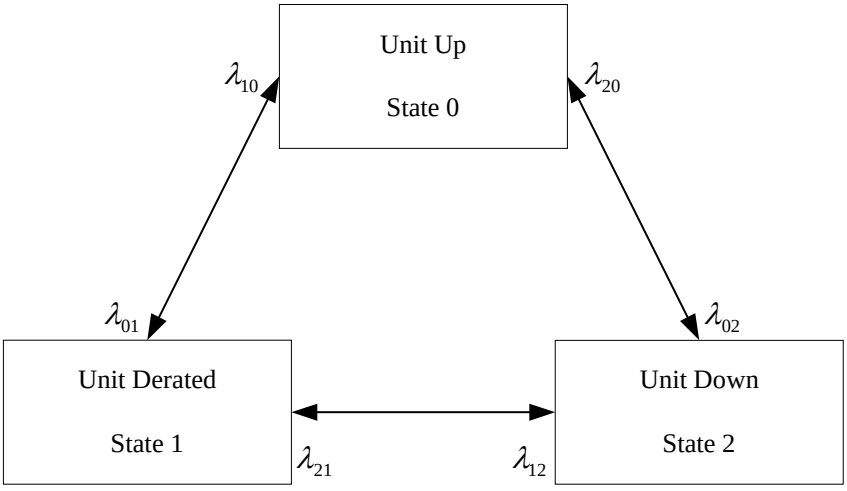

Figure 2.2: Three-state model for a base load unit

λ_{ij} is the transition rate between state "i" and state "j". The probability of existence at state "i", P_i, can be calculated as shown in Reference [26].

$$\alpha P_m = \alpha \qquad (2.3)$$

where $\alpha = [P_0 \quad P_1 \quad P_2]$ is the limiting state probability vector.

P_m is the stochastic transitional probability matrix.

The transitional probability matrix P_m for the model of Figure 2.2 is as follows.

$$P_m = \begin{bmatrix} (1-\lambda_{01}-\lambda_{02}) & \lambda_{01} & \lambda_{02} \\ \lambda_{10} & (1-\lambda_{10}-\lambda_{12}) & \lambda_{12} \\ \lambda_{20} & \lambda_{21} & (1-\lambda_{20}-\lambda_{21}) \end{bmatrix}$$

The two models shown in Figure 2.1 and 2.2 are suitable for base load units which have relatively long operating cycles. They are used to estimate the probability of existence in each state. In the case of peaking load units or intermittent operating units, the demand cycle is relatively short and therefore the models shown earlier cannot provide an adequate estimate. These models also do not include any recognition of the times when the unit is unavailable but is not required by the system. The IEEE Subcommittee on the Application of the Probability Methods [24] proposed the four-state model for peaking units shown in Figure 2.3. This model includes the reserve shutdown and forced out but not needed states.

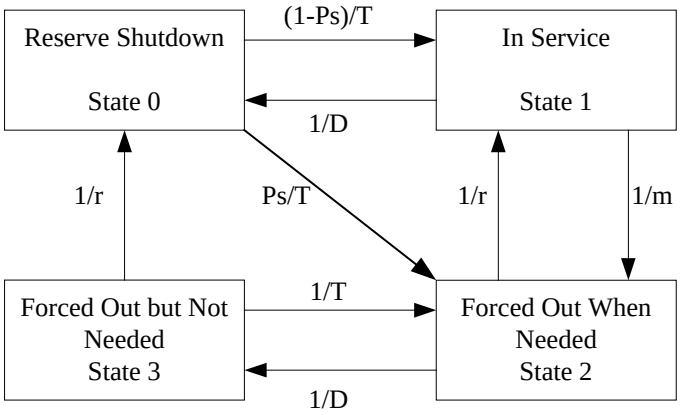

Figure 2.3: IEEE four-state model for a peaking load unit

T : Average reserve shutdown time between periods of need

D : Average in service time per occasion of demand

Ps : Probability of starting failure

In this case, the conditional probability that the unit will not be available when needed is P, where

$$P = \frac{P_2}{P_1 + P_2} \tag{2.4}$$

The demand factor f can be defined as follows.

$$f = \frac{P_2}{P_2 + P_3} \tag{2.5}$$

The conditional forced outage rate P can be calculated by:

$$P = \frac{f(P_2 + P_3)}{P_1 + f(P_2 + P_3)} = \frac{f(FOT)}{ST + f(FOT)} \tag{2.6}$$

where:

FOT is the forced outage time,

ST is the service time.

Recursive Algorithm

A capacity outage probability table (COPT) is an array of the capacity levels and their probabilities of existence. It is used in the loss of load method and can be formed using a recursive algorithm.

The recursive algorithm [2] for adding two state generating units is given by Equation (2.7). This equation shows the cumulative probability of a certain capacity outage state of X MW calculated after one unit of capacity C MW, with a forced outage rate U, is added.

$$P(X) = (1-U)P'(X) + (U)P'(X - C) \tag{2.7}$$

where

$P'(X)$ and $P(X)$: The cumulative probability of the capacity outage state of X MW before and after the unit is added.

Equation (2.7) is modified as shown in Equation (2.8) for generating units with derated states.

$$P(X) = \sum_{i=1}^{n} p_i P'(X - C_i) \tag{2.8}$$

where n = number of unit states

C_i = capacity outage of state i for the unit being added

p_i = probability of existence of the unit state i.

The capacity outage probability table is complete after all the generating units are added.

Loss of Load Method

The generation model is convolved with the load model as shown in Figure 1.4. The load model used depends on the required reliability index. One common load model represents each day by the daily peak load, while another one represents the load using the individual hourly load values. If the daily peak loads are arranged in descending order, the formed cumulative load model is called the daily peak load variation curve. The load duration curve is created by arranging the hourly load values in descending order.

In the loss of load method, the daily peak load (or hourly values) are combined with the capacity outage probability table to obtain the expected number of days (or hours) in the given period in which the daily peak load (or hourly load) exceeds the available capacity. The index in this case is designated as the loss of load expectation (LOLE). The LOLE is given by:

$$LOLE = \sum_{k=1}^{n} p_k t_k = \sum_{k=1}^{n} (t_k - t_{k-1}) P_k \qquad (2.9)$$

where n is the total number of capacity outage states.

p_k is the individual probability of the capacity outage state k.

P_k is the cumulative probability of the capacity outage state k.

t_k is the number of time units when there is a loss of load.

The relationship between load, capacity and reserve is shown in Figure 2.4. When the load duration curve is used, the shaded area E_k represents the energy that cannot

be supplied in a capacity outage state k. The probable energy curtailed in this case is $p_k E_k$. The loss of energy expectation (LOEE) is given by:

$$LOEE = \sum_{k=1}^{n} p_k E_k \tag{2.10}$$

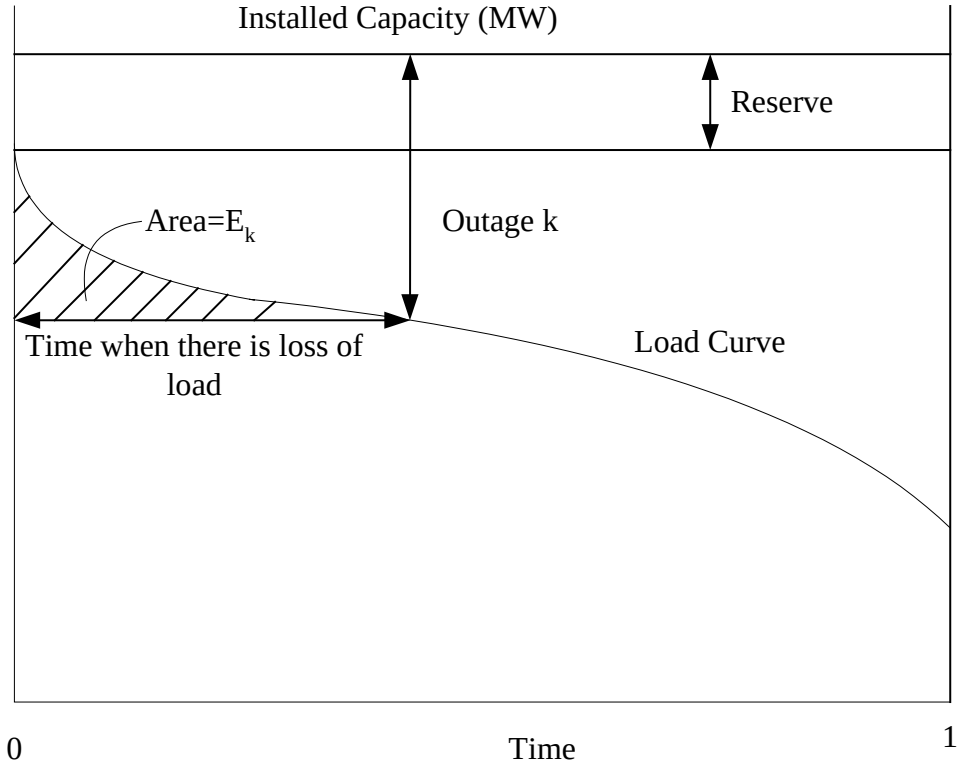

Figure 2.4: Relationship between capacity, load and reserve

The LOEE can be normalized using the total energy E under the load duration curve as shown in Equation (2.11).

$$LOEE_{p.u.} = \sum_{k=1}^{n} p_k E_k / E \tag{2.11}$$

An index designated as the energy index of reliability (EIR) can be calculated using Equation (2.12).

$$EIR = 1 - LOEE_{p.u.} \tag{2.12}$$

Load Forecast Uncertainty

The load data used to perform the evaluation is usually predicted using past

experience [2] and therefore the actual peak load will differ from the forecast values. Load forecast uncertainty can be incorporated in the reliability evaluation. The approach used in the analytical program is as follows.

The load forecast probability distribution can be divided into class intervals, the number of which depend on the required accuracy. The LOLE can be calculated for each load level represented by a class interval and multiplied by the probability that the load level occurs. The sum of the products is the LOLE for the forecast load.

2.2.2 Sequential Monte Carlo Simulation Method

The general steps used to apply the simulation method [2, 3, 26] to generating capacity reliability evaluation are as follows. The basic elements of the Monte Carlo simulation method, the inverse transform method to generate a random variate, the state duration sampling method and the stopping rules used in the simulation program are briefly described in the following.

General Steps

The general steps to perform the evaluation are as follows:

Step 1: Generate operating histories for each generating unit.

Step 2: Combine the operating cycles of all units and produce the system available capacity.

Step 3: Superimpose the system available capacity on the chronological load curve.

Step 4: Calculate the appropriate reliability indices.

Step 5: Check the stopping rules.

Random Variate Generation----Inverse Transform Method

A random variate is a random variable that follows a given distribution. Usually the development environment provides a random generator that can generate a random variate uniformly distributed between [0, 1]. The methods to generate a non-uniformly

distributed random variate can be categorized into three types, the inverse transform method, the composition method and the acceptance-rejection method. The inverse transform method is applied in the developed simulation program. The procedure to generate a random variate using the inverse transform method is as follows:

Step 1: Generate a uniformly distributed random number U between [0,1].

Step 2: Calculate the random variate X which has the cumulative probability distribution function F(x) using

$$X = F^{-1}(U) \tag{2.13}$$

Exponential and Weibull distributions are utilized in the simulation program.

The probability density function for the exponential distribution is,

$$f(x) = \lambda e^{-\lambda x} \tag{2.14}$$

The cumulative probability distribution function is:

$$F(x) = 1 - e^{-\lambda x} \tag{2.15}$$

Using the inverse transform method:

$$U = F(x) = 1 - e^{-\lambda x}$$

$$X = F^{-1}(U) = -\frac{1}{\lambda}\ln(1-U) = -\frac{1}{\lambda}\ln(U) \tag{2.16}$$

U is a uniformly distributed random number and therefore (1-U) distributes uniformly in the same way as U in the interval [0,1].

The random variate X then follows an exponential distribution.

The probability density function for the Weibull Distribution is,

$$f(x) = \frac{\beta}{\alpha^{\beta}} x^{\beta-1} \exp[-(\frac{x}{\alpha})^{\beta}] \tag{2.17}$$

Using the inverse transform method,

$$U = F(x) = 1 - \exp[-(\frac{x}{\alpha})^{\beta}]$$

$$X = \alpha[-\ln U]^{1/\beta} \tag{2.18}$$

The random variate X then follows a Weibull distribution.

State Duration Sampling Method

The basis of the state duration sampling method is to sample the probability distribution of the component state durations and to simulate the transition processes. The base load units and the peaking load units have different models and therefore their sampling procedures are different.

Base load units:

The model for a base load unit with N states (N>=2) is shown in Figure 2.5.

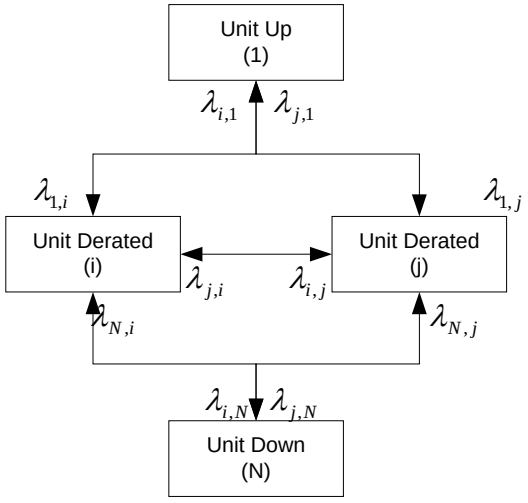

Figure 2.5: State model for a base load unit

$\lambda_{i,j}$ represents the transition rate from state "i" to state "j".

The steps to simulate a generating unit with N states are as follows:

Step 1: Specify the initial state of the unit and generate uniformly distributed random seeds $U_k, (k = 1,2...N)$ for each unit state.

Step 2: Sample the duration of the unit in the present state i. The time duration can be calculated using the inverse transform method. If the duration is exponentially distributed, $T_{i.j}$ is the time duration at state i if the unit is going to transfer to state j.

$$T_{i,j} = -\frac{1}{\lambda_{i,j}} * \ln(U_j),\ j = 1,2...N,\ j <> i \qquad (2.19)$$

The time duration at state i is : $T_i = \min(T_{i,j}) = T_{i,Nexti}$, the next state of the unit is

the one which has the shortest $T_{i.j}$.

Step 3: Repeat Step 2 in the given time span and obtain the operating cycle for this unit. Figure 2.6 shows a possible chronological operating cycle for the unit.

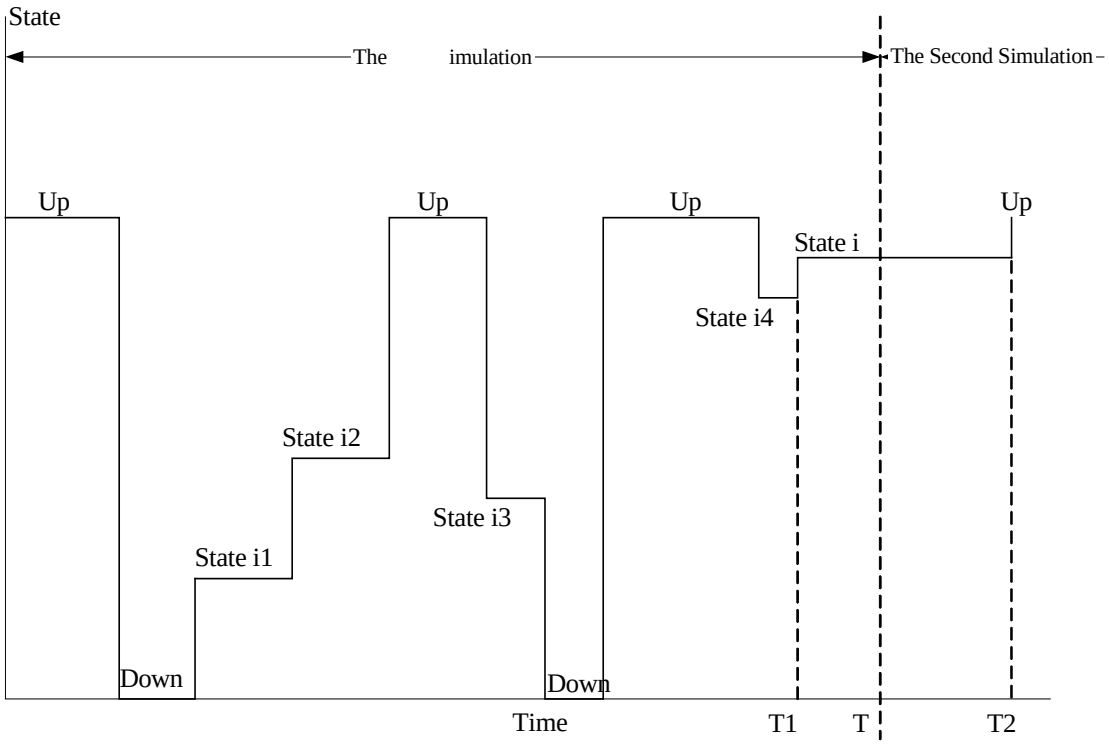

Figure 2.6: Possible Operating cycle for an N state unit

In Figure 2.6, T is the time span for one simulation. The last state of this unit is used as the initial state for the next simulation. In the situation shown in Figure 2.6, State i is the initial state of the second simulation and at time T2, the unit state changes to the up state. The second simulation therefore starts at time T2 and samples the duration of the unit in the up state.

Peaking load units:

The model for a peaking load unit is shown in Figure 2.3.

A uniformly distributed random seed is used to sample the starting failure condition. When the peaking load unit is needed, a random number between [0,1] is generated. If the number is smaller than P_s, the unit fails to start. If otherwise, it starts successfully.

After the peaking unit is started, the simulation process is basically the same as that used for a base load unit. In the case of a peaking load unit, the simulation time span depends on the period when the unit is needed.

Reliability Index Calculation

After the operating histories of all the generating units are generated, the system available capacity during one simulation time span is calculated. The superimposition of the available capacity on the load is shown in Figure 2.7.

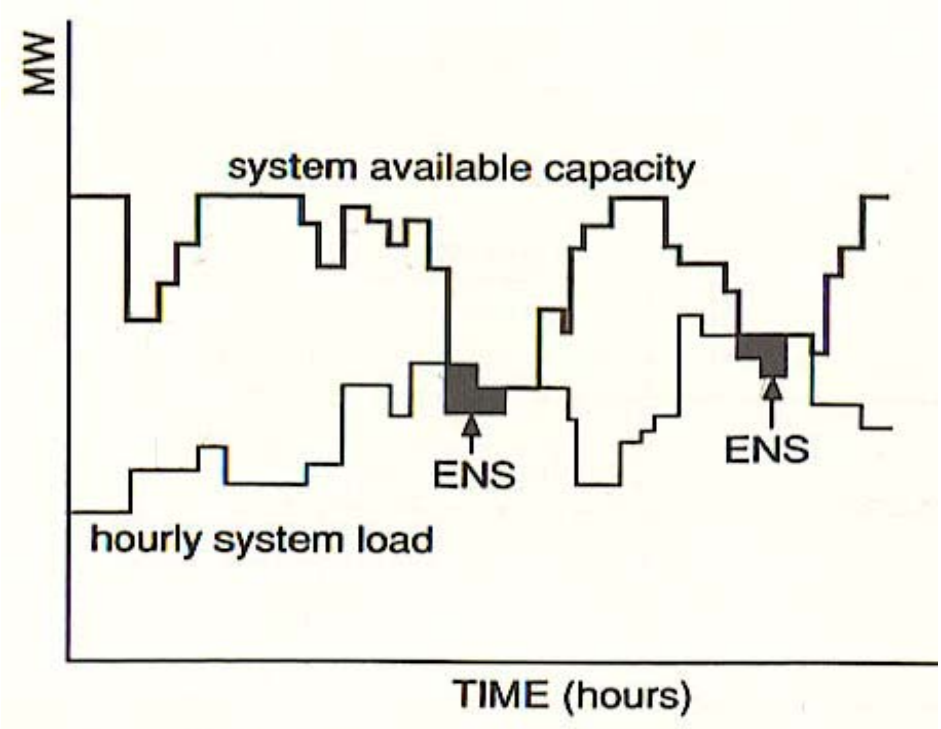

Figure 2.7: Superimposition of the available capacity on the load

The reliability indices can be calculated for each sampled year (if the time span is one year). The loss of load duration (LLD) is the summation of the time durations when the load exceeds the available capacity. The loss of load occurrence (LLO) is the total number of occurrences of loss of load. The shaded area in Figure 2.7 is the energy not supplied (ENS).

Annual system indices:

The LOLE, LOEE and LOLF can be calculated using the following equations.

$$LOLE = \frac{\sum_{i=1}^{N} LLD_i}{N} \tag{2.20}$$

The unit of the LOLE depend on the load model used. If the daily peaks are used, the unit is days/yr. If the hourly values are used, the unit is hr/yr.

$$LOEE = \frac{\sum_{i=1}^{N} ENS_i}{N} \quad MWh/yr \tag{2.21}$$

$$LOLF = \frac{\sum_{i=1}^{N} LLO_i}{N} \tag{2.22}$$

Where N is the total number of sampling years, LLD_i, ENS_i, LLO_i respectively are the loss of load duration, energy not supplied, loss of load occurrence for the sampling year i.

Interruption Indices

Duration of Interruption (DOI): $DOI = LOLE / LOLF$

The unit of the DOI depends on the load model used. If the daily peaks are used, the unit is day/int. If the hourly values are used, the unit is hr/int.

Energy Not Supplied per Interruption (ENSI):

$ENSI = LOEE / LOLF \quad MWh/\text{int}$

Load Curtailed per Interruption (LCI): $ENSI = LOEE / LOLE \quad MW/\text{int}$

Stopping Rules

Stopping rules are used to decide when to stop a simulation. The objective of a stopping rule is to facilitate a compromise between accuracy and computation cost.

Two stopping rules:

Rule 1: The simulation stops when the coefficient of the variation is less than a specified tolerance value.

Rule 2: The simulation pauses at a given number of samples to check if the coefficient of variation is acceptable. If not, the number is increased and the simulation resumes until the desired coefficient of variation is obtained.

The first stopping rule is applied in the simulation program.

The coefficient of variation of an index is:

$$\alpha = \frac{s}{E(x)\sqrt{N}} \tag{2.23}$$

Where N is the total number of sampling years.

E(x) is the expected value of the index.

s is the standard deviation of the index.

When multiple indices are determined, the one with the slowest convergence speed should be chosen as the convergence criterion.

2.3 Analytical Program

The analytical program was developed using the analytical method described earlier in this chapter. The structure, input data and output data are illustrated in the following.

2.3.1 Structure

Hardware Environment

Processor: Intel Pentium M, 1400 MHZ.

RAM: 384 MB.

Software Environment

Operating System: Windows XP home edition, version 2002.

Developing Environment: Visual C++ .NET 2003.

Block Diagram of the Analytical Program

The basic block diagram of the analytical program is shown in Figure 2.10. The detailed flow charts for steps 1 and 2 are shown in Appendix B.

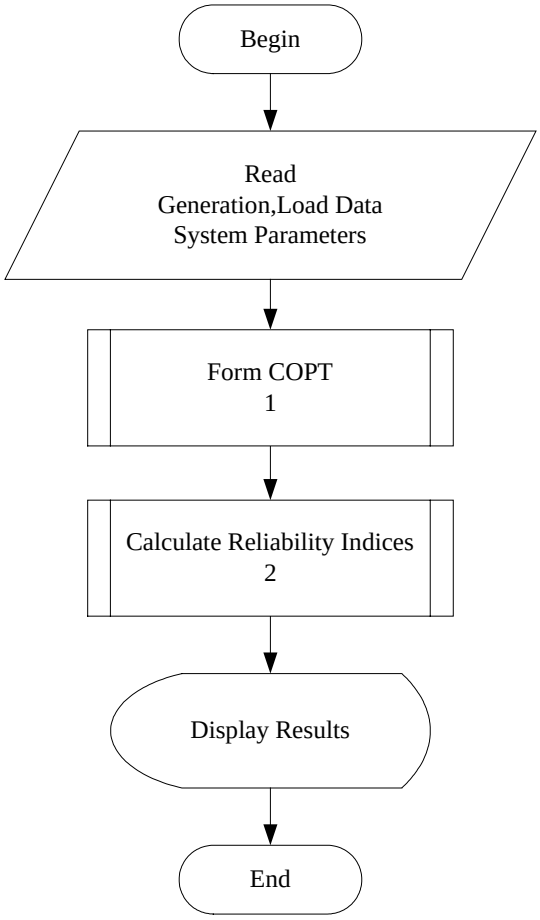

Figure 2.8: The Block Diagram for the Analytical Program

2.3.2 Input Data

Three data segments are needed to perform generating capacity adequacy evaluation using the analytical program. These segments are designated as system parameters, generation data and load data.

System Parameters

Figure 2.9 shows the system parameters that need to be inputted.

Rounding

The formed COPT can be rounded according to the rounding increment inputted in the text box by selecting the check box “Rounding COPT to Group”. The rounding process introduces some error, which depends on the rounding increment used and on the load characteristic.

Truncating

If this checkbox is checked, then the COPT is truncated by omitting all capacity outage states for which the cumulative probability is smaller than the specified amount in the text box. This results in a considerable saving in computation time.

Sensitivity Studies

This option is used to conveniently perform sensitivity studies with changes in the peak load. The max and min values represent the maximum and minimum peak load level. Steps means the total number of peak load levels. The maximum number of peak load levels the program can deal with is 50.

Selecting the Reliability Indices to Calculate

The required indices are checked.

Accuracy level

This option determines how many digits the reliability indices have.

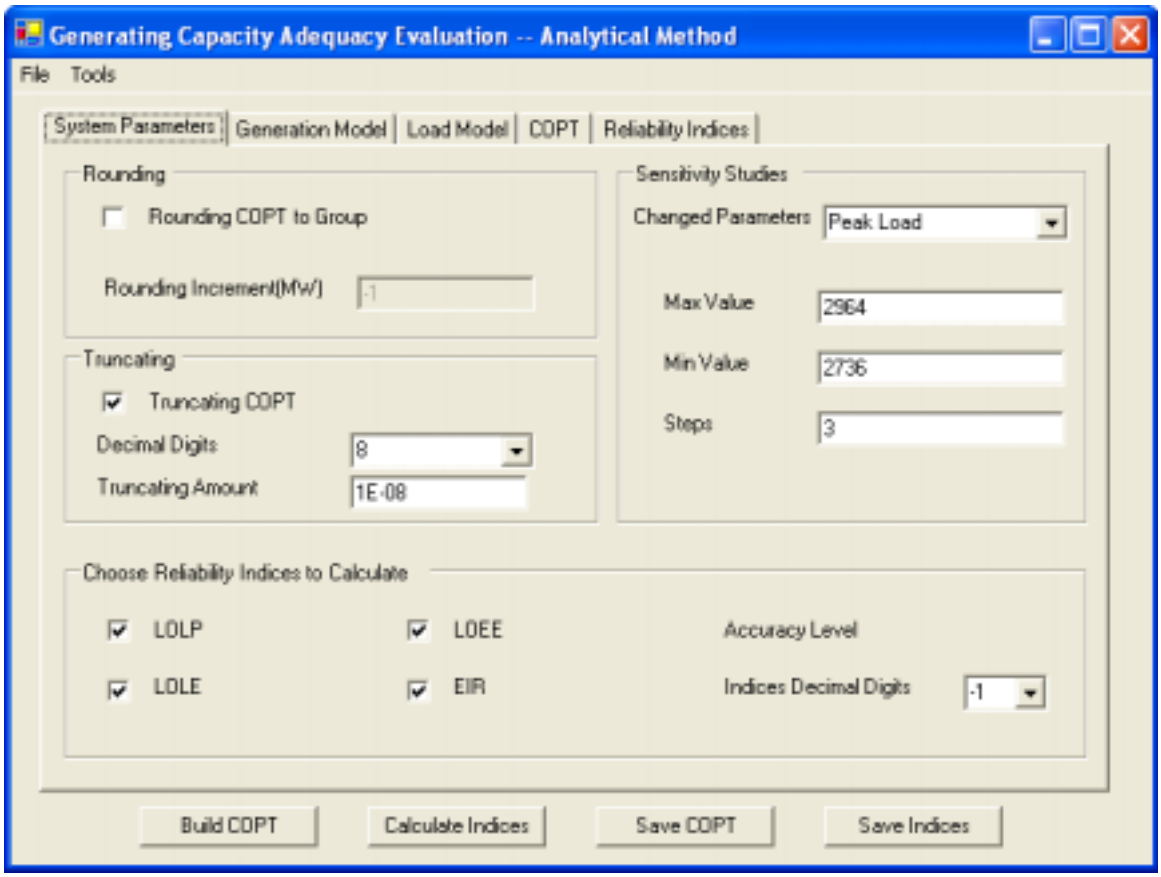

Figure 2.9: User interface to input the system parameters in the analytical program

Generation Data

Figure 2.10 shows the required generation data. The maximum number of similar generating unit groups and the number of generating unit derated states that the program can deal with is 200 and 20 respectively.

No. of Units----The number of similar generating units in a group.

Capacity----The unit capacity of this group of generating units.

No. of States----The number of the states of this group of generating units.

Capacity out and probability----For each generating unit state, the capacity out of service and the associated probability are inputted in the left text box.

The above is the required information for one group of generating units.

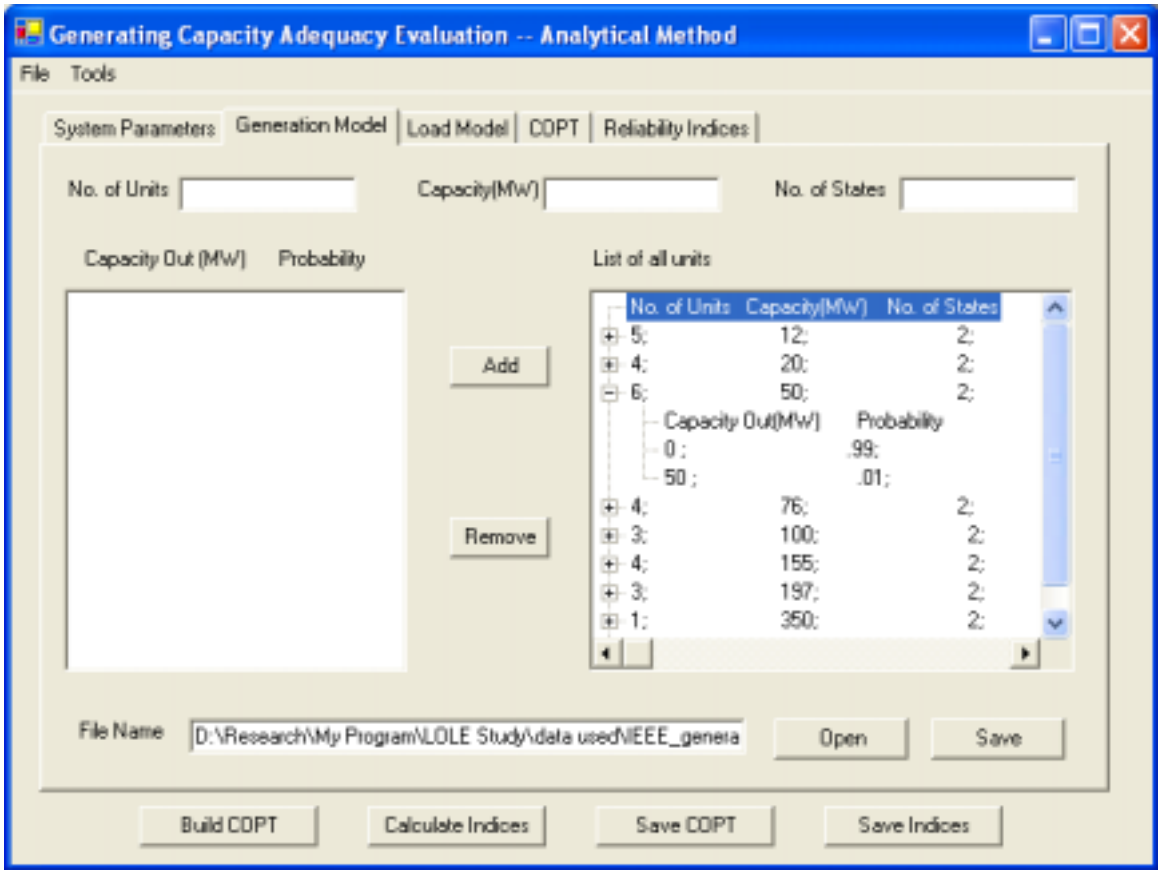

Figure 2.10: User interface to input the generation data in the analytical program

The following is the function of the buttons in the generation model page.

"Add": After the information for one group of generating units is completely inputted, the "Add" button is pressed to include this group in the generating unit list.

"Remove": Select the group of generating units to be removed. Pressing this button removes the group from the unit list.

"Open": If there is an existing stored generation data file, press this button and locate it, the generation data can be listed in the list.

"Save": After inputting the data for all generating units in the system, press this button and save the data to a specific file.

Load Data

Figure 2.11 shows the graphical user face to input load data.

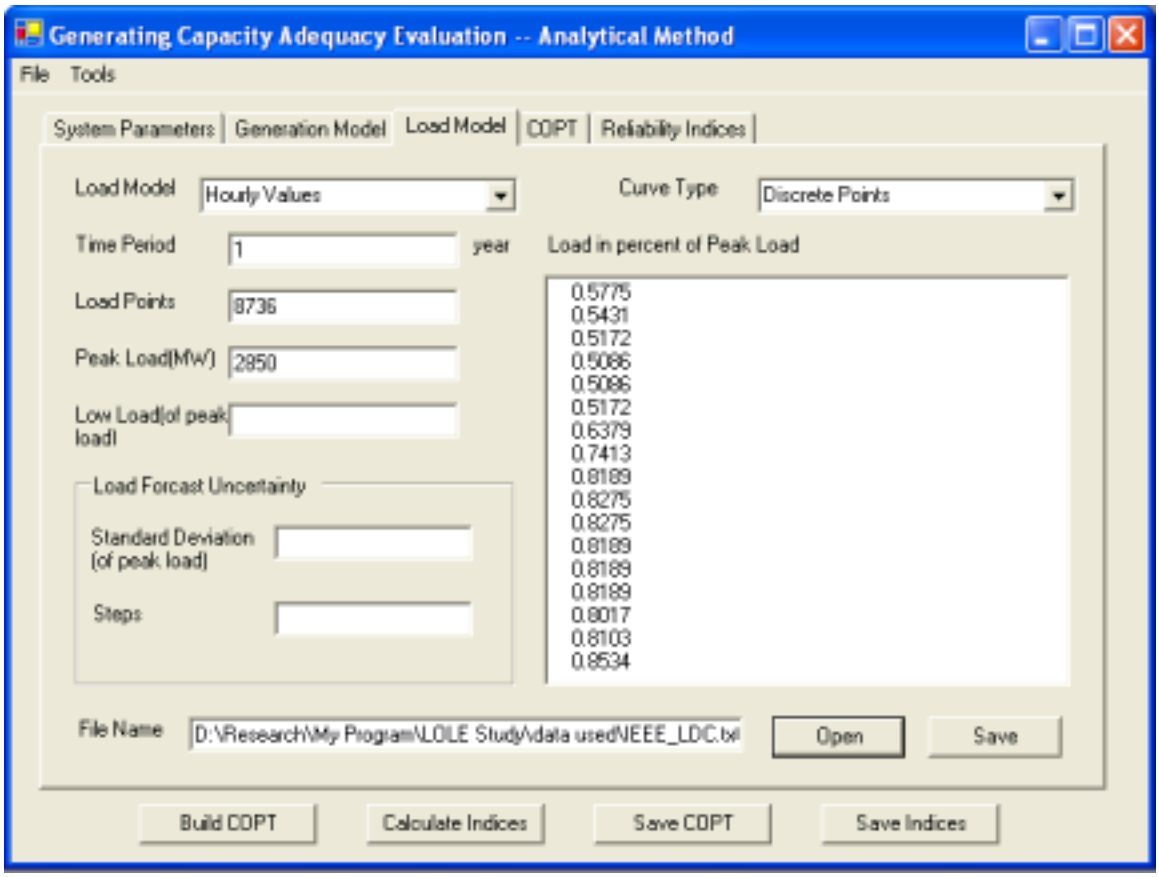

Figure 2.11: User interface to input the load data in the analytical program

Load Model: Can be selected through the List Box. The allowable load models are constant load, daily peaks or hourly values.

Curve Type: Select from the list box. The allowable load curve types are straight line, discrete points or multi step representation.

Time period: Input the time period in years for the load data.

Peak Load: The peak load in MW for the year.

If the curve type is “Discrete Points”, the number of load points has to be inputted. All of the load points should be inputted in the right text box in percent of the peak load.

If the curve type is “Straight Line”, leave the load points text box blank. The low load has to be inputted in percent of the peak load.

If the curve type is “Multi Steps”, the load steps must be inputted. The load in percent of the peak load for each step and the associated probability of this step should be inputted, i.e., 0.95; 0.55;.

Load Forecast Uncertainty: The analytical program assumes that the load forecast uncertainty follows a normal distribution. The distribution mean is the forecast peak load.

Standard Deviation (in percent of peak load)

Steps: The number of discrete steps in the distribution.

The function of the buttons “Open” and “Save”:

“Open”: If there is an existing load model file, press this button and locate that file, the load data can be loaded and displayed.

“Save”: If the load data has been inputted completely, press this button and save the data in a specific file.

2.3.3 Output Data

The program determines the COPT and the reliability indices for the system using the specified information.

The maximum number of states for a COPT is 10,000. As shown in Figure 2.12, the output includes the capacity out, individual probability and cumulative probability for each state.

The calculated reliability indices, LOLP, LOLE, LOEE and EIR are shown in Figure 2.13.

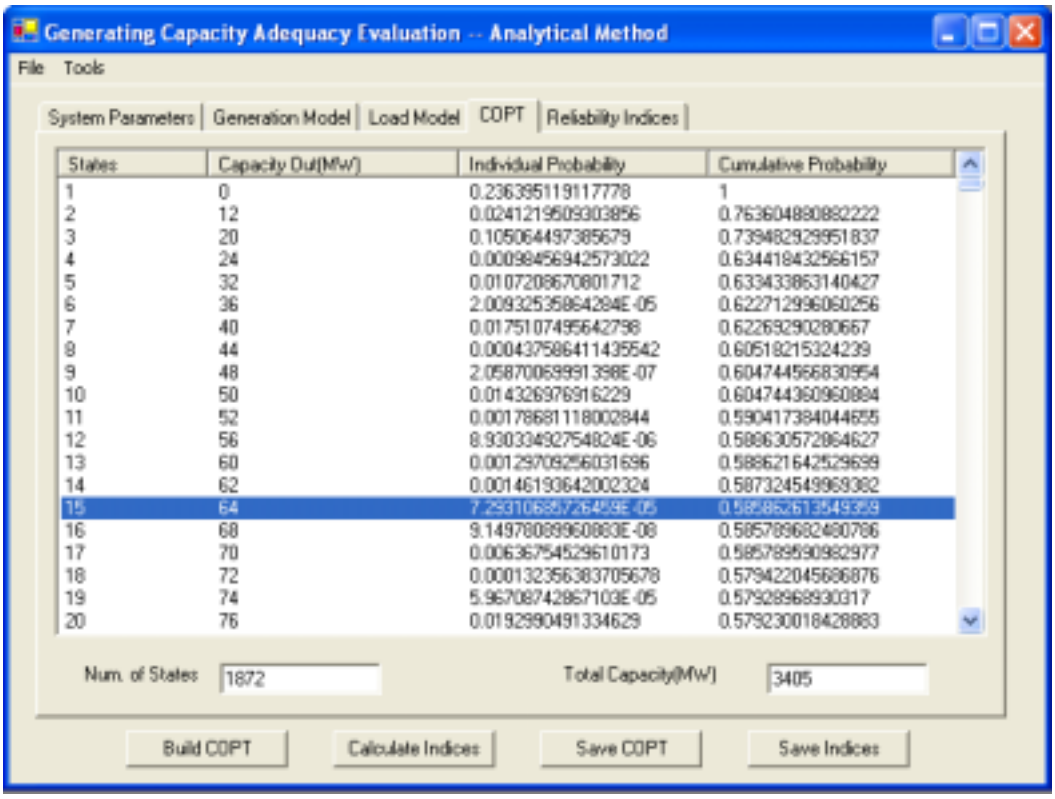

Figure 2.12: The output of the COPT from the analytical program

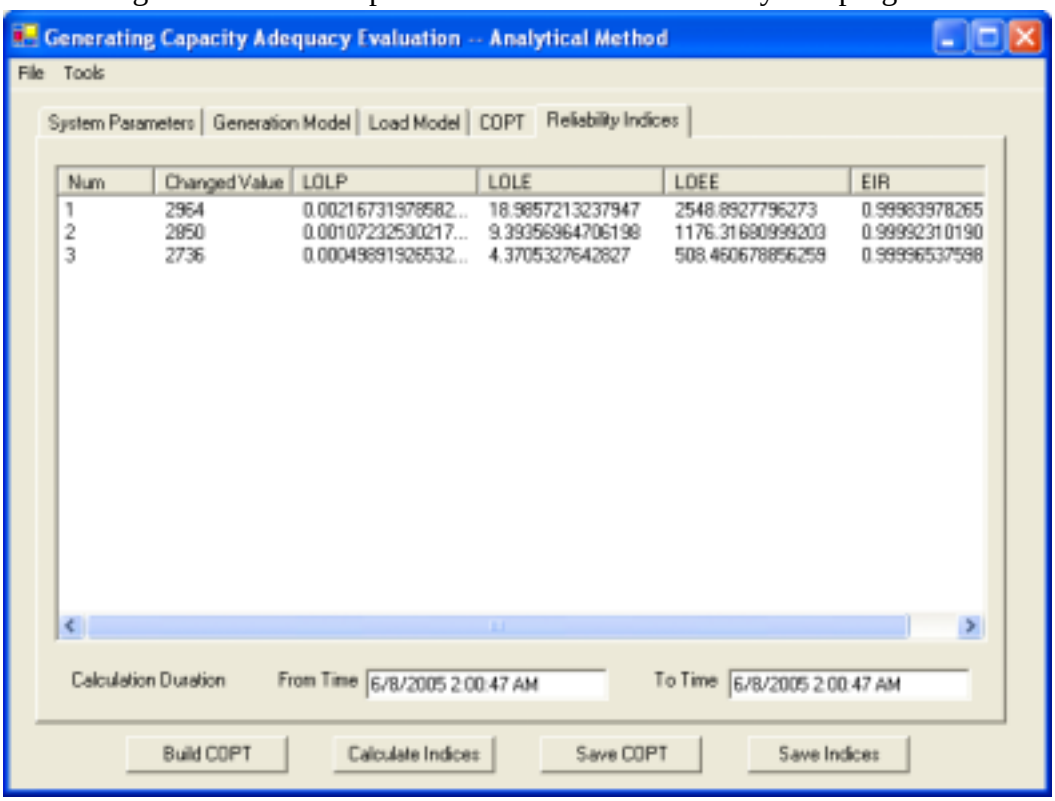

Figure 2.13: The output of the reliability indices from the analytical program

2.4 Simulation Program

The simulation program was developed using the sequential Monte Carlo method described earlier in this chapter. The structure, input data and output data are illustrated in the following.

2.4.1 Structure

Hardware Environment

Processor: Intel Pentium M, 1400 MHZ.

RAM: 384 MB.

Software Environment

Operating System: Windows XP home edition, version 2002.

Developing Environment: Visual C++ .NET 2003.

Block Diagram of the Simulation Program

The basic block diagram of the simulation program is shown in Figure 2.14. The detailed flow charts of the program are presented in Appendix C.

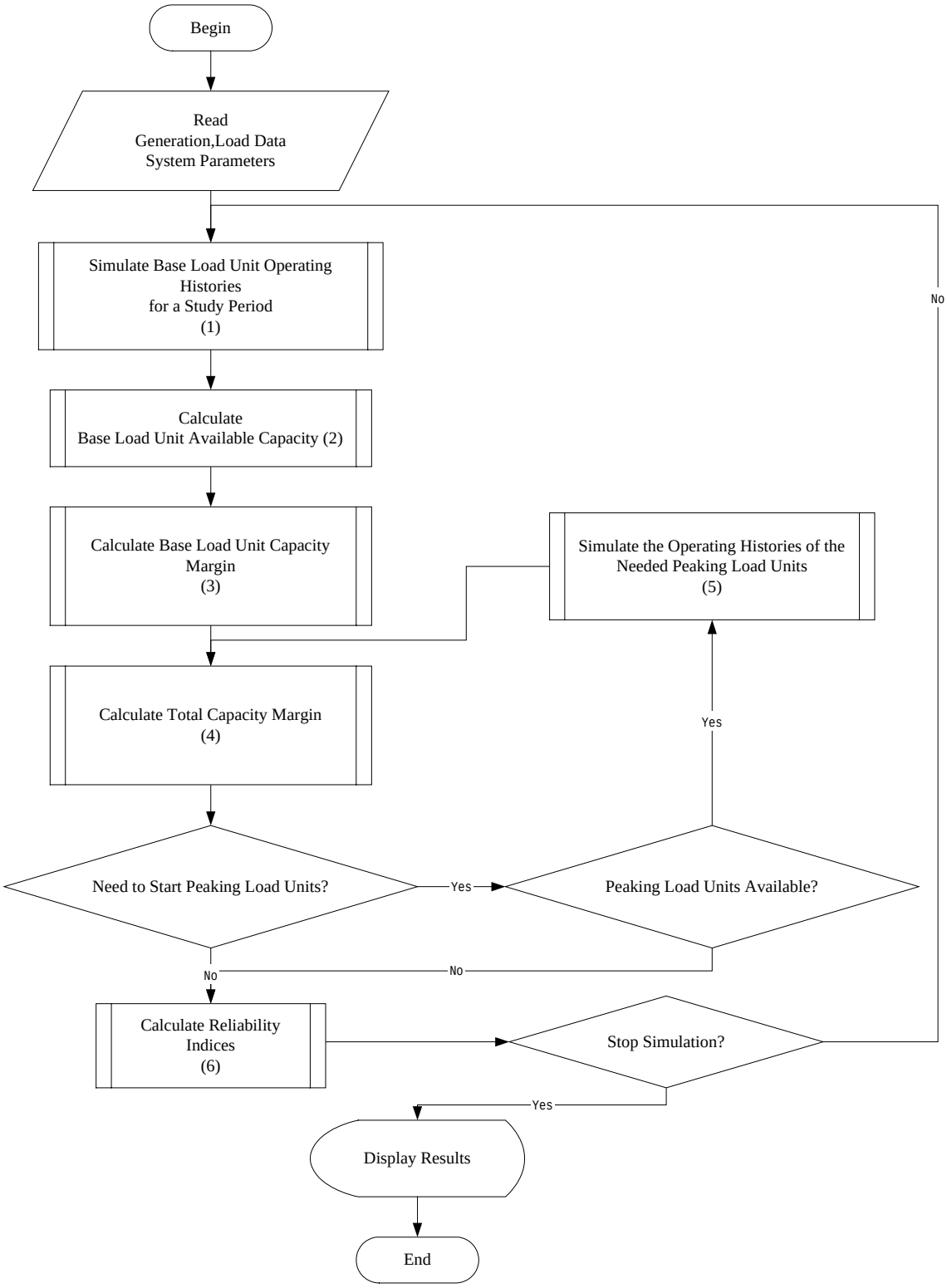

Figure 2.14: Block diagram for the simulation program

2.4.2 Input Data

Three data segments are needed to perform generating capacity adequacy evaluation using the simulation program. These segments are designated as system parameters, generation data and load data.

System Parameters

Figure 2.15 shows the interface to input the system parameters.

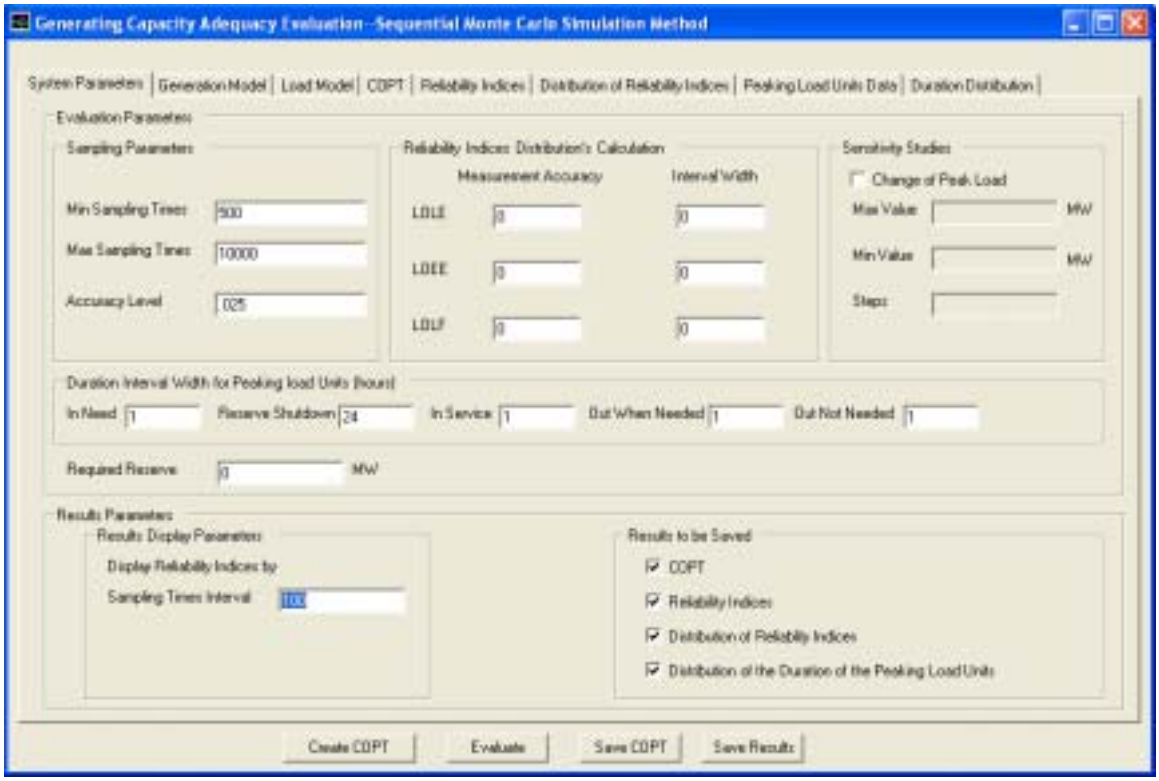

Figure 2.15: User interface to input the system parameters in the simulation program

Sampling Parameters

Min Sampling Time: The minimum number of simulation years.

Max Sampling Time: The maximum number of simulation years.

Accuracy Level: If the calculated index coefficient of variation is less than this value, the simulation stops.

Reliability Index Distribution Calculations

Interval Width: The class interval for the LOLE, LOEE and LOLF distributions.

Measurement Accuracy: The class end values are determined by adding to the

class starting values the quantity of (w-e), where w and e are the interval width and the measurement accuracy respectively.

Sensitivity Studies:

These parameters are the same as the ones used in the analytical program. The maximum number of peak load steps that the simulation program can deal with is 25.

Duration Interval Width for Peaking Load Units:

These are the interval widths for the peaking load unit state residence time distributions.

Results to be Saved:

The selected reliability indices are saved.

Generation Data

The interface to input the generation data is shown in Figure 2.16.

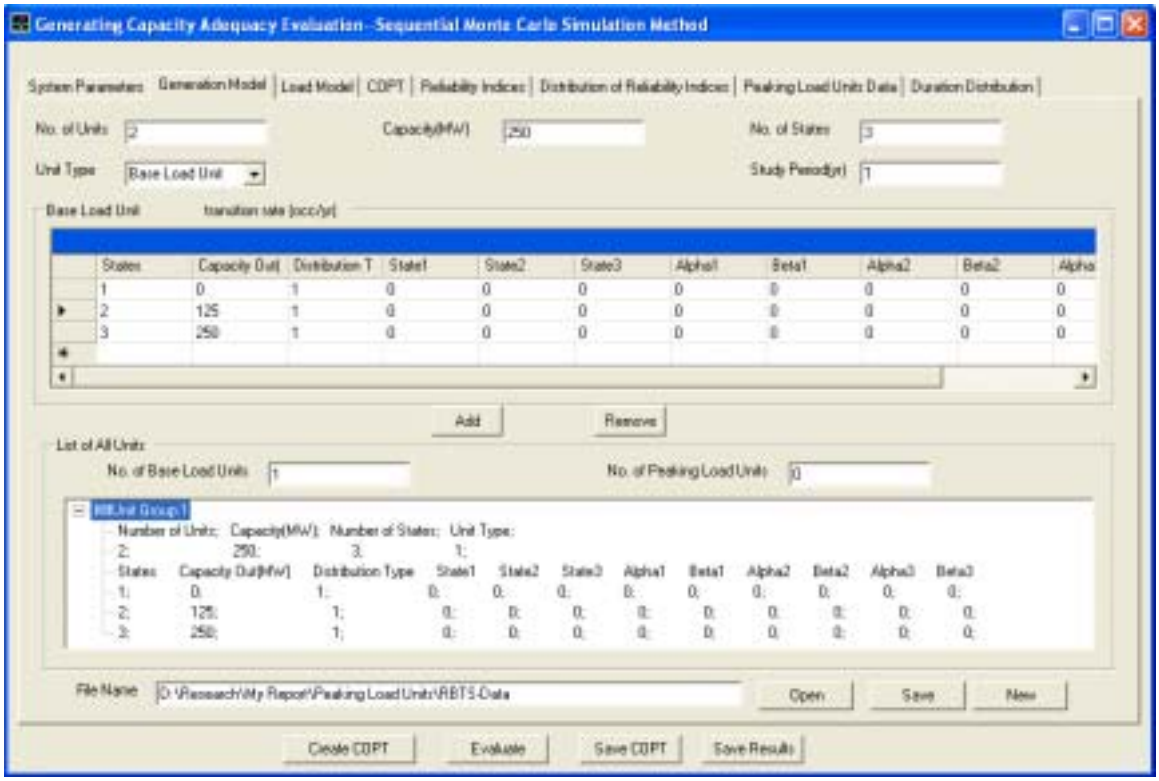

Figure 2.16: User interface to input generation data in simulation program

There are some constraints on the generation data.

The maximum number of similar generating unit groups is 50.

The maximum number of generating units is 100.

The maximum number of peaking load units is 20.

The maximum number of derated states for a generating unit is 8.

No. of Units----The number of similar generating units in a group.

Capacity----The unit capacity of this group of generating unit.

No. of States----The number of states in this group of generating units.

Unit Type----Select from the list box. It could be a base load unit or a peaking load unit.

Study Period----The study period for one simulation.

In the data grid in the middle of the interface:

Distribution Type----The generating unit state residence time distribution.

“1” represents an Exponential Distribution.

“3” represents a Weibull Distribution.

Transition Rate----The transition rate between the associated states.

The following two parameters are required if the generating unit state residence time follows a Weibull distribution.

Alpha----The scale parameter of the Weibull distribution.

Beta---- The shape parameter of the Weibull distribution.

The following are the functions of the buttons in the generation model page.

“Add”: After the information for one group of generating units is completely inputted, the “Add” button is pressed to include this group in the generating unit list.

“Remove”: Select the group of generating units to be removed. Pressing this button removes this group from the unit list.

“Open”: If there is an existing stored generation data file, press this button and locate it, the generation data will then be shown in the list.

“Save”: After inputting the data for all the generating units in the system, press this button to save the data to a specific file.

Load Data

The interface to input load data in the simulation program shown in Figure 2.17 is almost the same as the one used in the analytical program. Only one curve type is considered in the simulation program. The curve type in this case is the chronological load represented by discrete load points.

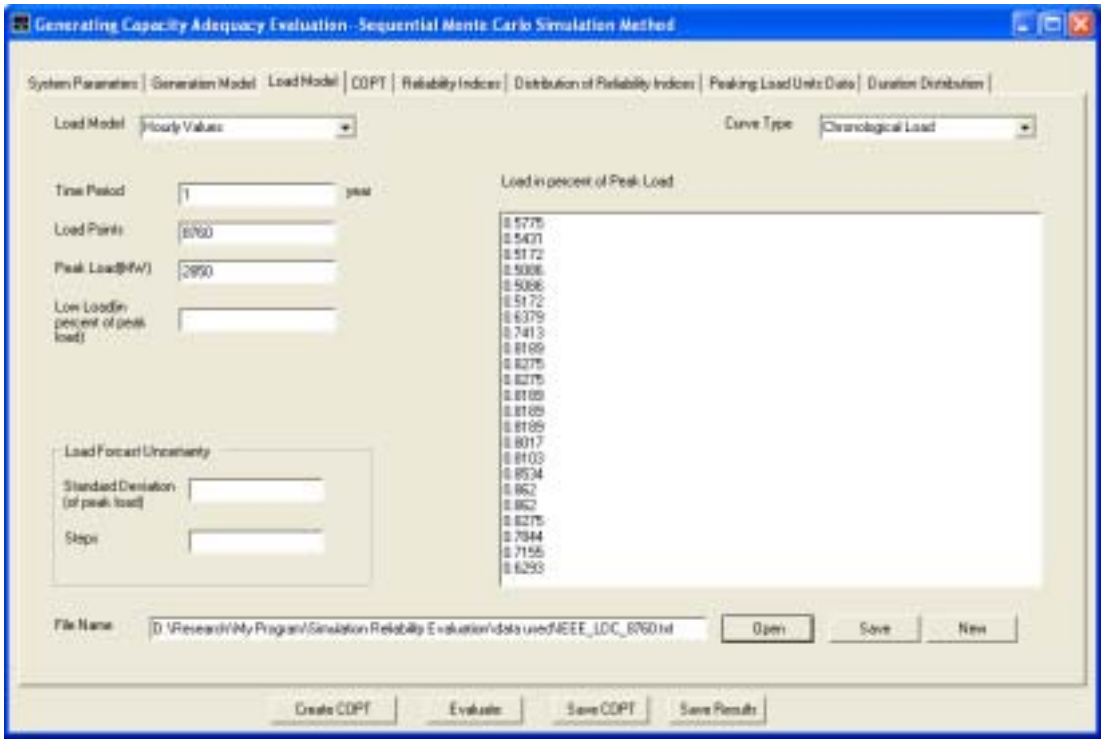

Figure 2.17: User interface to input the load data in the simulation program

2.4.3 Output Data

The simulation program produces four groups of results.

The first group is the reliability indices LOLE, LOEE, LOLF, DOI, ENSI and LCI. The output interface is shown in Figure 2.18.

The second group is the reliability index probability distributions for the LOL, LOE and LOLF shown in Figure 2.19.

The third group is the peaking load unit data, which are the peaking load unit state residence times, average state residence times, demand factors and UFOP shown in Figure 2.20.

The fourth group is the peaking load unit state residence time distributions shown

in Figure 2.21.

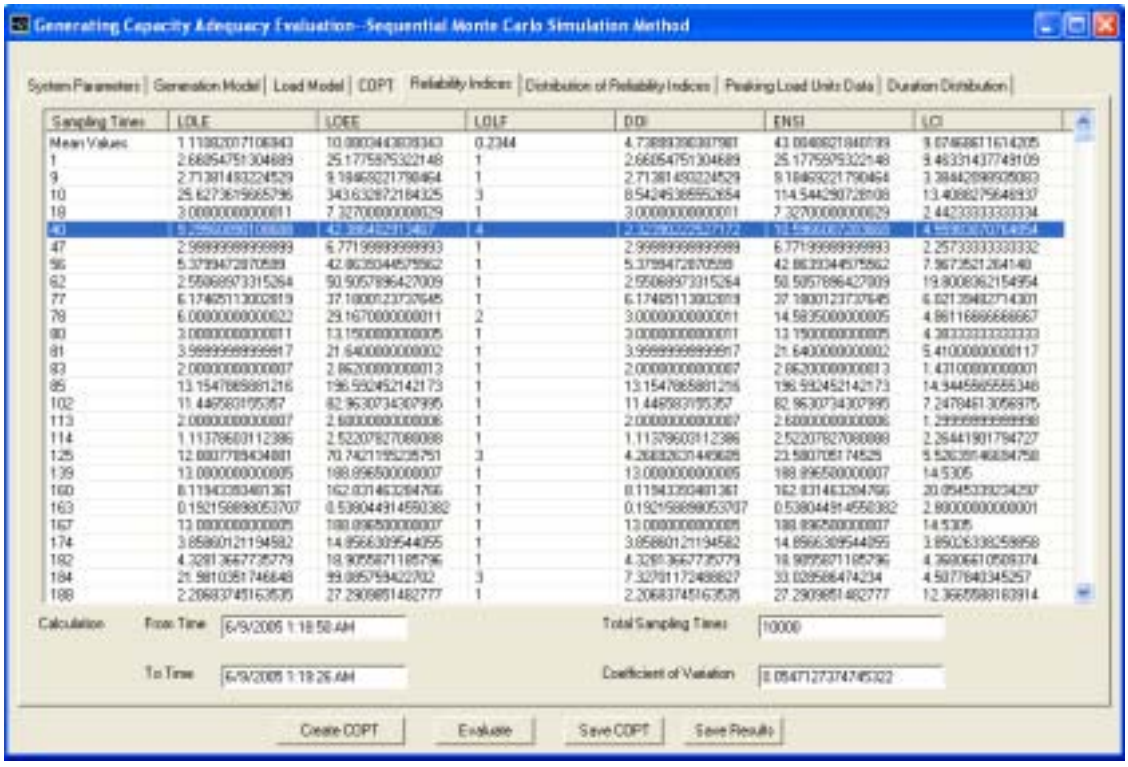

Figure 2.18: The output of the first group of results from the simulation program

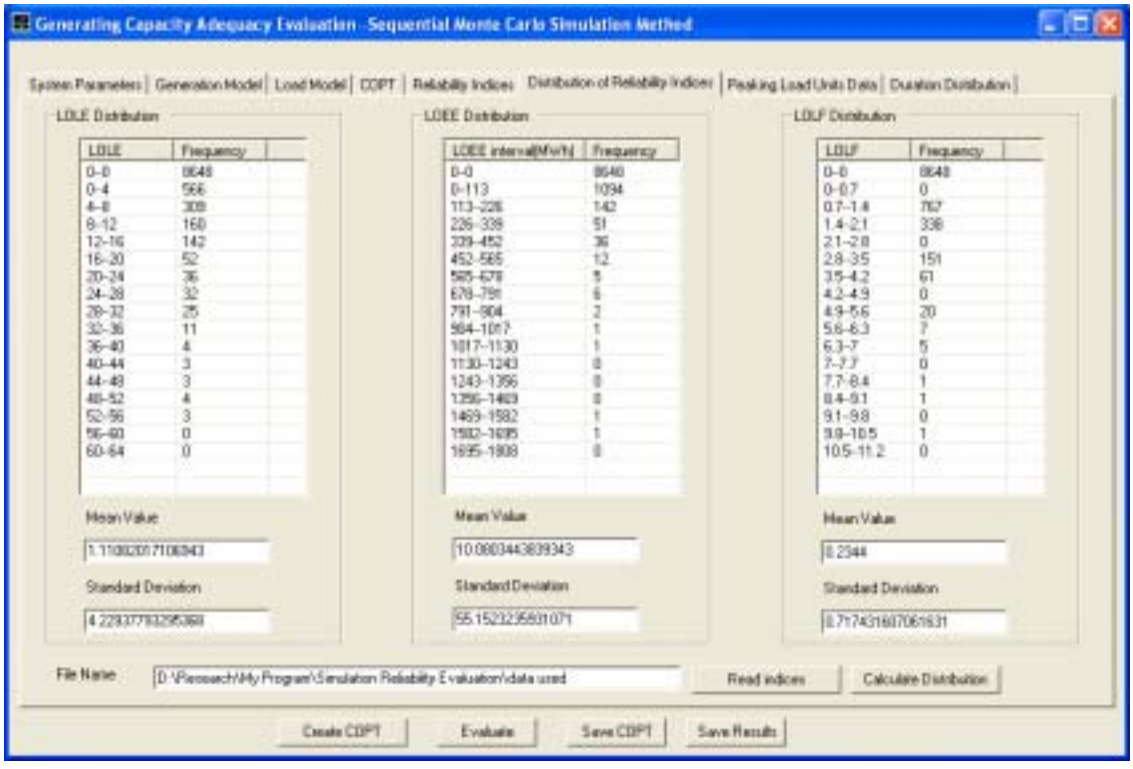

Figure 2.19: The output of the second group of results from the simulation program

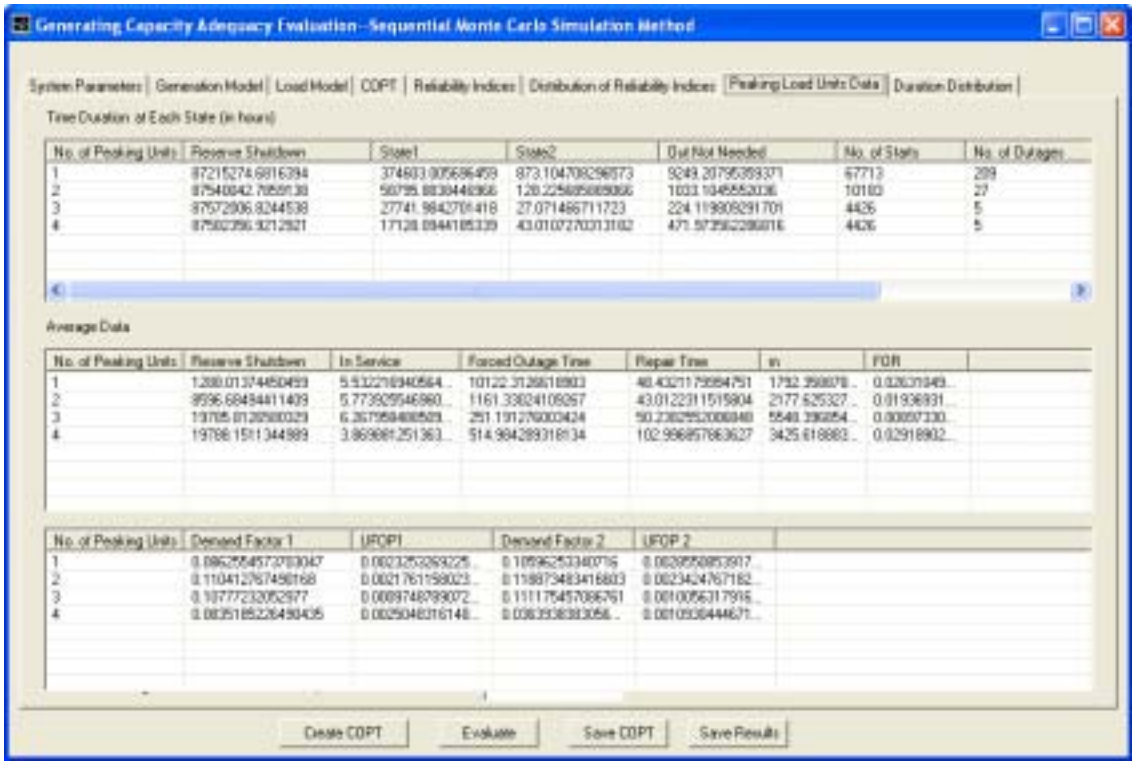

Figure 2.20: The output of the third group of results from the simulation program

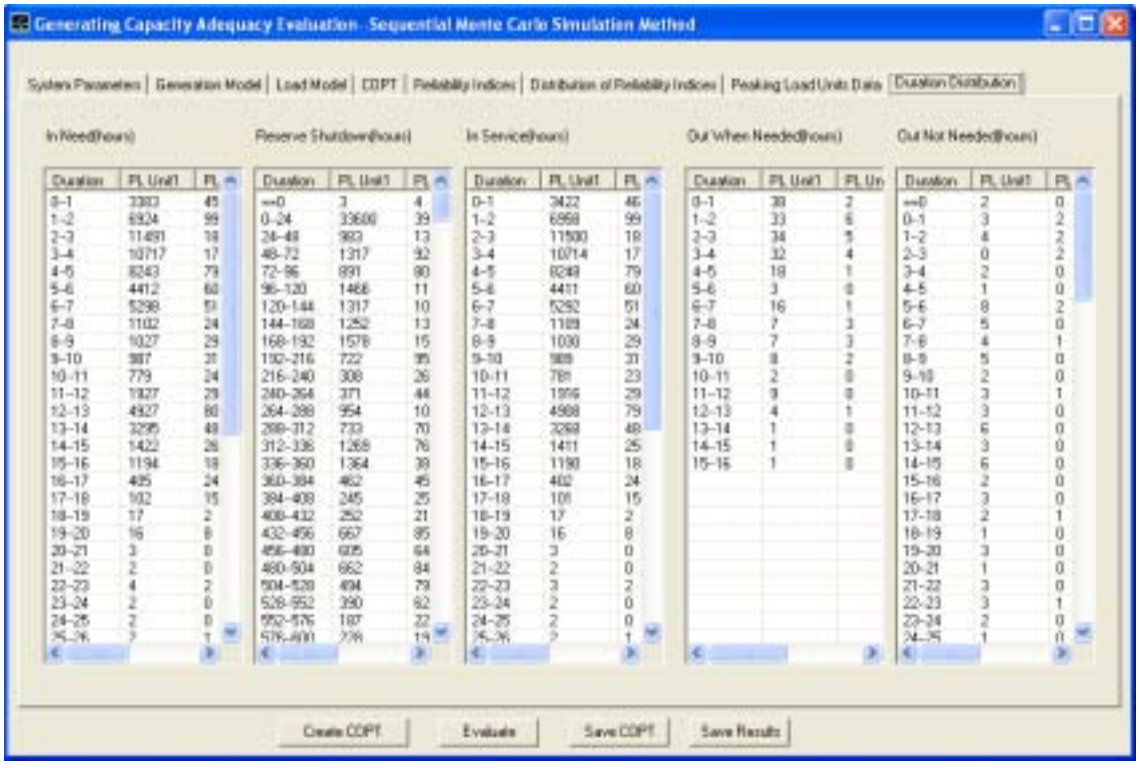

Figure 2.21: The output of the fourth group of results from the simulation program

2.5 Conclusion

Two computer programs were developed using the analytical and sequential Monte Carlo simulation approaches. The basic methods used in the programs are described in this chapter. The structures, the input and output data and the constraints of the programs are introduced.

Both programs consider generating unit derated states. The effects of load forecast uncertainty using a normal distribution can be incorporated in a reliability evaluation using either program. The two programs provide a convenient platform to perform sensitivity and related reliability studies. The two programs produce virtually identical results for the LOLE and the LOEE indices, as shown in Appendix D.

Non-exponential unit state residence time distributions can be utilized in the simulation program. The effects on the system reliability of peaking load units with derated states can be examined using the simulation program. This program can also produce accurate frequency and duration indices and reliability index probability distributions.

Only the basic block diagrams of the two programs are shown in this chapter. The detailed flow charts for the two programs are presented in Appendices B and C. The programs were specifically designed to provide the ability to examine a range of research issues. The research conducted using these programs is described in detail in the following chapters.

3. BASIC CONSIDERATIONS IN RELIABILITY EVALUATION AT HLI

3.1 Introduction

As noted earlier, there are several basic indices commonly used to evaluate generating system capacity adequacy. The indices of LOLE, LOEE and LOLF have been in use for some time, but there are still misconceptions that need to be examined and discussed.

The different reliability indices are obtained using different load models. The LOLE index in hours is obtained using hourly load values. The LOLE index in days is evaluated using daily peak load values. It is not valid to obtain the LOLE in hours by simply multiplying the days/year value by 24. This is because the hourly load profile is normally quite different from that of the daily peak load. The basic LOLE in days/year is often inverted to produce a years per day index and subsequently interpreted as a frequency parameter. The LOLE however, is simply the average number of time units (days or hours) that the load exceeds the available generating capacity. The reciprocal of the LOLE is not a frequency parameter and should not be interpreted as the LOLF.

The basic misconceptions noted above are illustrated numerically by applying the two developed programs to the IEEE-RTS and the RBTS. The simulation program was also applied to the two systems to create the reliability index probability distributions.

3.2 LOLE (hrs/yr) and LOLE (days/yr)

The LOLE (hrs/yr) and LOLE (days/yr) are compared using the results from the analytical program.

3.2.1 Different Generation Models

The normalized hourly load values and the daily peaks are taken from the IEEE-RTS and have 8736 and 364 points respectively.

RBTS Results

The LOLE in hrs/yr and days/year for various peak loads are shown in Table 3.1.

Table 3.1: The LOLE for the RBTS for varying peak loads

Num	Peak Load (MW)	LOLE (days/yr)	LOLE (hrs/yr)	Ratio of the LOLE (hrs/yr) over the LOLE (days/yr)
1	125	0.0003	0.0022	7.7483
2	135	0.0009	0.0073	7.8746
3	145	0.0030	0.0223	7.5665
4	155	0.0071	0.0578	8.1911
5	165	0.0224	0.1527	6.8230
6	175	0.0578	0.4117	7.1246
7	185	0.1469	1.0919	7.4305
8	195	0.3333	2.5154	7.5469
9	205	0.7400	5.3529	7.2339
10	215	1.7117	12.0549	7.0425
11	225	3.3549	25.1940	7.5096
12	235	6.7474	51.0714	7.5691

The ratio of the LOLE (hrs/yr) over the LOLE (days/yr) is shown in Figure 3.1.

It can be seen from Figure 3.1 that in the case of the RBTS, the ratio of the LOLE (hrs/yr) over the LOLE (days/yr) varies from 6.8 to 8.2 with changes in the peak load.

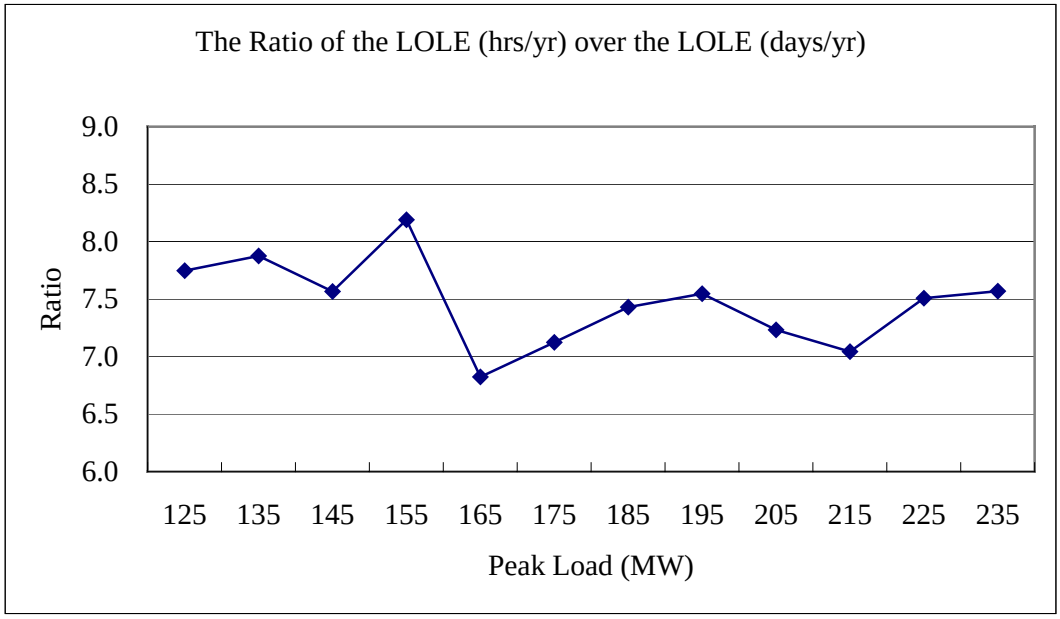

Figure 3.1: The ratio of the LOLE (hrs/yr) over the LOLE (days/yr) for the RBTS

IEEE-RTS Results

The LOLE in hrs/yr and days/year for changes in peak load are shown in Table 3.2.

Table 3.2: The LOLE for the IEEE-RTS with varying peak loads

Num	Peak Load (MW)	LOLE (days/yr)	LOLE (hrs/yr)	Ratio of the LOLE (hrs/yr) over the LOLE (days/yr)
1	2622	0.2973	1.9256	6.4765
2	2679	0.4437	2.9134	6.5666
3	2736	0.6526	4.3705	6.6973
4	2793	0.9717	6.5011	6.6901
5	2850	1.3687	9.3936	6.8630
6	2907	1.9217	13.4560	7.0020
7	2964	2.6720	18.9857	7.1053
8	3021	3.7785	26.6393	7.0502
9	3078	5.0568	36.2567	7.1699
10	3135	6.6807	49.1528	7.3574
11	3192	8.8934	66.0406	7.4258
12	3249	11.5165	87.0621	7.5598

The ratio of the LOLE (hrs/yr) over the LOLE (days/yr) is shown in Figure 3.2.

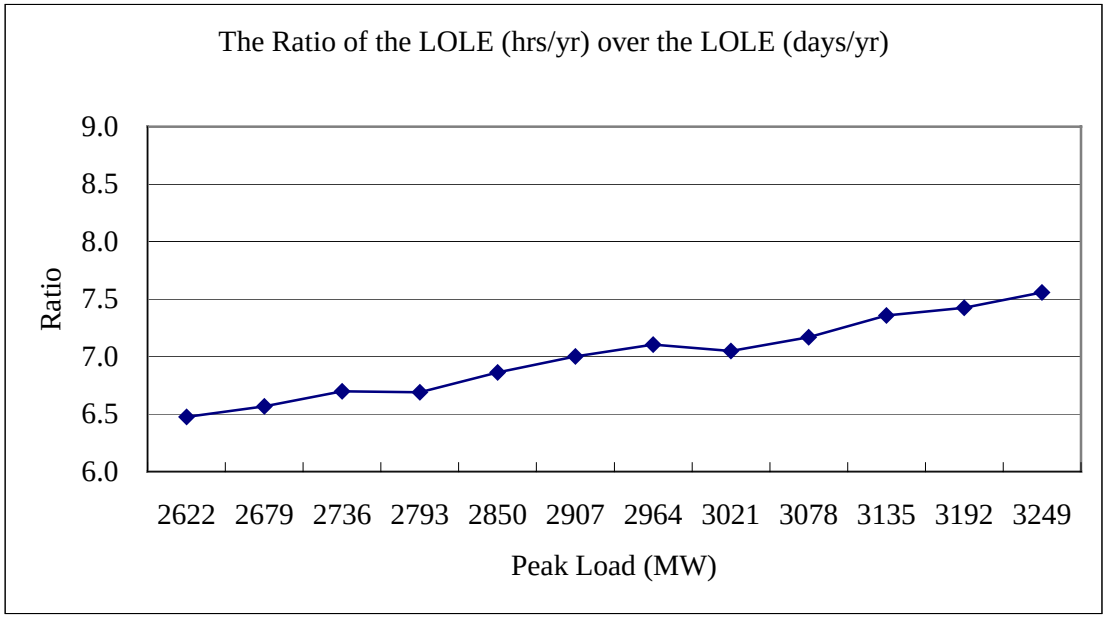

Figure 3.2: The Ratio of the LOLE (hrs/yr) over the LOLE (days/yr) for the IEEE-RTS

Figure 3.2 shows that the ratios for the IEEE-RTS are in the range of 6.4 to 7.6 for the indicated peak loads.

It can be seen from Figure 3.1 and 3.2 that while both the LOLE in hrs/yr and days/yr change with increase in the peak load, the ratio between them is not constant. Figures 3.1 and 3.2 show that the ratio of the LOLE (hrs/yr) and the LOLE (days/yr) in these two cases is far from the value of 24. The LOLE in days/year provides a more pessimistic appraisal than that given by the LOLE in hours/year.

The two test systems have the same normalized chronological hourly load model and therefore the same daily and annual load duration curves. The ratio difference in this case is therefore due to the different generation compositions.

3.2.2 Different Load Models

The normalized load profile for the RBTS and the IEEE-RTS are identical. A new load profile was created to examine the load profile effect on the LOLE ratio.

The load factor of the hourly value in percent of the daily peak was increased and decreased by 10% as shown in Tables 3.3 and 3.4. The weekly peak in percent of the

annual peak and the daily peak in percent of the weekly peak remain the same.

The daily peak in percent of the annual peak is obtained by combining the weekly peak in percent of the annual peak and the daily peak in percent of the weekly peak and remains the same as the original value. The LOLE (days/yr) for both the RBTS and the IEEE-RTS in this case have the same values shown in Section 3.2.1.

Table 3.3: Hourly peak in percent of daily peak (load factor increased by 10%)

	winter weeks		**summer weeks**		**spring/fall weeks**	
	1 -8 & 44 - 52		**18 -30**		**9-17 & 31 - 43**	
Hour	**Wkdy**	**Wknd**	**Wkdy**	**Wknd**	**Wkdy**	**Wknd**
12-1 am	86.4118	90.9095	85.0732	89.0000	84.7647	90.0754
1--2	84.7647	88.4303	83.4146	87.3077	84.3529	89.2814
2--3	83.5294	86.7775	82.5854	85.6154	83.5294	87.6935
3--4	83.1176	85.9511	81.7561	85.1923	82.7059	86.5025
4--5	83.1176	85.1247	81.7561	84.7692	83.1176	86.1055
5--6	83.5294	85.5379	82.5854	83.9231	85.5882	86.1055
6--7	89.2941	85.9511	85.0732	83.9231	88.4706	87.2965
7--8	94.2353	87.6039	90.0488	85.6154	93.8235	89.6784
8--9	97.9412	91.7359	94.6098	91.9615	97.9412	93.2513
9--10	98.3529	95.0416	97.9268	94.0769	99.5882	95.6332
10--11	98.3529	95.8680	99.5854	96.1923	100.0000	96.8241
11-noon	97.9412	96.2812	100.0000	97.0385	99.5882	97.6181
Noon-1pm	97.9412	95.8680	99.5854	97.0385	97.1176	96.4271
1--2	97.9412	95.0416	100.0000	96.6154	96.7059	96.0302
2--3	97.1176	94.6284	100.0000	96.1923	95.8824	96.0302
3--4	97.5294	94.6284	98.7561	96.1923	95.0588	94.4422
4--5	99.5882	96.2812	98.3415	96.6154	95.8824	94.0452
5--6	100.0000	100.0000	98.3415	97.4615	96.7059	95.2362
6--7	100.0000	99.5868	97.0976	97.8846	98.3529	96.8241
7--8	98.3529	98.7604	96.6829	97.8846	99.1765	100.0000
8--9	96.2941	97.5208	96.6829	100.0000	98.3529	98.8090
9--10	93.0000	96.6944	97.0976	97.0385	95.8824	98.0151
10--11	88.8824	94.6284	94.6098	94.9231	91.7647	96.0302
11--12	84.7647	92.1491	88.3902	91.5385	87.6471	94.0452
Average	93.0000	92.9583	92.9167	92.6667	93.0000	93.4167

Table 3.4: Hourly Peak in percent of daily peak (load factor decreased 10%)

	winter weeks		summer weeks		spring/fall weeks	
	1 -8 & 44 - 52		18 -30		9-17 & 31 - 43	
Hour	**Wkdy**	**Wknd**	**Wkdy**	**Wknd**	**Wkdy**	**Wknd**
12-1 am	47.5882	65.0905	42.9268	59.0000	41.2353	59.9246
1--2	41.2353	55.5697	36.5854	52.6923	39.6471	56.7186
2--3	36.4706	49.2225	33.4146	46.3846	36.4706	50.3065
3--4	34.8824	46.0489	30.2439	44.8077	33.2941	45.4975
4--5	34.8824	42.8753	30.2439	43.2308	34.8824	43.8945
5--6	36.4706	44.4621	33.4146	40.0769	44.4118	43.8945
6--7	58.7059	46.0489	42.9268	40.0769	55.5294	48.7035
7--8	77.7647	52.3961	61.9512	46.3846	76.1765	58.3216
8--9	92.0588	68.2641	79.3902	70.0385	92.0588	72.7487
9--10	93.6471	80.9584	92.0732	77.9231	98.4118	82.3668
10--11	93.6471	84.1320	98.4146	85.8077	100.0000	87.1759
11-noon	92.0588	85.7188	100.0000	88.9615	98.4118	90.3819
Noon-1pm	92.0588	84.1320	98.4146	88.9615	88.8824	85.5729
1--2	92.0588	80.9584	100.0000	87.3846	87.2941	83.9698
2--3	88.8824	79.3716	100.0000	85.8077	84.1176	83.9698
3--4	90.4706	79.3716	95.2439	85.8077	80.9412	77.5578
4--5	98.4118	85.7188	93.6585	87.3846	84.1176	75.9548
5--6	100.0000	100.0000	93.6585	90.5385	87.2941	80.7638
6--7	100.0000	98.4132	88.9024	92.1154	93.6471	87.1759
7--8	93.6471	95.2396	87.3171	92.1154	96.8235	100.0000
8--9	85.7059	90.4792	87.3171	100.0000	93.6471	95.1910
9--10	73.0000	87.3056	88.9024	88.9615	84.1176	91.9849
10--11	57.1176	79.3716	79.3902	81.0769	68.2353	83.9698
11--12	41.2353	69.8509	55.6098	68.4615	52.3529	75.9548
Average	73.0000	72.9583	72.9167	72.6667	73.0000	73.4167

The hourly load in percent of the annual peak is obtained by combing the weekly peak in percent of the annual peak and the daily peak in percent of the weekly peak and the hourly load value in percent of the daily peak. The load duration curves are produced by sorting the hourly load values in descending order as shown in Figure 3.3.

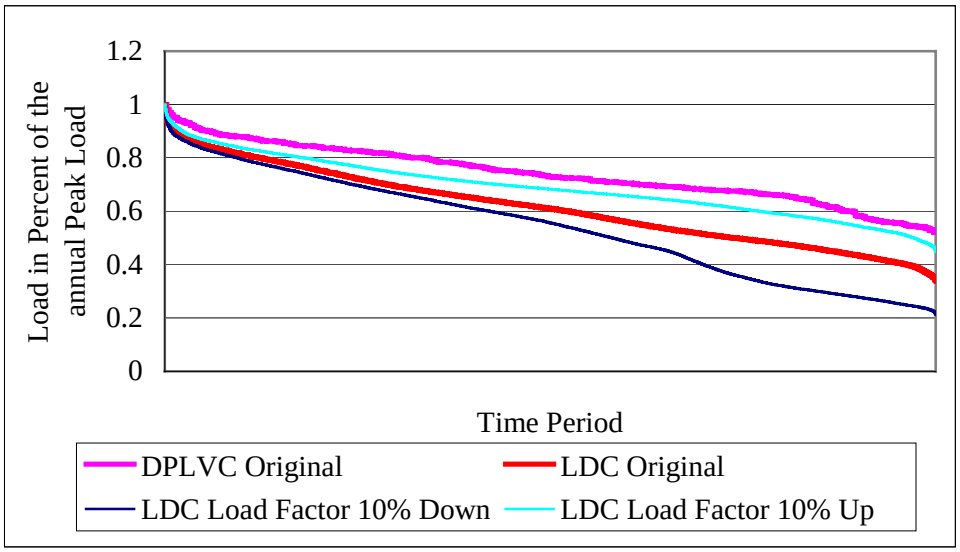

Figure 3.3: The DPLVC and LDC with different load factors

RBTS Results

The LOLE for the RBTS with the modified load factors are shown in Table 3.5 for a range of peak loads.

Table 3.5: The LOLE for the RBTS with different load models

Num	Peak Load (MW)	LOLE (days/yr)	LOLE (hrs/yr) Load Factor 10% Up	LOLE (hrs/yr) Load Factor 10% Down
1	125	0.0003	0.0034	0.0017
2	135	0.0009	0.0109	0.0053
3	145	0.0030	0.0346	0.0170
4	155	0.0071	0.0899	0.0431
5	165	0.0224	0.2438	0.1195
6	175	0.0578	0.6904	0.3157
7	185	0.1469	1.7104	0.8307
8	195	0.3333	3.9199	1.9106
9	205	0.7400	8.3329	4.1354
10	215	1.7117	18.6499	8.8524
11	225	3.3549	38.7413	18.3056
12	235	6.7474	79.1073	38.6240

The ratios of the LOLE (hrs/yr) over the LOLE (days/yr) for the modified load factors are shown in Figure 3.4.

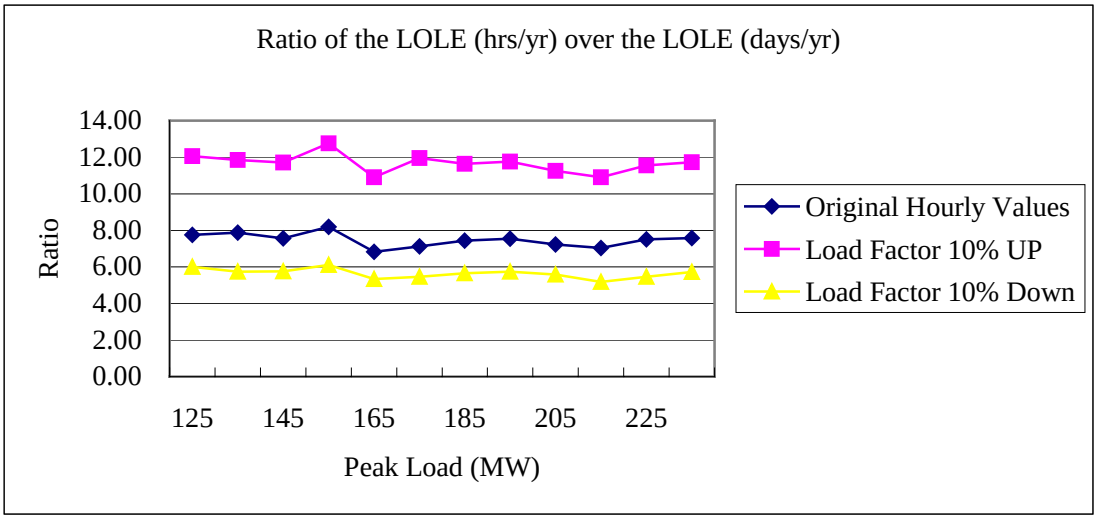

Figure 3.4: The ratio of the LOLE (hrs/yr) over the LOLE (days/yr) for the RBTS with different load models

It can be seen from Figure 3.4 that the ratio increases with increase in the load factor. As the load factor increases, the hourly load values move toward the daily peaks and the ratio increases.

IEEE-RTS Results

The LOLE obtained by applying the modified load factors to the IEEE-RTS are shown in Table 3.6.

Table 3.6: The LOLE for the IEEE-RTS with different load models

Num	Peak Load (MW)	LOLE (days/yr)	LOLE (hrs/yr) Load Factor 10% Up	LOLE (hrs/yr) Load Factor 10% Down
1	2622	0.297324654	3.06797114	1.42172778
2	2679	0.443676422	4.67032696	2.16530611
3	2736	0.65257997	6.981414544	3.236775531
4	2793	0.971745025	10.30983239	4.835124517
5	2850	1.368730589	14.94946711	7.001012241
6	2907	1.921732057	21.25360908	10.00146116
7	2964	2.672041145	29.64434106	14.1191587
8	3021	3.778490601	41.36045103	19.97518312
9	3078	5.056819548	57.02035589	27.34462732
10	3135	6.680708428	76.71539058	36.68923492
11	3192	8.893406603	101.8908647	49.28394253
12	3249	11.51650411	133.8677747	65.28948517

The ratios of the LOLE (hrs/yr) over the LOLE (days/yr) for the modified load factors are shown in Figure 3.5.

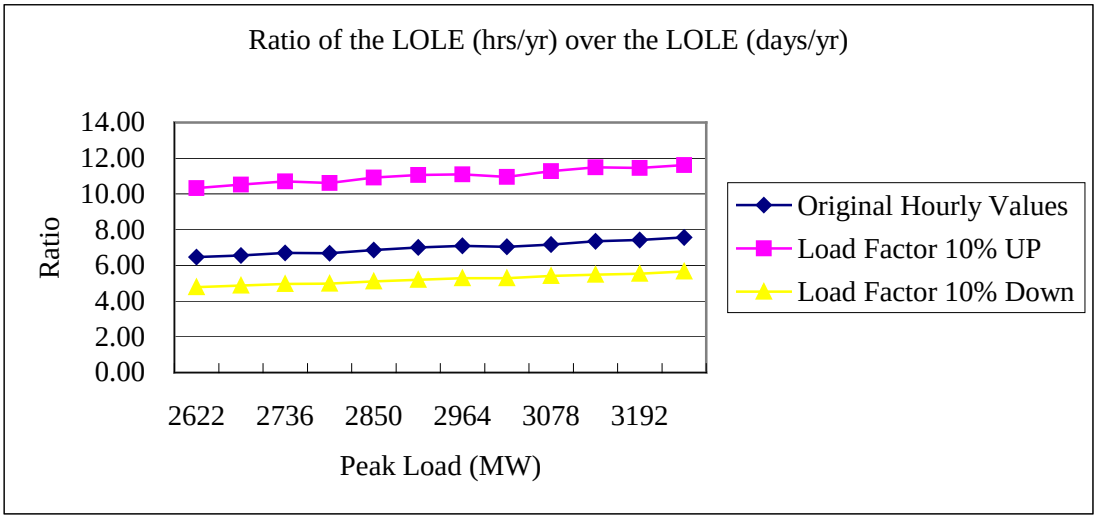

Figure 3.5: The ratio of the LOLE (hrs/yr) over the LOLE (days/yr) for the IEEE-RTS with different load models

The ratio curve moves upward as the load factor increases.

The general trend for both the RBTS and the IEEE-RTS are similar. The numerical values are, however, quite different. The LOLE ratio is affected by both the generation system compositions and the shape of the load profiles.

3.3 LOLE and LOLF

The reciprocal of the LOLE in years per day is commonly misinterpreted as a frequency index. As an example, the commonly used LOLE index of 0.1 days/year is often expressed as one day in ten years and extended to imply “once in ten years”. This is not a valid extension. A comparison of the LOLE (days/yr) with the LOLF (occ/yr) was made to illustrate the difference between the two indices. The analytical and simulation programs were used in this analysis. The daily peak load model was utilized for both the RBTS and the IEEE-RTS. The LOLE (days/yr) was obtained from the analytical program. The LOLF (occ/yr) was produced using the simulation program. The hourly load values are also used to show the difference between the LOLE (hrs/yr) and

the LOLF (occ/yr). The sampling years are 100,000 for the RBTS and 20,000 for the IEEE-RTS. The coefficient of variation for both systems is less than 1%.

3.3.1 Different Generation Models

RBTS Results

The LOLF (occ/yr) for the RBTS using the daily peaks and hourly values are shown in Table 3.7.

Table 3.7: The LOLF (occ/yr) for the RBTS using Daily Peaks and Hourly Values

Peak Load (MW)	LOLF (occ/yr) Using Daily Peaks	LOLF (occ/yr) Using Hourly Values
145	0.00594	0.00516
155	0.01288	0.01277
165	0.03907	0.03628
175	0.08805	0.09258
185	0.2116	0.22903
195	0.43562	0.51192
205	0.9111	1.10601
215	1.84762	2.56819
225	3.29473	5.02937
235	6.06173	9.5183

The ratio of the reciprocal of the LOLE over the reciprocal of the LOLF for the RBTS is shown in Figure 3.6.

Figure 3.6 shows that the ratio decreases with increase in the peak load. The range of the ratio is from 0.88 to 2.02 and indicates that the LOLF increases more slowly than the LOLE, as the peak load increases. It is important to note that the average duration per interruption increases with increase in the peak load.

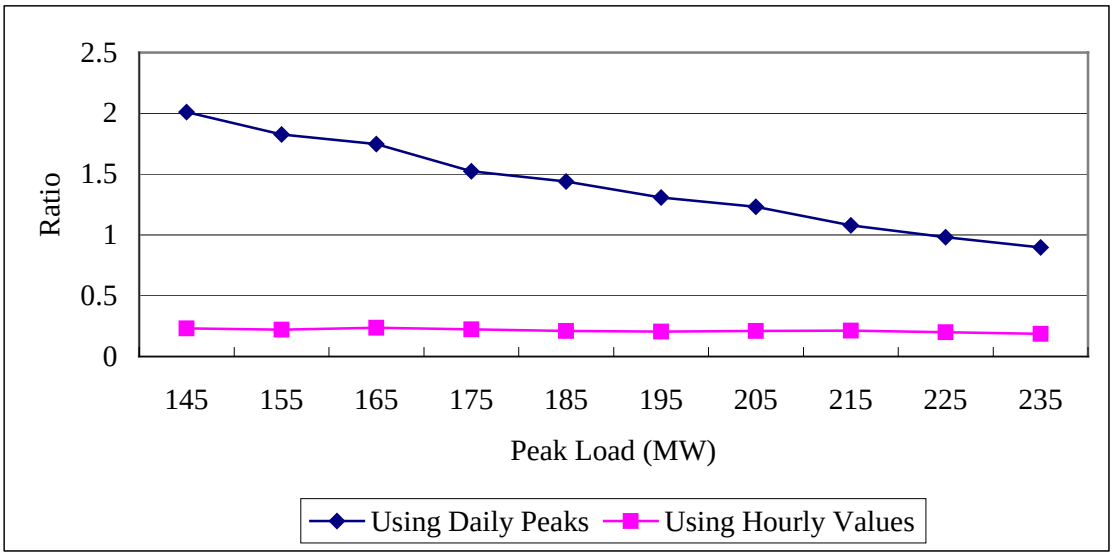

Figure 3.6: The ratio of the reciprocal of the LOLE over the reciprocal of the LOLF for the RBTS

IEEE-RTS Results

The LOLF (occ/yr) for the IEEE-RTS using the daily peaks and the hourly values are shown in Table 3.8. The ratio of the reciprocal of the LOLE over the reciprocal of the LOLF for the IEEE-RTS is shown in Figure 3.7.

Table 3.8: The LOLF (occ/yr) for the IEEE-RTS using daily peaks and hourly values

Peak Load (MW)	**LOLF (occ/yr) Using Daily Peaks**	**LOLF (occ/yr) Using Hourly Values**
2736	0.8284	0.983
2793	1.15745	1.43605
2850	1.57465	2.02855
2907	2.1381	2.8372
2964	2.8538	3.9514
3021	3.82325	5.45085
3078	4.8589	7.2241
3135	6.0984	9.6304
3192	7.82535	12.71085
3249	9.615	16.26285

The IEEE-RTS ratio in Figure 3.7 changes the same way as the RBTS ratio in Figure 3.6, but at a different rate. The ratio ranges from 0.84 to 1.3.

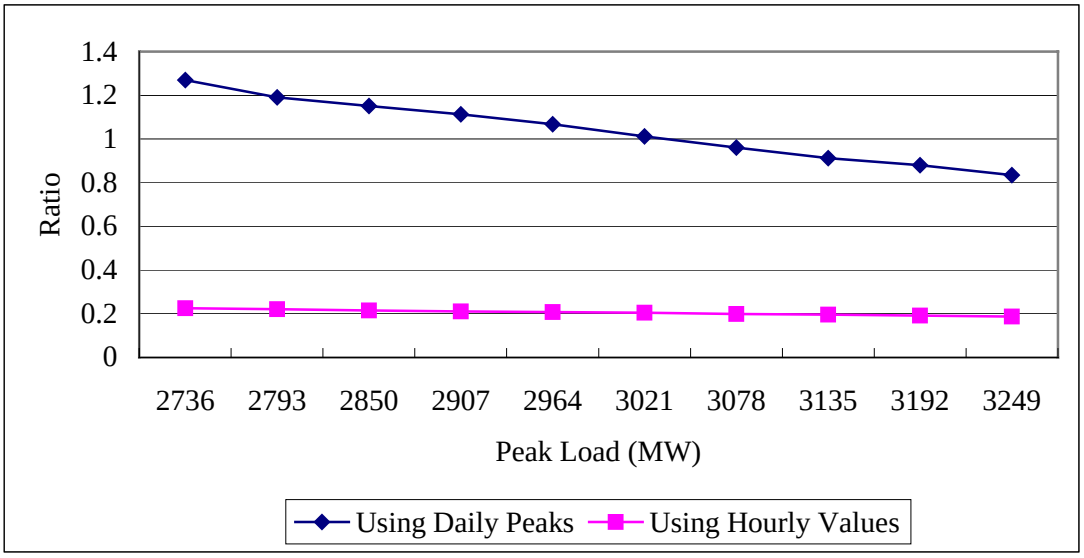

Figure 3.7: The ratio of the reciprocal of the LOLE over the reciprocal of the LOLF for the IEEE-RTS

It can be seen from Figures 3.6 and 3.7 that the ratio is not 1 when the daily peaks are used. Both figures show that the ratio becomes 1 at a high load level and then decreases when the peak load increases further. The LOLE in these two cases is at a level that would normally be considered to be unacceptable. When the hourly load is used, the ratio between the reciprocal of the LOLE over the reciprocal of the LOLF is considerable less than 1.

The LOLE index is simply the expected time in a given period that the load exceeds the available capacity. It does not provide any basic system frequency information.

3.3.2 Different Load Models

Different load models were applied to the RBTS and the IEEE-RTS to examine the difference between the reciprocals of the LOLE and LOLF.

The weekly peak load as a percentage of the annual peak was changed to make the load factor increase and decrease by 10%. The daily peaks in percent of the weekly peak and the hourly values in percent of the daily peak remain the same.

Table 3.9 shows the weekly peaks in percent of the annual peak after the load factor increases and decreases by 10%.

Table 3.9: Weekly Peak in Percent of Annual Peak

Week	Peak Load			Week	Peak Load		
	Original	Load Factor 10% Up	Load Factor 10% Down		Original	Load Factor 10% Up	Load Factor 10% Down
1	86.2	93.8081	78.5919	**27**	75.5	89.0072	61.9928
2	90	95.5131	84.4869	**28**	81.6	91.7442	71.4558
3	87.8	94.5260	81.0740	**29**	80.1	91.0712	69.1288
4	83.4	92.5518	74.2482	**30**	88	94.6158	81.3842
5	88	94.6158	81.3842	**31**	72.2	87.5265	56.8735
6	84.1	92.8659	75.3341	**32**	77.6	89.9494	65.2506
7	83.2	92.4621	73.9379	**33**	80	91.0263	68.9737
8	80.6	91.2955	69.9045	**34**	72.9	87.8406	57.9594
9	74	88.3342	59.6658	**35**	72.6	87.7060	57.4940
10	73.7	88.1996	59.2004	**36**	70.5	86.7638	54.2362
11	71.5	87.2125	55.7875	**37**	78	90.1289	65.8711
12	72.7	87.7509	57.6491	**38**	69.5	86.3151	52.6849
13	70.4	86.7189	54.0811	**39**	72.4	87.6163	57.1837
14	75	88.7829	61.2171	**40**	72.4	87.6163	57.1837
15	72.1	87.4817	56.7183	**41**	74.3	88.4688	60.1312
16	80	91.0263	68.9737	**42**	74.4	88.5137	60.2863
17	75.4	88.9623	61.8377	**43**	80	91.0263	68.9737
18	83.7	92.6864	74.7136	**44**	88.1	94.6606	81.5394
19	87	94.1671	79.8329	**45**	88.5	94.8401	82.1599
20	88	94.6158	81.3842	**46**	90.9	95.9170	85.8830
21	85.6	93.5389	77.6611	**47**	94	97.3079	90.6921
22	81.1	91.5198	70.6802	**48**	89	95.0645	82.9355
23	90	95.5131	84.4869	**49**	94.2	97.3976	91.0024
24	88.7	94.9299	82.4701	**50**	97	98.6539	95.3461
25	89.6	95.3337	83.8663	**51**	100	100	100
26	86.1	93.7633	78.4367	**52**	95.2	97.8463	92.5537
load factor	81.8615%	91.8615%	71.8615%				

The weekly peaks in percent of the annual peak load are also shown in Figure 3.8.

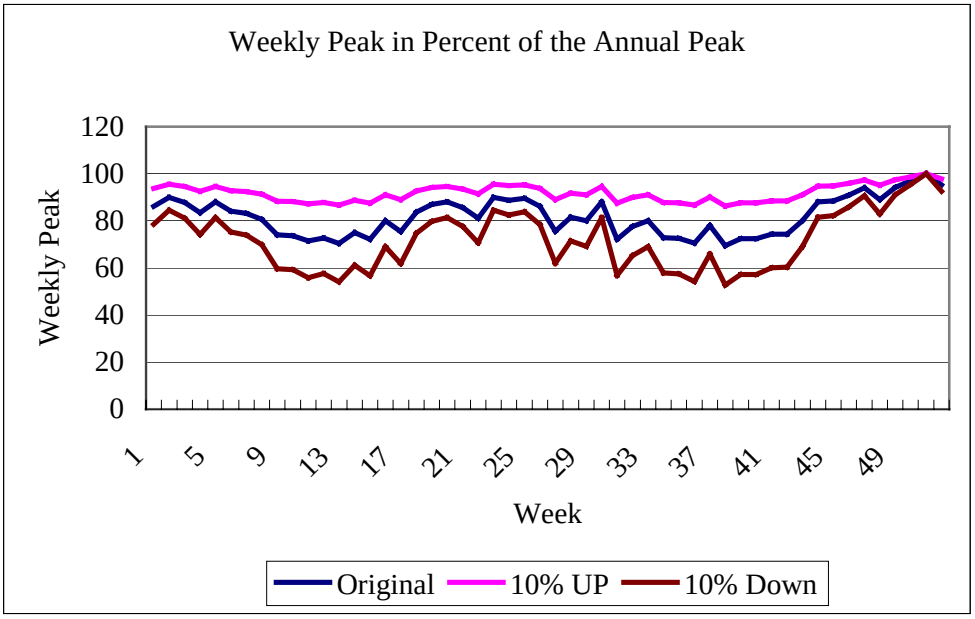

Figure 3.8: The weekly peak in percent of the annual peak

The daily peaks and hourly values in percent of the annual peak will change with the corresponding changes in the weekly peaks. The daily peak load variation curve and load duration curve produced by sorting the daily peaks and hourly values in descending order are shown in Figure 3.9.

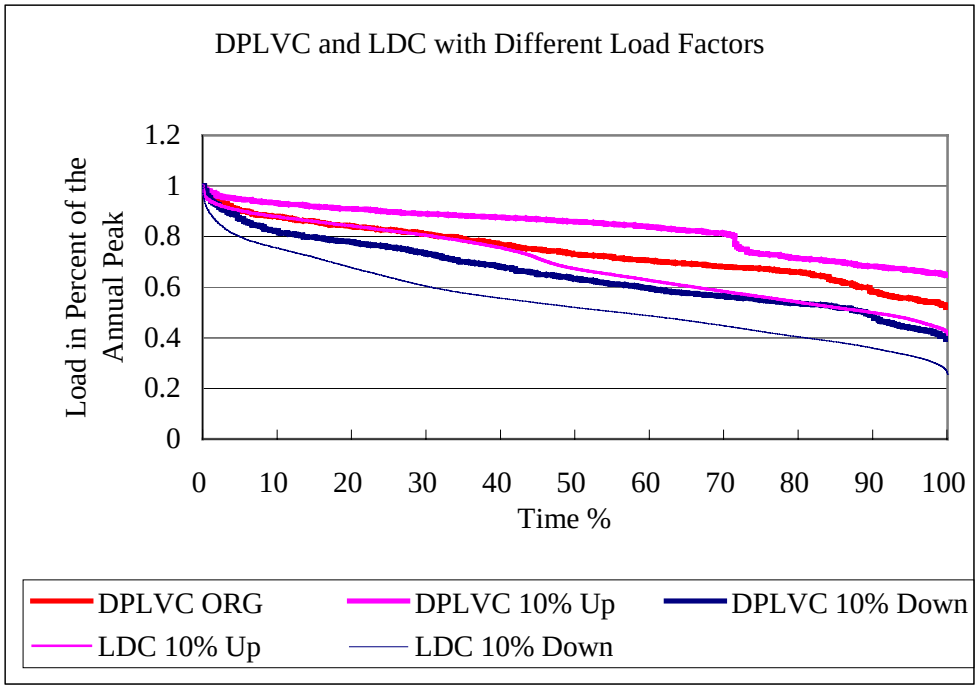

Figure 3.9: The DPLVC and LDC with different load factors

RBTS Results

The results for the RBTS using the daily peak load are shown in Table 3.10 for a range of peak loads.

Table 3.10: The results for the RBTS using daily peaks with the modified load factors

Peak Load (MW)	Load Factor 10% Down		Load Factor 10% Up	
	LOLE (days/yr)	LOLF (occ/yr)	LOLE (days/yr)	LOLF (occ/yr)
145	0.0014	0.0026	0.0072	0.0125
155	0.0042	0.0078	0.0214	0.0373
165	0.0117	0.0186	0.057	0.0976
175	0.0319	0.0478	0.1925	0.285
185	0.0762	0.1061	0.4565	0.6243
195	0.1574	0.2145	0.8945	1.1661
205	0.4402	0.5189	1.8453	2.2579
215	0.8937	0.9202	4.8967	5.2781
225	1.7923	1.7418	10.988	9.5558
235	3.0523	2.648	19.085	15.468

The ratio of the reciprocal of the LOLE (days/yr) over the reciprocal of the LOLF (occ/yr) for the RBTS is shown in Figure 3.10.

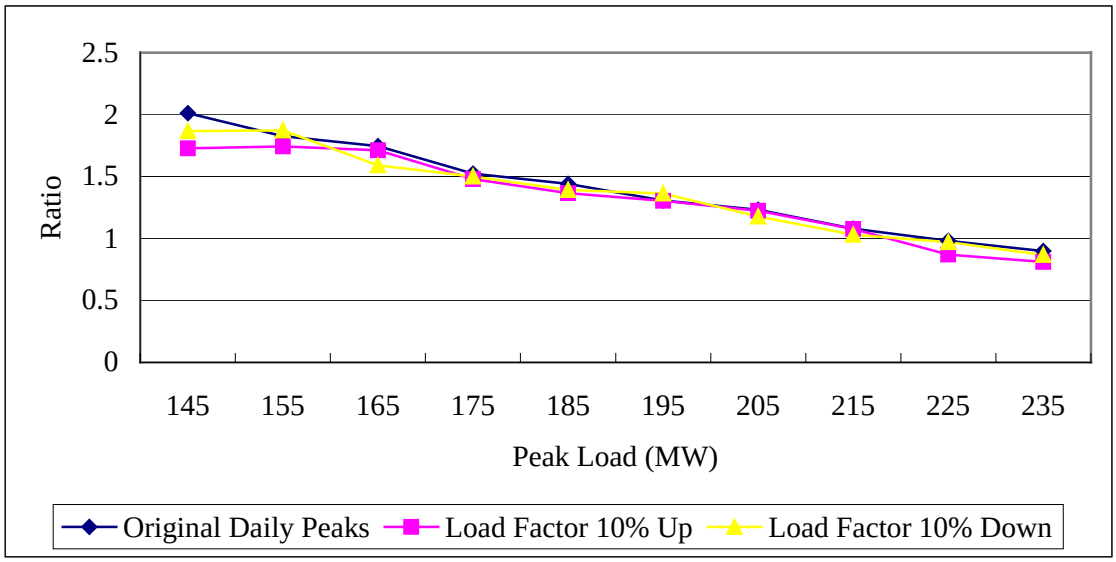

Figure 3.10: The ratio of the reciprocal of the LOLE (days/yr) over the reciprocal of the LOLF (occ/yr) for the RBTS using daily peaks with the modified load factors

The LOLE (hrs/yr) and the LOLF (occ/yr) using the hourly values with the

modified load factors are shown in Table 3.11.

Table 3.11: The results for the RBTS using hourly values with the modified load factors

Peak Load (MW)	Load Factor 10% Down		Load Factor 10% Up	
	LOLE (hrs/yr)	LOLF (occ/yr)	LOLE (hrs/yr)	LOLF (occ/yr)
145	0.0104	0.0025	0.0592	0.0133
155	0.0304	0.0072	0.1577	0.0370
165	0.0814	0.0187	0.4123	0.0931
175	0.2273	0.0522	1.2437	0.3095
185	0.5584	0.1171	3.3808	0.7306
195	1.2096	0.2380	6.9828	1.4593
205	2.8040	0.6099	14.0924	2.9037
215	6.5223	1.3474	32.2886	7.3709
225	13.2746	2.5753	77.4656	16.3635
235	25.4967	4.5862	152.5914	28.5428

The ratio between the reciprocal of the LOLE (hrs/yr) over the reciprocal of the LOLF (occ/yr) for the RBTS is shown in Figure 3.11.

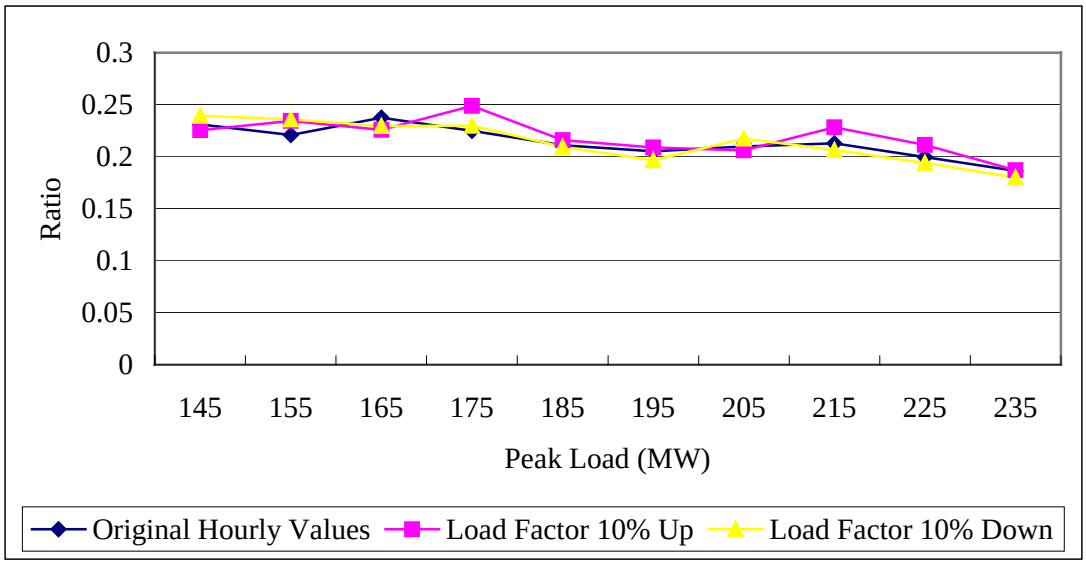

Figure 3.11: The ratio of the reciprocal of the LOLE (hrs/yr) over the reciprocal of the LOLF (occ/yr) for the RBTS using hourly values with the modified load factors

IEEE-RTS Results

The LOLE (days/yr) and LOLF (occ/yr) for the IEEE-RTS using daily peaks with modified load factors are shown in Table 3.12 for various peak loads.

Table 3.12: The results for the IEEE-RTS using daily peaks with the modified load factors

Peak Load (MW)	Load Factor 10% Down		Load Factor 10% Up	
	LOLE (days/yr)	LOLF (occ/yr)	LOLE (days/yr)	LOLF (occ/yr)
2736	0.348374379	0.4275	2.026578533	2.51695
2793	0.500023398	0.58585	2.975017474	3.4512
2850	0.707072645	0.79845	4.246364071	4.65145
2907	0.996055199	1.1013	5.846669243	6.0984
2964	1.3433061	1.4418	7.928614963	7.9834
3021	1.901940949	1.9246	10.82767086	10.52785
3078	2.574156003	2.42425	14.55367368	13.54515
3135	3.426459269	3.0772	19.17867622	16.99665
3192	4.394547424	3.8742	25.36553726	21.35135
3249	5.812722547	4.77265	33.16808719	25.5756

The ratio of the reciprocal of the LOLE (days/yr) over the reciprocal of the LOLF (occ/yr) for the IEEE-RTS is shown in Figure 3.12.

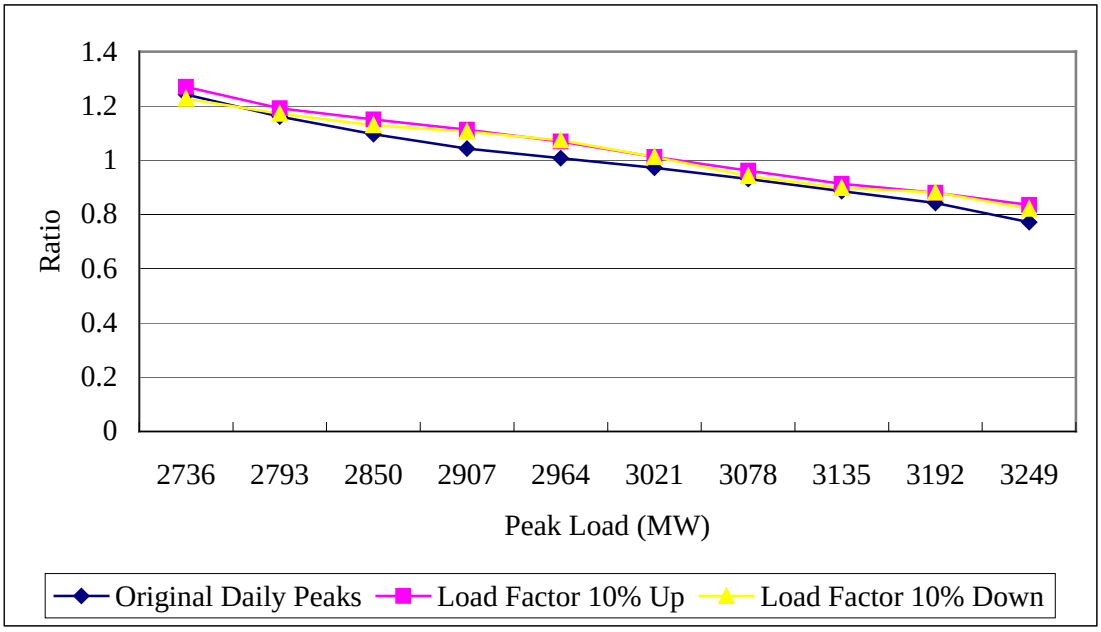

Figure 3.12: The ratio of the reciprocal of the LOLE (days/yr) over the reciprocal of the LOLF (occ/yr) for the IEEE-RTS using daily peaks with the modified load factors

The LOLE (hrs/yr) and the LOLF (occ/yr) using hourly values with the modified load factors are shown in Table 3.13.

Table 3.13: The results for the IEEE-RTS using hourly values with the modified load factors

Peak Load (MW)	Load Factor 10% Down		Load Factor 10% Up	
	LOLE (hrs/yr)	LOLF (occ/yr)	LOLE (hrs/yr)	LOLF (occ/yr)
2736	2.2814	0.5175	13.4948	3.1372
2793	3.3740	0.7474	19.9877	4.5613
2850	4.8724	1.0431	29.1156	6.4528
2907	6.9205	1.4488	41.2255	8.8444
2964	9.6342	1.9530	57.2408	11.9614
3021	13.4548	2.6908	78.7135	16.1478
3078	18.2815	3.6093	106.0666	21.4939
3135	24.7749	4.8538	141.2277	28.3359
3192	32.9465	6.2458	187.6085	37.3407
3249	43.8584	8.1341	248.1732	48.2233

The ratio between the reciprocal of the LOLE (hrs/yr) over the reciprocal of the LOLF (occ/yr) for the IEEE-RTS is shown in Figure 3.13.

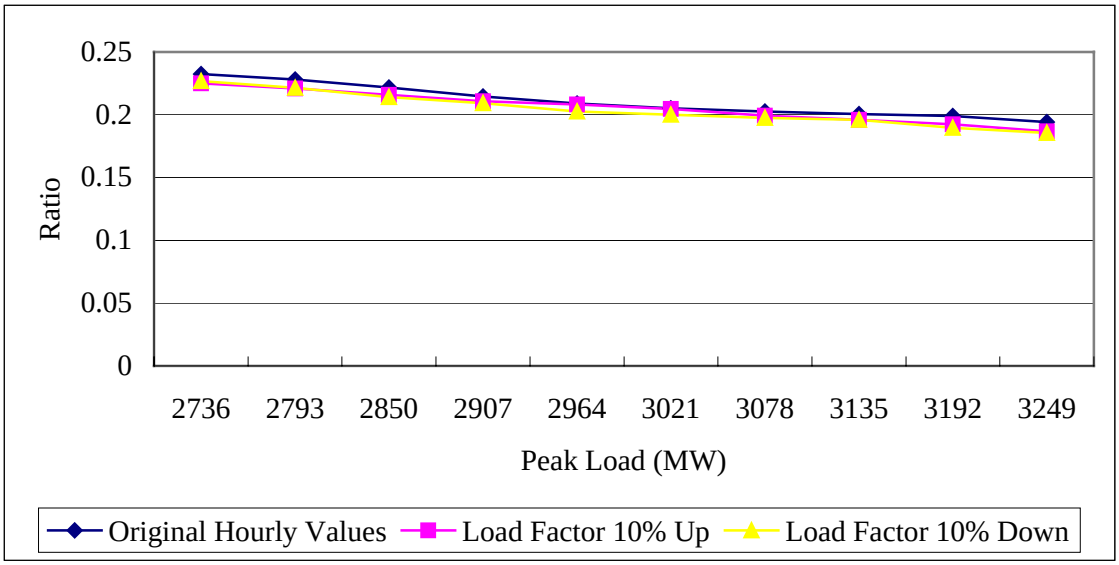

Figure 3.13: The ratio of the reciprocal of the LOLE (hrs/yr) over the reciprocal of the LOLF (occ/yr) for the IEEE-RTS using daily peaks with the modified load factors

It can be seen from Figures 3.10 to 3.13 that the ratio of the reciprocal of the LOLE over the reciprocal of the LOLF remains almost the same when the load factor changes, for both the RBTS and the IEEE-RTS, using either the daily peaks or the hourly values.

The LOLE and the LOLF both increase with increase in the load factor and therefore the effects of the two indices on the ratio are relatively balanced.

The analyses conducted using the original load data and the modified load data clearly indicate that the LOLE does not provide a consistent estimate of the LOLF.

3.4 Reliability Index Probability Distributions

The simulation program was used to create a series of reliability index probability distributions for the RBTS and the IEEE-RTS. The hourly load values are used in this study. The sampling size for the RBTS is 100,000 sampling years and 20,000 for the IEEE-RTS. This provides a coefficient of variation less than 1%.

3.4.1 RBTS Results

Probability distribution of the loss of load

The LOLE for the RBTS at a 185 MW peak load is 1.0901 hours/year. In the 100,000 sampling years, there are 86,492 years in which the system experienced no shortage of capacity. This can be interpreted as the relative frequency or probability (86.49%) that in a given year with a peak load of 185 MW there will be no loss of load. The numbers of years with no loss of load are 73,703 (73.70%) and 52,587 (52.59%) respectively when the peak load is 195 MW and 205 MW. The probability of having a year with no load loss decreases rapidly when the system reserve margin is less than the capacity of the largest generating unit. This is 40 MW in the case of the RBTS. Figure 3.14 shows the relative frequencies of having various loss of load durations for peak loads of 185, 195 and 205 MW. The relative frequencies of having no loss of load at these peak load levels are not included in these figures.

A class interval width of 1.5 hours/year is used to present the data. The last class interval shown contains the cumulative relative frequencies of the loss of load durations greater than 33 hours/year. In Figure 3.13 (a), (b) and (c), the last interval is 33 to 111, 33 to 124.5 and 33 to 198 hrs/yr respectively.

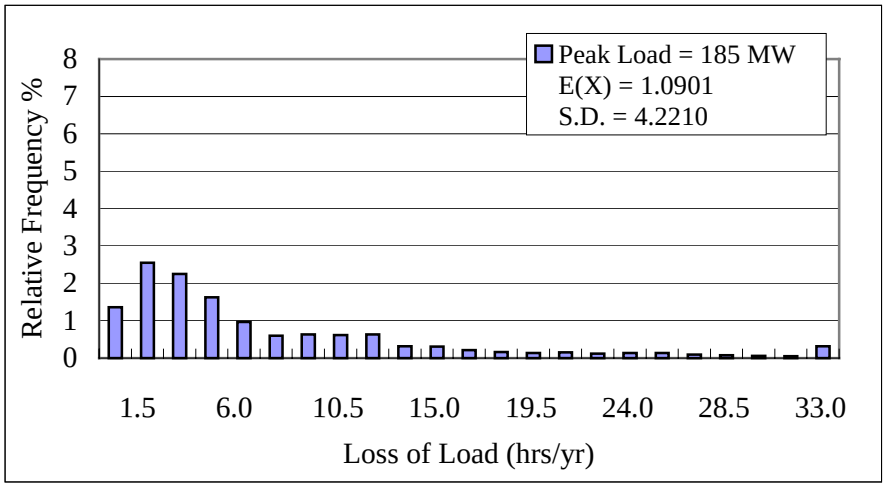

(a) Peak load = 185 MW

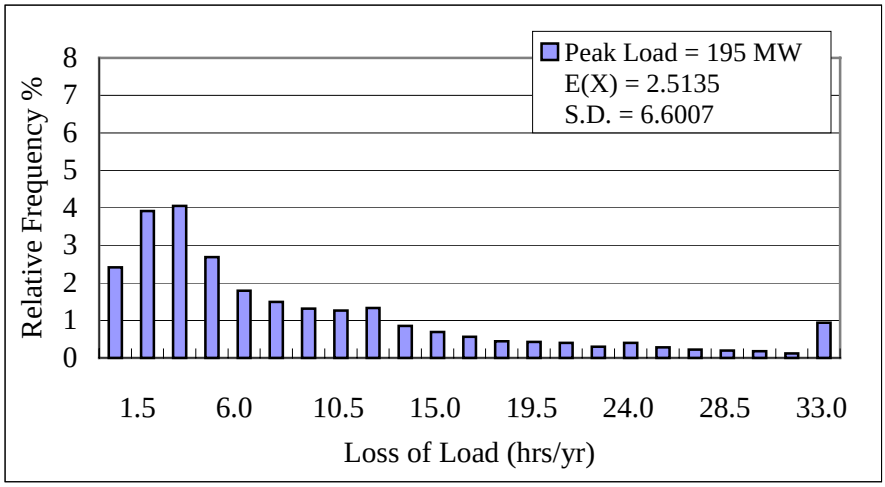

(b) Peak load = 195 MW

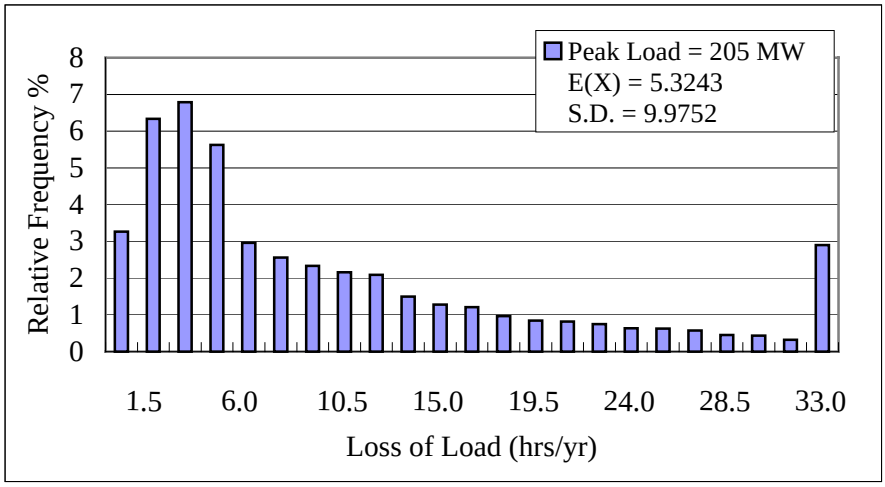

(c) Peak load = 205 MW

Figure 3.14: Probability distributions of the loss of load for the RBTS

The range of the loss of load increases with increase in the peak load. The mean value and standard deviation of the loss of load in hours/year increase as the peak load increases and the distributions shown in Figure 3.13 move to the right. The relative frequency of having a year with more than 6 hours/year of loss of load are 5.72%, 13.23% and 25.41% respectively for the peak load levels of 185, 195 and 205 MW. These values are 0.314%, 0.937% and 2.902% for loss of load durations greater than 33 hours/year.

The LOLE is a valuable parameter and is used by many utilities as their basic generating capacity adequacy index. It should be appreciated, however, that it is simply the long run average value of the annual loss of load and contains no information on the dispersion or the distribution of this index.

Probability distribution of the loss of energy

Figure 3.15 shows the distribution of the loss of energy for the RBTS.

The relative frequencies of no energy loss in a given year are not shown in these figures. The expected value and the standard deviation increase with increase in the peak load. The distributions are exponential in form and extend further to the right as the peak load increases. The relative frequencies of having an energy deficiency in excess of 220 MWh/year are 1.18%, 3.03% and 7.82% respectively at the 185, 195 and 205 MW peak load levels.

As noted earlier, the LOLE index is the most commonly used adequacy index in generating capacity planning. The LOLE does not contain any information on the magnitude of load loss due to insufficient generation. It simply indicates the expected number of hours of load loss in a given year. The LOEE is a more complex index and is a composite of the frequency, duration and magnitude of load loss. The LOEE can be combined with an index known as the Interrupted Energy Assessment Rate (IEAR) to give the expected customer economic loss due to capacity deficiencies [2].

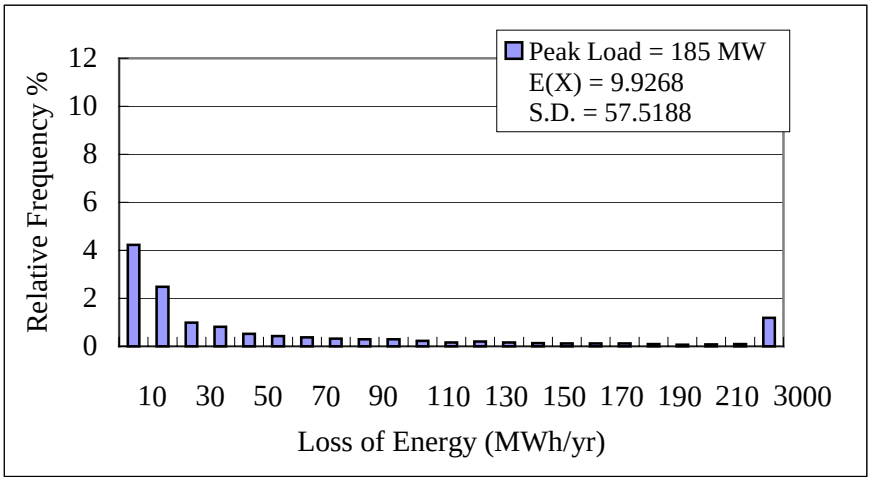

(a) Peak load = 185 MW

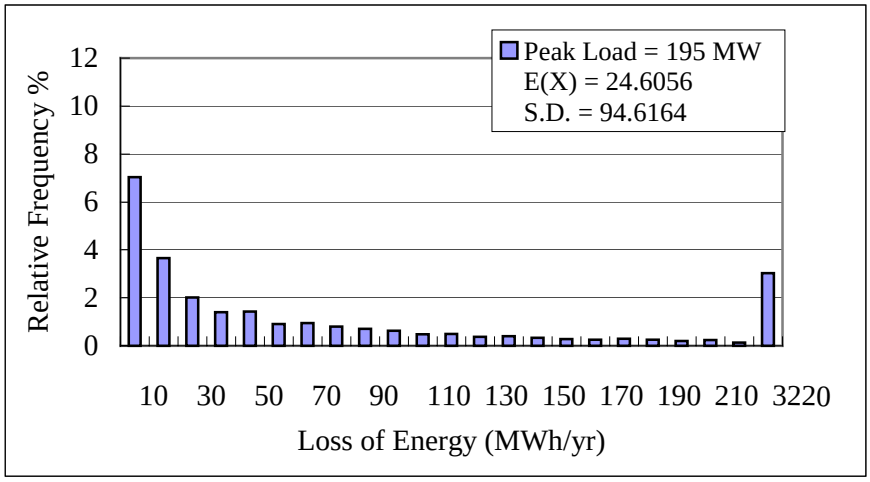

(b) Peak load = 195 MW

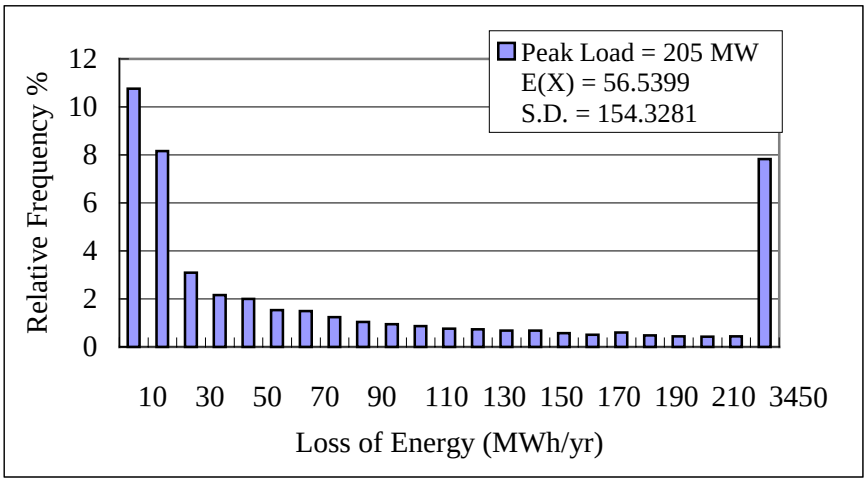

(c) Peak load = 205 MW

Figure 3.15: Probability distributions of the loss of energy for the RBTS

Assuming an IEAR of 15.00/kWh of unserved energy, the expected customer interruption costs (ECOST) are $149,000, $369,000 and $ 848,000 respectively at the 185, 195 and 205 MW peak load levels. These values were obtained by taking the product of the IEAR and the respective LOEE.

Additional information on the likelihood of encountering a particular level of monetary loss can be obtained using the distribution in Figure 3.15. As an example, the relative frequencies of encountering a monetary loss exceeding 1.05 million dollars are 3.67%, 8.91% and 18.22% respectively for the 185, 195 and 205 MW peak load levels. The distributions provide considerable additional information that can be used in electricity utility risk assessment and management.

Probability distribution of the loss of load frequency

The same concept can be applied to the loss of load frequency. The probability distribution for the LOLF is shown in Figure 3.16. The relative frequencies of having no occurrence of loss of load at these peak load levels are not included in these figures. A class interval width of 1 occ/yr is used to present the data. The last class interval shown contains the cumulative relative frequencies of the loss of load frequency greater than 10 occ/yr. For Figure 3.16 (a), (b) and (c), the last interval is 10, 10 to 13, and 10 to 23 occ/yr respectively. The range of the loss of load frequency increases with increase in the peak load.

The mean value and standard deviation of the loss of load frequency in occ/yr increase as the peak load increases and the distributions shown in Figure 3.16 move to the right. It can be seen from the Figure 3.16 that not only are the expected values of the LOL and LOLF different, but their probability distributions are also quite different. The range of the distribution for the loss of load is much wider than that for the loss of load frequency.

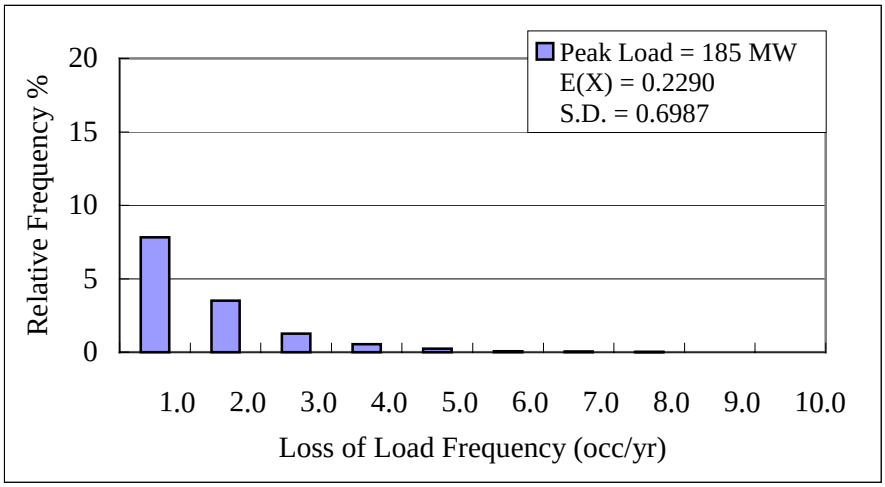

(a) Peak Load = 185 MW

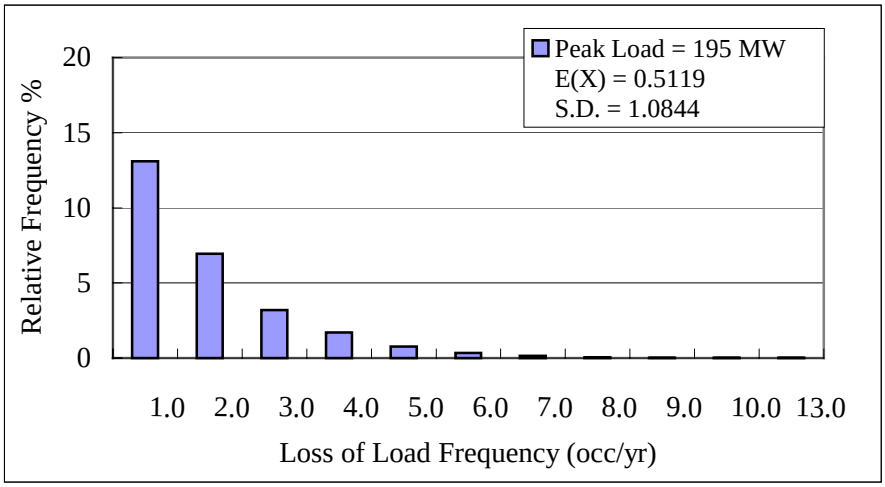

(b) Peak Load = 195 MW

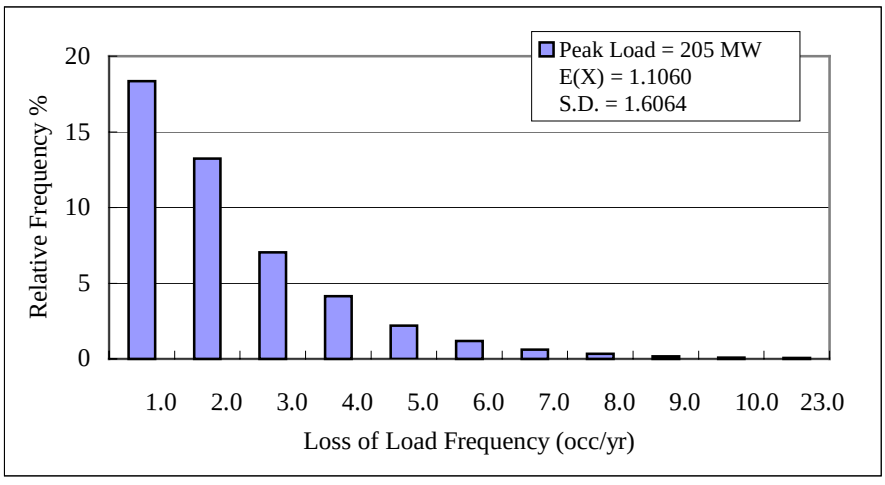

(c) Peak Load = 205 MW

Figure 3.16: Probability distributions of the loss of load frequency for the RBTS

3.4.2 IEEE-RTS Results

Probability distribution of the loss of load

The LOLE for the IEEE-RTS at a 2850 MW peak load is 9.3868 hours/year. In the 20,000 sampling years, there are 8,670 years in which the system experienced no shortage of capacity. The numbers of years with no loss of load are 8,670 (43.350%), 4,223 (21.12%) and 1,407 (7.04%) respectively when the peak load is 2850 MW, 2964 MW and 3078MW.

Figure 3.17 shows the relative frequencies of having various loss of load durations for the different peak load levels. The probability of having a year with no load loss decreases rapidly when the system reserve margin is less than the capacity of the largest generating unit, which is 400 MW for the IEEE-RTS. The relative frequencies of having no loss of load at these peak load levels are not included in these figures. The class interval in this case is 4 hrs/yr. The last class interval shown contains the cumulative relative frequencies of the loss of load durations greater than 120 hours/year. It is obvious that the cumulative relative frequency increases sharply with increase in the peak load. The mean values and the standard deviations also increase and the distribution moves to the right. The relative frequency of encountering no loss of load for the IEEE-RTS is much smaller than for the RBTS. The IEEE-RTS has a low HLI reliability compared to the RBTS.

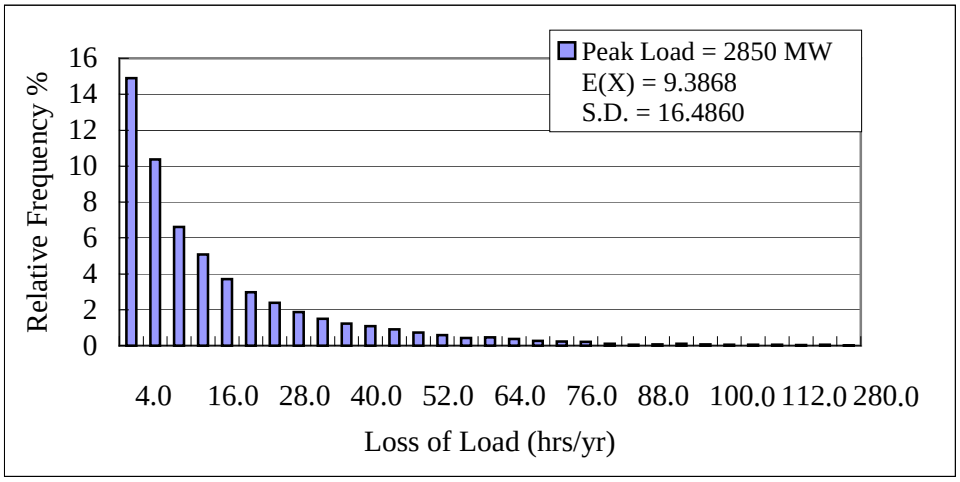

(a) Peak Load = 2850 MW

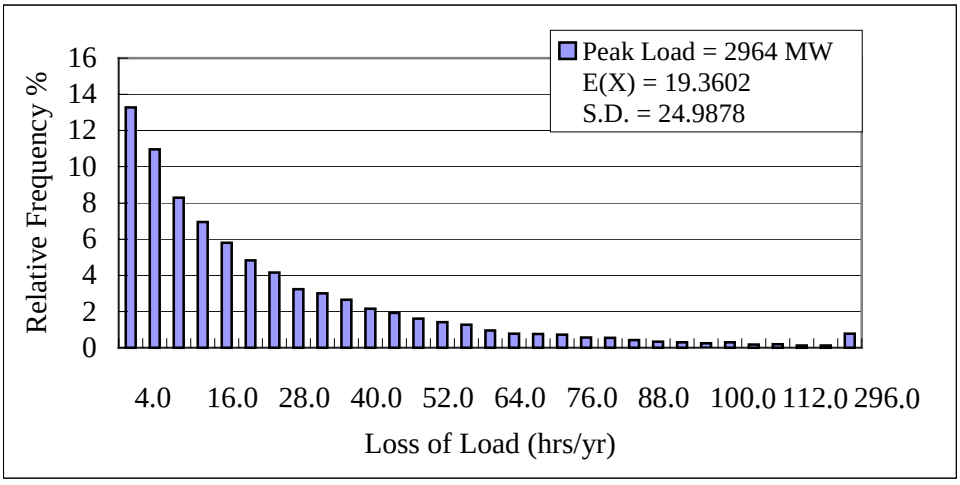

(b) Peak Load = 2964 MW

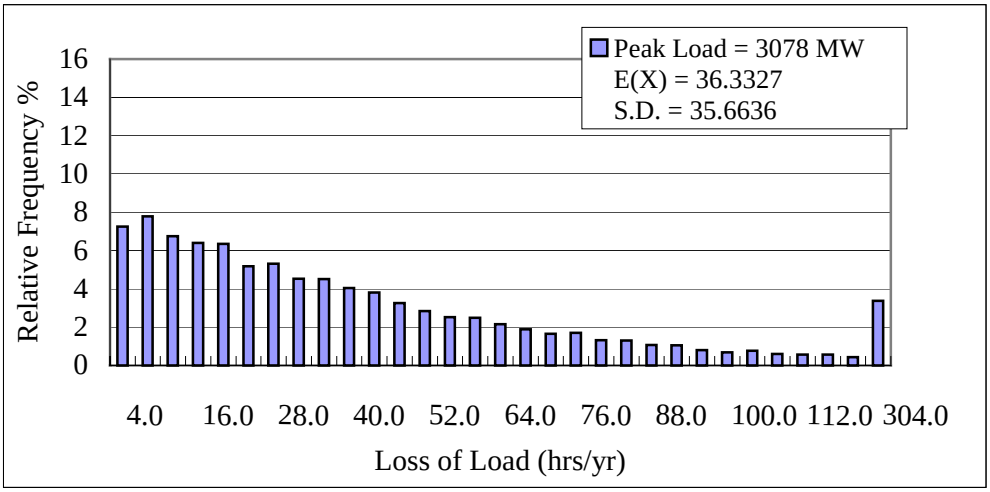

(c) Peak Load = 3078 MW

Figure 3.17: Probability distributions of the loss of load for the IEEE-RTS

Probability distribution of the loss of energy

The probability distributions of the loss of energy for the IEEE-RTS are shown in Figure 3.18. The relative frequencies of no energy loss in a given year are not shown in these figures. The expected values and the standard deviations increase with increase in the peak load. The distributions are exponential in form and extend further to the right as the peak load increases. The last interval for this distribution is 6,500 MWh to 41,000 MWh, 61,000 MWh and 108,500 MWh respectively. The relative frequencies of having an energy deficiency in excess of 6,500 MWh/year are 0.28%, 12.15% and 26.15% for the three peak load levels.

It can be seen from Figure 3.18 that the distribution of the loss of energy is generally exponential. The relative cumulative frequency of the last interval of the loss of energy increases greatly with the increasing peak load levels. The cumulative relative frequency of the last interval when the peak load is equal to 3078 MW is even greater than the frequency of the first interval. The range of the distribution increases as the peak load increases.

Additional information on the likelihood of encountering a particular level of monetary loss can be obtained as shown in Section 3.4.1.

Probability distribution of the loss of load frequency

Figure 3.19 shows the probability distribution of the loss of load frequency for the IEEE-RTS. The relative frequencies of having no occurrence of loss of load at these peak load levels are not included in these figures. A class interval width of 1 occ/yr is used to present the data. The last class interval shown contains the cumulative relative frequencies of the loss of load frequency greater than 23 occ/yr. For Figure 3.19 (a), (b) and (c), the last interval is 23, 23 to 33, and 23 to 42 occ/yr respectively. The cumulative relative frequency for the last interval is: 0.01%, 0.19% and 1.77% respectively. The range of the loss of load frequency increases with increase in the peak load.

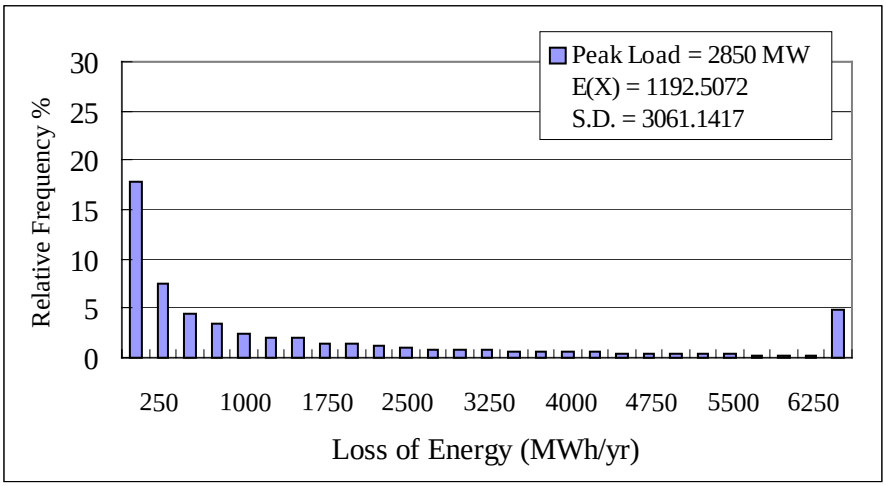

(a) Peak Load = 2850 MW

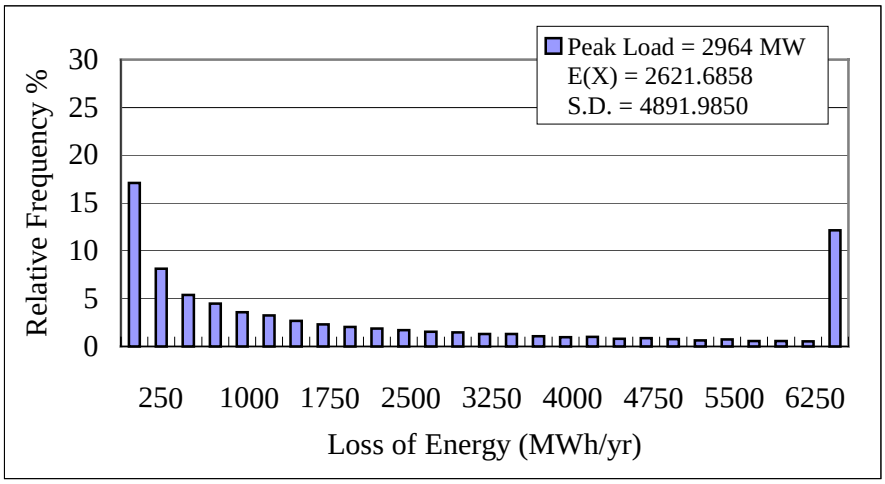

(b) Peak Load = 2964 MW

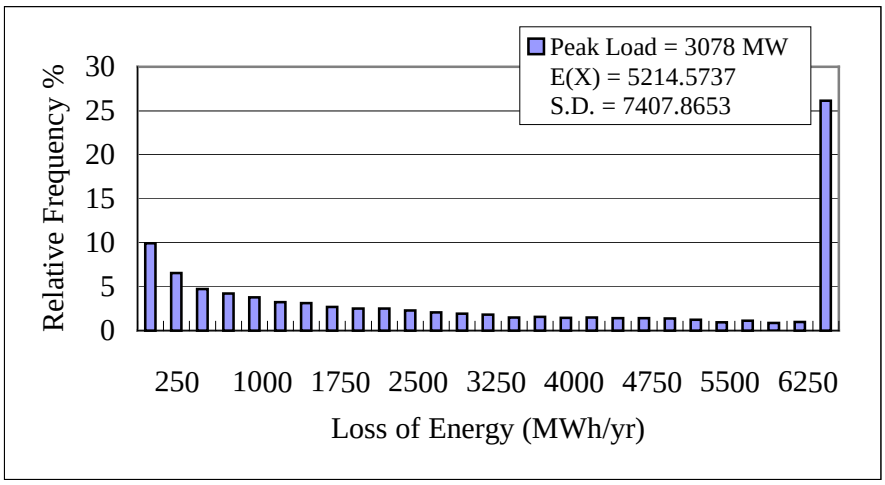

(c) Peak Load = 3078 MW

Figure 3.18: Probability distributions of the loss of energy for the IEEE-RTS

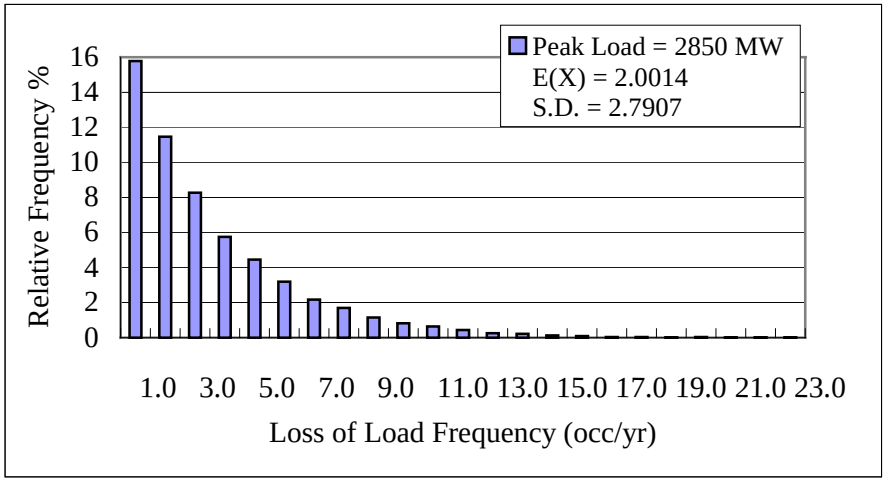

(a) Peak Load = 2850 MW

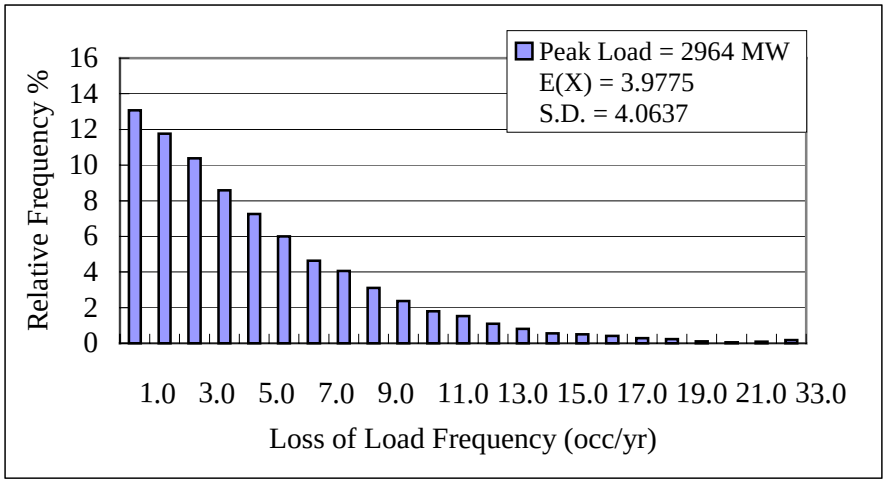

(b) Peak Load = 2964 MW

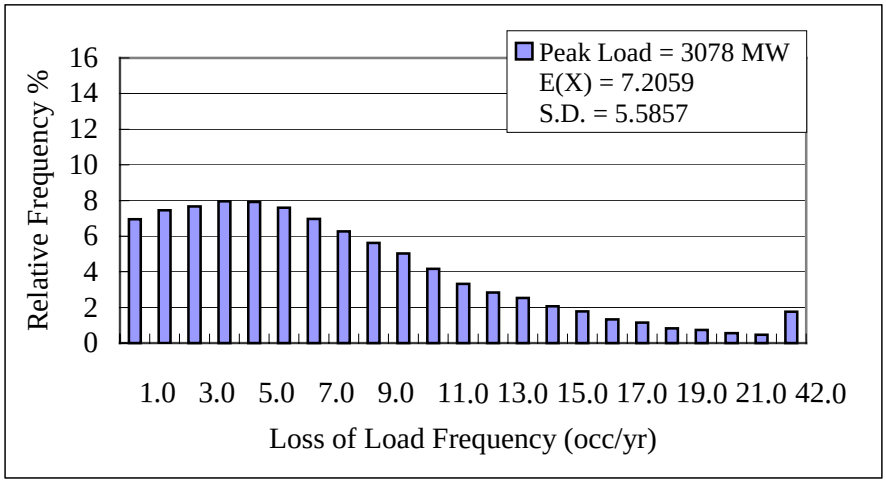

(c) Peak Load = 3078 MW

Figure 3.19: Probability distributions of the loss of load frequency for the IEEE-RTS

3.5 Conclusion

This chapter illustrates the application of the two developed computer programs to the RBTS and the IEEE-RTS. Two commonly encountered misconceptions are presented and examined using the results obtained from the two programs. The two misconceptions are further examined by using different load models on the two test systems.

The simulation program can provide a wider range of indices than the analytical program. The simulation program can also provide the data required to create reliability index probability distributions. The index distributions for the RBTS and the IEEE-RTS illustrate the concept of creating distributions and the additional information that can be obtained and utilized in generating capacity risk assessment.

The studies described in this chapter show that the LOLE (hrs/yr) cannot be obtained by multiplying the LOLE (days/yr) by a factor of 24. The ratio of the LOLE (hrs/yr) over the LOLE (days/yr) is always less than the value of 24 in an actual power system. The LOLE (days/yr) gives a pessimistic appraisal of the system reliability. The multiplication factor is not the same for the RBTS and the IEEE-RTS and changes with peak load level. The difference is due to the different generation compositions since the two systems have the same normalized load profile. The multiplication factor moves towards the value of 24 when the load factor of the hourly load in percent of daily peak increases. The ratio between the LOLE (hrs/yr) and LOLE (days/yr) is equal to 24 only when the load factor is unity.

The LOLE (days/yr) does not include any frequency information and should not be interpreted as a frequency index. The results for the RBTS and IEEE-RTS show that the ratio of the reciprocal of the LOLE (days/yr) over the reciprocal of the LOLF (occ/yr) is not unity for all peak load levels. The ratio decreases with increase in the peak load, which indicates that the LOLF (occ/yr) increases more slowly than the LOLE (days/yr). The average duration per interruption increases with increase in the peak load. The ratio

between the two indices becomes unity at a high load level. The LOLE in this case would normally be considered to be unacceptable. It's also obvious that when the hourly load is used, the ratio between the reciprocal of the LOLE (hrs/yr) over the reciprocal of the LOLF (occ/yr) is considerable less than unity. The ratios for both the RBTS and the IEEE-RTS remain almost constant at each peak load level when the load factor of the normalized load profile changes. This is because both the LOLE and the LOLF increase with increase in the load factor.

Reliability index probability distributions provide considerable additional information on the system reliability. The expected values of LOLE, LOEE and LOLF are basic generating adequacy indices. They are, however, only the long run average values and contain no information on the dispersion and the annual variability of the index. Considerable additional information can be obtained by using probability distributions. As shown in this chapter, the likelihood of encountering a particular level of monetary loss can be obtained from the distribution of the annual loss of energy and used by utilities in risk assessment and management.

4. THE EFFECT OF GENERATING UNIT STATE RESIDENCE TIME DISTRIBUTIONS ON SYSTEM RELIABILITY

4.1 Introduction

Generating unit residence time distributions can be generally categorized as being either exponential or non-exponential in form. The exponential distribution is utilized, however, in virtually all practical system studies. Normal or Weibull distributions are used in aging failure analysis of power system components. Generating unit residence time distributions are usually assumed to be exponential in the analytical method while non-exponential distributions can be considered in the simulation method.

The RBTS and the IEEE-RTS generation data were modified to contain units with Weibull distributed generating unit state residence time distributions. The generation data were further modified to incorporate units with derated states having Weibull distributions. The developed simulation program was applied to the modified test systems. The reliability indices and the reliability index probability distributions for the two systems when the Weibull shape parameters change are compared in this chapter to show the effect of Weibull distributed generating unit state residence time distributions on the system reliability.

4.2 Generating Units without Derated States

The repair times of the generating units in the RBTS and the IEEE-RTS are assumed to have a Weibull distribution. The shape parameters were changing in the following cases. The scale parameters are calculated to retain the original unit MTTR. Hourly load values are used in this study.

Case 0: The generating unit repair times follow Weibull distributions with a shape parameter of 0.5.

Case 1: The generating unit repair times follow Weibull distributions with a shape parameter of 1.

Case 2: The generating unit repair times follow Weibull distributions with a shape parameter of 2.

Case 3: The generating unit repair times follow Weibull distributions with a shape parameter of 4.

The expected value of the Weibull distribution is given by:

$$E(t) = \alpha \int_0^{\infty} t^{\frac{1}{\beta}} e^{-t} dt \qquad (4.1)$$

The scale parameter α can be calculated as in Equation (4.2).

$$\alpha = E(t) / \int_0^{\infty} t^{\frac{1}{\beta}} e^{-t} dt \qquad (4.2)$$

The scale parameter α for each case is shown in Table 4.1.

Table 4.1: Parameters of the Weibull Distribution for each case

Cases	α	β
Case 0	=MTTR/2	0.5
Case 1	=MTTR	1
Case 2	= MTTR * 1.13	2
Case 3	=MTTR*1.1	4

The sampling size is set at 100,000 for the RBTS. The sampling size for the IEEE-RTS is 20,000 years.

4.2.1 RBTS Results

Comparison of the reliability indices

The reliability indices obtained for the four cases are given in Table 4.2.It can be seen from Table 4.2 that the reliability indices are very similar for the four cases. The mean values of the reliability indices are not affected by the shape parameters as long as the mean values of the unit repair time distributions remain the same. The variations in the indices are due to the simulation process.

Table 4.2: The reliability indices of each case for the RBTS

Case Num	LOLE (hrs/yr)	LOEE (MWh/yr)	LOLF(occ/yr)
Case 0	1.1041	9.8027	0.2308
Case 1	1.1021	9.9303	0.2306
Case 2	1.0942	9.8464	0.2285
Case 3	1.0993	9.8034	0.2301

Comparison of the reliability index probability distributions

The probability distributions of the loss of load for the four cases are shown in Figure 4.1. The interval class is 1.5 (hrs/yr) and the last interval in (a), (b), (c) and (d) shows the cumulative relative frequency of loss of load from 45 to 223.5 (hrs/yr), 90 (hrs/yr), 57 (hrs/yr) and 57 (hrs/yr) respectively. The relative frequency of encountering no loss of load is 88.49%, 86.44%, 85.82% and 85.64% for the four cases respectively. The relative frequency of encountering no loss of load is not shown in Figure 4.1. It can be seen from Figure 4.1 that the loss of load distributions change and the standard deviations of the loss of load decrease with increase in the shape parameter. The relative frequency of encountering loss of load in the first interval (0-1.5 hrs/yr) decreases. The relative frequencies of the next few class intervals increase as the shape parameter increases, as shown in Table 4.3. The range of the loss of load decreases with increasing shape parameter. The relative frequencies of large LOL values decrease quickly as the shape parameter increases.

The changes in the relative frequency and the range of the loss of load have opposite effects on the LOLE, therefore the LOLE remains the same.

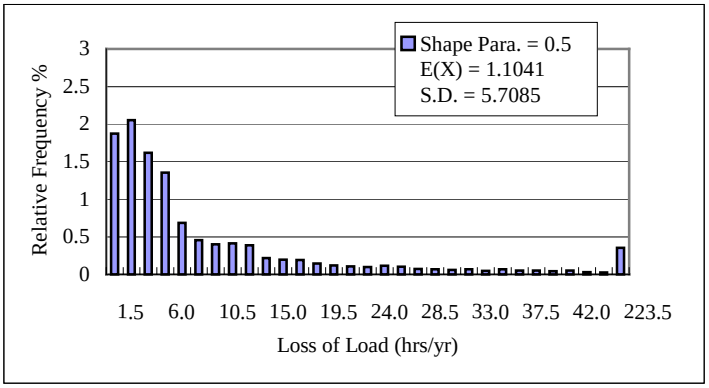

(a) Shape Parameter = 0.5

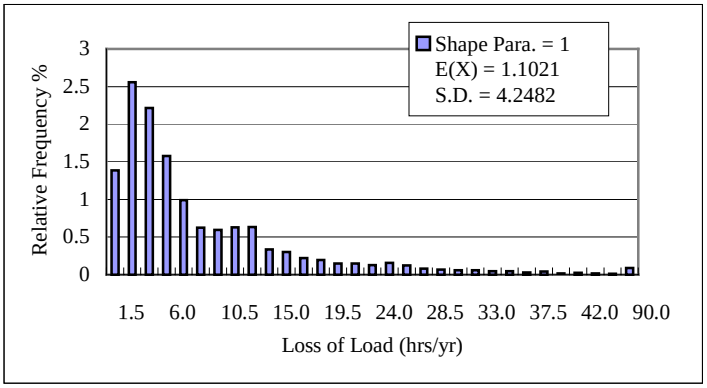

(b) Shape Parameter = 1.0

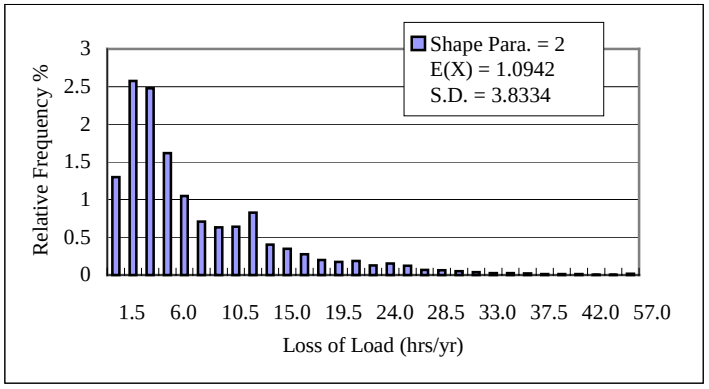

(c) Shape Parameter = 2.0

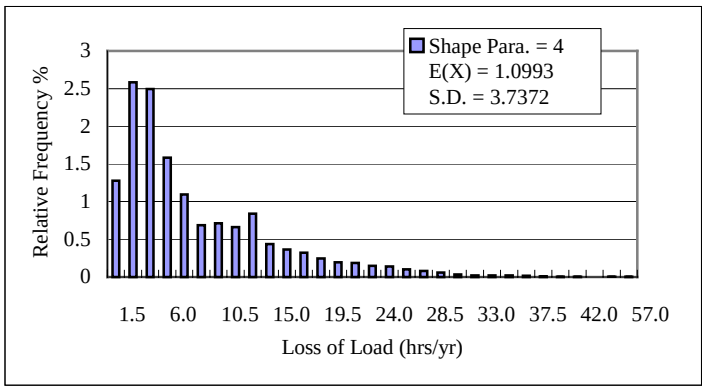

(d) Shape Parameter = 4.0

Figure 4.1: Probability distributions of the LOL for the RBTS

Table 4.3: The relative frequency of the LOL for the RBTS

Interval hrs/yr	Case 0	Case 1	Case 2	Case 3
0--1.5	1.873	1.384	1.297	1.278
1.5--3	2.05	2.557	2.575	2.585
3--4.5	1.618	2.216	2.476	2.494
>45	0.355	0.089	0.019	0.005

The loss of energy distributions are shown in Figure 4.2. The class interval width is 10 MWh/yr. The relative frequency of encountering no shortage of energy is the same as the one for the loss of load and is not shown in the figures.

The expected values of the loss of energy are identical for the four cases, while the standard deviation for the four cases decreases. The frequencies for the first several intervals increase and the cumulative relative frequency for the last interval decreases with increase in the shape parameter as shown in Table 4.4. The range of the loss of energy decreases with increase in the shape parameter.

Table 4.4: The relative frequency of the LOE for the RBTS

Interval Mwh/yr	Case 0	Case 1	Case 2	Case 3
0-10	4.024	4.338	4.477	4.464
10-20	2.017	2.308	2.442	2.467
20-30	0.789	1.029	1.055	1.116
>300	0.795	0.757	0.663	0.636

The loss of load frequency distributions are shown in Figure 4.3. The relative frequency when no loss of load occurs is not shown in the figure. The LOLF are very similar for the four cases with the various shape parameters. The relative frequencies for the first several class intervals increase and the cumulative relative frequencies for the last interval decrease as shown in Table 4.5. The range of the loss of load frequency decreases with increase in the shape parameter.

Table 4.5: The relative frequency of the LOLF for the RBTS

Interval occ/yr	Case 0	Case 1	Case 2	Case 3
1	6.453	7.814	8.377	8.352
2	2.548	3.511	3.809	4.091
>=7	0.336	0.051	0.014	0.009

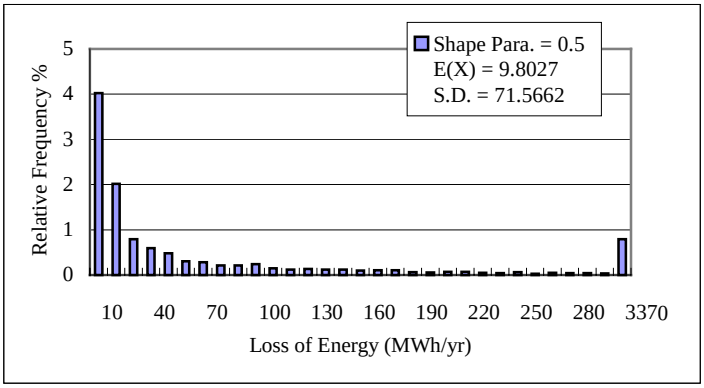

(a) Shape Parameter = 0.5

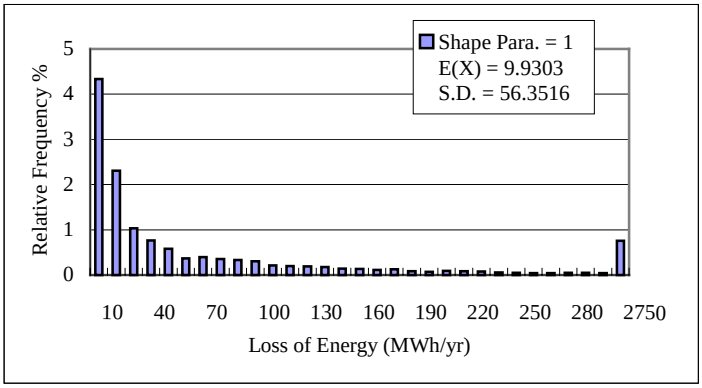

(b) Shape Parameter = 1.0

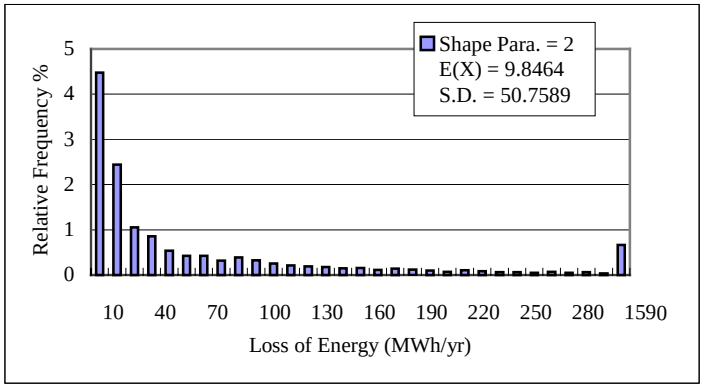

(c) Shape Parameter = 2.0

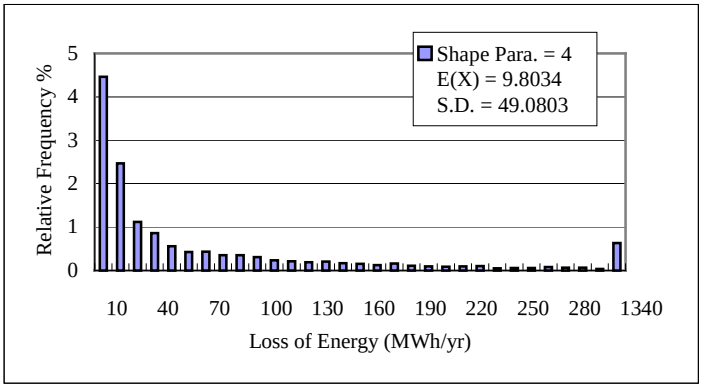

(d) Shape Parameter = 4.0

Figure 4.2: Probability distributions of the LOE for the RBTS

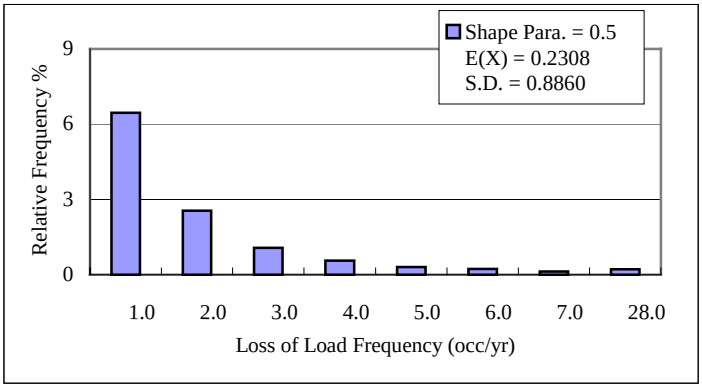

(a) Shape Parameter = 0.5

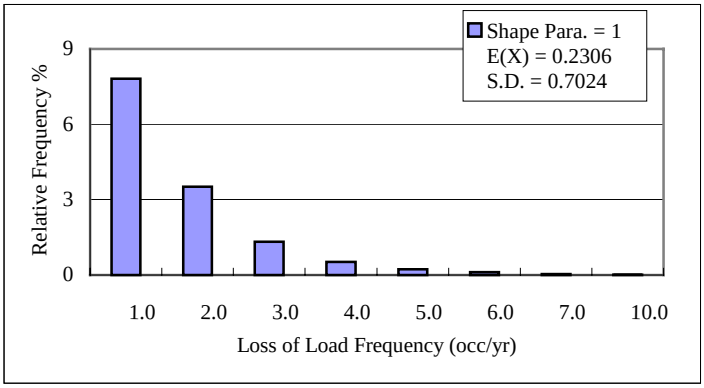

(b) Shape Parameter = 1.0

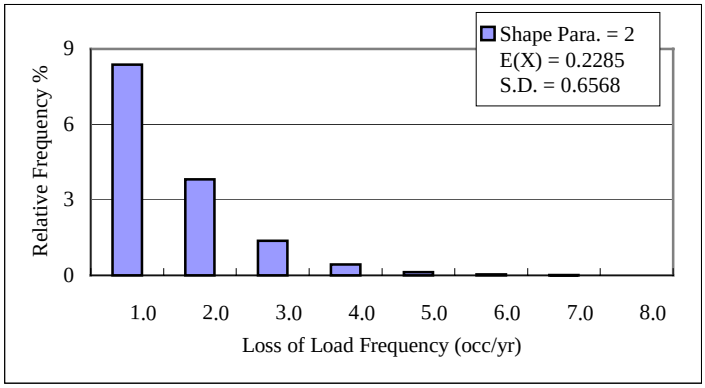

(c) Shape Parameter = 2.0

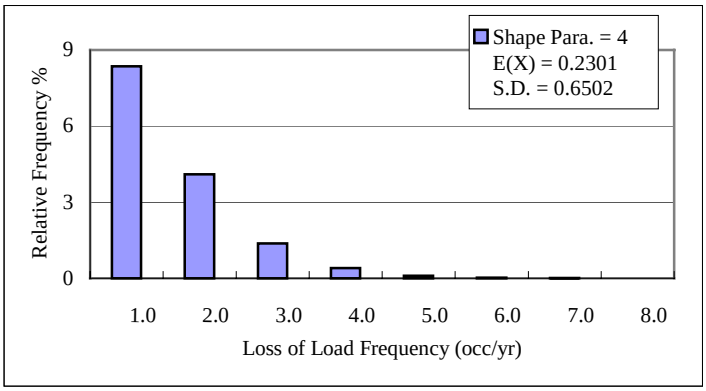

(d) Shape Parameter = 4.0

Figure 4.3: Probability distributions of the LOLF for the RBTS

4.2.2 IEEE-RTS Results

Comparison of the reliability indices

The reliability indices obtained for the four cases are given in Table 4.6.

Table 4.6: The reliability indices of each case for the IEEE-RTS

Case Num	LOLE (hrs/yr)	LOEE (MWh/yr)	LOLF(occ/yr)
Case 0	9.2813	1184.3020	2.0005
Case 1	9.3868	1192.5072	2.0014
Case 2	9.3839	1169.3402	2.0339
Case 3	9.3056	1173.0227	1.9990

The results in Table 4.6 show that the reliability indices are almost the same for the four cases.

Comparison of the reliability index probability distribution

The probability distributions of the loss of load for the IEEE-RTS are shown in Figure 4.4. The interval class is 4 (hrs/yr) and the last interval in (a), (b), (c) and (d) represents the cumulative relative frequency of loss of load from 120 to 400 (hrs/yr), 280 (hrs/yr), 148 (hrs/yr), 132 (hrs/yr) respectively. The relative frequency of encountering no loss of load is 51.65%, 43.35%, 39.12% and 38.56% for the four cases respectively. The relative frequency of encountering no loss of load is not shown in the figure.

The relative frequencies for the first several class intervals and the last interval are shown in Table 4.7. It can be seen from Table 4.7 that the relative frequencies for the first several intervals increase while the cumulative frequency for the last interval decreases with increase in the shape parameter. The range of the loss of load decreases with increase in shape parameter. The relative frequency of encountering a certain level of loss of load drops more quickly when the shape parameter increases.

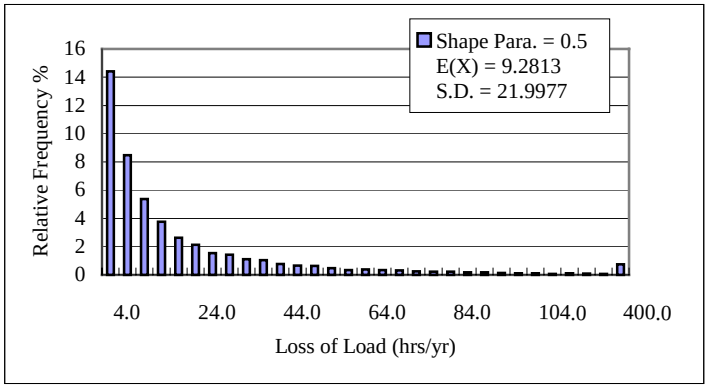

(a) Shape Parameter = 0.5

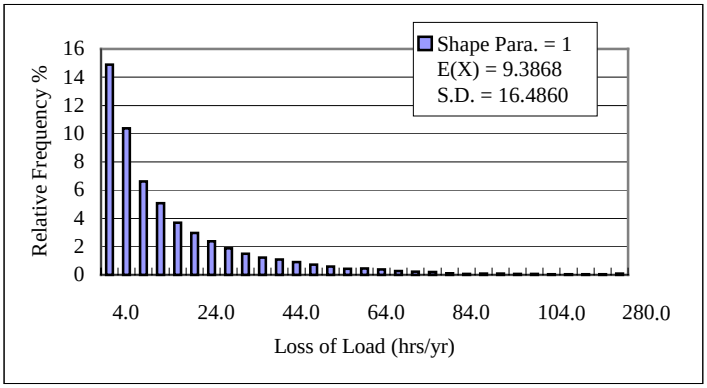

(b) Shape Parameter = 1.0

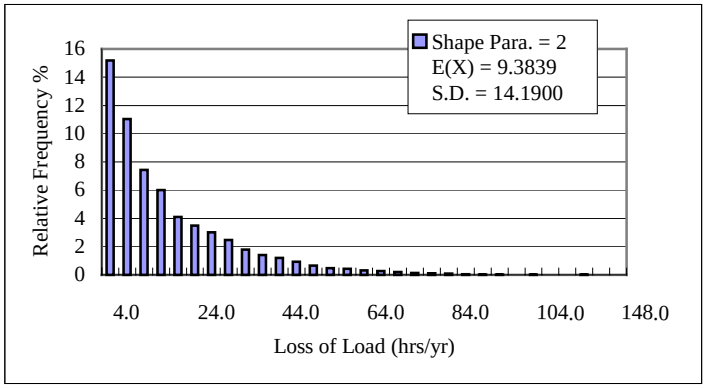

(c) Shape Parameter = 2.0

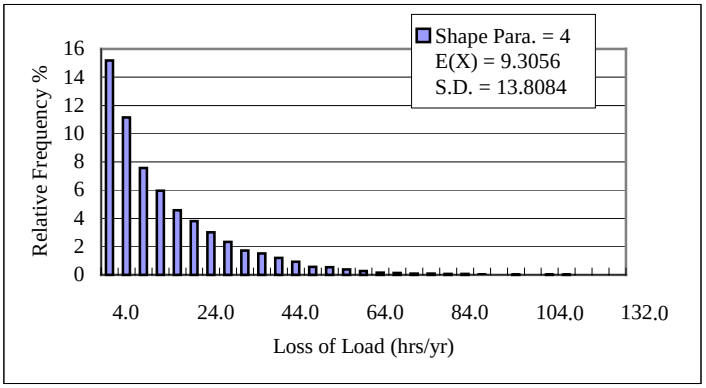

(d) Shape Parameter = 4.0

Figure 4.4: Probability distributions of the LOL for the IEEE-RTS

Table 4.7: The relative frequency of the LOL for the IEEE-RTS

Interval hrs/yr	Case 0	Case 1	Case 2	Case 3
0—4	14.42	14.9	15.195	15.18
4—8	8.465	10.375	11.04	11.155
8—12	5.37	6.61	7.43	7.56
>120	0.75	0.085	0.01	0.005

The probability distributions of the loss of energy for the IEEE-RTS are shown in Figure 4.5. The class interval width is 250 MWh/yr in this case. The frequency when there is no shortage of energy is not shown in the figures. The last interval shown in the figure is from 7,500 (MWh/yr) to 105,250 (MWh), 84,500 (MWh), 51,500 (MWh) and 33,750 (MWh) respectively.

The expected values of the loss of energy remain almost the same, while the standard deviations decrease for the four cases. The relative frequencies of the first several intervals increase while the cumulative relative frequency for the last interval decreases with increase in the shape parameter, as shown in Table 4.8.

Table 4.8: The relative frequency of the LOE for the IEEE-RTS

Interval MWh /yr	Case 0	Case 1	Case 2	Case 3
0—250	16.78	17.82	18.53	18.32
250—500	6.15	7.425	7.95	8.08
>7500	4.18	3.83	3.35	3.29

The loss of load frequency distributions are shown in Figure 4.6. The relative frequency when no loss of load occurs is not shown in the figure. The last interval is when a loss of load occurs more than 10 occ/yr. The expected LOLF remains the same for the four cases with increase in the shape parameter while the range of the loss of load frequency decreases. The changes in the relative frequency for the first several and the last intervals are shown in Table 4.9.

Table 4.9: The relative frequency of the LOLF for the IEEE-RTS

Interval occ/yr	Case 0	Case 1	Case 2	Case 3
1	14.275	15.79	16.26	16.305
2	9.27	11.45	12.565	12.97
3	5.835	8.265	9.475	9.74
>10	3.85	1.76	1.005	0.71

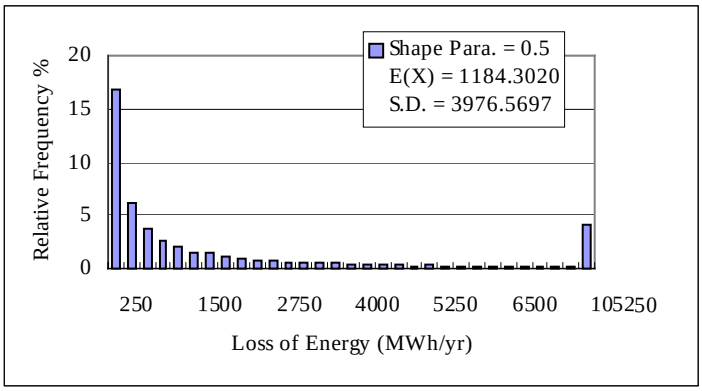

(a) Shape Parameter = 0.5

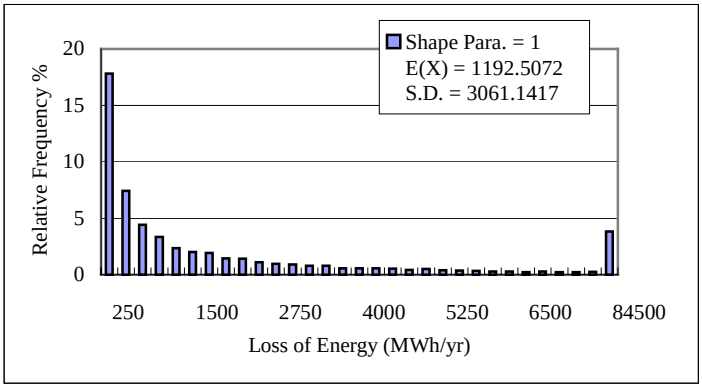

(b) Shape Parameter = 1.0

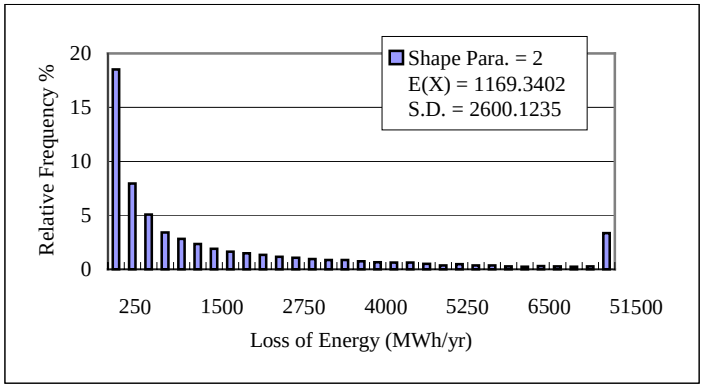

(c) Shape Parameter = 2.0

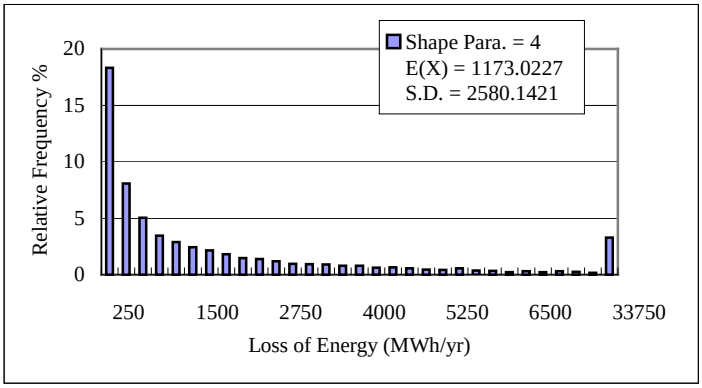

(d) Shape Parameter = 4.0

Figure 4.5: Probability distributions of the LOE for the IEEE-RTS

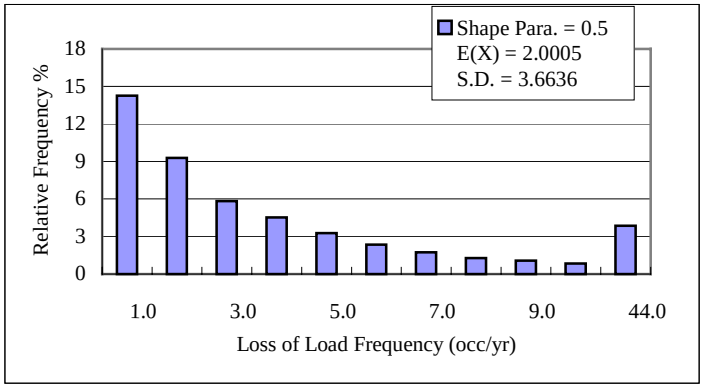

(a) Shape Parameter = 0.5

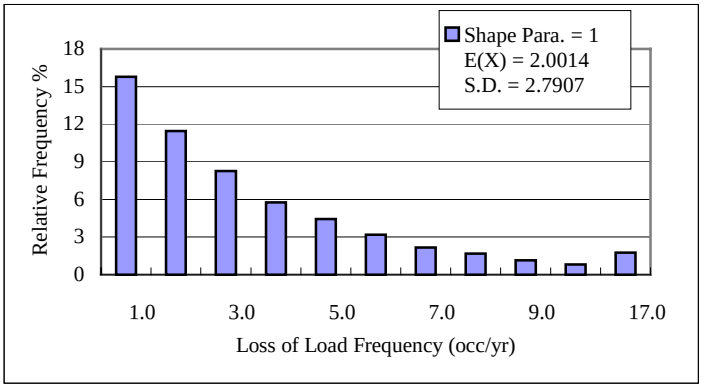

(b) Shape Parameter = 1.0

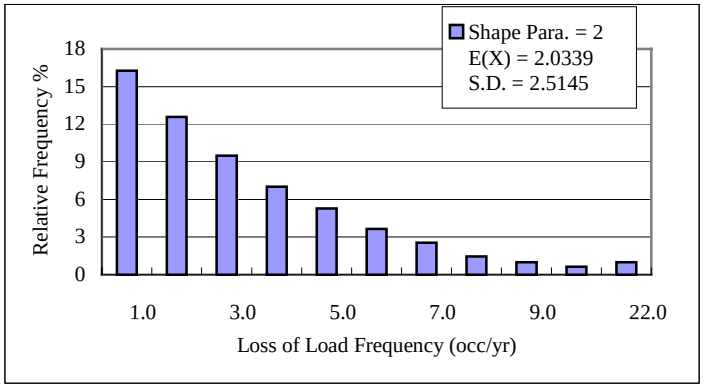

(c) Shape Parameter = 2.0

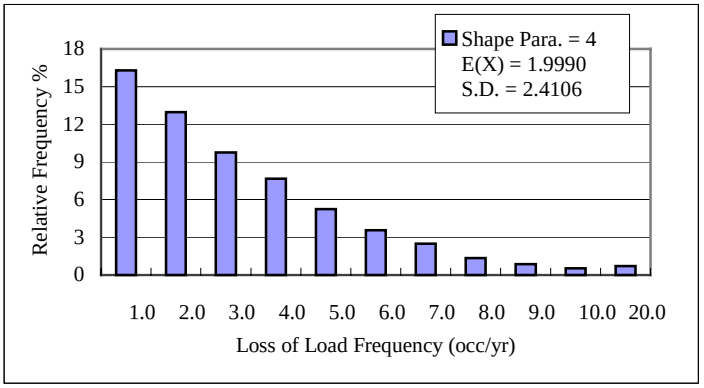

(d) Shape Parameter = 4.0

Figure 4.6: Probability distributions of the LOLF for the IEEE-RTS

The studies in the previous section illustrate the changes in the reliability index distributions due to varying the generating unit repair time distributions. The unit repair time distributions for the two test systems were assigned Weibull distributions with different shape parameters. The scale parameter was set to keep the mean value of the repair time constant.

As expected, the mean values of the reliability indices for both the RBTS and the IEEE-RTS remain the same. The standard deviations of the reliability index distributions, however, decrease with increase in the shape parameter and the ranges of the distributions decrease.

4.3 Generating Units with Derated States

The IEEE-RTS data were modified in order to examine the effects of state residence time distributions in generating units with derated states. One 350 MW and two 400 MW units were assume to each have one derated state. The corresponding transition rates occ/yr when all the state residence times are exponentially distributed are shown in Tables 4.10 and 4.11.

Table 4.10: Transition rates for a 350 MW unit with exponential distributions

State	Capacity Out (MW) Transition Rate (/yr)	0	175	350
0	0	0	3.8087	3.8087
1	175	73	0	73
2	350	62.5714	62.5714	0

Table 4.11: Transition rates for a 400 MW unit with exponential distributions

State	Capacity Out (MW) Transition Rate (/yr)	0	200	400
0	0	0	3.74359	3.74359
1	200	43.8	0	43.8
2	400	43.8	43.8	0

The derated and down states of one 350 MW and two 400 MW units are assumed to have a Weibull distribution. The Weibull distribution shape and scale parameters are

given in Table 4.12.

Table 4.12: Shape and scale parameters for a unit with derated states

From State \ To State	0		1		2	
	α	β	α	β	α	β
0	-	-	-	-	-	-
1	$\alpha_{1,0}$	$\beta_{1,0}$	0	0	$\alpha_{1,2}$	$\beta_{1,2}$
2	$\alpha_{2,0}$	$\beta_{2,0}$	$\alpha_{2,0}$	$\beta_{2,1}$	0	0

Where $\alpha_{i,j}, \beta_{i,j}$ are the scale and shape parameters respectively for the Weibull distributed residence time at state i when the unit transits from state i to state j. The shape parameter $\beta_{i,j}$ changes from 0.5, 1, 2 to 4 for Cases 0,1,2 and 3. The scale paramter $\alpha_{i,j}$ is calculated according to Equation (4.2). In this case the E(t) in Equation (2) is equal to the expected value of the residence time in state i. The simulation program was applied to the modified IEEE-RTS using the hourly load values. The sampling size is 20,000 years.

4.3.1 Comparison of the reliability indices

The reliability indices are shown in Table 4.13.

Table 4.13: The reliability indices of each case for the IEEE-RTS with derated states

Case Num	LOLE (hrs/yr)	LOEE (MWh/yr)	LOLF(occ/yr)
Case 0	1.5955	162.8154	0.4390
Case 1	5.3855	615.3270	1.2614
Case 2	9.5742	1156.7574	2.0996
Case 3	12.8032	1586.6165	2.7084

Table 4.13 shows that the reliability indices increase considerably with increase in the shape parameter.

4.3.2 Comparison of the reliability index probability distribution

The loss of load distributions for the modified IEEE-RTS are shown in Figure 4.7. The relative frequency of encountering no loss of load is not shown in this figure.

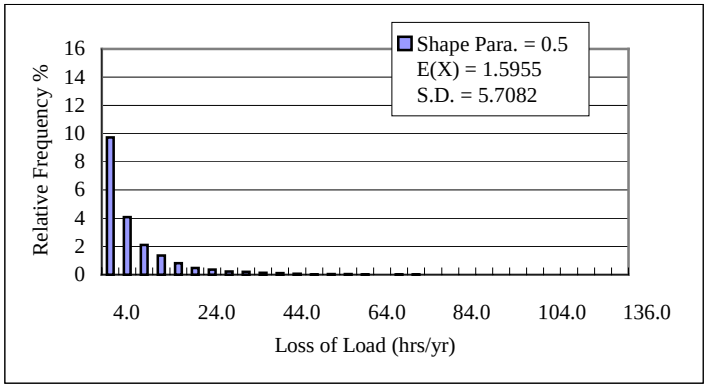

(a) Shape Parameter = 0.5

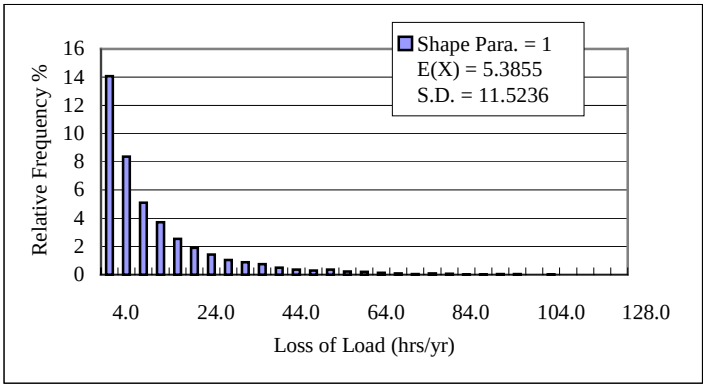

(b) Shape Parameter = 1.0

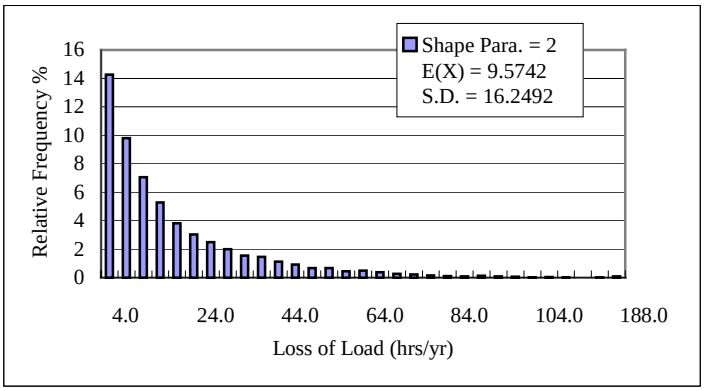

(c) Shape Parameter = 2.0

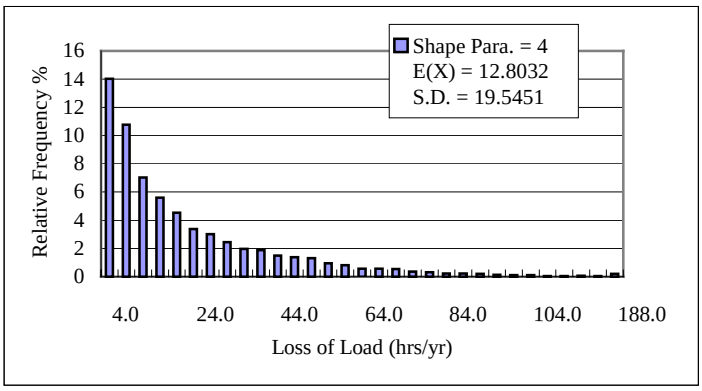

(d) Shape Parameter = 4.0

Figure 4.7: Probability distributions of the LOL for the IEEE-RTS with derated states

The interval width in Figure 4.7 is 4 (hrs/yr). The relative frequency of encountering no loss of load is 80.09%, 57.68%, 43.18% and 35.62% for the four cases respectively. The last interval in the figures shows the cumulative relative frequency of loss of load from 120 to 136 (hrs/yr), 128 (hrs/yr), 188 (hrs/yr), 188 (hrs/yr) respectively. The relative frequency of the first two intervals and the last interval is shown in Table 4.14. Both the mean value and standard deviation of loss of load increase with increase in the shape parameter.

Table 4.14: The relative frequency of the LOL for the IEEE-RTS with derated states

Interval hrs/yr	Case 0	Case 1	Case 2	Case 3
0—4	9.725	14.065	14.265	14.03
4—8	4.075	8.37	9.805	10.77
>120	0.01	0.005	0.1	0.205

The loss of energy distributions for the IEEE-RTS with derated states are shown in Figure 4.8. The class interval width is 250 MWh/yr in this case. The frequency when there is no shortage of energy is not shown in the figures. The last interval in the figure is 7,500 (MWh/yr) to 29,500 (MWh), 38,500 (MWh), 47,250 (MWh) and 49500 (MWh) respectively.

The cumulative relative frequency for the last interval increases. The relative frequency of the first several intervals and the last interval is shown in Table 4.15. Both the expected value and the standard deviation of the loss of energy increase considerably with increase in the shape parameter. The range of loss of energy increases with increase in the shape parameter.

Table 4.15: The relative frequency of the LOE for the IEEE-RTS with derated states

Interval MWh /yr	Case 0	Case 1	Case 2	Case 3
0—250	10.345	16.455	17.565	18.035
250—500	3	5.91	7.6	7.97
500—750	1.46	3.47	4.595	4.87
>7500	0.265	1.69	3.61	5.70

The loss of load frequency distributions for the modified IEEE-RTS are shown in Figure 4.9. The relative frequency when no loss of load occurs is not shown.

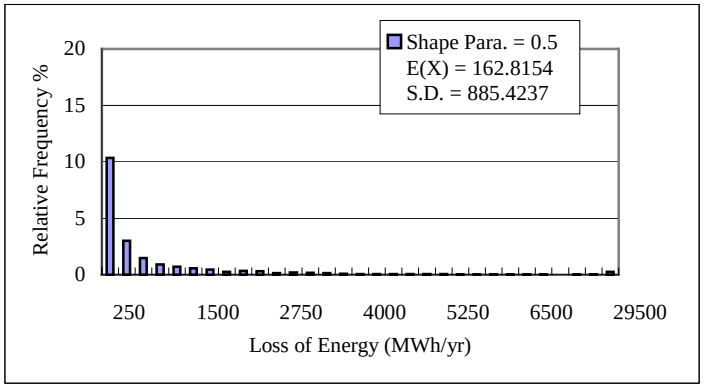

(a) Shape Parameter = 0.5

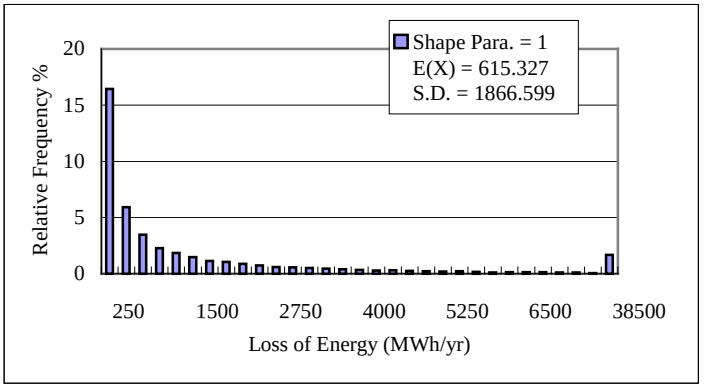

(b) Shape Parameter = 1.0

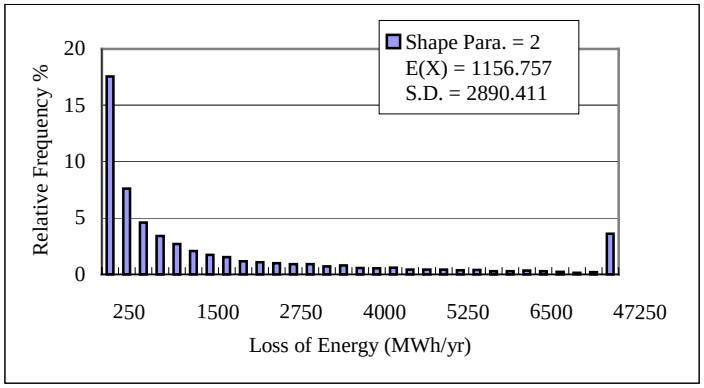

(c) Shape Parameter = 2.0

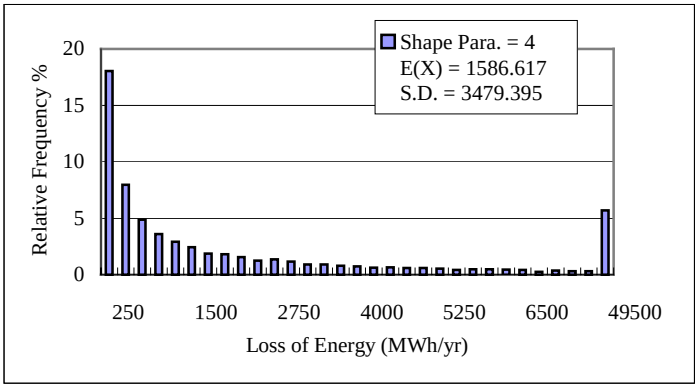

(d) Shape Parameter = 4.0

Figure 4.8: Probability distributions of the LOE for the IEEE-RTS with derated states

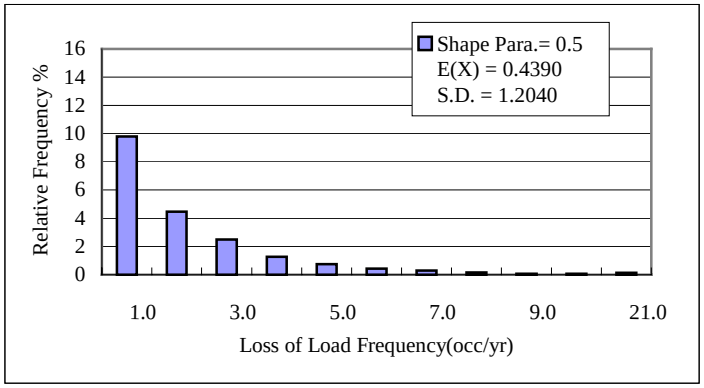

(a) Shape Parameter = 0.5

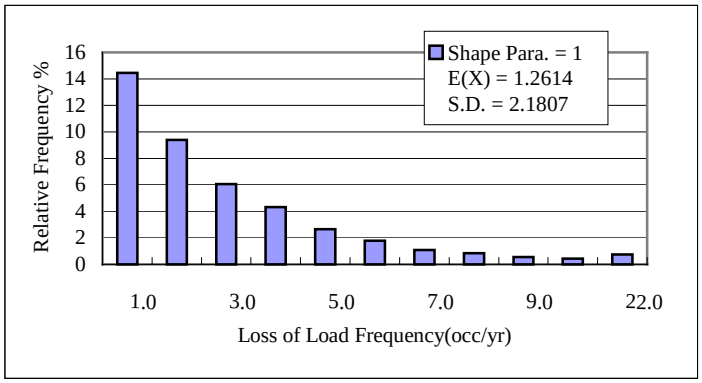

(b) Shape Parameter = 1.0

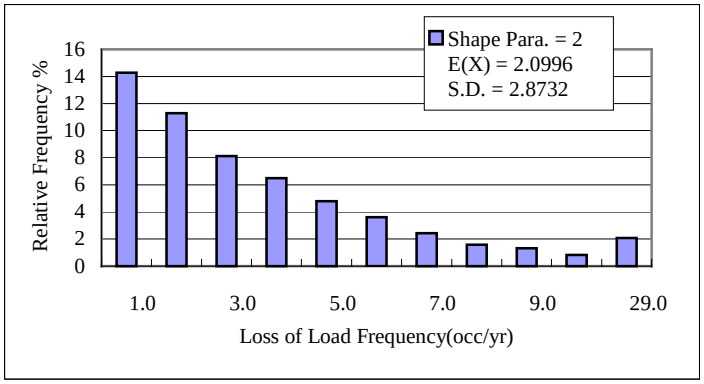

(c) Shape Parameter = 2.0

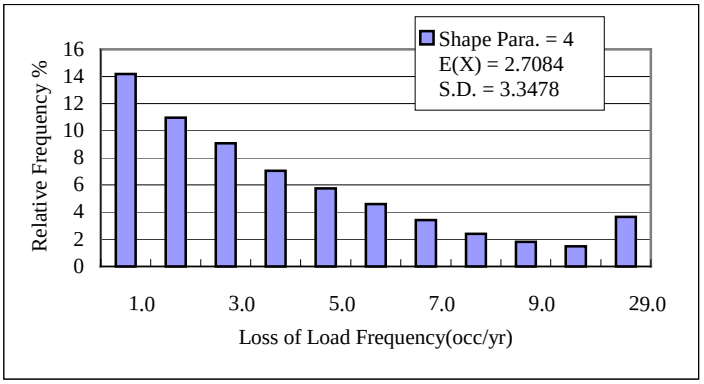

(d) Shape Parameter = 4.0

Figure 4.9: Probability distributions of the LOLF for the IEEE-RTS with derated states

The last interval in Figure 4.9 shows the cumulative frequency when the loss of load occurs 10 (occ/yr) to 21 (occr/yr), 22 (occ/yr), 29 (occ/yr) and 29 (occ/yr) for the four cases.

It can be seen from Figure 4.9 that the cumulative relative frequency for the last interval increases significantly. Both the expected value and standard deviation of the LOLF increase considerably with increase in the shape parameter while the range of the loss of load frequency decreases with increase in the shape parameter. The relative frequencies for the first three intervals and the last interval are shown in Table 4.16.

Table 4.16: The relative frequency of the LOLF for the IEEE-RTS with derated states

Interval occ/yr	Case 0	Case 1	Case 2	Case 3
1	9.785	14.46	14.285	14.185
2	4.465	9.385	11.28	10.96
3	2.5	6.05	8.125	9.08
>10	0.125	0.74	2.075	3.655

The results for the IEEE-RTS show that both the expected values and the standard deviations of the reliability indices increase with increase in the shape parameter.

4.4 Conclusion

The RBTS and the IEEE-RTS generation data were modified to contain units with Weibull distributed generating unit state residence time distributions with various shape parameters. The IEEE-RTS generation data were further modified to incorporate units with derated states that have Weibull distributions with changing shape parameters. The developed simulation program is applied to the modified RBTS and the IEEE-RTS. The reliability indices and the index probability distributions for these cases are compared in this chapter.

In the studies including units without derated states,

1. The relative frequency of encountering no shortage of capacity decreases with increase in the shape parameter.

2. The expected values of the reliability indices are constant for the various shape parameters when the mean residence time remains unchanged.
3. The standard deviations of the index distributions decrease with increase in the shape parameter.
4. The range of the reliability index probability distributions decreases when the shape parameter increases.

In the studies including units with derated states,

1. The relative frequency of encountering no shortage of capacity decreases with increase in the shape parameter.
2. Both the expected values and the standard deviations of the reliability indices increase when the shape parameter increases.
3. The range of the reliability index distributions decreases with increase in the shape parameter.

5. RELIABILITY EVALUATION AT HLI CONSIDERING PEAKING LOAD UNITS

5.1 Introduction

Base load units have relatively long operating cycles while peaking load units or intermittent operating units normally operate for relatively short periods. Peaking units are started when they are needed and are frequently interrupted by economy shutdowns, which depend greatly on generating unit conditions, operating constraints and load levels. The operation of peaking load units can be described by the frequency and duration of their service and shutdown states and the transitions between these states. A peaking load unit has many more startups and shutdowns compared to a base load unit, which brings extra starting stress to the unit since the starting period is the most critical period in the operation of a unit [2, 3, 24, 33-35].

The two-state model for a base load unit is extended to a four-state model in Reference [24]. There are several indices used to describe the unavailability of peaking load units based on the four-state model. The Utilization Forced Outage Probability (UFOP) is the probability of a generating unit not being available when needed [25]. The Derated Adjusted Utilization Forced Outage Probability (DAUFOP) is the probability of a generating unit with derated states not being available when needed [25]. The UFOP and DAUFOP for peaking load units are used in the analytical method to evaluate the system reliability instead of the conventional Forced Outage Rate (FOR). The UFOP used in the analytical method is usually a fixed value calculated at a

certain system condition and used for a range of situations.

The UFOP, however, is not a constant value for a peaking load unit. It varies with changes in the system operating conditions such as the peak load level, required operating reserve and so on. It is important to examine how the UFOP varies with changes in the system operating conditions. Not only does the UFOP of a peaking load unit change, but also the peaking load unit state residence time distributions change with the system operating conditions. The changes in the UFOP and the state residence time distributions need to be examined.

The simulation program was developed to incorporate peaking load units in a generating capacity adequacy assessment at HLI. The simulation process for peaking load units and the assumptions made are described in this chapter.

The developed simulation program was applied to both the RBTS and the IEEE-RTS. The two test systems were modified to contain some peaking load units. Hourly load values are used in this study. The UFOP are computed using the peaking load unit state residence time durations produced by the simulation program. The variation in UFOP with changes in the unit loading order, the peaking load level, the required reserve and the unit residence time distributions are calculated and compared in this study.

The peaking load unit state residence time distributions are produced using the simulation program. The four-state model used to represent a peaking load unit assumes that the peaking load unit state residence times are exponentially distributed. The actual peaking load unit residence time distributions are shown using the results for both the RBTS and the IEEE-RTS from the simulation program. The peaking load unit repair time durations were modified to follow Weibull distributions with varying shape parameters. The effect of the Weibull distribution shape parameters on the actual peaking load unit state residence time distributions are shown in this chapter.

5.2 Simulation of the Peaking Load Unit Operation

A four-state model is used to represent a peaking load unit as shown in Figure 2.3. The general process used to simulate generating units including both base load units and peaking load units is described in Chapter 2. The basic rules and assumptions made in the peaking load unit simulation processes are stated in the following. The steps used in selecting the required set of peaking load units and simulating the selected peaking load units are illustrated using Figure 5.1.

Figure 5.1 shows the base load unit capacity margin and the required reserve. The base load unit capacity margin is obtained by superimposing the system capacity generated by all the base load units on the chronological load. The total capacity margin is obtained by superimposing the total system capacity generated by both the base load units and the peaking load units on the chronological load.

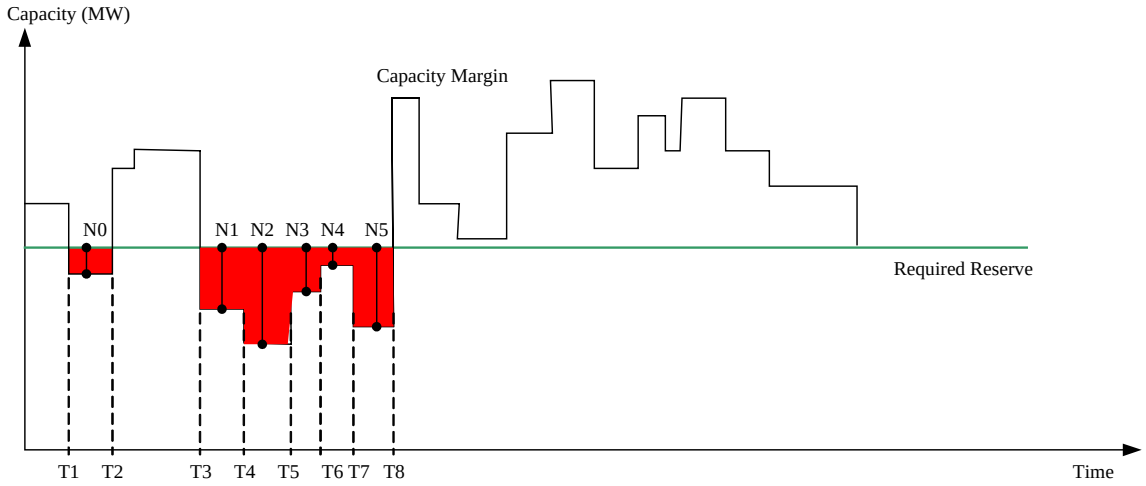

Figure 5.1: The basic capacity margin and the required reserve

The basic rules and assumptions for the peaking load unit simulation procedure are as follows.

The base load unit capacity margin is checked for each time interval. In the case shown in Figure 5.1, the base load unit capacity margin is less than the required reserve during the time intervals between T1 and T2, T3 and T4, … T7 and T8. The total capacity margins are also checked for these intervals. Peaking load units are required for

the time intervals in which the total system capacity margin is less than the required reserve.

The required peaking load unit capacity = the required reserve – the total capacity margin.

The in-need time for the selected peaking load units is the continuous time interval in which the total capacity margin is less than the required reserve. The in-need time for the peaking load units is not exactly the in-need time for each peaking load unit. The process to determine the exact in-need time for each peaking load unit is complex and time consuming. An approximation is used to save computation time. The time interval in which the base load unit capacity margin is less than the required reserve is usually not very long and the simplification in this case is reasonable. The total capacity margin may change during the in-need time and therefore the actual needed capacity could be less than the calculated one. There will be some redundant peaking capacity due to avoiding starting up and shutting down the peaking load units too often.

Assume there is no peaking load unit started before time T1 in the case shown in Figure 5.1. There are two in-need time intervals of [T1, T2] and [T3, T8]. The in-need capacity for [T1, T2] is N0. The calculated in-need capacity for the interval [T3, T8] is N1 as shown. The total capacity margin is checked again in the interval [T4, T5] since the base load unit capacity margin is less than the required reserve and different from the one for the interval [T3, T4]. More peaking load units are needed if the total capacity margin is less than the require reserve. The in-need time for the selected peaking units in this case is the time interval of [T4, T8].

The available peaking load units, which are in a reserve shutdown state, are selected according to the loading order. This process stops when the sum of the selected peaking load unit capacity exceeds the required capacity, or there are no available peaking load units left. The selected peaking load units are then simulated to produce the unit operating histories.

The steps to select peaking load units and simulate the unit operating histories are as follows.

Step 1 : Judge if the peaking load units need to be started.

Step 2 : Calculate the in-need capacity.

Step 3 : Select the required set of peaking load units to be started according to the in-need capacity and the loading order.

Step 4 : Calculate the in-need time for the selected peaking load units.

Step 5 : Simulate the selected peaking load units for the calculated in-need time.

The peaking load unit simulation process is shown in Figure 5.2.

The simulation program was extended to incorporate the simulation of peaking load units. The peaking load unit state residence time durations are produced using the simulation program. The UFOP and the DAUFOP are calculated using these obtained time durations. The UFOP and the DAUFOP [33] are given by Equations (5.1) and (5.2).

$$UFOP = \frac{f * FO}{f * FO + O} \tag{5.1}$$

$$DAUFOP = \frac{f * FO + O(FD)_{adj}}{f * FO + O + O(FD)} \tag{5.2}$$

where f is the demand factor and is calculated as follows.

$$f = \frac{P_{out\ \ when\ \ needed}}{P_{out\ \ when\ \ needed} + P_{out\ \ not\ \ needed}} \tag{5.3}$$

where,

FO : Forced Outage Time

FD : Forced Derated Time

O : Operating Time

O(FD) : Operating Time under forced derated state

$O(FD)_{adj}$: Adjusted outage time

$$O(FD)_{adj} = \frac{100 - X}{100} * O(FD) \tag{5.4}$$

where,

X : The unit operates under the derated level X% of the maximum continuous rating.

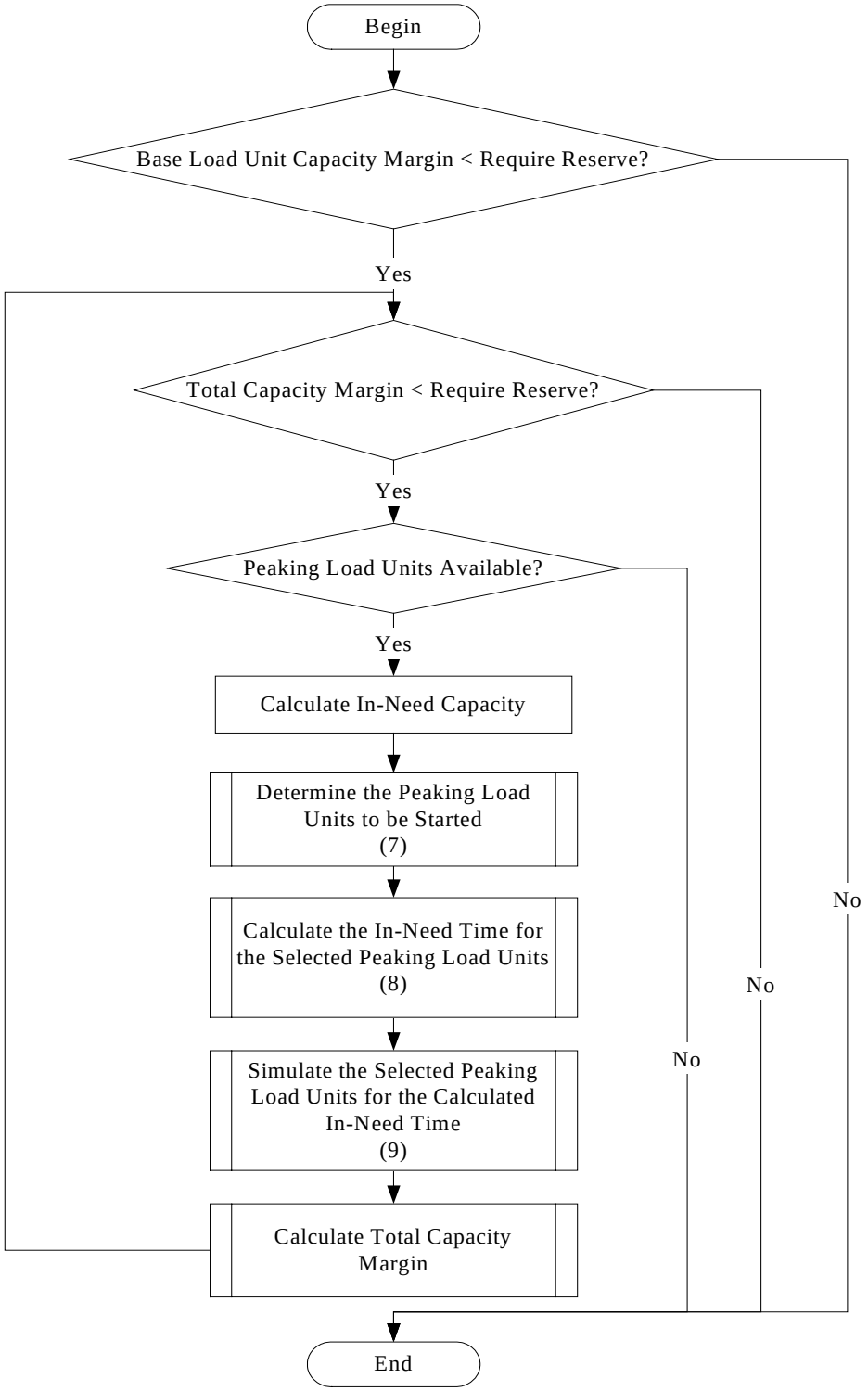

Figure 5.2: The simulation process for peaking load units

5.3 The Effect of Operating Conditions on the UFOP

The simulation program was applied to the RBTS to show the effect of operating conditions on the UFOP. The sampling size is 5,000 sampling years in this study. The starting failure probability is set to 0 for all units and hourly load values are used in this case.

5.3.1 Study Cases

Case 0 is the base case of the RBTS.

All the units in the RBTS are considered as peaking load units in Cases 1 and 2. The loading orders and reliability data for Cases 1 and 2 are shown in Table 5.1 and 5.2 respectively.

Table 5.1: The loading order and reliability data for the RBTS Case 1

Units (MW)	Loading order	MTTF (hr)	MTTR (hr)	FOR
1*40 Hydro	1	2920	60	0.02
4*20 Hydro	2-5	3650	55	0.015
2*5 Hydro	6-7	4380	45	0.01
2*40 Lignite	8-9	1460	45	0.03
1*20 Lignite	10	1752	45	0.025
1*10 Lignite	11	2190	45	0.02

Table 5.2: The loading order and reliability data for the RBTS Case 2

Units (MW)	Loading order	MTTF (hr)	MTTR (hr)	FOR
1*40 Hydro	1	2920	60	0.02
2*40 Lignite	2,3	1460	45	0.03
4*20 Hydro	4-7	3650	55	0.015
1*20 Lignite	8	1752	45	0.025
1*10 Lignite	9	2190	45	0.02
2*5 Hydro	10,11	4380	45	0.01

The simulation program was applied to the two modified RBTS cases with various peak load levels and required reserves. The results for the two cases are shown and compared in the following.

5.3.2 Changes in the Required Reserve

The required reserves are set at 0 MW, 20MW, 40 MW and 60 MW for the RBTS Cases 1 and 2. The peak load is 185 MW in this study.

RBTS Case 1 Results

The reliability indices for the RBTS Case 1 are shown in Table 5.3.

Table 5.3: The reliability indices with various required reserves for the RBTS Case 1

Reserve (MW)	LOLE(hrs/year)	LOEE(MWh/year)	LOLF(occ/year)
0	0.3537	3.3281	0.0778
20	0.5504	4.6109	0.1154
40	0.8358	6.7383	0.1784
60	0.8877	7.7332	0.1888

It can be seen from Table 5.3 that the reliability indices increase with increase in the required reserve. This is because the peaking unit operating times increase and function more like base load units when the required reserve increases.

The demand factor and the UFOP were calculated using the peaking load unit state durations produced by the simulation program and shown in Table 5.4.

Table 5.4: The demand factor and the UFOP versus required reserve for the RBTS Case 1

	Required Reserve							
	0 MW		20 MW		40 MW		60 MW	
Unit	**Demand Factor**	**UFOP**	**Demand Factor**	**UFOP**	**Demand Factor**	**UFOP**	**Demand Factor**	**UFOP**
40 H	0.9906	0.0200	0.9928	0.0198	0.9925	0.0196	0.9929	0.0201
20 H	0.9950	0.0149	0.9918	0.0146	0.9951	0.0148	0.9915	0.015
20 H	0.9943	0.0150	0.9932	0.0149	0.9943	0.0151	0.9926	0.0152
20 H	0.9941	0.0151	0.9926	0.0148	0.9945	0.0149	0.991	0.0146
20 H	0.9939	0.0147	0.9925	0.0145	0.9941	0.0148	0.9925	0.015
5 H	0.5346	0.0054	0.9957	0.0099	0.9964	0.0101	0.9943	0.0103
5 H	0.5047	0.0052	0.9967	0.0102	0.9955	0.0099	0.9958	0.0103
40 L	0.4413	0.0135	0.6461	0.0194	0.9869	0.0292	0.9904	0.0292
40 L	0.1559	0.0046	0.2539	0.0075	0.4437	0.0136	0.6719	0.0199
20 L	0.2563	0.0081	0.1536	0.0040	0.1731	0.0046	0.2722	0.007
10 L	0.2961	0.0048	0.1999	0.0033	0.1599	0.0031	0.1678	0.0036

It can be seen from Table 5.4 that the first five unit demand factors are almost unity

when the required reserve is 0 MW. The calculated UFOP of the five units are almost equal to the FOR of these units, which shows that in this case these five peaking load units function as base load units.

The demand factor and the UFOP of the peaking load units in Case 1 due to changes in the required reserve are also shown in Figures 5.3 and 5.4 respectively.

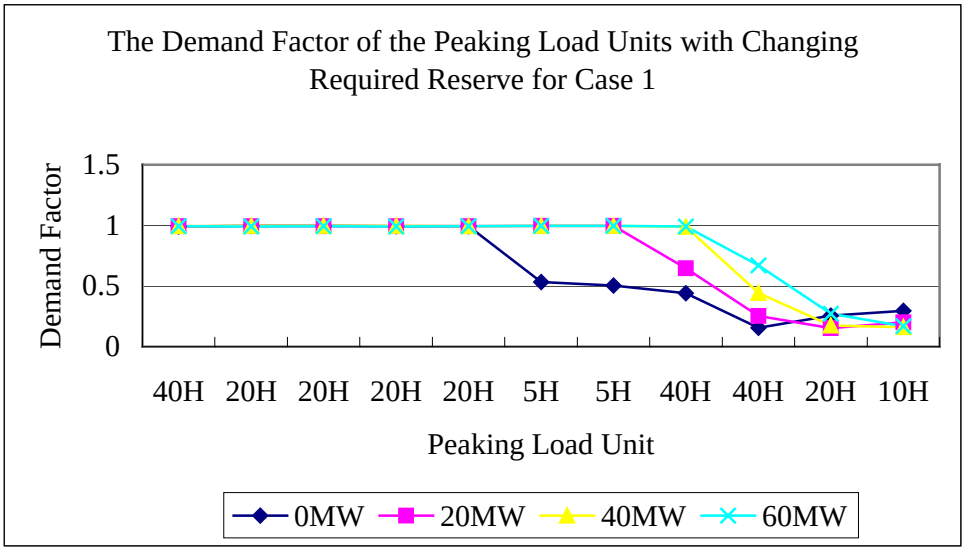

Figure 5.3: The demand factors with various required reserves for the RBTS Case 1

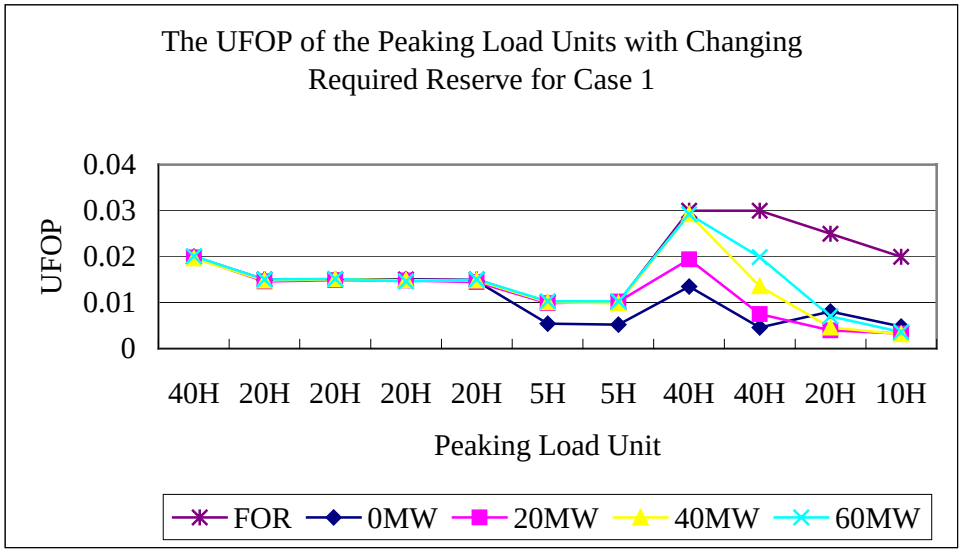

Figure 5.4: The UFOP with various required reserves for the RBTS Case 1

Figure 5.3 shows that more peaking load unit demand factors move towards unity with increase in the required reserve. The demand factors of the peaking load units

decrease with the loading order but there are fluctuations for the last two units. This is because the last two units are not used as much as the first nine units. The prespecified sampling size for the simulation program is therefore not big enough to produce accurate results for the last two units. It can be seen, however, that the demand factors decrease with the unit loading order when the required reserves are 40 MW and 60 MW.

Figure 5.4 shows that the UFOP move towards the FOR values with increase in the required reserve. The UFOP for more peaking load units become close to their FOR as the required reserve increases. The changes in the UFOP for the last two units also fluctuate because of the sampling size.

RBTS Case 2 Results

The developed simulation program was applied to the RBTS Case 2. The reliability indices are shown in Table 5.5.

Table 5.5: The reliability indices with various required reserves for the RBTS Case 2

Reserve (MW)	LOLE(hrs/year)	LOEE(MWh/year)	LOLF(occ/year)
0	0.8357	7.0479	0.1812
20	0.9059	8.0636	0.1906
40	0.9889	8.57502	0.206
60	1.1327	10.6455	0.229

The reliability indices for Case 2 also increase with increase in the required reserve. The values in Table 5.5, however, are quite different from the ones in Table 5.3. The differences in the reliability indices for the two cases are due to the different unit loading orders.

The calculated demand factors and the UFOP for all the peaking load units in Case 2 are shown in Table 5.6. It can be seen from this table that the demand factors for the first three units are almost unity when the required reserve is 0 MW. The calculated UFOP of these three units are almost equal to the FOR. This shows that these three peaking load units function as base load units in this case.

The number of peaking load units that function as base load units in Case 2 is different from that in Case 1. This is because the larger units have higher loading priority

in Case 2 compared to that in Case 1.

Table 5.6: The demand factor and the UFOP versus required reserve for the RBTS Case 2

	Required Reserve							
	0 MW		20 MW		40 MW		60 MW	
Unit	**Demand Factor**	**UFOP**	**Demand Factor**	**UFOP**	**Demand Factor**	**UFOP**	**Demand Factor**	**UFOP**
40 H	0.9903	0.01958	0.9910	0.0201	0.9912	0.0203	0.9904	0.0202
40 L	0.9857	0.0295	0.9857	0.0294	0.9872	0.0296	0.9871	0.0296
40 L	0.9868	0.02924	0.9871	0.0296	0.9854	0.0296	0.9874	0.0296
20 H	0.5406	0.00809	0.9937	0.0150	0.9936	0.0149	0.9932	0.0149
20 H	0.4029	0.00597	0.5492	0.0082	0.9932	0.0146	0.9928	0.0142
20 H	0.178	0.00265	0.4037	0.0061	0.5601	0.0083	0.9916	0.0148
20 H	0.1628	0.00273	0.1857	0.0028	0.4098	0.0061	0.5711	0.0087
20 L	0.1584	0.00434	0.1999	0.0048	0.2099	0.0055	0.4256	0.0108
10 L	0.293	0.00696	0.1825	0.0038	0.1921	0.0041	0.2142	0.0044
5 H	0.117	0.00168	0.3057	0.0026	0.1852	0.0018	0.2054	0.0019
5 H	0	0	0.3068	0.0038	0.1848	0.0018	0.2065	0.0019

The demand factors and the UFOP with changes in the required reserve for Case 2 are shown in Figures 5.5 and 5.6 respectively.

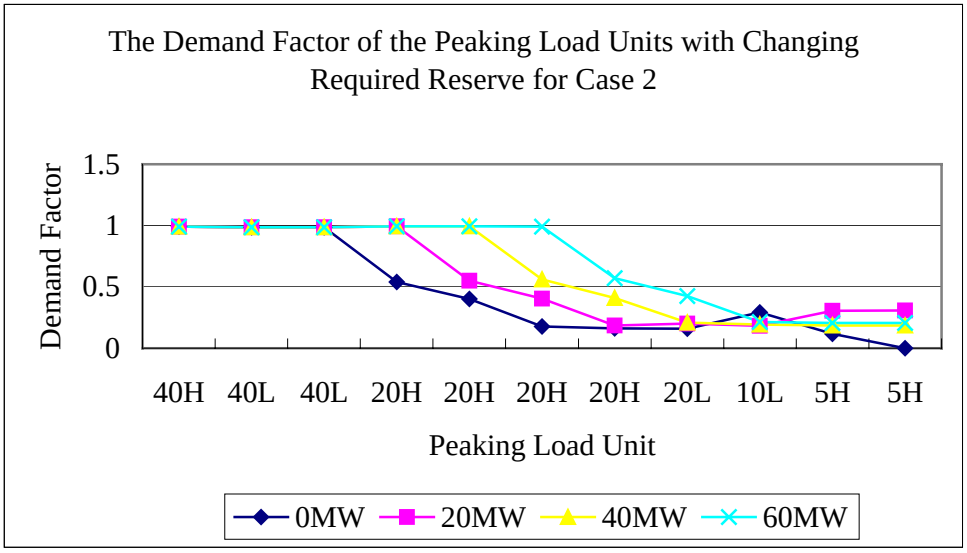

Figure 5.5: The demand factors with various required reserves for the RBTS Case 2

It can be seen from Figure 5.5 that the demand factors for the first eight units move upward with increase in the required reserve while there are fluctuations for the last three units. More peaking load unit demand factors become close to unity when the

required reserve increases. This means that more peaking load units act like base load units with increasing required reserve.

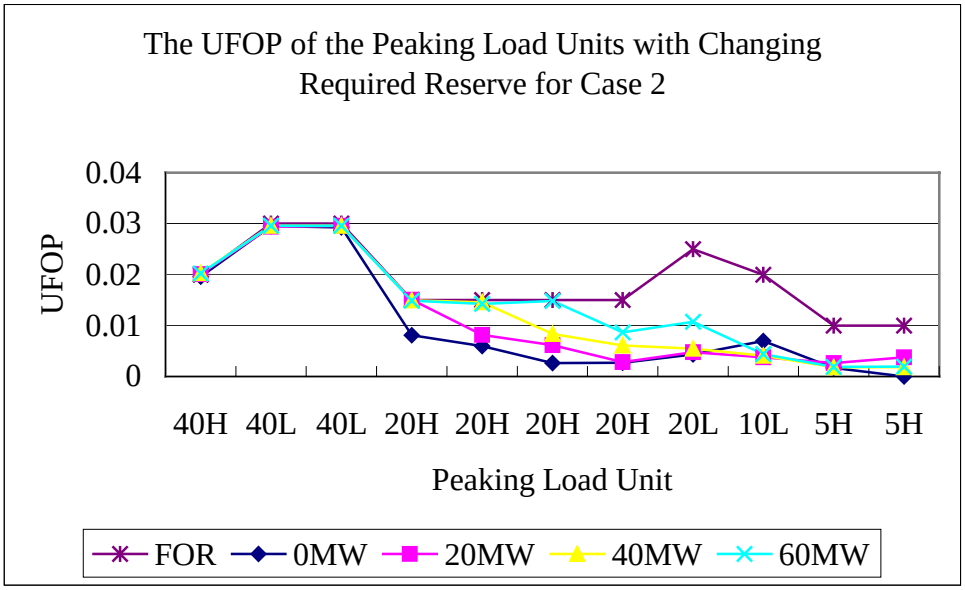

Figure 5.6: The UFOP with various required reserves for the RBTS Case 2

5.3.3 Changes in the Peak Load

The peak loads for the RBTS cases are set to be 185, 195 and 205 MW. The required reserve is 0 MW in this case.

Reliability Indices for RBTS Cases 1 and 2

The reliability indices for the RBTS Cases 0-2 are shown in Table 5.7.

Table 5.7: The reliability indices with various peak loads for the RBTS Cases 0-2

Peak Load (MW)	LOLE (hrs/year)			LOEE (MWh/year)			LOLF (occ/year)		
	Case 0	Case 1	Case 2	Case 0	Case 1	Case 2	Case 0	Case 1	Case 2
185	1.0919	0.3537	0.8357	9.9268	3.3281	7.0479	0.2290	0.0778	0.1812
195	2.5154	1.0952	2.1094	24.6056	11.6046	20.2884	0.5119	0.2274	0.4146
205	5.3529	2.7235	4.1390	56.5399	30.2102	45.1409	1.1060	0.5840	0.8358

It can be seen from Table 5.7 that the reliability indices drop in Cases 1 and 2 compared to Case 0. The reliability indices for Case 1 and Case 2 also have large differences although both cases consider all units to be peaking load units. This is because the larger units have higher loading priorities and function more like base load units in Case 2. The large size units have significant effects on the system reliability

when they are used as peaking load units.

The reliability indices for the three cases increase with increase in the peak load and are shown in Figure 5.7.

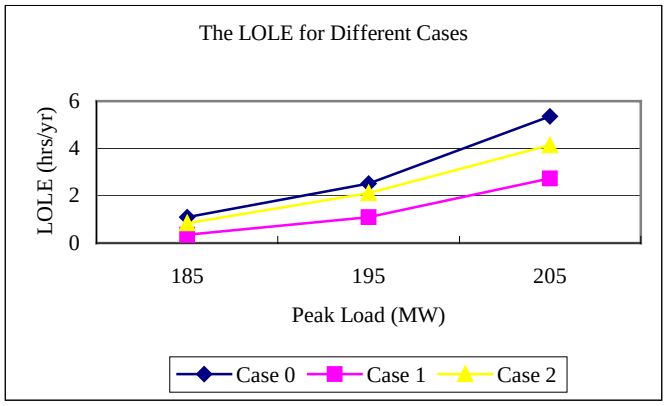

(a) LOLE

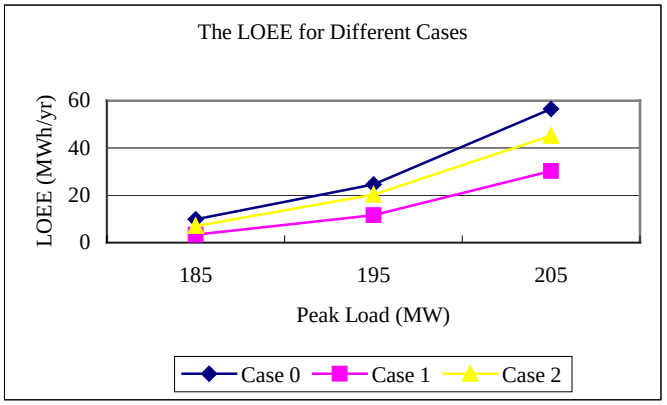

(b) LOEE

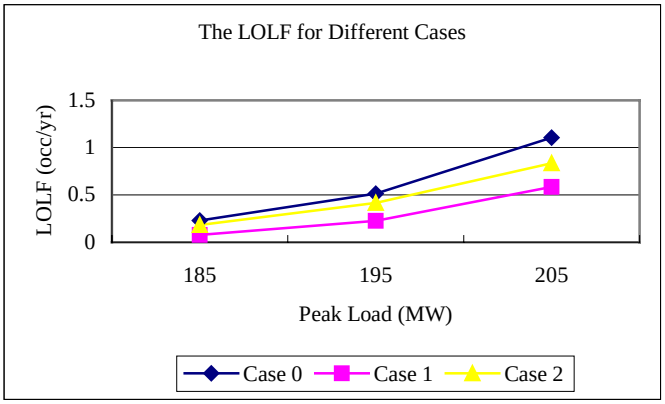

(c) LOLF

Figure 5.7: The reliability indices for various peak loads for the RBTS cases

It can be seen from Figure 5.7 that Case 1 has the smallest rate of increase in the reliability indices when the peak load increases while Case 0 has the largest rate of

increase. This shows that considering the units to be peaking load units slows down the increase in the reliability indices as the peak load increases. The unit loading order also has a significant effect on the system reliability.

The Demand Factors and UFOP for RBTS Case 1

The demand factors and the UFOP for various peak loads are shown in Table 5.8. The demand factors and the UFOP increase with increase in the peak load. The first five units behave almost the same as base load units. This condition continue to exist as the peak load increases.

Table 5.8: The demand factors and UFOP with various peak loads for the RBTS Case 1

Unit	Peak Load					
	185 MW		195 MW		205 MW	
	Demand Factor	UFOP	Demand Factor	UFOP	Demand Factor	UFOP
40 H	0.9906	0.0200	0.9902	0.0199	0.9902	0.0200
20 H	0.9950	0.0149	0.9924	0.0147	0.9922	0.0148
20 H	0.9943	0.0150	0.9919	0.0150	0.9918	0.0148
20 H	0.9941	0.0151	0.9925	0.0148	0.9932	0.0149
20 H	0.9939	0.0147	0.9929	0.0151	0.9923	0.0150
5 H	0.5346	0.0054	0.5998	0.0063	0.6552	0.0068
5 H	0.5047	0.0052	0.5708	0.0060	0.6319	0.0064
40 L	0.4413	0.0135	0.5341	0.0163	0.6016	0.0182
40 L	0.1559	0.0046	0.1722	0.0051	0.2146	0.0066
20 L	0.2563	0.0081	0.1553	0.0041	0.1577	0.0042
10 L	0.2961	0.0048	0.3414	0.0069	0.1707	0.0043

The demand factors and the UFOP are also shown in Figures 5.8 and 5.9 respectively.

It can be seen from Figure 5.8 that the demand factors move upwards with increase in the peak load for the first nine peaking units. Figure 5.8 also shows that the demand factors decrease with the unit loading order. The demand factors for the last two units fluctuate because of the simulation sampling size.

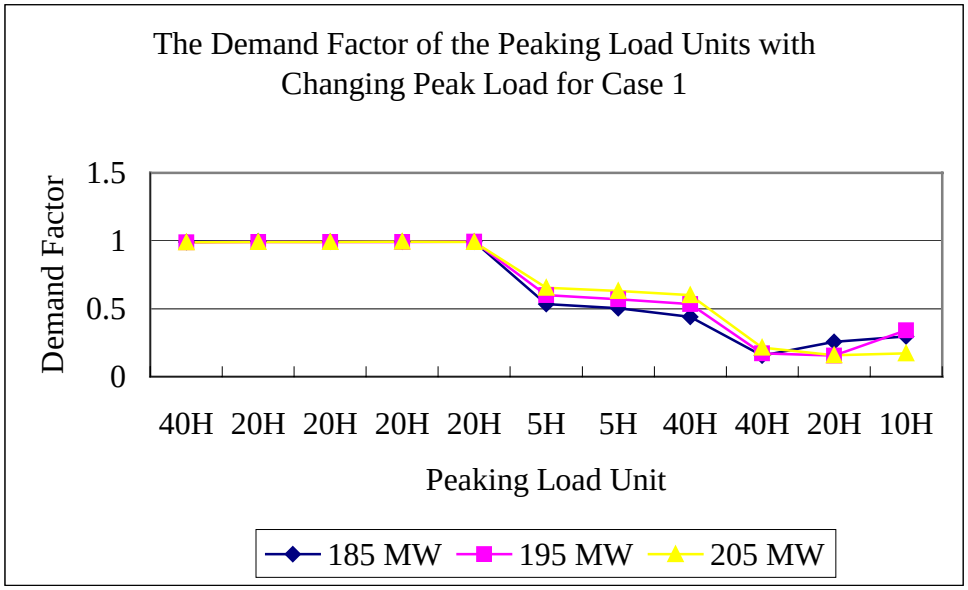

Figure 5.8: The demand factors with various peak loads for the RBTS Case 1

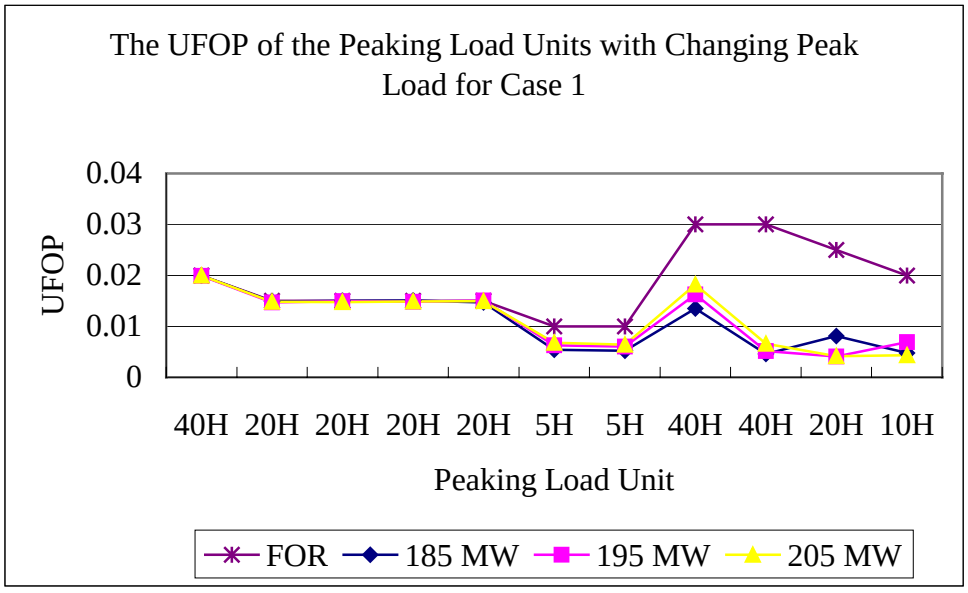

Figure 5.9: The UFOP with various peak loads for the RBTS Case 1

Figure 5.9 shows that the UFOP for the first 9 peaking units move towards the unit FOR values with increase in the peak load. There are fluctuations for the last two units because of the sampling size.

The Demand Factors and UFOP for RBTS Case 2

The demand factors and UFOP for the RBTS Case 2 are shown in Table 5.9.

Table 5.9: The demand factors and the UFOP versus peak load for the RBTS Case 1

Unit	Peak Load					
	185 MW		195 MW		205 MW	
	Demand Factor	UFOP	Demand Factor	UFOP	Demand Factor	UFOP
40 H	0.9903	0.01958	0.9917	0.0200	0.9941	0.0199
40 L	0.9857	0.0295	0.9891	0.0293	0.9901	0.0294
40 L	0.9868	0.02924	0.9896	0.0295	0.9893	0.0294
20 H	0.5406	0.00809	0.5995	0.0091	0.6538	0.0095
20 H	0.4029	0.00597	0.4351	0.0064	0.4833	0.0071
20 H	0.178	0.00265	0.2273	0.0033	0.2915	0.0044
20 H	0.1628	0.00273	0.1642	0.0021	0.1560	0.0022
20 L	0.1584	0.00434	0.1754	0.0044	0.1636	0.0040
10 L	0.293	0.00696	0.1715	0.0047	0.1713	0.0029
5 H	0.117	0.00168	0.4487	0.0028	0.2259	0.0022
5 H	0	0	0.1848	0.0019	0.3545	0.0036

It can be seen that the first three peaking units act like base load units in this case. The demand factors of the other peaking units increase but are not close to unity when the peak load increases. The UFOP of the other nine peaking load units also increase with increase in the peak load but are much less than the FOR. The demand factors and the UFOP are also shown in Figures 5.10 and 5.11 respectively.

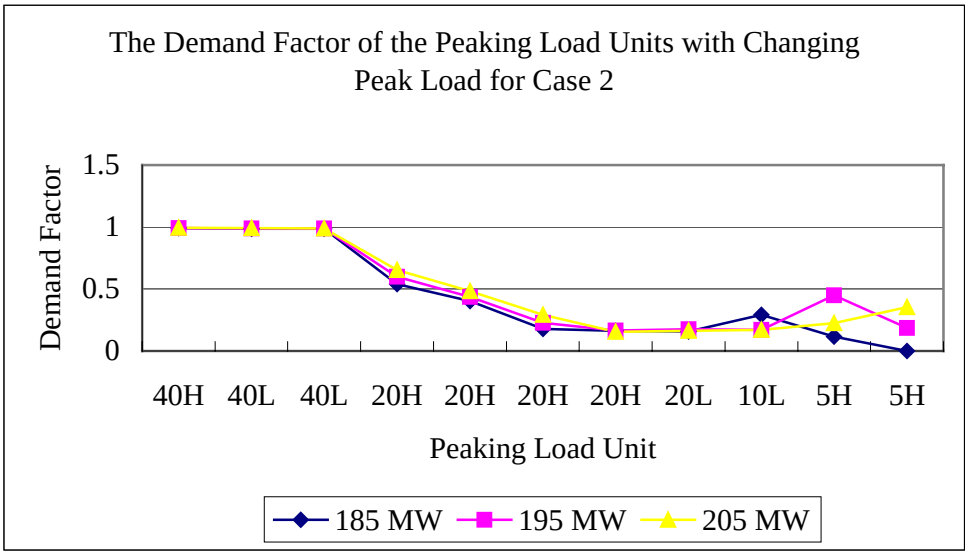

Figure 5.10: The demand factors with various peak loads for the RBTS Case 2

It can be seen from Figure 5.10 that the demand factor moves towards unity with

increase in the peak load. However, the demand factor in this case does not change as much as it did in the required reserve study.

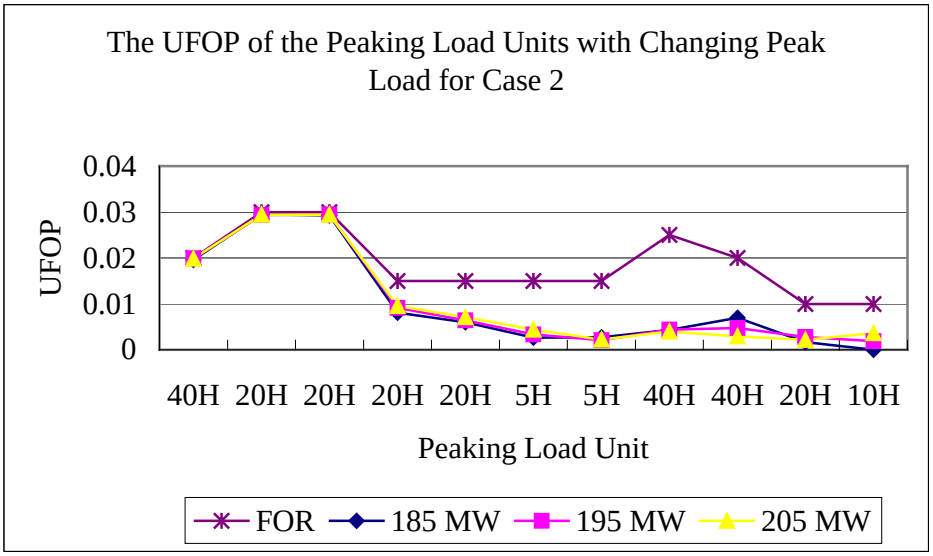

Figure 5.11: The UFOP with various peak loads for the RBTS Case 2

In Figure 5.11, the UFOP of the peaking load units moves towards the FOR. The UFOP do not change as much as they did in the required reserve case. There are fluctuations for the last three peaking units.

5.4 Peaking Load Unit State Residence Time Distributions

The state residence time is assumed to be exponential distributed when the four-state model is used to represent the peaking load unit. This is not necessarily true since the in-need times of the peaking load units are determined by the system available capacity and the load profile. As an example, the in-service time of the peaking load units are determined by the in-need time and the unit reliability data. The developed simulation program can be used to produce the peaking load unit state residence time distributions. The peaking load unit state residence distributions are examined in this section by applying the simulation program to the modified RBTS and the IEEE-RTS. The modified RBTS and IEEE-RTS cases are described in the following. The results are shown and compared later.

5.4.1 Study Cases

The RBTS and the IEEE-RTS were modified to contain some peaking load units.

RBTS Case 3 is the same as Case 2 except that only the last four units are considered to be peaking load units. The capacity of the peaking load units is 16.67% of the total installed capacity of 240 MW.

IEEE-RTS Case 4 sets the 4*20 MW units in the IEEE-RTS to be peaking load units. The reliability data for the 4*20 MW units are: MTTF = 450 hours. MTTR = 50 hours. FOR = 0.1. The capacity of the peaking load units is about 2.35% of the total installed capacity of 3405 MW.

The required reserve is set to be 0 MW in this study. The sampling sizes are 150,000 and 50,000 sampling years for the RBTS Case 3 and the IEEE-RTS Case 4 respectively.

5.4.2 Average State Durations for the Peaking Load Units

RBTS Case 3 Results

The average state durations for the peaking load units in the RBTS Case 3 are shown in Table 5.10.

Table 5.10: Average state durations of the peaking load units in the RBTS Case 3

Unit	Reserve Shutdown (hours)	In Service (hours)	MTTF (hours)	MTTR (hours)	FOR	UFOP
20 L	1278.2110	5.5553	1636.5624	44.2635	0.0263	0.0031
10 L	8378.8411	5.8895	2136.4721	47.3945	0.0217	0.0025
5 H	18512.4040	6.3044	4518.4892	50.9235	0.0111	0.0012
5 H	18514.7815	3.9608	2838.7575	26.6802	0.0093	0.0012

It can be seen from Table 5.10 that the reserve shutdown time increases considerably with the unit loading order. The MTTF, MTTR and the calculated FOR are close to the ones shown in Table 5.2 except for the last peaking unit. This is because the last unit is not needed as much as the first three units and therefore the sampling size is not big enough to obtain an accurate result. The obtained UFOP are much smaller than the FOR.

IEEE-RTS Case 4 Results

The average state durations of the peaking load units in the IEEE-RTS Case 4 are shown in Table 5.11.

Table 5.11: Average state durations of the peaking load units in the IEEE-RTS Case 4

Unit	Reserve Shutdown (hours)	In Service (hours)	MTTF (hours)	MTTR (hours)	FOR	UFOP
1	2682.1689	4.8417	448.8429	51.0905	0.1022	0.0099
2	2682.7196	4.3638	404.5394	44.3474	0.0988	0.0099
3	2683.2120	3.8938	360.9686	42.2709	0.1048	0.0099
4	2683.6498	3.5138	325.7447	36.9037	0.1018	0.0099

The reserve shutdown time in Table 5.11 does not change very much with the loading order. The calculated FOR of the four units are close to the given values as described in Section 5.4.1. The UFOP is much smaller than the FOR.

5.4.3 Distribution of the Total Residence Times in Each State

RBTS Case 3 Results

The class interval width for the reserve shutdown distribution is 24 hrs. Table 5.12 shows the frequencies of the first two and the last reserve shutdown class intervals for the RBTS Case 3.

Table 5.12: The frequency of the first two and the last reserve shutdown class intervals for the RBTS Case 3

Duration (hours)	Frequency			
	20 L	**10 L**	**5 H**	**5 H**
==0	32	64	58	56
0--24	511971	61060	25879	15983
==8760	4826	80220	111751	122612

It can be seen from Table 5.12 that peaking units with high loading priorities are required for more time. The frequency when the reserve shutdown time equals 8760 hrs increases significantly with the loading order. There are many years where the reserve shutdown time is 0 to 24 hrs for the 20L unit. This shows that this unit is required to operate for almost the whole year. There are 122,612 occurrences (81.74% of the total sampling years) for the last 5H unit. This shows that the unit is not needed very much as

it is in the reserve shutdown time for most of the years.

The reserve shutdown time distributions for other intervals are shown in Figure 5.12.

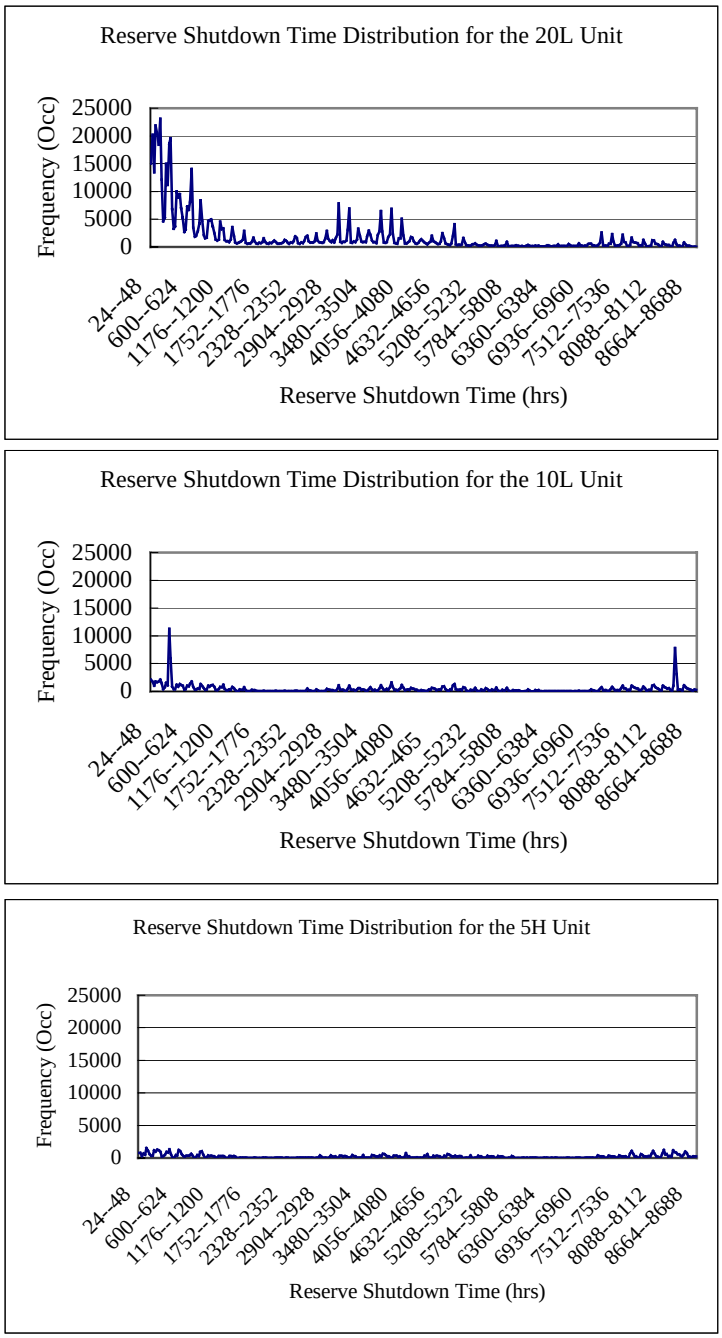

Figure 5.12: The peaking load unit reserve shutdown time distributions for the RBTS Case 3

Figure 5.12 shows that the frequencies when the reserve shutdown time is less than

1200 hrs is relatively high for the 20L unit. The frequency decreases when the reserve shutdown time approaches the value of 8760 hrs. This shows that the 20L unit is needed for most of the time in a year. The frequency when the reserve shutdown time equals 8760 hrs is relatively high for the other three peaking units, which means those three units are not needed for most of the time in a year.

The peaking load unit in-need time distributions for the RBTS Case 3 are shown in Table 5.13.

Table 5.13: The peaking load unit in-need time distributions for the RBTS Case 3

Duration (hours)	**Frequency**			
	20 L	**10 L**	**5 H**	**5 H**
0--1	50026	6846	2971	2342
1--2	106444	15035	7824	4953
2--3	170371	27957	10139	8636
3--4	163359	26859	11047	5465
4--5	121788	12390	5759	4839
5--6	67978	9131	4182	2426
6--7	80067	8270	2473	1427
7--8	17424	3683	2493	1600
8--9	16388	5033	2634	1908
9--10	14927	4618	1995	1146
10--11	11621	3666	2086	1045
11--12	28923	4783	2486	1900
12--13	75208	12777	6616	4156
13--14	48491	7206	5102	3010
14--15	21727	4128	1476	724
15--16	18776	3365	1268	842
16--17	6527	436	173	89
17--90	3390	530	231	135

Figure 5.13 shows the peaking load unit in-need time distributions for the 20L, 10L and the first 5H units in Case 3. The class interval is 1 hour for these distributions. The last interval shows the cumulative frequency when the in-need time is larger than 17 hours.

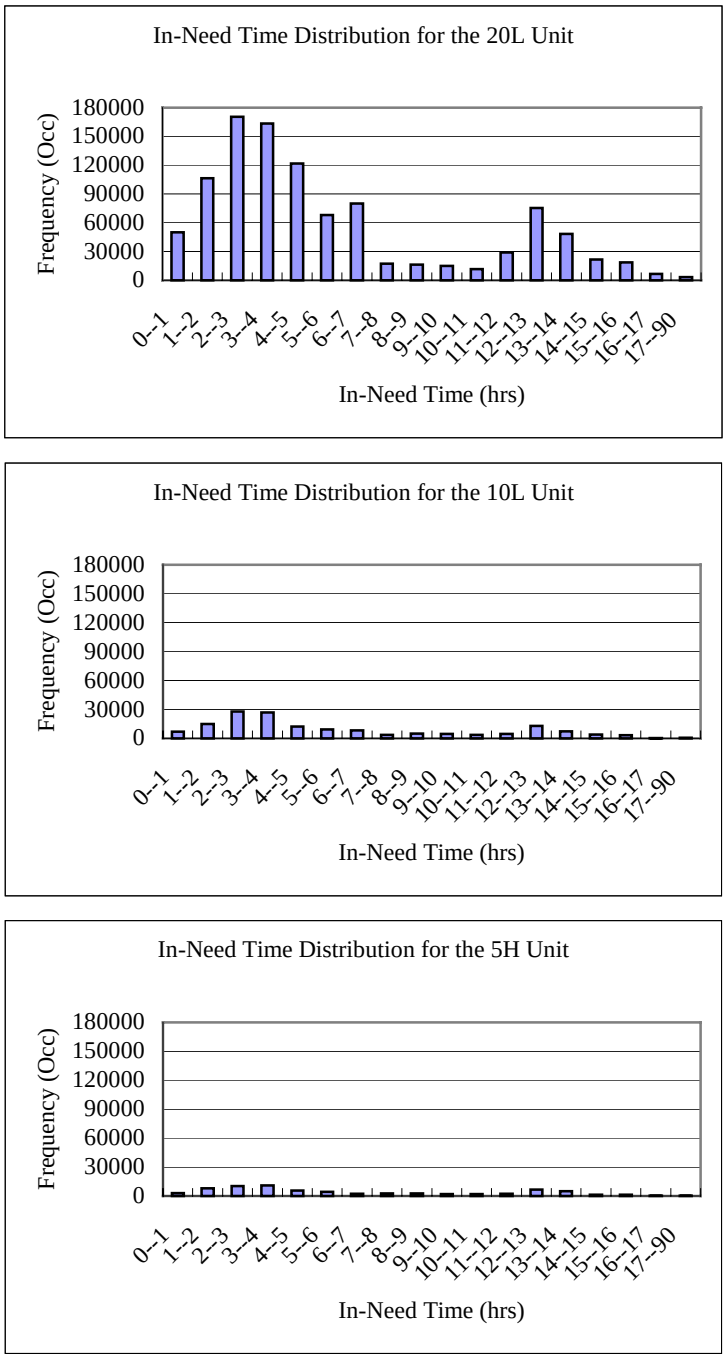

Figure 5.13: The peaking load unit in-need time distributions for the RBTS Case 3

It can be seen from Figure 5.13 that the in-need time is not exponentially distributed. The in-need time distributions for the three peaking units have similar shapes but with different magnitudes.

The peaking load unit in-service time distributions for the RBTS Case 3 are shown in Table 5.14. The class interval width is 1 hour in this case.

Table 5.14: The peaking load unit in-service time distributions for the RBTS Case 3

Duration (hours)	Frequency			
	20 L	**10 L**	**5 H**	**5 H**
0--1	50737	6930	2988	2352
1--2	106965	15097	7839	4964
2--3	170627	27995	10147	8643
3--4	163394	26873	11045	5469
4--5	121737	12383	5765	4841
5--6	67953	9129	4183	2425
6--7	79930	8279	2476	1430
7--8	17513	3695	2498	1600
8--9	16469	5027	2637	1907
9--10	15001	4618	1994	1145
10--11	11689	3662	2086	1049
11--12	28860	4781	2482	1895
12--13	74730	12724	6596	4143
13--14	48174	7152	5092	3002
14--15	21557	4106	1476	724
15--16	18582	3342	1258	837
16--17	50737	6930	2988	2352
17--90	3364	527	231	135

It can also be seen by comparing Table 5.14 with Table 5.13 that the frequency of the in-service time is larger than that of the in-need time when the duration is short. The frequency of the in-service time will be less than that of the in-need time when the duration increases. This is because a unit may fail during the in-need time especially when it is required for a long time.

The first three peaking unit in-service time distributions in the RBTS Case 3 are also shown in Figure 5.14. The last interval represents the cumulative frequency when the in-service time is larger than 17 hours.

It can be seen from Figure 5.14 that the frequency decreases with the unit loading order because a unit with lower loading priority is required for less time. Figures 5.13 and 5.14 show that the shape and the magnitude of the in-service time distributions are similar to those of the in-need time distributions.

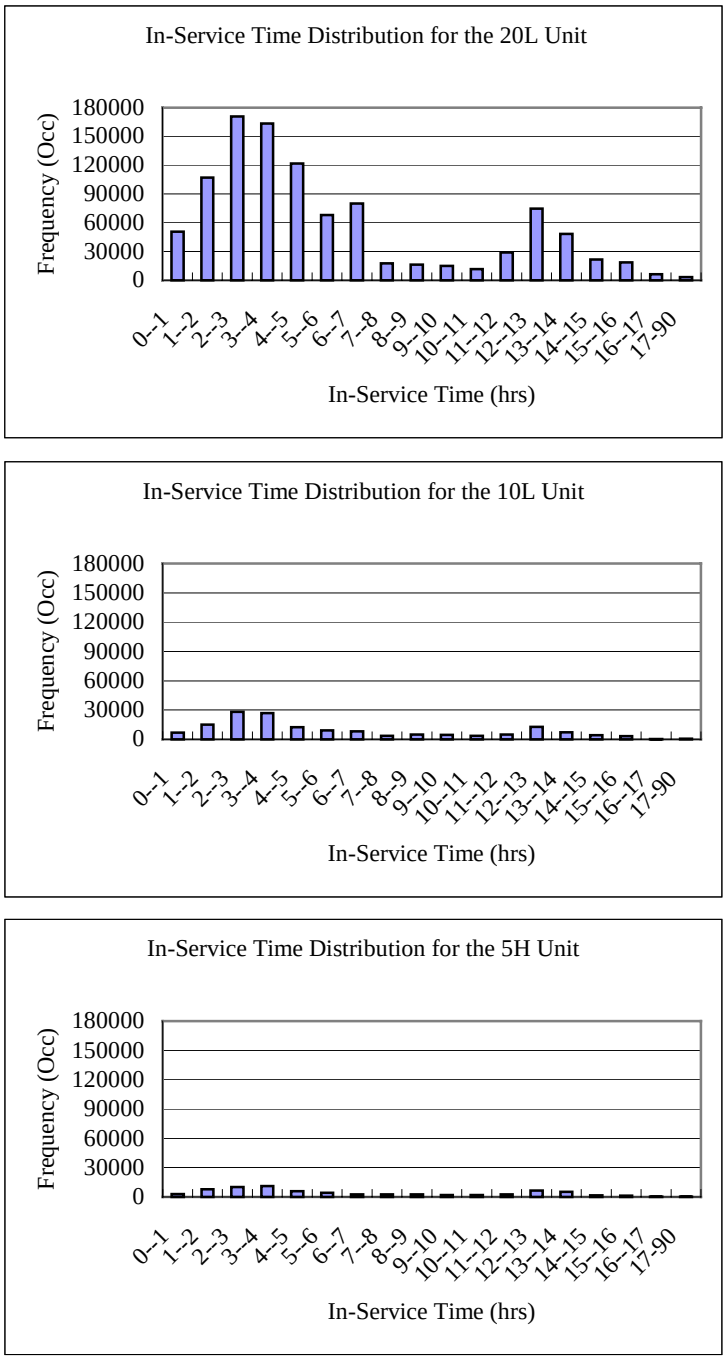

Figure 5.14: The peaking load unit in-service time distributions for the RBTS Case 3

The forced out when needed time distributions for the RBTS Case 3 are shown in Table 5.15. The class interval width for the forced out when need state is 1 hour.

The frequency of the forced out when needed state is much less than that of the in-service time or the in-need time. This is because peaking load units are relatively reliable and the probability that a peaking unit fails during the in-need time is small.

Table 5.15: The peaking unit forced out when needed distributions for the RBTS Case 3

Duration (hours)	**Frequency**			
	20 L	**10 L**	**5 H**	**5 H**
0--1	706	88	8	10
1--2	643	74	26	8
2--3	544	65	17	14
3--4	387	55	9	5
4--5	282	40	10	6
5--6	220	35	9	5
6--7	149	16	9	3
7--8	143	24	10	4
8--9	136	39	5	4
9--10	122	23	2	5
10--11	107	16	7	7
11--12	99	11	3	3
12--13	69	12	2	4
13--14	44	9	2	3
14--15	24	2	0	0
15--65	16	1	1	1

The forced out when needed distributions for the first three peaking units are shown in Figure 5.15. The last interval represents the cumulative frequency when the forced out when needed time is larger than 15 hours.

It can be seen that the frequency decreases significantly with the loading order. This is because a peaking load unit with a lower loading priority is not needed as often, and for as long as a unit with a higher loading priority. The probability that a unit fails during the in-need period decreases as the in-need time decreases. It is also worth noting that the range of the forced out when needed state time is smaller than that of the in-need time.

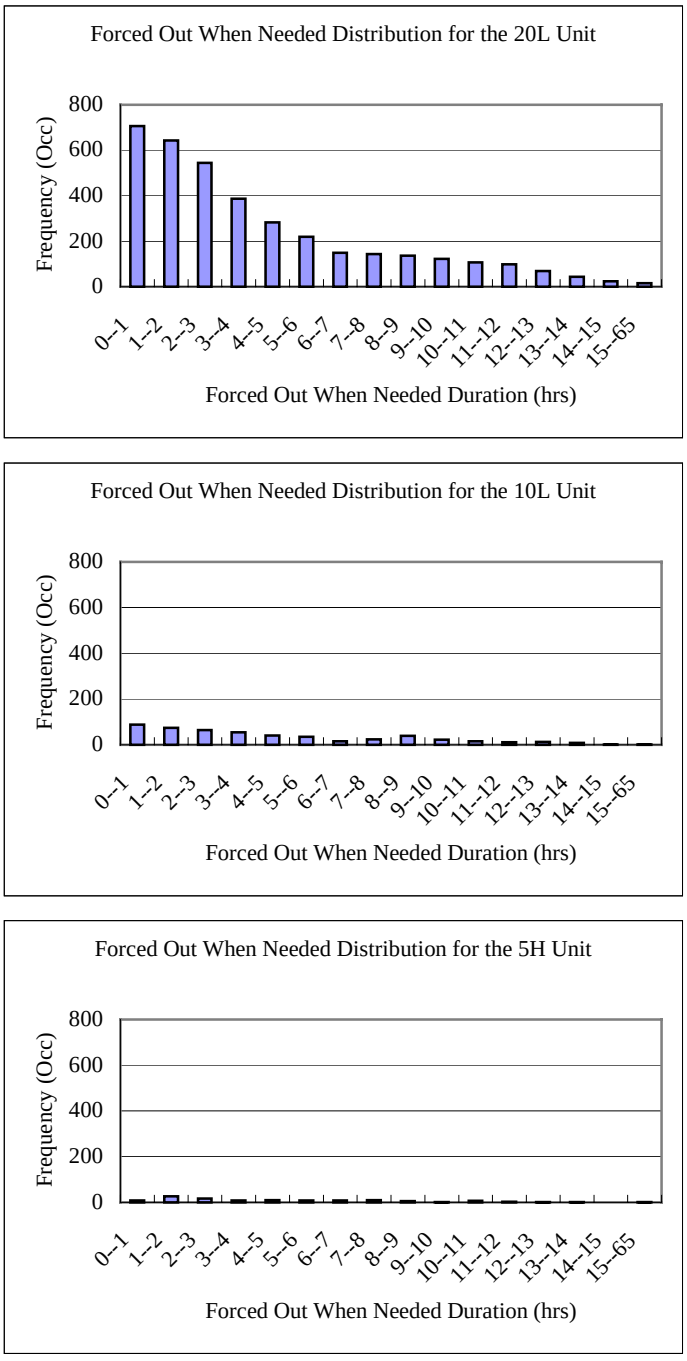

Figure 5.15: The peaking unit forced out when needed distributions for the RBTS Case 3

The peaking load units forced out but not needed distributions are shown in Figure 5.16. The range of the forced out but not needed distribution is much bigger than that of the forced out when needed distribution. The frequency of the forced out but not needed state decreases considerably with the loading order.

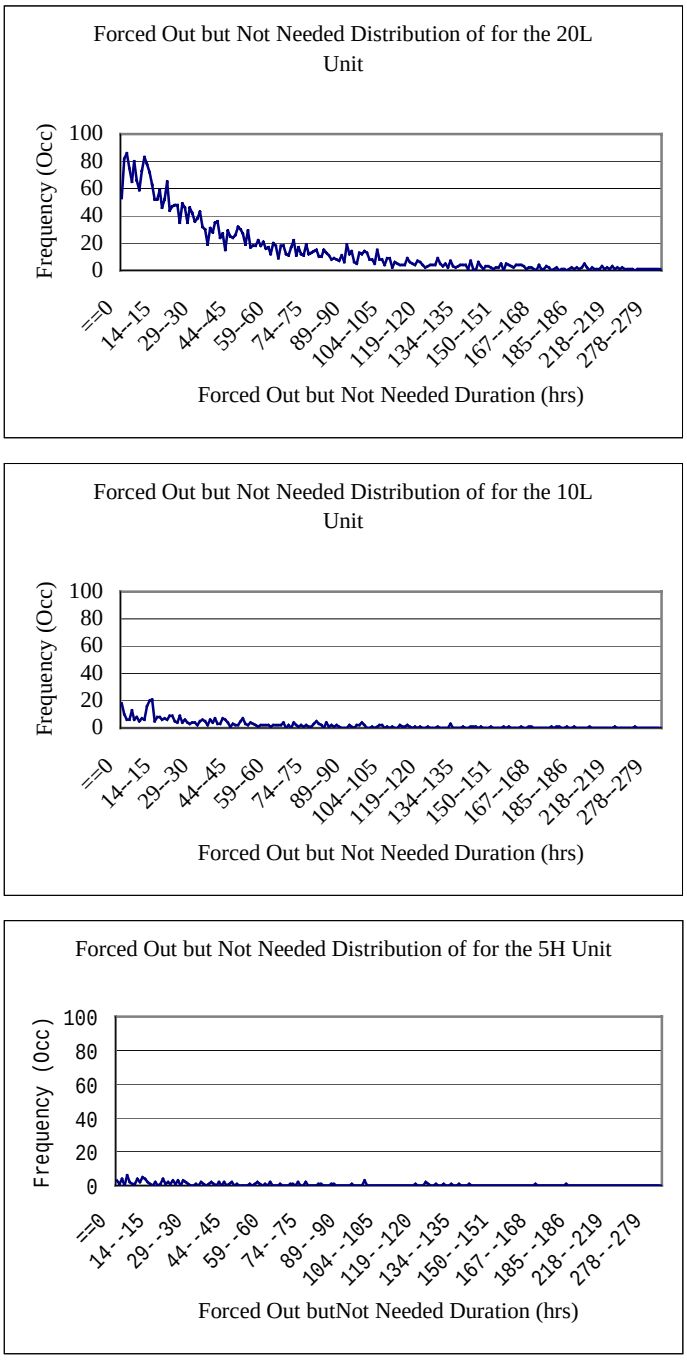

Figure 5.16: The peaking load unit forced out but not needed distributions for the RBTS Case 3

IEEE-RTS Case 4 Results

The class interval width for the reserve shutdown distribution is 24 hrs. Table 5.16 shows the frequencies of the first two and the last class intervals of reserve shutdown for the IEEE-RTS Case 4.

It can be seen from Table 5.16 that the frequency increases with the loading order when the reserve shutdown duration is 8760 hours. Peaking units 1, 2, 3 and 4 are not needed in 26.81%, 30.82%, 35.74% and 39.44% of the total 50,000 sampling years.

Table 5.16: The frequency of the first two and the last class intervals of reserve shutdown for the IEEE-RTS Case 4

Duration (hours)	**Frequency**			
	Unit 1	**Unit 2**	**Unit 3**	**Unit 4**
==0	198	99	21	20
0--24	87913	73021	59084	48520
==8760	13407	15412	17868	19722

The frequencies of the other class intervals are shown in Figure 5.17.

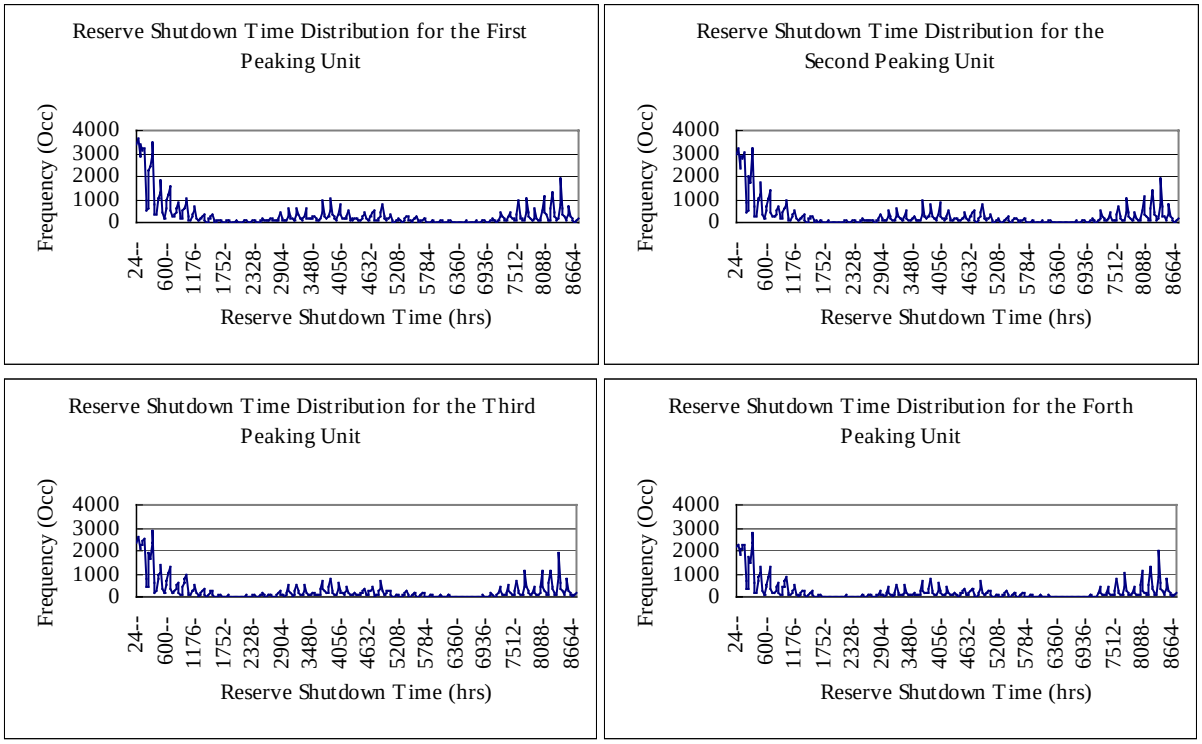

Figure 5.17: The peaking load unit reserve shutdown time distributions for the IEEE-RTS Case 4

Figure 5.17 shows that the frequency decreases gradually with the loading order. It does not change as fast as in the RBTS Case 3. This is because of the different generation compositions in the two systems. The proportional capacity of the peaking load in percent of the total installed capacity is different in the two systems. The shapes of the reserve shutdown distributions for the four peaking units are similar.

The peaking units in-need time distributions for the IEEE-RTS Case 4 are shown in Table 5.17. It can be seen from this table that the frequency of the in-need time decreases with the peaking unit loading order.

Table 5.17: The peaking load unit in-need time distributions for the IEEE-RTS Case 4

Duration (hours)	**Frequency**			
	Unit 1	**Unit 2**	**Unit 3**	**Unit 4**
0--1	12408	9371	7289	5810
1--2	16935	14556	11480	9470
2--3	30622	25177	19998	17953
3--4	28215	23426	17811	12089
4--5	17115	17059	16799	16612
5--6	12701	8082	5172	3369
6--7	11348	8808	5724	3529
7--8	2849	3362	3714	3989
8--9	3205	3137	2852	3034
9--10	2589	2124	1985	1627
10--11	1435	1447	1455	1278
11--12	3252	3327	3358	3213
12--13	8677	8866	8933	8834
13--14	6562	6488	6577	6400
14--15	3199	2971	2569	2377
15--16	1622	1408	1294	1202
16--17	181	172	142	128
17--41	58	55	46	33

It can be seen by comparing Table 5.17 with Table 5.13 that the ranges of the in-need time for the RBTS Case 3 and the IEEE-RTS Case 4 are different. The in-need time is determined by both the generation system and the load profile. Although Cases 3 and 4 share the same normalized load profile, the generation compositions are different.

The in-need time distributions for Case 4 are also shown in Figure 5.18. The class interval width is 1 hour in this case. The last interval represents the cumulative frequency when the in-need time is between 17 to 41 hours. It can be seen from Figure 5.18 that the shapes of the in-need time distributions for the four units are similar. The magnitudes of the four distributions again decrease with the loading order.

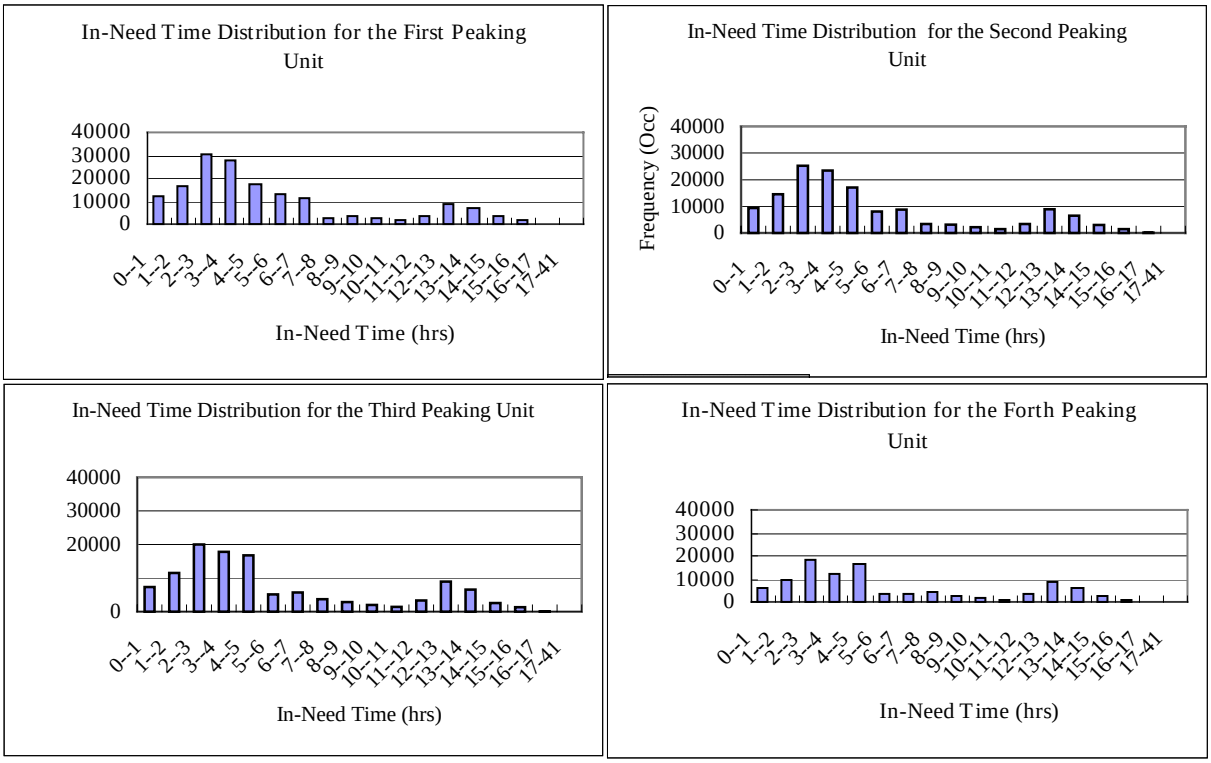

Figure 5.18: The peaking load unit in-need time distributions for the IEEE-RTS Case 4

The peaking load unit in service distributions for Case 4 are shown in Table 5.18.

The in-service time distributions and the in-need time distributions are similar. It can be seen by comparing Table 5.18 with Table 5.17 that the frequency of the in-service time is larger than that of the in-need time. The in-need time and in-service time distributions should be the same if the peaking load units are 100% reliable.

The difference in the frequencies of the in-need time and in-service time is bigger in the IEEE-RTS Case 4 than in the RBTS Case 3. This is because the peaking load units in Case 4 have relatively higher unavailabilities than in Case 3.

The in-service time distributions for the four peaking load units in the IEEE-RTS Case 4 are also shown in Figure 5.19. The class interval width is 1 hour. The last interval represents the cumulative frequency when the in-service time is between 17 hrs and 41 hours. It can be seen from Figure 5.19 that the frequency decreases gradually with the peaking load unit loading order.

Table 5.18: The peaking load unit in-service time distributions for the IEEE-RTS Case 4

Duration (hours)	Frequency			
	Unit 1	**Unit 2**	**Unit 3**	**Unit 4**
0--1	12763	9667	7535	6042
1--2	17221	14768	11712	9670
2--3	30730	25293	20119	18041
3--4	28209	23454	17822	12148
4--5	17101	17054	16789	16526
5--6	12673	8080	5200	3434
6--7	11284	8770	5732	3556
7--8	2881	3389	3738	3989
8--9	3222	3148	2851	3042
9--10	2587	2125	2008	1645
10--11	1459	1445	1456	1301
11--12	3239	3275	3338	3176
12--13	8451	8680	8715	8624
13--14	6382	6314	6377	6232
14--15	3094	2899	2486	2306
15--16	1573	1369	1256	1165
16--17	177	164	135	123
17--41	55	53	46	33

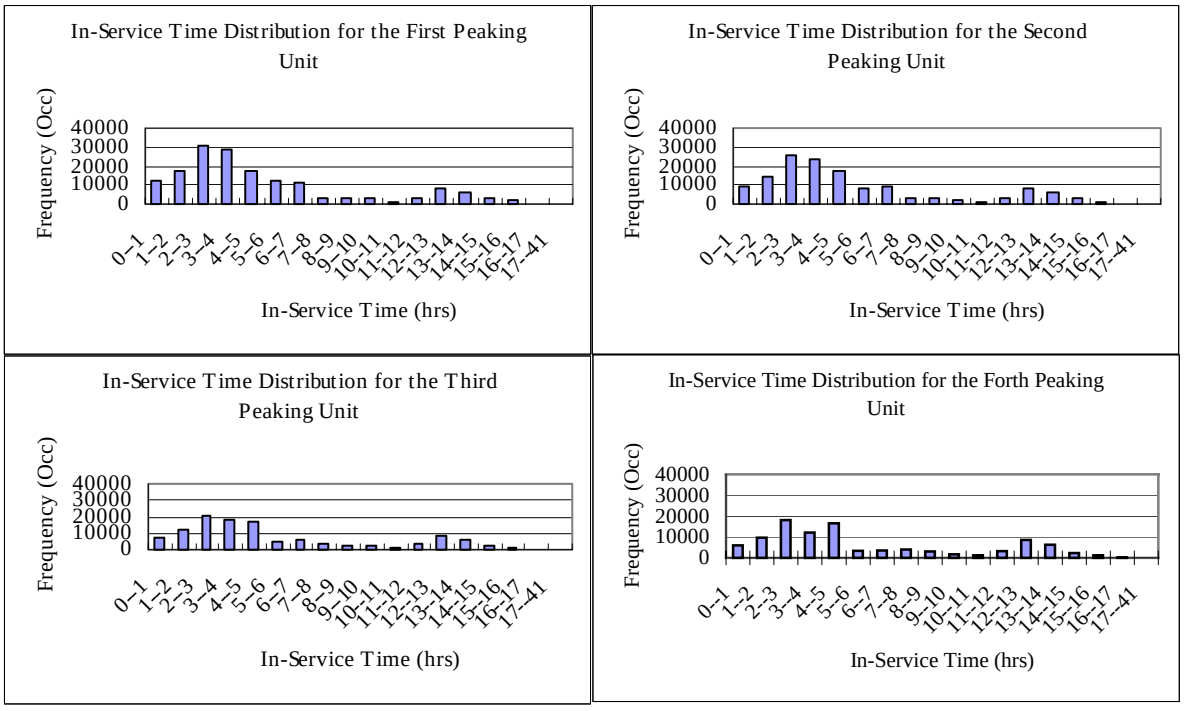

Figure 5.19: The peaking load unit in-service time distributions for the IEEE-RTS Case 4

The peaking load unit forced out when needed distributions are shown in Table 5.19.

Table 5.19: The peaking load unit forced out when needed distributions for the IEEE-RTS Case 4

Duration (hours)	**Frequency**			
	Unit 1	**Unit 2**	**Unit 3**	**Unit 4**
0--1	447	404	361	289
1--2	392	368	297	276
2--3	411	306	324	280
3--4	297	251	235	235
4--5	352	279	258	216
5--6	130	135	136	98
6--7	116	77	102	105
7--8	104	90	103	93
8--9	96	79	80	96
9--10	72	55	81	74
10--11	75	73	71	50
11--12	70	68	82	64
12--13	121	120	123	112
13--14	88	75	80	56
14--15	37	29	47	23
15--18	28	28	18	21

It can be seen from Table 5.19 that the frequency at a certain forced out but not needed duration decreases with the peaking unit loading order. It can also be seen by comparing Table 5.19 with Table 5.17 that the range of the forced out when needed duration is narrower than that of the in-need time.

The forced out but not needed distributions are shown in Figure 5.20. The class interval width is 1 hour. The last class interval represents the cumulative frequency when the forced out when needed duration is between 15 and 18 hours.

It can be seen from Figure 5.20 that the shapes of the distributions for the four units are similar. The magnitude of the distributions decreases gradually with the unit loading order.

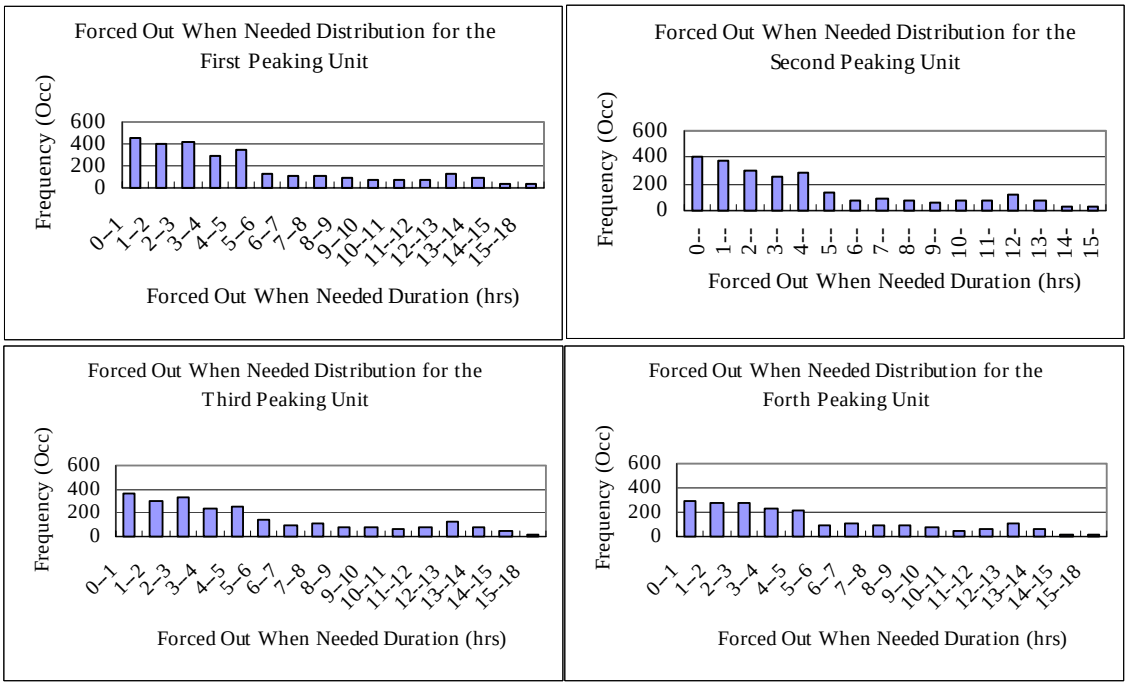

Figure 5.20: The peaking load unit forced out when needed distributions for the IEEE-RTS Case 4

The peaking unit forced out but not needed distributions are shown in Figure 5.21.

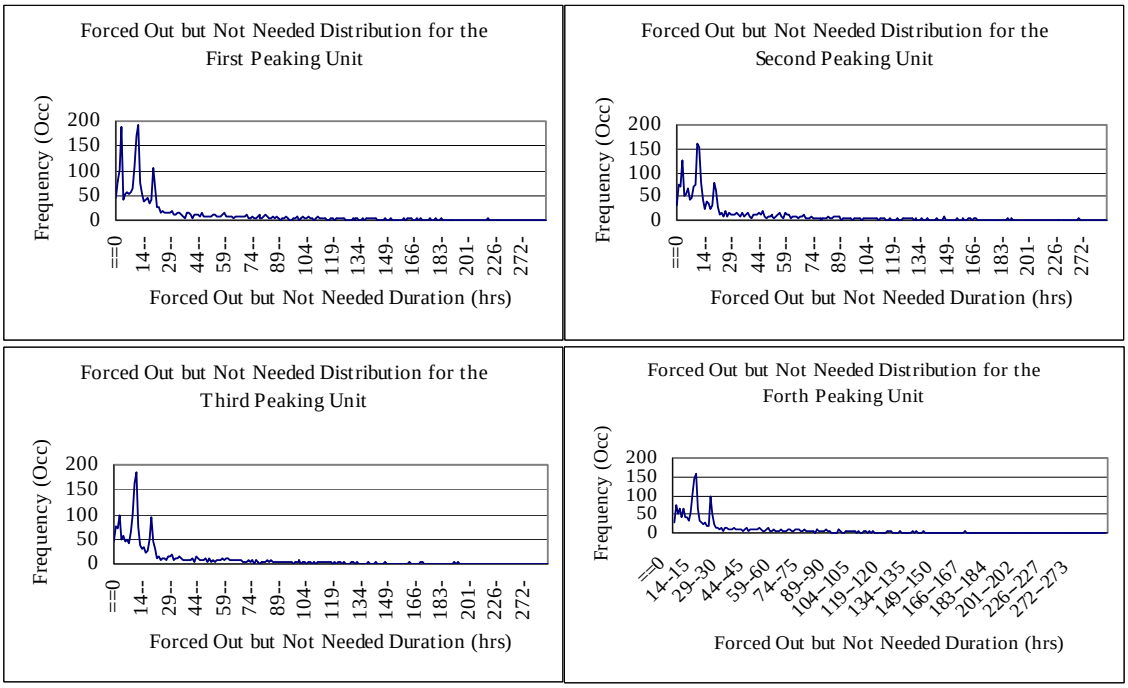

Figure 5.21: The peaking load unit forced out but not needed distributions for the IEEE-RTS Case 4

The maximum forced out but not needed duration is about 413 hours, which is larger than that of the forced out when needed state. The frequency decreases with the unit loading order, but the shapes of the distributions remain almost the same.

5.4.4 The Effect of the Unit Weibull Distributed Repair Time Shape Parameters on the Peaking Unit State Residence Time Distributions

The RBTS Case 3 is used in this study. The peak load is 185 MW and the required reserve is 0 MW. The repair times of the four peaking units are assumed to follow Weibull distributions. The Weibull distribution shape parameters used are 0.5, 1, 2 and 4. The Weibull distribution scale parameter is set to keep the mean value of the repair time constant. The calculation of the scale parameter is the same as in Table 4.1. The sampling size in the simulation program is 150,000 sampling years for this study.

The 20L unit reserve shutdown distributions with varying shape parameters are shown in Figure 5.22. Table 5.20 shows the first two intervals and the last interval of the distribution.

Table 5.20: The frequency of the first two and last classes of reserve shutdown for the 20L Unit in the RBTS Case 3 with varying shape parameters

Duration (hours)	**Frequency**			
	$\beta = 0.5$	$\beta = 1$	$\beta = 2$	$\beta = 3$
==0	32	32	44	46
0--24	511230	511971	511654	511277
==8760	4779	4826	4923	4875

It can be seen from Table 5.42 that the frequencies of the reserve shutdown times for various shape parameters are very similar.

The reserve shutdown time distributions for the other class intervals of the 20L unit with changing shape parameters are shown in Figure 5.22. The class interval width is 24 hours. It can be seen that the reserve shutdown time distributions with changes in the Weibull distribution shape parameters remain almost the same. This is because the reserve shutdown time of the peaking load units is mainly determined by the load data and the generated capacity due to the base load units.

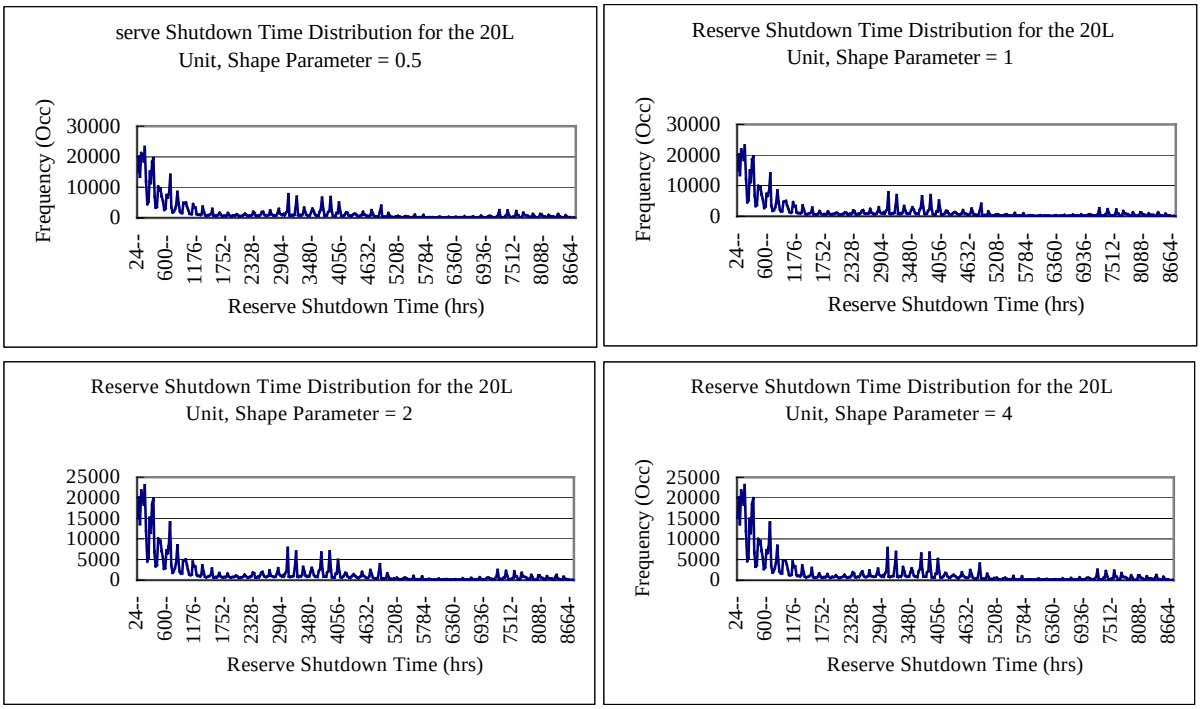

Figure 5.22: The 20L unit reserve shutdown time distribution versus shape parameter

The 20L peaking unit in-need time distributions for various Weibull shape parameters are shown in Table 5.21.

The frequencies for the four shape parameters are similar for each class interval. The shape, the magnitude and the range of the in-need time distributions for the four shape parameters are almost the same. This is because the in-need time of the peaking load units is mainly determined by the available capacity associated with the base load units, and the load data.

The 20L peaking unit in-need time distributions with changes in the shape parameters are also shown in Figure 5.23. The class interval width is 1 hour and the last class interval in Figure 5.23 represents the cumulative frequency when the in-need time is larger than 17 hours.

The peaking load unit in-service time distributions are almost the same as the in-need time distributions and are not shown in this section.

Table 5.21: The 20L unit in-need time distributions versus shape parameter

Duration (hours)	Frequency			
	$\beta = 0.5$	$\beta = 1$	$\beta = 2$	$\beta = 3$
0--1	50063	50026	50027	50125
1--2	106514	106444	106725	106382
2--3	169601	170371	169728	169911
3--4	163526	163359	163511	163417
4--5	122105	121788	121936	122251
5--6	68319	67978	68263	67353
6--7	80078	80067	80339	79879
7--8	17510	17424	17296	17372
8--9	16437	16388	16412	16363
9--10	14597	14927	14875	15033
10--11	11620	11621	11547	11620
11--12	28961	28923	28682	28990
12--13	74966	75208	75836	75270
13--14	48624	48491	48798	49138
14--15	21542	21727	21642	21751
15--16	18173	18776	18467	18699
16--17	6327	6527	6325	6392
>17	3182	3390	3417	3386

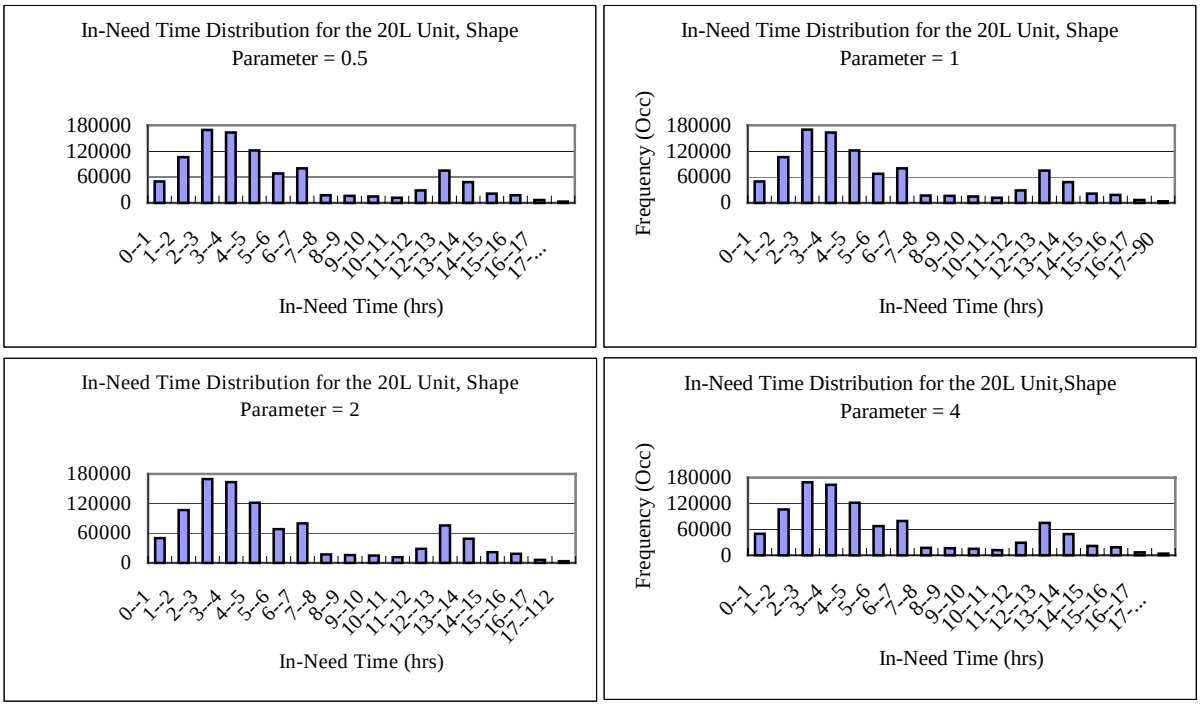

Figure 5.23: The 20L unit in-need time distribution versus shape parameter

The forced out when needed distributions for the 20L peaking load unit with changes in the Weibull shape parameter are shown in Table 5.22. The time that the unit resides in the forced out state is directly affected by the repair time distribution. It can be seen from Table 5.22 that the frequency of the first class interval drops with increase in the shape parameter.

Table 5.22: The 20L unit forced out when needed distribution versus shape parameter

Duration (hours)	Frequency			
	$\beta = 0.5$	$\beta = 1$	$\beta = 2$	$\beta = 3$
0--1	1084	706	637	623
1--2	590	643	571	527
2--3	417	544	470	482
3--4	252	387	373	371
4--5	210	282	287	276
5--6	158	220	244	214
6--7	114	149	145	173
7--8	115	143	144	170
8--9	83	136	130	141
9--10	58	122	127	131
10--11	66	107	119	117
11--12	51	99	103	106
12--13	40	69	100	92
13--14	27	44	31	42
14--15	12	24	25	41
>15	6	16	23	21

The forced out when needed distributions are also shown in Figure 5.24. The class interval width is 1 hour and the last interval represents the cumulative frequency when the forced out when needed time is larger than 15 hours. It can be seen that the frequency decreases relatively quickly when the shape parameter is 0.5. The range of the distribution when the shape parameter is equal to 0.5 is smaller than that for the other three conditions.

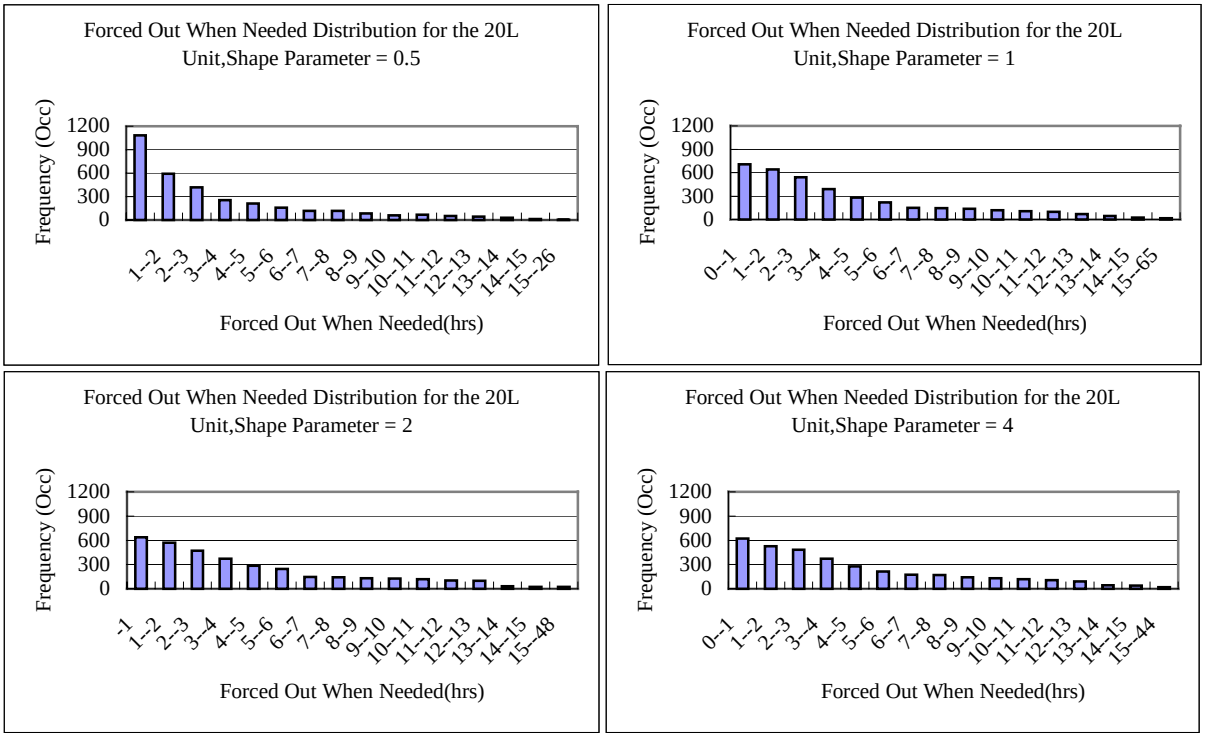

Figure 5.24: The 20L unit forced out when needed distribution versus shape parameter

The forced out but not needed distributions for various shape parameters are shown in Figure 5.25.

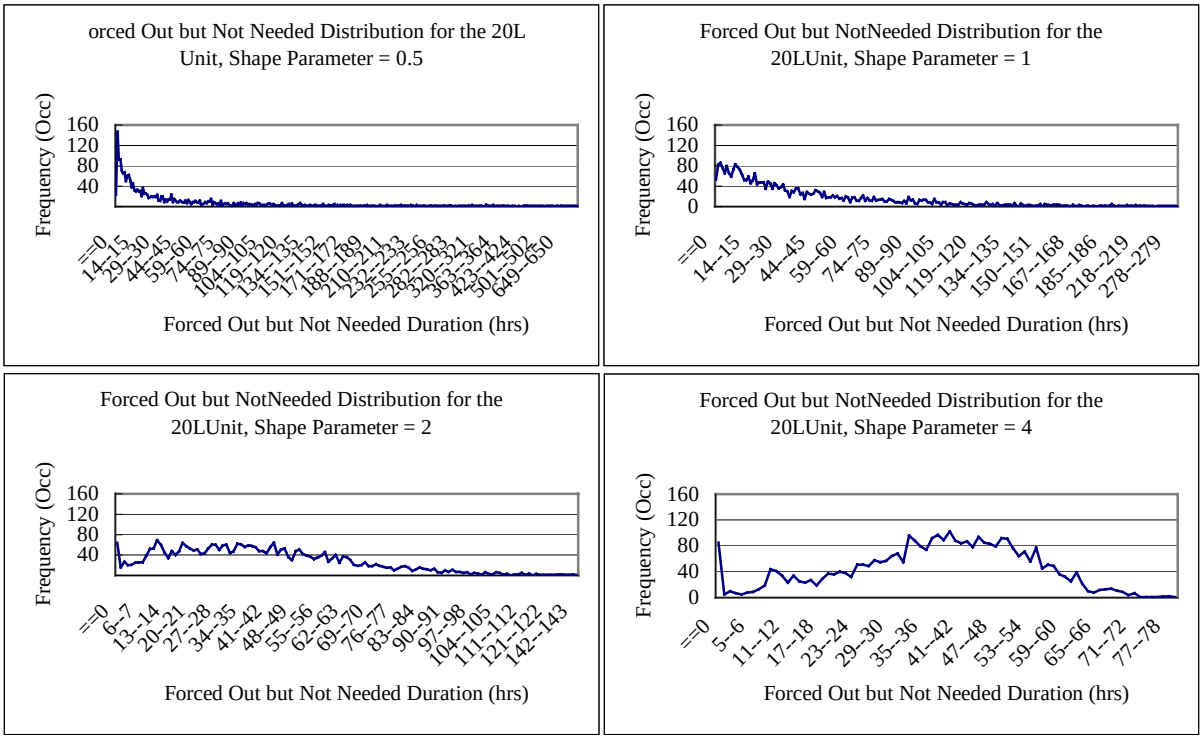

Figure 5.25: The 20L unit forced out but not needed distribution versus shape parameter

It can be seen from Figure 5.25 that the mode of the distribution moves to the right with increase in the shape parameter. The range of the forced out but not needed distribution decreases with increase in the shape parameter.

5.5 Conclusion

The peaking load units and base load units have different operating characteristics. The four-state model is normally used to represent peaking load units and the conventional two-state model is usually applied to base load units.

The RBTS was modified by considering all units to be peaking load units. The effect of system conditions on the UFOP is examined in this chapter by applying the developed simulation program to the modified RBTS to perform a detailed study.

The results show that:

Increasing the required reserve results in higher peaking load unit operating times and therefore more peaking load units act like base load units. The demand factors of the peaking load units move towards unity with increasing required reserves. The demand factor of a peaking load unit decreases with the peaking unit loading order. The UFOP of the peaking load units move towards the FOR with increase in the required reserve. The UFOP is almost equal to the FOR when the demand factor is close to unity. A peaking load unit has a larger UFOP when it is given a higher loading priority.

The peaking unit loading order affects the system reliability. System reliability indices such as the LOLE, LOEE and LOLF decrease when the larger units have lower loading priorities.

Both the demand factors and the UFOP of the peaking load units increase with increase in the peak load. The rate of increase in this case is different from the rate with increase in the required reserve. The peaking load units slow down the rate of increase of the reliability indices such as the LOLE, LOEE and LOLF when the peak load increases.

The peaking load unit state residence time distributions in the four-state model are

normally assumed to be exponential. The RBTS and the IEEE-RTS are modified to contain peaking load units in Cases 3 and 4. The unit state residence time distributions are illustrated and show that:

The frequency of the reserve shutdown time at the value of 8760 hrs is relatively high for peaking loading units with low loading priority. The shapes of the peaking unit reserve shutdown time distributions for other class intervals are similar but the magnitude of the distributions decrease with the loading order.

The peaking load unit in-need time distributions are mainly determined by the load data and the available system capacity of the base load units. The distributions are not exponential and the frequencies decrease with the loading order. The peaking load unit in-service time distributions are almost the same as the in-need time distributions. This is because the peaking load units are started when they are needed and the units are relatively reliable.

The in-need time also significantly affects the unit forced out when needed distributions. The ranges of the forced out when needed distributions are narrower than those of the in-need time distributions. The ranges of the peaking unit forced out but not needed distributions are larger than those of the forced out when needed distributions. This is because the forced out but not needed time durations are more dependent on the unit characteristics. The frequencies of the forced out when needed and forced out but not needed durations decrease with the loading order. This is because the peaking load units with lower loading priority are not needed as often and for as long as the units with higher loading priorities. The shorter the in-need time is, the less probable that a unit will fail during this period.

The frequency decrease rates of the unit state residence time distributions with loading order are different for the two test systems. This is because of the different system generation compositions and the different proportions of peaking load units in the installed capacities.

The RBTS was modified to include peaking load units with Weibull distributed repair times with various shape parameters. The peaking unit state residence time distributions were examined by applying the simulation program to the modified RBTS. The results show that:

The unit reserve shutdown time distributions, in-need time distributions and in-service time distributions remain almost the same when the shape parameter is changed from 0.5 to 4. These distributions are mainly dependent on the load data and the available system capacity of the base load units.

The forced out when needed distributions and the forced out but not needed distributions change significantly for the various Weibull shape parameters. The frequency of the forced out when needed duration decreases relatively quickly when the shape parameter is equal to 0.5. The ranges of the forced out but not needed distributions decrease when the shape parameter increases. The mode of the distribution moves to the right with increase in the shape parameter.

The studies shown in this chapter on the four-state model used to represent peaking load units in generating capacity reliability evaluation are extended in the next chapter. The application of the UFOP and DAUFOP statistics using the analytical method are illustrated by application to the RBTS and the IEEE-RTS.

6. THE UFOP AND THE DAUFOP

6.1 Introduction

The process used to simulate peaking load units and applied to calculate the UFOP and the DAUFOP are illustrated in Chapter 5. The effects of the system operating conditions on the UFOP are also shown in Chapter 5.

In this chapter, the obtained UFOP are used to modify the generation data used in the analytical method. The UFOP for a peaking load unit used in the analytical method is usually a fixed value obtained at a certain system condition and used in a wide range of situations. This introduces error in generating capacity adequacy evaluations because the UFOP are not constant values and vary with changes in the peak load level, required reserves and so on. The fixed UFOP and the actual UFOP are used in the analytical program and the results are compared to show how pessimistic or optimistic the results might be when fixed UFOP are used.

Derated states of peaking load units can impact the system reliability. The RBTS and the IEEE-RTS are modified to include peaking load units with derated states. The simulation program was applied to the modified test systems and the results from different cases are compared to show the effect of peaking load unit derated states on the system reliability.

The DAUFOP can be calculated using the peaking unit state durations provided by the simulation program. The generation data in the analytical program are modified using the DAUFOP and the results are compared with those obtained when the UFOP are used. The effects of the UFOP and DAUFOP on the system reliability are examined.

6.2 Fixed UFOP and Actual UFOP

The RBTS Case 3 and the IEEE-RTS Case 4 described in Section 5.4.1 are used in this study. The simulation program was applied to the two modified test systems with changes in the required reserve, peak load, starting failure probability and Weibull shape parameter. The UFOP obtained for each system condition was used to modify the generation data applied in the analytical program. The results from the analytical program using the fixed UFOP and the actual UFOP are compared to show the errors introduced when fixed UFOP are used.

The simulation sampling sizes are 5,0000 and 30,000 sampling years for the RBTS and the IEEE-RTS respectively. The hourly load data are used in this study.

6.2.1 Changes in the Required Reserve

The required reserve was varied in Cases 3 and 4. The peak loads are 185 MW and 2850 MW for Cases 3 and 4 respectively.

RBTS Case 3 Results

The reliability indices obtained from the simulation program for the RBTS Case 3 are shown in Table 6.1.

Table 6.1: The reliability indices with changing required reserves for the RBTS Case 3

Reserve (MW)	LOLE(hrs/year)	LOEE(MWh/year)	LOLF(occ/year)
0	0.9531	8.3639	0.1987
20	0.9658	8.5595	0.2027
40	0.9668	8.5658	0.2023
60	1.0298	9.2105	0.2165

It can be seen from Table 6.1 that the reliability indices increase with increase in the required reserve.

The obtained UFOP for the four peaking load units are shown in Table 6.2. The UFOP for the peaking load units increase with increase in the required reserve from 20 MW to 60 MW. The UFOP are also shown in Figure 6.1.

Table 6.2: The UFOP with changing required reserves for the RBTS Case 3

Unit	UFOP for Various Required Reserves			
	0 MW	**20 MW**	**40 MW**	**60 MW**
20 L	0.0030	0.0039	0.0049	0.0089
10 L	0.0021	0.0025	0.0032	0.0040
5 H	0.0015	0.0012	0.0016	0.0018
5 H	0.0013	0.0012	0.0015	0.0018

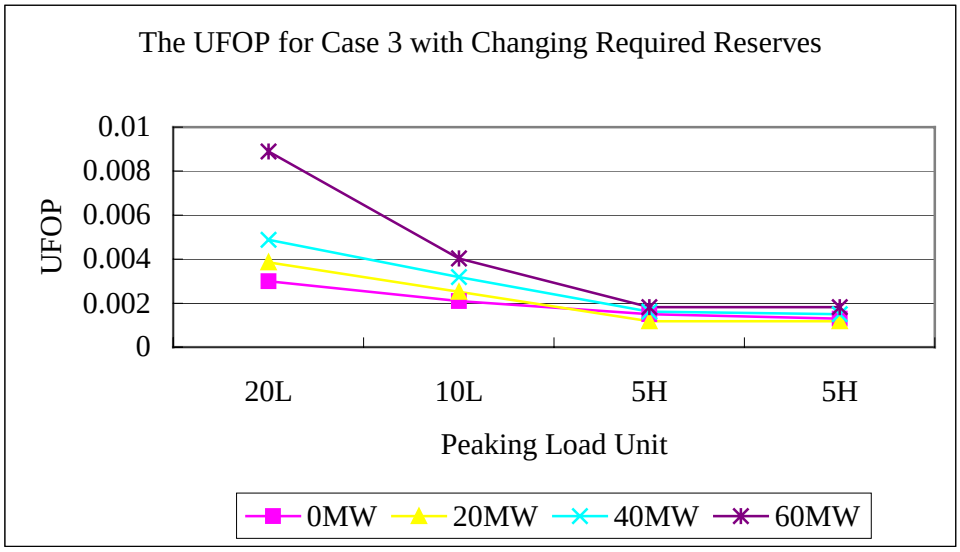

Figure 6.1: The UFOP with changing required reserves for the RBTS Case 3

The UFOP obtained from the simulation program were used to modify the RBTS generation data used in the analytical program. Assume that UFOP1 are the calculated UFOP when the required reserve is 0 MW, and UFOP 2 when the required reserve is 60 MW. The LOLE and LOEE obtained from the analytical program using the different UFOP are shown in Table 6.3.

The LOLE and LOEE shown in Table 6.3 both increase with increase in the required reserve. This is true because the UFOP obtained from the simulation program increase when the required reserve increases. The system LOLE and the LOEE will be smaller than they really are using the fixed UFOP1 while the system is operating with other required reserves. The results are optimistic in this case. The indices are larger than they really are when the fixed UFOP2 are used. The results are pessimistic in this case.

Table 6.3: The reliability indices and deviations using fixed and actual UFOP at various required reserves for the RBTS Case 3

Required Reserve (MW)	LOLE Using Actual UFOP	Deviation in the LOLE Using UFOP1	Deviation in the LOLE Using UFOP2
0	0.9426	0.00%	-3.45%
20	0.9474	0.51%	-2.93%
40	0.9540	1.19%	-2.22%
60	0.9751	3.33%	0.00%
Required Reserve (MW)	**LOEE Using Actual UFOP**	**Deviation in the LOEE Using UFOP1**	**Deviation in the LOEE Using UFOP2**
0	8.1889	0.00%	-4.54%
20	8.2441	0.67%	-3.84%
40	8.3172	1.54%	-2.92%
60	8.5604	4.34%	0.00%

The deviations in the two indices are also shown in Figure 6.2.

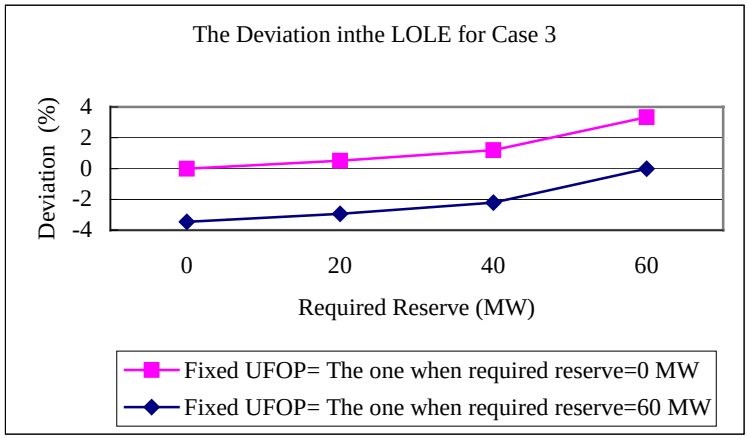

(a) LOLE

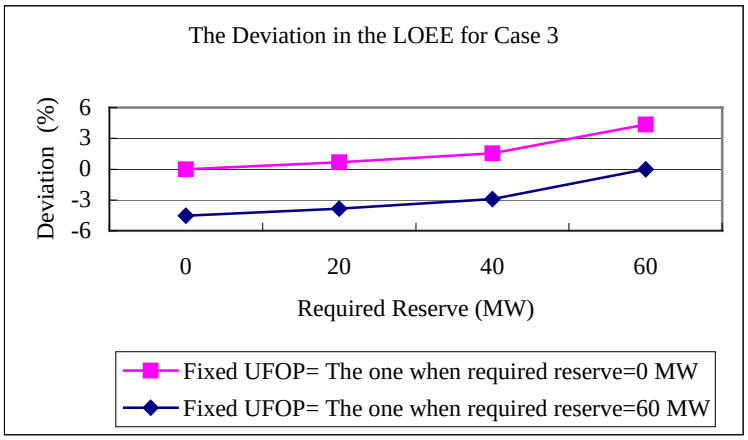

(b) LOEE

Figure 6.2: The deviations in the LOLE and LOEE using fixed and actual UFOP with changing required reserves for the RBTS Case 3

It can be seen from Figure 6.2 that the absolute value of the deviation increases as the required reserve moves further away from the values on which the UFOP are based.

IEEE-RTS Case 4 Results

The reliability indices for the IEEE-RTS Case 4 for various required reserves are shown in Table 6.4. The intervals of the changes in the required reserve are larger in the IEEE-RTS Case 4 than those in the RBTS Case 3.

Table 6.4: The reliability indices with changing required reserves for the IEEE-RTS Case 4

Reserve (MW)	LOLE(hrs/year)	LOEE(MWh/year)	LOLF(occ/year)
0	8.9031	1121.2728	1.9202
80	8.9860	1125.6402	1.9270
120	9.0204	1133.2926	1.9300
160	9.0617	1138.4613	1.9428

Table 6.4 shows that the reliability indices increase with increase in the required reserve. The peaking load units are needed more and function more like base load units when the required reserve increases. The UFOP for the peaking load units also increase with increase in the required reserve as shown in Table 6.5.

Table 6.5: The UFOP with changing required reserves for the IEEE-RTS Case 4

Unit	UFOP for Various Required Reserves			
	0 MW	**80 MW**	**120 MW**	**160 MW**
1	0.0167	0.0180	0.0189	0.0186
2	0.0164	0.0171	0.0189	0.0199
3	0.0175	0.0188	0.0190	0.0186
4	0.0159	0.0177	0.0184	0.0186

The UFOP are also shown in Figure 6.3. The UFOP are expected to increase with increase in the required reserve. There are still some fluctuations in Figure 6.3, as the capacity of the peaking load units is only 2.35% of the total capacity. These peaking units are not needed for much of the time and the simulation sampling size in this case is not big enough.

The generation data used in the analytical program for the IEEE-RTS are

modified using the obtained UFOP. The calculated UFOP when the required reserve is 0 MW are designated as UFOP1, while UFOP 2 represent the UFOP when the required reserve is equal to 160 MW.

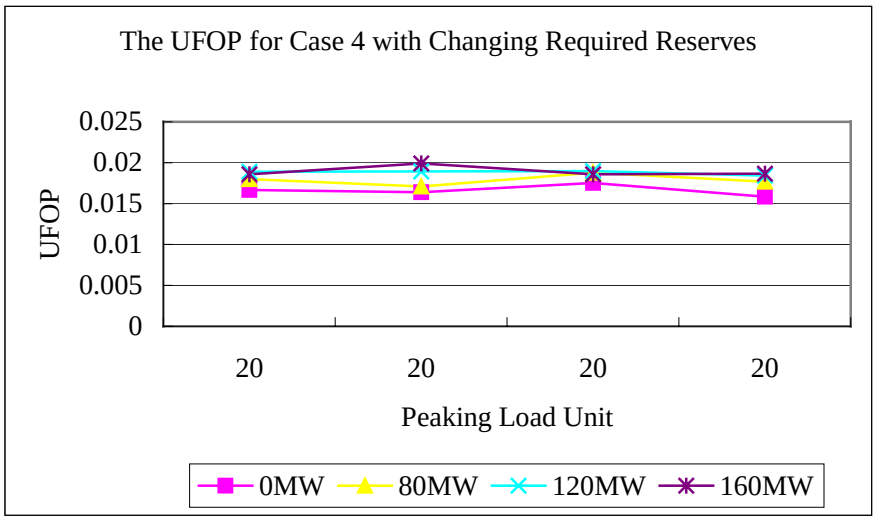

Figure 6.3: The UFOP with changing required reserves for the IEEE-RTS Case 4

The LOLE and LOEE obtained from the analytical program using the fixed UFOP and actual UFOP are shown in Table 6.6. Table 5.6 shows that the LOLE and LOEE both increase as in the RBTS Case 3. The magnitudes of the deviations for the two cases, however, are different.

Table 6.6: The reliability indices and deviations using fixed and actual UFOP with changing various required reserves for the IEEE-RTS Case 4

Required Reserve (MW)	**LOLE Using Actual UFOP**	**Deviation in the LOLE Using UFOP1**	**Deviation in the LOLE Using UFOP2**
0	8.9098	0.0000%	0.0000%
80	8.9173	0.0840%	0.0893%
120	8.9228	0.1448%	0.1538%
160	8.9234	0.1520%	0.1615%
Required Reserve (MW)	**LOEE Using Actual UFOP**	**Deviation in the LOEE Using UFOP1**	**Deviation in the LOEE Using UFOP2**
0	1111.4293	-0.1522%	-0.1617%
80	1112.4225	-0.0680%	-0.0723%
120	1113.1418	-0.0072%	-0.0076%
160	1113.2269	0.0000%	0.0000%

The deviations in the LOLE and LOEE for the IEEE-RTS Case 4 are also shown

in Figure 6.4. It can be seen from Figure 6.4 that the LOLE and LOEE obtained when the fixed UFOP1 are used are slightly less than they really are, which gives an optimistic appraisal of the system reliability. The indices are larger than they really are when the fixed UFOP2 are used which provides a slightly pessimistic appraisal of the system reliability.

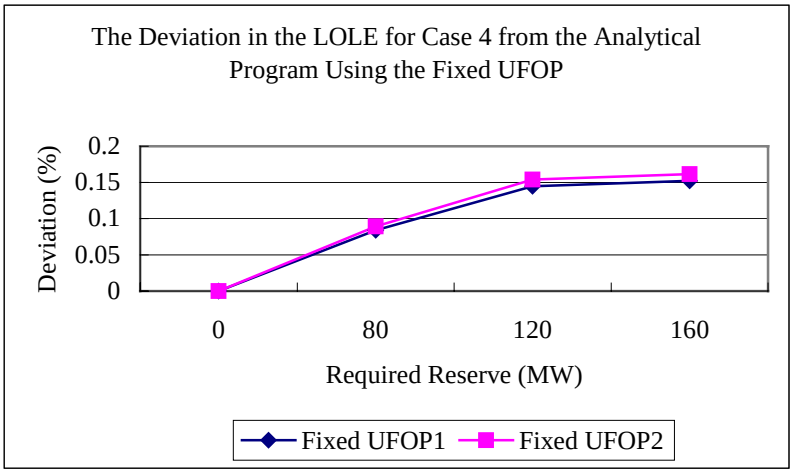

(a) LOLE

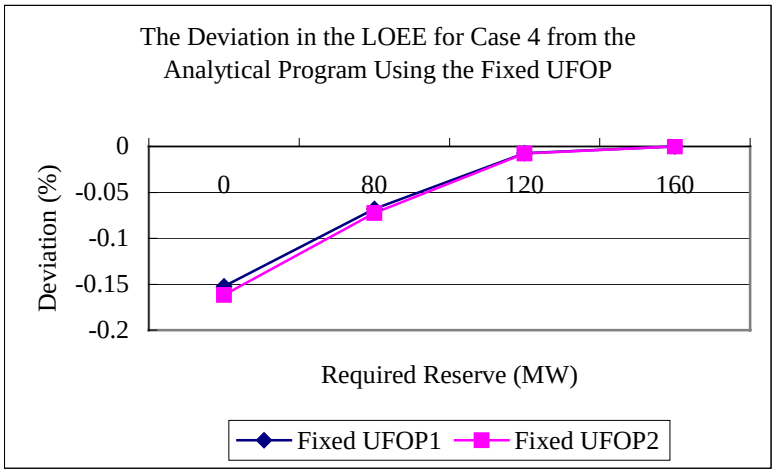

(b) LOEE

Figure 6.4: The deviations in the LOLE and LOEE with changing required reserves for the IEEE-RTS Case 4

6.2.2 Changes in the Peak Load

The required reserve is 0 MW for both Cases 3 and 4 in this section. The starting failure probability for each peaking load unit is assumed to be 0. The results for the RBTS Case 3 and the IEEE-RTS Case 4 with changes in the peak load are shown in the following.

RBTS Case 3 Results

The reliability indices for the RBTS Case 3 are shown in Table 6.7. The reliability indices increase considerably with increase in the peak load.

Table 6.7: The reliability indices with changing peak loads for the RBTS Case 3

Peak Load (MW)	LOLE(hrs/year)	LOEE(MWh/year)	LOLF(occ/year)
175	0.3485	2.9836	0.0794
185	0.9531	8.3639	0.1987
195	2.2690	22.4163	0.4552
205	4.8052	51.7538	0.9856
215	10.8132	112.9180	2.3048

The UFOP for the four peaking load units are shown in Table 6.8. There are fluctuations in the UFOP for the last two peaking units due to the sampling size. The generation data in the analytical program are modified using the obtained UFOP as in Section 6.2.1. The UFOP1 are the obtained UFOP when the peak load is equal to 185 MW, while the UFOP2 are the obtained UFOP when the peak load is 215 MW.

Table 6.8: The UFOP with changing peak loads for the RBTS Case 3

	UFOP for Various Peak Loads				
Unit	**175 MW**	**185 MW**	**195 MW**	**205 MW**	**215 MW**
20 L	0.0027	0.0030	0.0033	0.0035	0.0037
10 L	0.0019	0.0021	0.0020	0.0023	0.0025
5 H	0.0017	0.0015	0.0013	0.0011	0.0014
5 H	0.0012	0.0013	0.0013	0.0011	0.0012

The reliability indices from the analytical program for a range of peak load levels using different sets of the UFOP are shown in Table 6.9.

Table 6.9: The reliability indices using fixed and actual UFOP with changing peak loads for the RBTS Case 3

Peak Load (MW)	Actual UFOP		Fixed UFOP1		Fixed UFOP2	
	LOLE hrs/year	**LOEE MWh/year**	**LOLE hrs/year**	**LOEE MWh/year**	**LOLE hrs/year**	**LOEE MWh/year**
175	0.3339	2.9081	0.3346	2.9153	0.3406	2.9728
185	0.9426	8.1889	0.9426	8.1889	0.9540	8.3172
195	2.2074	21.3832	2.2040	21.3457	2.2279	21.6162
205	4.6542	49.6455	4.6397	49.4920	4.6950	50.0834
215	10.7168	111.0617	10.6031	109.7642	10.71680	111.0617

The deviations in the reliability indices using the actual UFOP and the fixed UFOP are shown in Table 6.10. The deviations are also shown in Figure 6.5.

Table 6.10: The deviations in the reliability indices using fixed and actual UFOP with changing peak loads for the RBTS Case 3

Peak Load (MW)	Fixed UFOP 1		Fixed UFOP 2	
	Deviation in the LOLE (%)	Deviation in the LOEE (%)	Deviation in the LOLE (%)	Deviation in the LOEE (%)
175	0.2213	0.2468	2.0073	2.2240
185	0.0000	0.0000	1.2018	1.5673
195	-0.1524	-0.1753	0.9285	1.0896
205	-0.3124	-0.3093	0.8766	0.8821
215	-1.0614	-1.1682	0	0

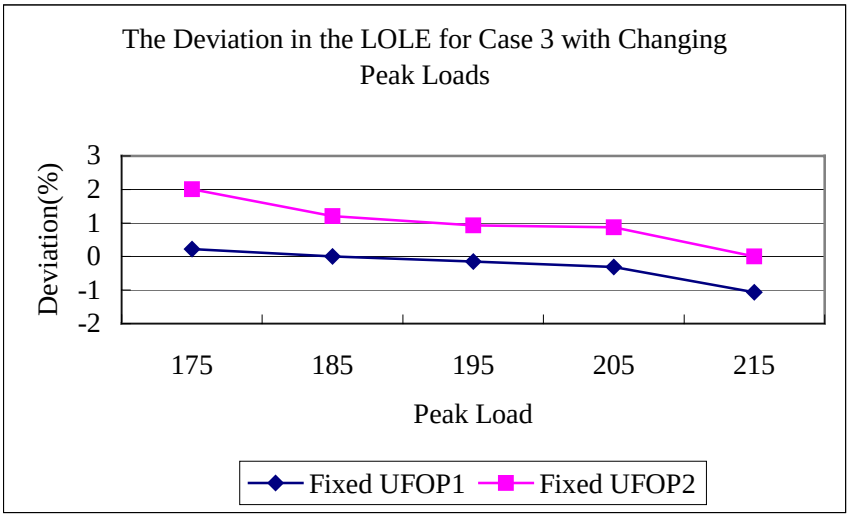

(a) LOLE

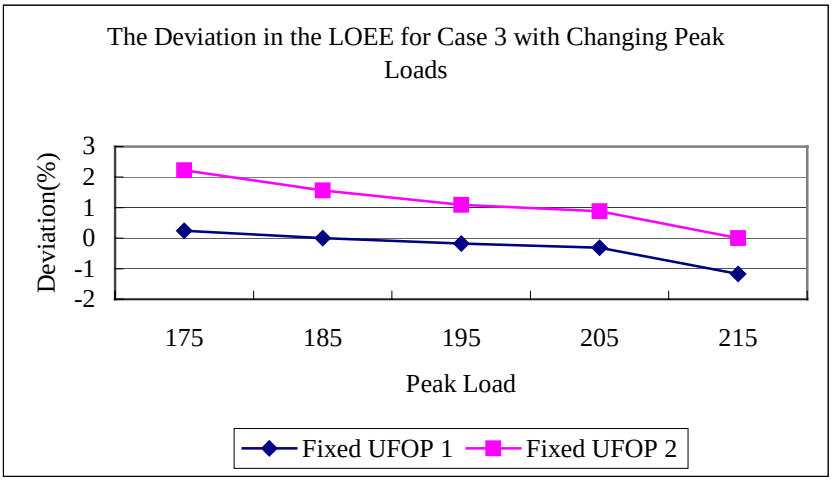

(b) LOEE

Figure 6.5: The deviations in the LOLE and LOEE with changing peak loads for the RBTS Case 3

It can be seen from Figure 6.5 that the reliability indices for the lower peak loads are larger than the real values when the fixed UFOP at a higher peak load level is used leading to a pessimistic appraisal of the system reliability. The reliability indices for the higher peak load levels are smaller than their real values, which is optimistic.

IEEE-RTS Case 4 Results

The reliability indices from the simulation program for the IEEE-RTS Case 4 are shown in Table 6.11. The reliability indices increase considerably with increase in the peak load.

Table 6.11: The reliability indices with changing peak loads for the IEEE-RTS Case 4

Peak Load (MW)	LOLE(hrs/year)	LOEE(MWh/year)	LOLF(occ/year)
2736	4.1150	486.6206	0.9234
2850	8.9031	1121.2728	1.9202
2964	18.0210	2411.2452	3.7484
3078	34.5841	4952.1958	6.8924

The UFOP obtained for various peak load levels are shown in Table 6.12. It can be seen from Table 6.12 that the UFOP increase with increase in the peak load.

Table 6.12: The UFOP with changing peak loads for the RBTS Case 3

Unit	UFOP for Various Peak Loads			
	2736 MW	2850 MW	2964 MW	3078 MW
1	0.0094	0.0097	0.0105	0.0106
2	0.0090	0.0096	0.0102	0.0108
3	0.0088	0.0101	0.0104	0.0105
4	0.0094	0.0098	0.0102	0.0108

The UFOP1 are the UFOP obtained from the simulation program when the peak load is 2850 MW. The UFOP2 are the UFOP when the peak load is equal to 3078 MW. The generation data used in the analytical program are modified using the UFOP1, UFOP2 and the actual UFOP. The reliability indices produced by the analytical program for various peak load levels using different UFOP are shown in Table 6.13.

The deviations in the calculated LOLE and LOEE using the fixed UFOP and the actual UFOP are shown in Table 6.14.

Table 6.13: The reliability indices using different UFOP with changing peak loads for the IEEE-RTS Case 3

Peak Load (MW)	Actual UFOP		Fixed UFOP 1		Fixed UFOP 2	
	LOLE hrs/year	LOEE MWh/year	LOLE hrs/year	LOEE MWh/year	LOLE hrs/year	LOEE MWh/year
2736	4.0952	475.4703	4.0971	475.7034	4.0998	476.0217
2850	8.8699	1106.1391	8.8699	1106.1391	8.8751	1106.8245
2964	18.0206	2409.5644	18.0151	2408.7773	18.0247	2410.1503
3078	34.5694	4964.3248	34.5524	4961.7113	34.5694	4964.3248

Table 6.14: The deviations in the reliability indices using fixed and actual UFOP for the IEEE-RTS Case 4

Peak Load (MW)	Fixed UFOP 1		Fixed UFOP 2	
	Deviation in the LOLE (%)	Deviation in the LOEE (%)	Deviation in the LOLE (%)	Deviation in the LOEE (%)
2736	0.0477	0.0490	0.1128	0.1160
2850	0.0000	0.0000	0.0584	0.0620
2964	-0.0307	-0.0327	0.0228	0.0243
3078	-0.0491	-0.0526	0.0000	0.0000

The deviations in the LOLE and LOEE with the changes in the peak load are also shown in Figure 6.6. The farther the peak load is from the one on which the fixed UFOP are based, the larger is the deviation. The deviations in the reliability indices for the IEEE-RTS Case 4 are relatively small.

The changes in the reliability index deviations for both Cases 3 and 4 have the same trend. It is worth noting, however, that the reliability index deviations for the IEEE-RTS Case 4 are much smaller than those for the RBTS Case 3. This is because Case 3 has a relatively large proportion of peaking load units compared to that in Case 4. The fixed UFOP do not introduce considerable error in the reliability indices when the capacity of the peaking load units is small compared to the total installed capacity. The effect of the fixed UFOP on the reliability evaluation accuracy increases with increase in the relative peaking load unit capacity.

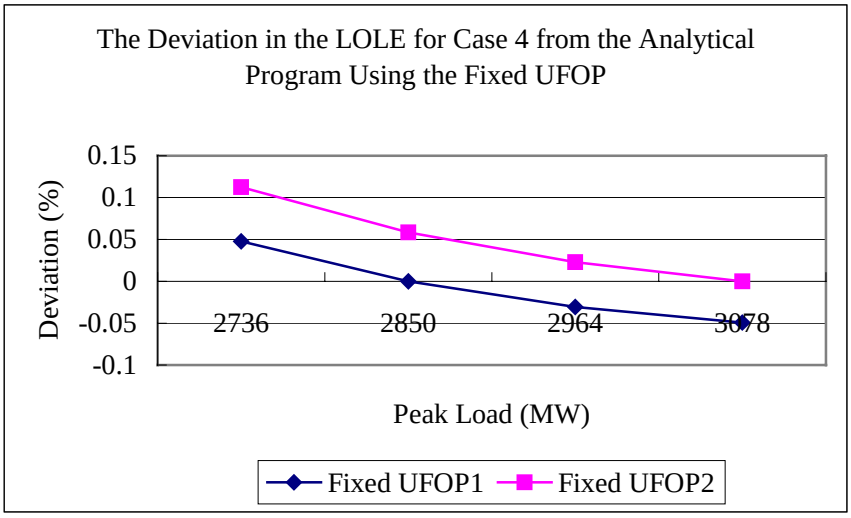

(a) LOLE

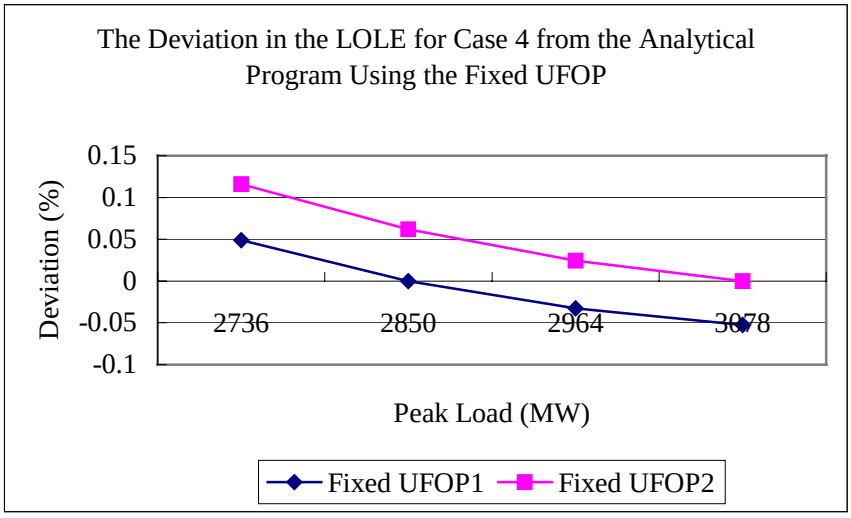

(b) LOEE

Figure 6.6: The deviations in the LOLE and LOEE with changing peak loads for the IEEE-RTS Case 4

6.2.3 Changes in the Starting Failure Probability

The peak loads for Cases 3 and 4 are 185 MW and 2850 MW respectively and the required reserve is 0 MW for both cases in this study. The starting failure probability is assumed to be 0, 0.05 and 0.10 for both systems.

The results are shown in the following.

RBTS Case 3 Results

The reliability indices for the RBTS Case 3 obtained from the simulation program are shown in Table 6.15. The indices increase considerably with increase in the starting failure probability.

Table 6.15: The reliability indices with different starting failure probabilities for the RBTS Case 3

Starting Failure Probability	LOLE(hrs/year)	LOEE(MWh/year)	LOLF(occ/year)
0	0.9531	8.3639	0.1987
0.05	1.3234	13.2744	0.2727
0.10	1.8103	20.1307	0.3710

The UFOP obtained using the simulation program are shown in Table 6.16. The UFOP increase significantly with increase in the starting failure probability. The UFOP are even bigger than the FOR of the units when the starting failure probability is equal to 0.05 and 0.1.

Table 6.16: The UFOP with different starting failure probabilities for the RBTS Case 3

Unit	UFOP for Various Starting Failure Probabilities		
	0	**0.05**	**0.1**
20 L	0.0030	0.0469	0.0871
10 L	0.0021	0.0448	0.0853
5 H	0.0015	0.0440	0.0820
5 H	0.0013	0.0442	0.0818

The UFOP are also shown in Figure 6.7. It can be seen from Figure 6.7 that the UFOP increase as the starting failure probability increases. The FOR of these units are relatively small and therefore the starting failure probability has a large effect on the UFOP. The benefit obtained by modeling the units as peaking load units are counteracted by the starting failure effects.

The UFOP are used to modify the generation data used in the analytical program. The calculated UFOP when the starting failure probability is 0 are assumed to be the fixed UFOP.

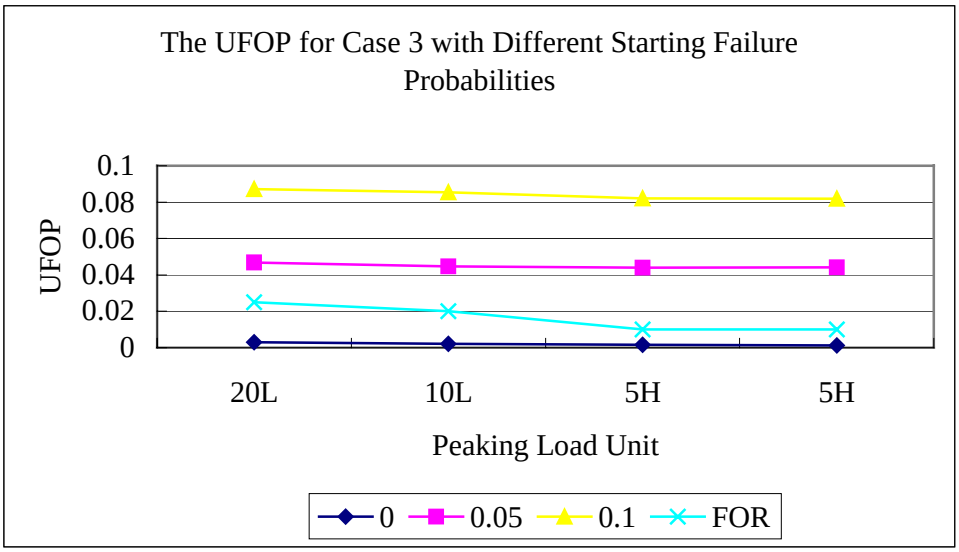

Figure 6.7: The UFOP with different starting failure probabilities for the RBTS Case 3

The LOLE and the LOEE obtained and the deviations in the indices when the fixed UFOP is used are shown in Table 6.17. The deviation is also shown in Figure 6.8.

Table 6.17: The reliability indices and deviations using fixed and actual UFOP with different starting failure probabilities for the RBTS Case 3

Starting Failure Probability	**LOLE Using Actual UFOP**	**Deviation in LOLE Using Fixed UFOP %**	**LOEE Using Actual UFOP**	**Deviation in LOEE Using Fixed UFOP %**
0	0.9413	0.0000	8.1804	0.0000
0.05	1.3056	-27.9029	12.1854	-32.8672
0.1	1.6917	-44.3577	16.4350	-50.2257

It can be seen from Table 6.17 that the reliability indices obtained are smaller than the actual ones when the fixed UFOP are used, which gives an optimistic evaluation of the system reliability.

The differences between the reliability indices using the fixed UFOP and the actual UFOP are large because the UFOP change significantly with increase in the starting failure probability.

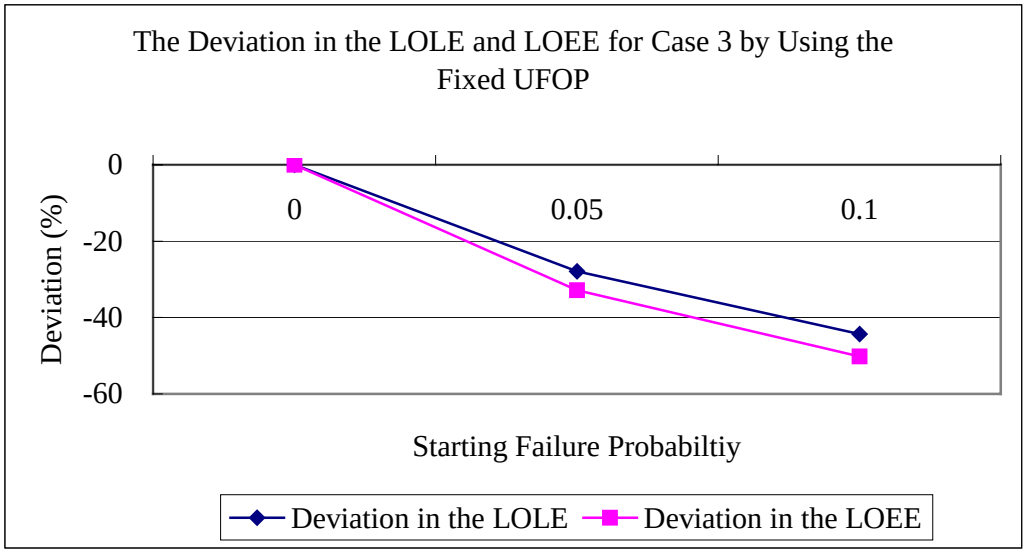

Figure 6.8: The deviations in the LOLE and LOEE with different starting failure probabilities for the RBTS Case 3

IEEE-RTS Case 4 Results

The reliability indices for the IEEE-RTS Case 4 for various starting failure probabilities are shown in Table 6.18.

Table 6.18: The reliability indices with different starting failure probabilities for the IEEE-RTS Case 4

Starting Failure Probability	LOLE(hrs/year)	LOEE(MWh/year)	LOLF(occ/year)
0	0.9531	8.3639	0.1987
0.05	9.2346	1168.4297	1.9609
0.10	9.5273	1212.0007	2.0087

The reliability indices increase significantly with increase in the starting failure probability. This is because the peaking load units are started and shut down very often. The starting failure probability directly affects a peaking load unit's performance.

The UFOP obtained from the simulation program for various starting failure probabilities are shown in Table 6.19. It can be seen that the UFOP increase with increase in the starting failure probability and decrease with the loading order. The UFOP are also shown in Figure 6.9.

Table 6.19: The UFOP with different starting failure probabilities for the IEEE-RTS Case 4

Unit	UFOP for Various Starting Failure Probabilities		
	0	**0.05**	**0.10**
1	0.0167	0.0524	0.0924
2	0.0164	0.0521	0.0919
3	0.0175	0.0518	0.0916
4	0.0159	0.0513	0.0913

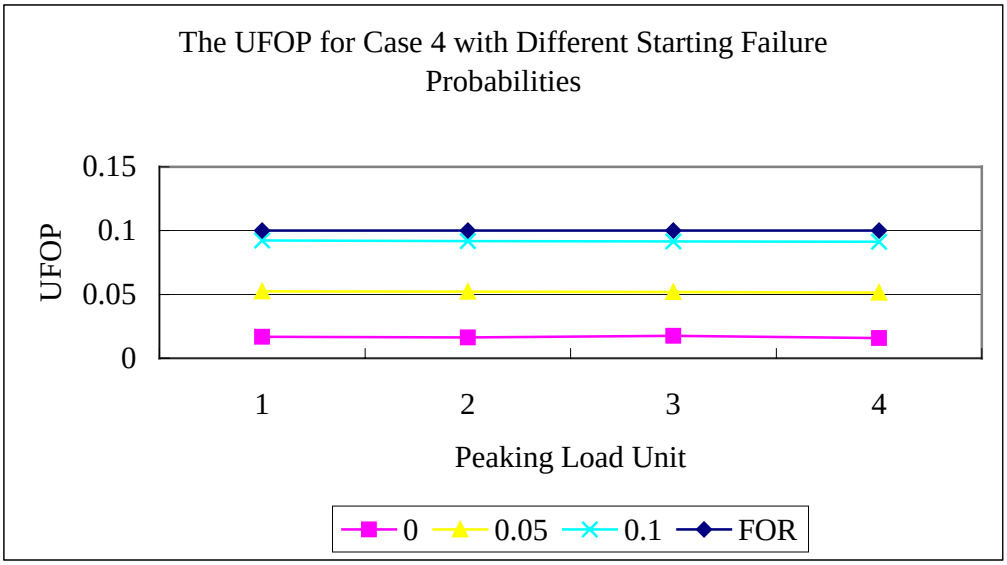

Figure 6.9: The UFOP with different starting failure probabilities for the IEEE-RTS Case 4

It can be seen from Figure 6.9 that the UFOP increases significantly when the starting failure probability increases. The UFOP become close to the FOR which is 0.1 for the four peaking units when the starting failure probability is 0.1. Peaking load units are able to improve the system reliability because they are in service only when they are required. This improvement is, however, affected by the starting failure stress they are faced with because of their frequent start-ups. The benefit of using units as peaking units is therefore counteracted when the starting failure probability increases.

The calculated UFOP when the starting failure probability is 0 are considered as the fixed UFOP in this case. The generation data for the analytical program are modified using both the fixed UFOP and the actual UFOP. The reliability indices and the deviations between the calculated indices using the fixed UFOP and the actual

UFOP are shown in Table 6.20.

Table 6.20: The reliability indices and deviations using fixed and actual UFOP with changing starting failure probabilities for the IEEE-RTS Case 4

Starting Failure Probablility	**LOLE Using Actual UFOP**	**Deviation in LOLE Using Fixed UFOP %**	**LOEE Using Actual UFOP**	**Deviation in LOEE Using Fixed UFOP %**
0	8.8986	0	1110.3895	0
0.05	9.1064	-2.2819	1137.9862	-2.4250
0.1	9.3443	-4.7698	1169.7307	-5.0731

The absolute values of the deviations increase when the starting failure probability is far from the one based on which the fixed UFOP are calculated. The deviations are also shown in Figure 6.10.

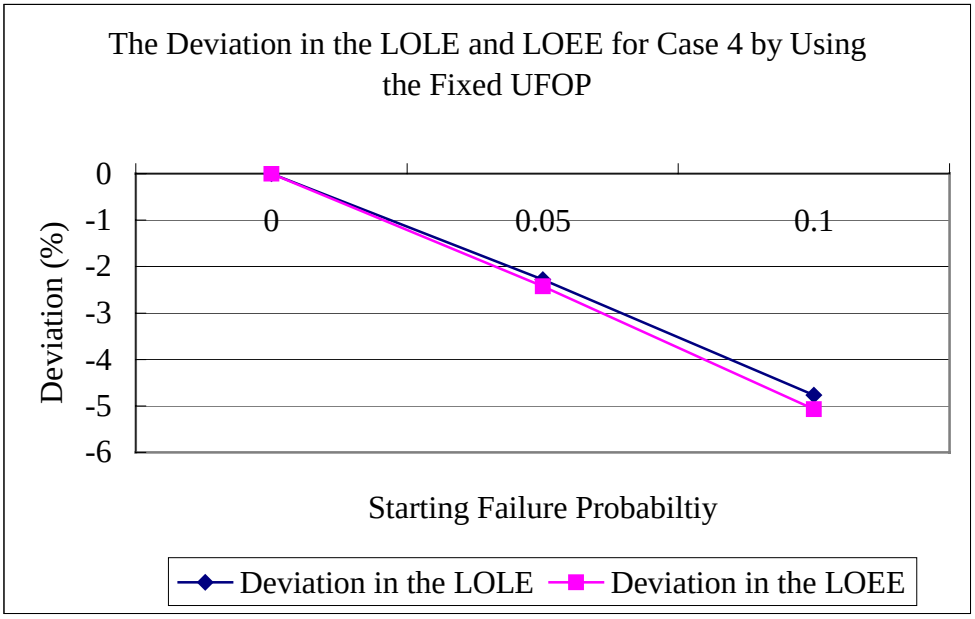

Figure 6.10: The deviations in the LOLE and LOEE with changing starting failure probabilities for the IEEE-RTS Case 4

It can be seen from the results for Cases 3 and 4 that the starting failure probability affects the units in RBTS Case 3 more than those in the IEEE-RTS Case 4. This is because the peaking units in Case 3 have relatively lower FOR compared to the ones in Case 4.

6.2.4 Changes in the Weibull Shape Parameters

The RBTS Case 3 was further modified to include peaking load units with repair times that follow Weibull distributions with various shape parameters. The scale parameters are set to keep the mean values of the repair times constant as in Table 4.1.

The simulation program was applied to the modified Case 3 and the reliability indices are shown in Table 6.21.

Table 6.21: The reliability indices with changing shape parameters for the RBTS Case 3

β	**LOLE(hrs/year)**	**LOEE(MWh/year)**	**LOLF(occ/year)**
0.5	0.9357	8.1833	0.19964
1	0.9531	8.3639	0.1987
2	0.9691	8.6189	0.2023
4	0.9716	8.6017	0.2023

It can be seen that the reliability indices increase with increase in the shape parameter.

The unit state residence time distributions are assumed to be exponential in the analytical program. The obtained UFOP in this case were not used in the analytical program. The LOLE and LOEE are 0.9426 hrs/yr and 8.1889 MWh/yr respectively as shown in Table 6.3 when the unit repair times follow exponential distributions, the peak load equals 185 MW and the required reserve is 0 MW. The LOLE and the LOEE are compared with those shown in Table 6.21 and the deviations in the indices are shown in Table .6.22.

Table 6.22: The deviations in the LOLE and LOEE with changing shape parameters for the RBTS Case 3

β	**Deviation in LOLE (%)**	**Deviation in LOEE (%)**
0.5	0.7447	0.0688
1	-1.1012	-2.0925
2	-2.7289	-4.9890
4	-2.9769	-4.7996

The deviations in the reliability indices are also shown in Figure 6.11.

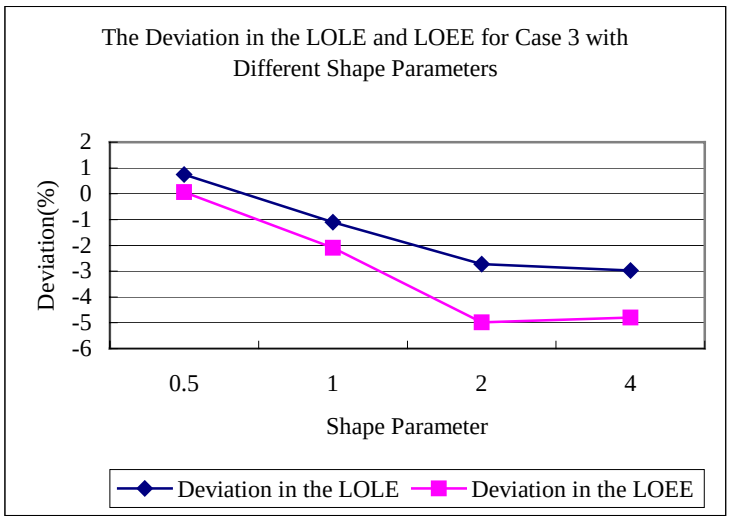

Figure 6.11: The deviations in the LOLE and LOEE with changing shape parameters for the RBTS Case 3

6.3 The UFOP and DAUFOP

Derated states for the peaking load units are not considered in the previous sections. The effects of peaking load unit derated states on the system reliability are examined in the following. The RBTS and the IEEE-RTS are modified to include peaking load units that have derated states.

The simulation program was applied to the modified RBTS and the IEEE-RTS. The tolerance values are 2% and 1.5% for the RBTS and the IEEE-RTS respectively in this study. The UFOP and DAUFOP were calculated as described in Section 5.2. The actual UFOP and the DAUFOP were applied to the analytical program and the reliability indices obtained using the UFOP and the DAUFOP are compared in this section.

6.3.1 Study Cases

Case 5: The four peaking load units in the RBTS Case 3 are modified to contain one derated state.

The transition rates (occ/yr) between the states for the four units in the RBTS

Case 5 are shown in Table 6.23.

Table 6.23: Transition rates of the four units in the RBT Cases 5

State	Capacity In (MW)	State 1	State 2	State 3
2*5H Unit				
State 1	5	0	1.0104	1.0104
State 2	2.5	98	0	98
State 3	0	97.3333	97.3333	0
1*10L Unit				
State 1	10	0	2.0419	2.0419
State 2	5	97.3333	0	97.3333
State 3	0	97.3333	97.3333	0
1*20L Unit				
State 1	20	0	2.5659	2.5659
State 2	10	97.3333	0	97.3333
State 3	0	97.3333	97.3333	0

Case 6: The four 20 MW units in the IEEE-RTS are considered to be peaking load units that have three states. The state transition rates (occ/yr) for this group of units are shown in Table 6.24.

Table 6.24: Transition rates of the 20 MW units in the IEEE-RTS Case 6

State	Capacity In (MW)	State 1	State 2	State 3
State 1	20	0	9.9545	9.9545
State 2	10	219	0	219
State 3	0	109.5	109.5	0

6.3.2 Changes in the Required Reserve

The required reserve was varied in Cases 5 and 6. The peak loads are 185 MW and 2850 MW for Cases 5 and 6 respectively. The starting failure probability for the peaking load units in this study is 0. The results for Cases 5 and 6 are shown and compared in the following.

RBTS Results

The reliability indices obtained from the simulation program for the RBTS Case 5 are shown in Table 6.25.

Table 6.25: The reliability indices with changing required reserves for the RBTS Case 5

Required Reserve (MW)	LOLE (hrs/year)	LOEE (MWh/year)	LOLF (occ/year)
0	0.9422	8.0661	0.1986
20	0.9459	8.2132	0.2004
40	0.9780	8.7191	0.2037

It can be seen from Table 6.25 that the reliability indices increase with increase in the required reserve. The reliability indices in Table 6.25 are less than the ones in Table 6.1 because the derated states are considered in this case.

The UFOP and DAUFOP for the four peaking load units in the RBTS Case 5 with changing required reserve are shown in Tables 6.26 and 6.27 respectively.

Table 6.26: The UFOP with changing required reserves for the RBTS Case 5

Unit	UFOP for Various Required Reserves		
	0 MW	**20 MW**	**40 MW**
20 L	0.0013	0.0015	0.0015
10 L	0.0009	0.0011	0.0013
5 H	0.0003	0.0005	0.0006
5 H	0.0005	0.0006	0.0006

Table 6.27: The DAUFOP with changing required reserves for the RBTS Case 5

Unit	DAUFOP for Various Required Reserves		
	0 MW	**20 MW**	**40 MW**
20 L	0.0019	0.0023	0.0023
10 L	0.0015	0.0016	0.0020
5 H	0.0006	0.0008	0.0009
5 H	0.0008	0.0009	0.0010

It can be seen by comparing Table 6.26 with Table 6.27 that the calculated DAUFOP is larger the UFOP for each peak load unit at each required reserve. Both the UFOP and the DAUFOP increase with increase in the required reserve.

The UFOP and DAUFOP were applied to modify the generation data in the analytical program and the LOLE and LOEE obtained for each required reserve are shown in Table 6.28. The deviations in the reliability indices using the UFOP and DAUFOP are shown in Table 6.28 and Figure 6.12.

Table 6.28: The reliability indices and deviations using UFOP and DAUFOP at various required reserves for the RBTS

Required Reserve (MW)	LOLE Using UFOP	LOLE Using DAUFOP	Deviation in the LOLE (%)
0	0.9299	0.9341	0.4496
20	0.9313	0.9364	0.5446
40	0.9317	0.9372	0.5869
Required Reserve (MW)	**LOEE Using UFOP**	**LOEE Using DAUFOP**	**Deviation in the LOEE (%)**
0	8.0531	8.1002	0.5815
20	8.0695	8.1261	0.6965
40	8.0734	8.1340	0.7450

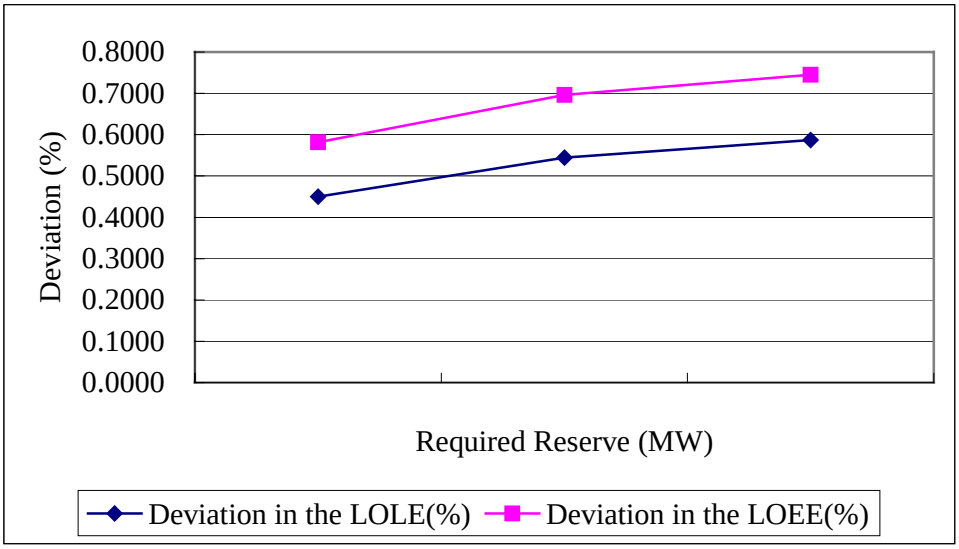

Figure 6.12: Deviations in the LOLE and the LOEE using the UFOP and the DAUFOP with changing required reserves for the RBTS

The deviations in the LOLE and the LOEE using the UFOP and the DAUFOP are less than 1% in the RBTS Case 5.

IEEE-RTS Results

The reliability indices obtained from the simulation program for the IEEE-RTS Case 6 are shown in Table 6.29.

Table 6.29: The reliability indices with changing required reserves for the IEEE-RTS Case 6

Required Reserve (MW)	LOLE (hrs/year)	LOEE (MWh/year)	LOLF (occ/year)
0	8.7301	1090.7664	1.8847
40	8.8248	1104.7904	1.9081
80	8.9414	1112.0557	1.9347

It can be seen from Table 6.29 that the reliability indices increase with increase in the required reserve. The reliability indices are less than those in Table 6.5 because peaking load unit derated states are considered in this case.

The UFOP and DAUFOP for the peaking load units in the IEEE-RTS Case 6 are shown in Tables 6.30 and 6.31 respectively.

Table 6.30: The UFOP with changing required reserves for the IEEE-RTS Case 6

Unit	UFOP for Various Required Reserves		
	0 MW	**40 MW**	**80 MW**
1	0.0047	0.0048	0.0047
2	0.0052	0.0049	0.0050
3	0.0053	0.0054	0.0052
4	0.0048	0.0056	0.0052

Table 6.31: The DAUFOP with changing required reserves for the IEEE-RTS Case 6

Unit	DAUFOP for Various Required Reserves		
	0 MW	**40 MW**	**80 MW**
1	0.0067	0.0068	0.0067
2	0.0073	0.0069	0.0074
3	0.0075	0.0076	0.0075
4	0.0071	0.0078	0.0076

The calculated DAUFOP is larger than the UFOP for each peaking load unit at the same required reserve condition. The UFOP and DAUFOP obtained at each required reserve are applied to the analytical program. The calculated LOLE and the LOEE and the deviations in the two indices are shown in Table 6.32.

The deviations are also shown in Figure 6.13.

Table 6.32: The reliability indices and deviations using UFOP and DAUFOP at various required reserves for the IEEE-RTS Case 6

Required Reserve (MW)	**LOLE Using UFOP**	**LOLE Using DAUFOP**	**Deviation in the LOLE (%)**
0	8.8307	8.8432	0.1414
40	8.8317	8.8440	0.1391
80	8.8311	8.8438	0.1436
Required Reserve (MW)	**LOEE Using UFOP**	**LOEE Using DAUFOP**	**Deviation in the LOEE (%)**
0	1101.3903	1103.0512	0.1506
40	1101.5254	1103.1477	0.1471
80	1101.4482	1103.1285	0.1523

The deviations in the reliability indices for the IEEE-RTS by using UFOP and DAUFOP are less than 0.2%.

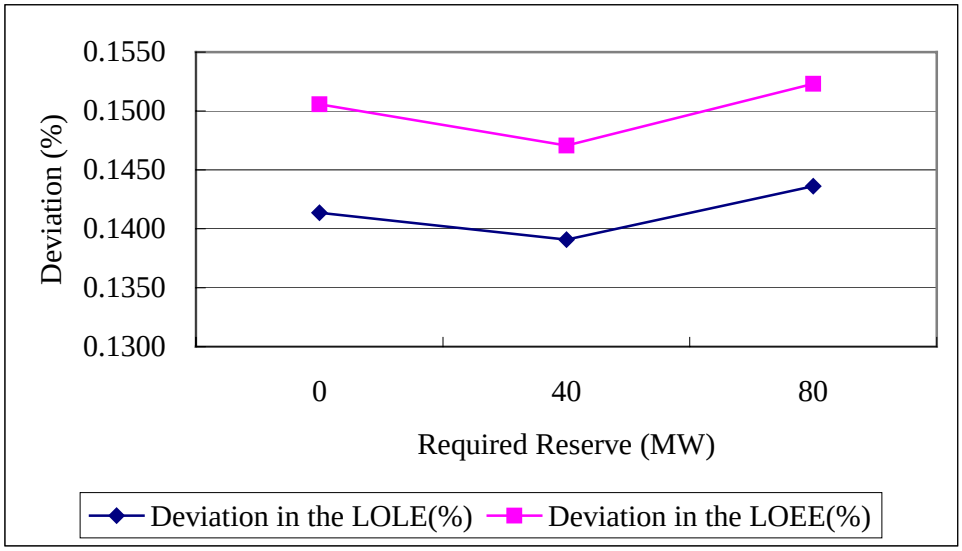

Figure 6.13: Deviations in the LOLE and the LOEE using the UFOP and the DAUFOP with changing required reserves for the IEEE-RTS

The deviations in the reliability indices by using the UFOP and the DAUFOP are smaller for the IEEE-RTS than those for the RBTS. This is because the peaking load unit proportional capacity of the IEEE-RTS is relatively small and therefore the peaking load unit derated states have relatively small effect on the system reliability.

6.3.3 Changes in the Peak Load

The peak loads are varied in this study. The required reserve is 0 MW for both the RBTS Case 5 and the IEEE-RTS Case 6. The starting failure probability for the peaking load units in this study is 0. The results for Cases 5 and 6 are shown and compared in the following.

RBTS Results

The simulation program was applied to the RBTS Case 5 and the reliability indices obtained for various peak loads are shown in Table 6.33.

Table 6.33: The reliability indices with changing peak loads for the RBTS Case 5

Peak Load (MW)	LOLE (hrs/year)	LOEE (MWh/year)	LOLF (occ/year)
185	0.9422	8.0661	0.1986
195	2.1914	21.2608	0.4403
205	4.6294	50.2090	0.9511

Table 6.33 shows that the reliability indices increase significantly with increase in the peak load.

The UFOP and DAUFOP for the peaking load units in the RBTS Case 5 with changing peak loads are shown in Tables 6.34 and 6.35 respectively.

Table 6.34: The UFOP with changing peak loads for the RBTS Case 5

Unit	UFOP for Various Peak Loads		
	185 MW	195 MW	205 MW
20 L	0.0013	0.0013	0.0014
10 L	0.0009	0.0010	0.0009
5 H	0.0003	0.0006	0.0005
5 H	0.0005	0.0007	0.0005

Table 6.35: The DAUFOP with changing peak loads for the RBTS Case 5

Unit	DAUFOP for Various Peak Loads		
	185 MW	195 MW	205 MW
20 L	0.0019	0.0020	0.0021
10 L	0.0015	0.0015	0.0014
5 H	0.0006	0.0008	0.0008
5 H	0.0008	0.0009	0.0007

It can be seen from Tables 6.34 and 6.35 that the DAUFOP is larger than the

UFOP for each peaking load unit at the same peak load level. Both the UFOP and the DAUFOP increase with increase in the peak load for the first two peaking units in the loading order. There are, however, some fluctuations for the last two units.

The actual UFOP and the DAUFOP for each peak load level were applied in the analytical program and the reliability indices obtained for each peak load level are shown in Table 6.36. The deviations in the reliability indices when the UFOP and the DAUFOP are used are shown in Table 6.36 and Figure 6.14.

Table 6.36: The reliability indices and deviations using UFOP and DAUFOP at various peak loads for the RBTS Case 5

Peak Load (MW)	**LOLE Using UFOP**	**LOLE Using DAUFOP**	**Deviation in the LOLE (%)**
185	0.9299	0.9341	0.4496
195	2.1798	2.1891	0.4248
205	4.5815	4.6031	0.4692
Peak Load (MW)	**LOEE Using UFOP**	**LOEE Using DAUFOP**	**Deviation in the LOEE (%)**
185	8.0531	8.1002	0.5815
195	21.0671	21.1722	0.4964
205	48.8905	49.1226	0.4725

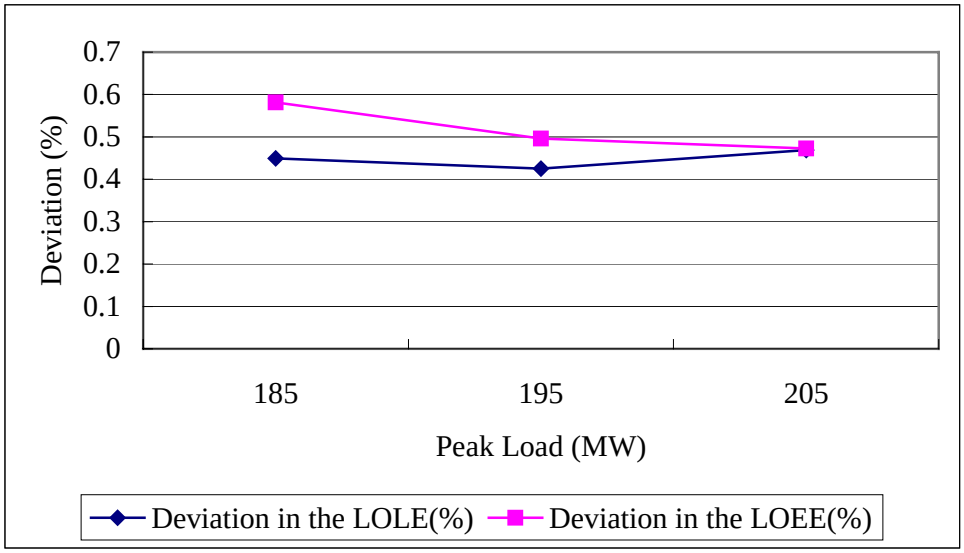

Figure 6.14: Deviations in the LOLE and the LOEE using the UFOP and the DAUFOP with changing peak loads for the RBTS Case 5

It can be seen from Table 6.36 that the deviations in the LOLE and the LOEE are

small. The values are less than 1%.

IEEE-RTS Results

The results for the IEEE-RTS Case 6 with changing peak loads are shown in Table 6.37.

Table 6.37: The reliability indices with changing peak loads for the IEEE-RTS Case 6

Peak Load (MW)	LOLE (hrs/year)	LOEE (MWh/year)	LOLF (occ/year)
2850	8.7301	1090.7664	1.8847
2964	18.0135	2397.1603	3.7639
3078	34.3460	4896.9892	6.8609

It can be seen from Table 6.37 that the reliability indices increase significantly with increase in the peak load.

The UFOP and DAUFOP for the peaking load units in the IEEE-RTS Case 6 with changing peak loads are shown in Tables 6.38 and 6.39 respectively.

Table 6.38: The UFOP with changing peak loads for the IEEE-RTS Case 6

Unit	UFOP for Various Peak Loads		
	2850 MW	2964 MW	3078 MW
1	0.0047	0.0047	0.0047
2	0.0052	0.0046	0.0050
3	0.0053	0.0051	0.0054
4	0.0048	0.0050	0.0052

Table 6.39: The DAUFOP with changing peak loads for the IEEE-RTS Case 6

Unit	DAUFOP for Various Peak Loads		
	2850 MW	2964 MW	3078 MW
1	0.0067	0.0068	0.0068
2	0.0073	0.0066	0.0072
3	0.0075	0.0075	0.0078
4	0.0071	0.0075	0.0076

It can be seen from Tables 6.38 and 6.39 that the DAUFOP is larger than the UFOP for a peaking load unit at a given peak load level. There are fluctuations in the UFOP with increase in the peak load. The actual UFOP and DAUFOP were applied to the analytical program at each peak load level. The calculated LOLE and the LOEE

and the deviations in the two indices when the UFOP and the DAUFOP are used are shown in Table 6.40.

Table 6.40: The reliability indices and deviations using UFOP and DAUFOP at various peak loads for the IEEE-RTS Case 6

Peak Load (MW)	**LOLE Using UFOP**	**LOLE Using DAUFOP**	**Deviation in the LOLE (%)**
2850	8.8307	8.8432	0.1414
2964	17.9367	17.9612	0.1364
3078	34.4137	34.4572	0.1262
Peak Load (MW)	**LOEE Using UFOP**	**LOEE Using DAUFOP**	**Deviation in the LOEE (%)**
2850	1101.3903	1103.0512	0.1506
2964	2398.6707	2402.1523	0.1449
3078	4942.2701	4948.9721	0.1354

The deviation in the LOLE and the LOEE are also shown in Figure 6.15.

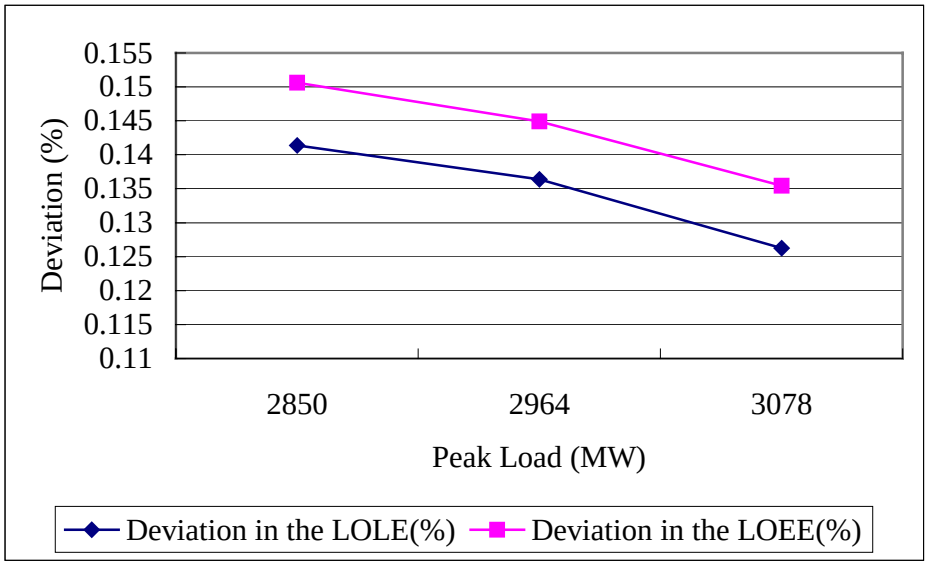

Figure 6.15: Deviations in the LOLE and the LOEE using the UFOP and the DAUFOP with changing peak loads for the IEEE-RTS Case 6

It can be seen that the deviations in the LOLE and the LOEE are small. The deviations for the IEEE-RTS using the UFOP and the DAUFOP are less than the ones for the RBTS.

It can also be seen by comparing Tables 6.28 and 6.36 that the deviations in the reliability indices for the RBTS do not change significantly with changes in the

required reserves and in the peak loads. The deviations for the IEEE-RTS also do not change materially for the changing required reserve and the peak loads.

6.3.4 Changes in the Starting Failure Probability

The starting failure probabilities of the peaking load units are varied in this case. The required reserve is 0 MW for both the RBTS and the IEEE-RTS. The peak loads for the two systems are 185 MW and 2850 MW respectively.

RBTS Case 5 Results

The results for the RBTS Case 5 with various starting failure probabilities are shown in Table 6.41.

Table 6.41: The reliability indices with changing starting failure probabilities for the RBTS Case 5

Starting Failure Probability	LOLE (hrs/year)	LOEE (MWh/year)	LOLF (occ/year)
0	0.9422	8.0661	0.1986
0.05	1.3742	13.0183	0.2860
0.1	1.8259	17.8432	0.3825

The reliability indices in Table 6.41 increase considerably with increase in the starting failure probability. This is because the starting failure probability greatly affects the unavailability of the generating unit.

The UFOP and the DAFUOP obtained are shown in Tables 6.42 and 6.43. The two indices increase significantly with increase in the starting failure probability.

Table 6.42: The UFOP with changing starting failure probabilities for the RBTS Case 5

Unit	UFOP for Various Starting Failure Probabilities		
	0	**0.05**	**0.1**
1	0.0013	0.0469	0.0917
2	0.0009	0.0452	0.0923
3	0.0003	0.0453	0.0898
4	0.0005	0.0464	0.0951

Table 6.43: The DAUFOP with changing starting failure probabilities for the RBTS Case 5

Unit	DAUFOP for Various Starting Failure Probabilities		
	0	**0.05**	**0.1**
1	0.0019	0.0484	0.0942
2	0.0015	0.0468	0.0946
3	0.0006	0.0468	0.0921
4	0.0008	0.0478	0.0973

The DAUFOP is larger than the UFOP for each peaking load unit.

The UFOP and DAUFOP were applied in the analytical program and the obtained results are shown in Table 6.44. The deviations in the reliability indices are shown in Table 6.44 and Figure 6.16.

Table 6.44: The reliability indices and deviations using UFOP and DAUFOP at various peak loads for the RBTS Case 5

Starting Failure Probability	**LOLE Using UFOP**	**LOLE Using DAUFOP**	**Deviation in the LOLE (%)**
0	0.9299	0.9341	0.4496
0.05	1.3093	1.3231	1.0430
0.1	1.7579	1.7835	1.4354
Starting Failure Probability	**LOEE Using UFOP**	**LOEE Using DAUFOP**	**Deviation in the LOEE (%)**
0	8.0531	8.1002	0.5815
0.05	12.2226	12.3738	1.2219
0.1	17.1520	17.4343	1.6192

It can be seen from Table 6.44 that the deviations in the LOLE and the LOEE increase with increase in the starting failure probability. It can also be seen by comparing Table 6.44 with Tables 6.28 and 6.36 that the deviations with changes in the starting failure probabilities are larger than in the required reserves and in the peak loads.

It is also worth noting that the deviations with changes in the starting failure probabilities are still small, i.e. less than 2% in the case of the RBTS.

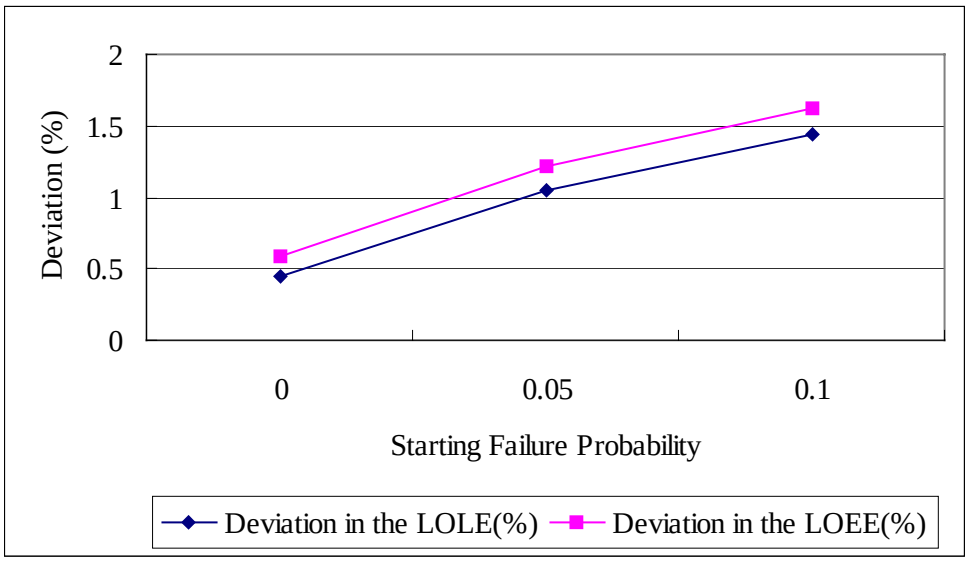

Figure 6.16: Deviations in the LOLE and the LOEE using the UFOP and the DAUFOP with changing starting failure probabilities for the RBTS Case 5

IEEE-RTS Case 6 Results

The results for the IEEE-RTS Case 6 with various starting failure probabilities are shown in Table 6.45.

Table 6.45: The reliability indices with changing starting failure probabilities for the IEEE-RTS Case 6

Starting Failure Probability	LOLE (hrs/year)	LOEE (MWh/year)	LOLF (occ/year)
0	8.7301	1090.7664	1.8847
0.05	9.3987	1185.8118	2.0087
0.1	9.4903	1180.7377	2.0396

The reliability indices increase with increase in the starting failure probability. The magnitudes of the changes, however, are smaller than for the RBTS. This is because the peaking load unit proportional capacity is relatively small and the unavailability of a peaking unit is relatively high in the IEEE-RTS. Changes in the starting failure probability therefore have less effect on the system reliability.

The obtained UFOP and the DAUFOP for the IEEE-RTS Case 5 are shown in Tables 6.46 and 6.47 respectively. It can be seen that the DAUFOP is larger than the UFOP and both indices increase significantly with increase in the starting failure

probability.

Table 6.46: The UFOP with changing starting failure probabilities for the IEEE-RTS Case 6

Unit	UFOP for Various Starting Failure Probabilities		
	0	**0.05**	**0.1**
1	0.0047	0.0494	0.0954
2	0.0052	0.0500	0.0953
3	0.0053	0.0502	0.0968
4	0.0048	0.0498	0.0969

Table 6.47: The DAUFOP with changing starting failure probabilities for the IEEE-RTS Case 6

Unit	DAUFOP for Various Starting Failure Probabilities		
	0	**0.05**	**0.1**
1	0.0067	0.0521	0.0991
2	0.0073	0.0527	0.0989
3	0.0075	0.0532	0.1006
4	0.0071	0.0529	0.1008

The UFOP and DAUFOP were used in the analytical program and the obtained reliability indices and the deviations in the indices are shown in Table 6.48. The deviations in the reliability indices are also shown in Figure 6.17.

Table 6.48: The reliability indices and deviations using UFOP and DAUFOP at various peak loads for the IEEE-RTS Case 6

Starting Failure Probability	**LOLE Using UFOP**	**LOLE Using DAUFOP**	**Deviation in the LOLE (%)**
0	8.8307	8.8432	0.1414
0.05	9.0943	9.1113	0.1866
0.1	9.3701	9.3927	0.2406
Starting Failure Probability	**LOEE Using UFOP**	**LOEE Using DAUFOP**	**Deviation in the LOEE (%)**
0	1101.3903	1103.0512	0.1506
0.05	1136.3704	1138.6368	0.1990
0.1	1173.1856	1176.2040	0.2566

It can be seen from Table 6.48 that the deviations in the LOLE and the LOEE are larger than when the required reserves or the peak loads are changed. The deviations in this case are still small, i.e. less than 0.3%.

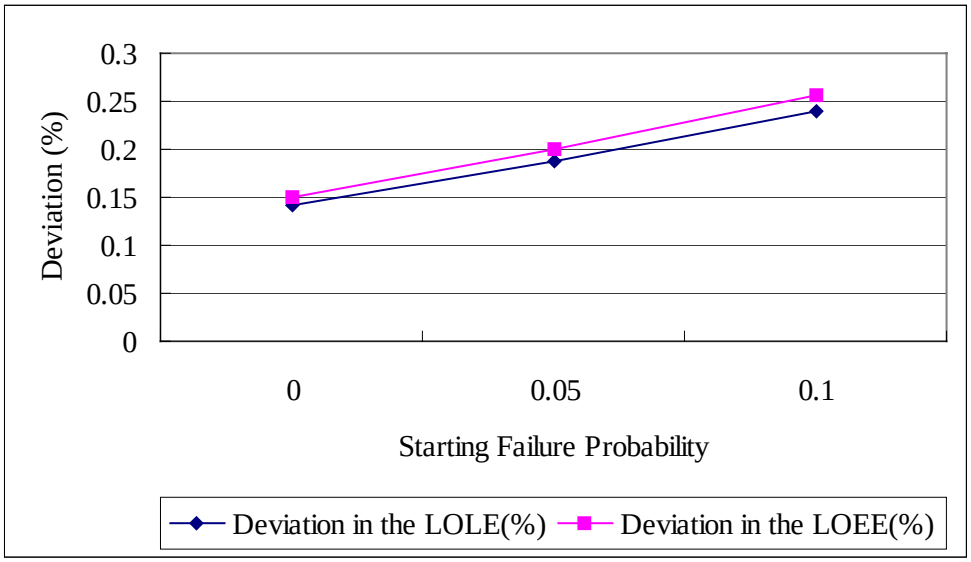

Figure 6.17: Deviations in the LOLE and the LOEE using the UFOP and the DAUFOP with changing starting failure probabilities for the IEEE-RTS Case 6

It can be seen from the results shown above that the deviations in the reliability indices by using the UFOP and the DAUFOP are relatively small with changes in the required reserve, in the peak load and in the starting failure probability.

6.4 Conclusion

Peaking load units and base load units have different operating characteristics. A four-state model is used to represent a peaking load unit instead of the two-state model usually used to represent a base load unit. The conditional probability of finding a peaking load unit in the failed state when it is required by the system (UFOP) or the DAUFOP when peaking unit derated states are considered, is used to calculate the system reliability indices in the analytical program.

The fixed UFOP calculated at a specific system condition are usually used for a range of other situations. This will introduce some error in the reliability indices. Both the RBTS and the IEEE-RTS are modified to contain some peaking load units. The simulation program was applied to the two systems under different operating conditions such as the required reserves, peak load levels, starting failure probabilities and unit state residence time distributions. The UFOP were calculated for each

condition and used to modify the generation data used in the analytical program. The results obtained from the analytical program using the fixed UFOP and the actual UFOP are compared. The results show that:

The absolute values of the reliability index deviations introduced by using the fixed UFOP increase when the system operating condition is different from the one on which the fixed UFOP are based. The absolute values of the reliability index deviations caused by the fixed UFOP increase when the peaking load unit proportional capacity increases. The magnitudes of the deviations in the RBTS Case 3 are bigger than those in the IEEE-RTS Case 4.

The starting failure probability directly affects the performance of peaking load units. The UFOP can exceed the conventional unit FOR under some conditions when the unit starting failure probability increases. The benefit in the system reliability obtained by using a unit as a peaking unit is counteracted by the unit starting failure probability. Changes in the starting failure probability cause big changes in the UFOP. The errors introduced in the reliability indices can be significant when the fixed UFOP are used to calculate reliability indices in the analytical program. The deviations in the LOLE and LOEE are up to 44.36% and 50.23% respectively for the RBTS Case 3. The deviations in the LOLE and LOEE are 4.77% and 5.07% for the IEEE-RTS Case 4.

The use of the fixed UFOP introduces errors in the system reliability indices. The error varies significantly with system unit conditions, operating conditions and load profiles. Whether accurate results can be produced by using fixed UFOP should be examined for each specific system.

The effect of the peaking load unit derated states on the system reliability is examined by applying the simulation program to the RBTS and the IEEE-RTS. The UFOP and DAUFOP for the peaking load units are calculated in the simulation program. The results show that the DAUFOP is larger than the UFOP for a peaking load unit. The generation data used in the analytical program are modified using the

obtained UFOP and the DAUFOP.

The deviations in the reliability indices using the UFOP and the DAUFOP depend on the peaking load unit size, peaking load unit proportional capacity and the system operating conditions. The results for the RBTS and the IEEE-RTS show that the LOLE and LOEE increase when the DAUFOP are used. The deviations in the LOLE and the LOEE using the UFOP and the DAUFOP are, however, small for both the RBTS and the IEEE-RTS with changes in the required reserve, in the peak load and in the starting failure probability.

7. SUMMARY AND CONCLUSIONS

Generating capacity adequacy evaluation is an important area of power system reliability evaluation and is used extensively in power system planning, design and operation. The concern in generating capacity adequacy assessment is on the total system generation and total system load. A wide range of techniques have been developed to perform generating capacity adequacy evaluation. Two computer programs were developed in this research work based on the analytical method and the sequential Monte Carlo simulation method. The research in this thesis is focused on investigating basic considerations in HLI adequacy assessment. The impacts of generating unit state residence time distributions and peaking load units on the system reliability are also examined. The research in this thesis was conducted by applying both the analytical and simulation programs to two reliability test systems, the RBTS and the IEEE-RTS.

Chapter 1 provides a brief introduction to the concept of power system reliability evaluation. Two basic aspects, system security and system adequacy and the three functional zones of a power system are introduced. The merits and demerits of both the analytical and simulation techniques are presented. An introduction to the basic reliability indices and the two reliability test systems is also presented.

The analytical and simulation methods employed in the two programs are described in Chapter 2. Some of the assumptions made in the programs are illustrated. The structures of the two programs are shown in the basic block diagrams presented in this chapter. The graphical user interfaces to input system data, the output of the program and some of the constraints in the programs are presented.

Both the analytical and the simulation programs can consider generating unit derated states. The effects of normally distributed load forecast uncertainty are also incorported in both programs. The two computer programs provide convenient tools to perform sensitivity studies with changing peak loads. The simulation program is able to simulate operating histories for a unit with Weibull distributed state residence times. The simulation program can also produce frequency and duration indices and the reliability index probability distributions.

There are two commonly encountered misconceptions that are made regarding the basic reliability indices. A series of studies to examine the two misconceptions are presented in Chapter 3 using the two computer programs applied to the RBTS and the IEEE-RTS.

The studies in Chapter 3 show that the LOLE (hrs/yr) cannot be obtained by multiplying the LOLE (days/yr) by 24. The LOLE (days/yr) gives a pessimistic appraisal of the system reliability. The ratio changes differently with changing peak loads for systems with different generation compositions. The ratio moves towards the value of 24 with increase in the system daily load factor.

The LOLE does not include any frequency information and cannot be interpreted as a frequency index. The ratio of the reciprocal of the LOLE (days/yr) over the reciprocal of the LOLF (occ/yr) is not unity in most practical situations and decreases with increase in the peak load. The LOLF (occ/yr) increases more slowly than that of the LOLE (days/yr). The average duration of an interruption increases with increase in the peak load. The ratio between the reciprocal of the LOLE expressed in hrs/yr over the reciprocal of the LOLF (occ/yr) is considerable less than unity. The LOLE is simply the expected time in a given period in which the load exceeds the available capacity. The ratios between the LOLE and the LOLF for both the RBTS and the IEEE-RTS remain almost the same for each peak load when the load factor of the normalized load profile changes.

The simulation program can provide a wider range of indices than the analytical program. It can also provide the data required to create reliability index probability distributions. The concept of creating distributions and the additional information that can be obtained and utilized in generating capacity risk assessment is briefly illustrated in Chapter 3. The expected values of LOLE, LOEE and LOLF are basic generating adequacy indices. They are, however, simply the long run average values and contain no information on the dispersion and the annual variability of the indices. Reliability index probability distributions provide additional information on system reliability. The likelihood of encountering a particular level of monetary loss can be obtained from the distribution of the loss of energy shown in Chapter 3 and can be used in utility risk assessment and management.

Non-exponential unit residence time distributions can be considered in the simulation program. The RBTS and the IEEE-RTS were modified to contain generating units that have Weibull distributed repair times with various shape parameters. The mean values of the unit repair times were held constant. The results from the simulation program for the modified RBTS and the IEEE-RTS in Chapter 4 show the impact of the unit state residence time distributions on the system reliability.

In the studies including units without derated states, the expected values of the reliability indices are constant for various Weibull shape parameters when the mean residence time is unchanged. The relative frequencies of encountering no shortage of capacity and the standard deviations of the reliability indices decrease with increase in the shape parameter. The range of the reliability index probability distribution decreases with increase in the shape parameter.

In the studies including units with derated states, both the expected values and the standard deviations of the reliability indices increase with increase in the shape parameter. The relative frequency of encountering no shortage of capacity decreases. The ranges of the reliability index probability distributions increase with increase in

the shape parameter.

Peaking load units and base load units have different operating characteristics. A four-state model is normally used to represent peaking load units and a two-state model is usually applied to base load units. The UFOP or the DAUFOP are used instead of the conventional FOR to calculate the reliability indices in the analytical program. The process to simulate the peaking load units based on the four-state model and the assumptions made in the process are described in Chapter 5. The calculation of the UFOP and DAUFOP is also illustrated.

The RBTS was modified by considering all units to be peaking load units with different loading orders. The effect of system conditions on the UFOP is examined. The results show that the demand factors move towards unity and the UFOP move towards the unit FOR with increase in the required reserve or in the peak load. The UFOP is almost equal to the FOR when the demand factor is close to unity. The demand factors of the peaking load units decrease with the loading order. A peaking load unit has a larger UFOP when it is given a higher loading priority. System reliability indices such as the LOLE, LOEE and LOLF decrease when the larger units have lower loading priorities. The results also show that the use of peaking load unit models decreases the rate of increase in the reliability indices of the LOLE, LOEE and LOLF as the peak load increases.

Chapter 5 also examines the peaking load unit state residence time distributions. The RBTS and the IEEE-RTS were modified to include peaking load units. The results for both systems show that the likelihood of a unit with low loading priority not being required at all in a given year is relatively high. The shape of the unit reserve shutdown time distributions are similar but the magnitudes of the distributions decrease with the loading order. The in-need time distributions are mainly determined by the available system capacity and load data and are not exponential distributed. The in-service time distribution for the peaking load units in both systems are almost the same as the

distribution of the in-need time because the peaking units are only started when they are needed and the units are relatively reliable. The in-need time also significantly affects the forced out when needed distributions. The ranges of the forced out but not needed distributions are larger than those of the forced out when needed distributions. This is because the forced out but not needed durations are more dependent on the unit characteristics. The forced out when needed time and forced out but not needed distributions are not exponential and the frequencies for both distributions decrease with the loading order.

The effects of unit state residence time distributions on the system reliability are examined in Chapter 5. The RBTS and the IEEE-RTS were further modified to include peaking units with Weibull distributed repair times with various shape parameters. The results show that the reserve shutdown time, in-need time and in-service time distributions remain almost the same for the various Weibull shape parameters because these distributions are mainly dependent on the available system capacity of the base load units and the load data. The forced out when needed and forced out but not needed distributions change significantly with changes in the shape parameter. The frequency of the forced out when needed duration decreases relatively quickly when the shape parameter is small. The range of the forced out but not needed distribution decreases and the mode of the distribution moves to the right with increase in the shape parameter.

The obtained UFOP were used to modify the generation data used in the analytical program to calculate system reliability indices in Chapter 6. Normally one fixed UFOP calculated at a certain system condition is used for a wide range of situations and therefore introduces errors in the results. The actual UFOP was calculated for each operating condition and used in the analytical program. The results obtained from the analytical program using the fixed UFOP and the actual UFOP are compared. The results show that the absolute values of the reliability index deviations

introduced by using the fixed UFOP increases when the system operating condition is different from the one on which the fixed UFOP is based. The absolute values of the deviations increase with increase in the peaking load unit proportional capacity. The benefit of the system reliability obtained by considering a unit as a peaking unit is counteracted by its starting failure probability. The UFOP may be even bigger than the unit FOR when the starting failure probability increases above a certain value. Changes in the starting failure probability can cause large changes in the UFOP. The introduced errors are considerable if the fixed UFOP is used to calculate reliability indices in this case. The use of the fixed UFOP introduces errors in the system reliability indices, which can be either pessimistic or optimistic. The utilization of a fixed UFOP should be examined for the specific system under consideration.

The impacts of peaking load unit derated states on the system reliability are also examined in Chapter 6. The system operating conditions such as the required reserve, peak load and the peaking load unit starting failure probability are varied to show the different effects of the peaking unit derated states on the system reliability. The RBTS and the IEEE-RTS are modified to include peaking load units with derated states. The results from the simulation program show that the obtained DAUFOP is always larger than the UFOP for a peaking load unit at a certain operating condition. The obtained UFOP and the DAUFOP are used in the analytical program and the results are compared. The LOLE and the LOEE are larger when using the DAUFOP than when using the UFOP. The deviations in the reliability indices depend on the peaking load unit size, peaking load unit proportional capacity and the system operating conditions. The deviations in the LOLE and the LOEE using the UFOP and the DAUFOP are relatively small for both the RBTS and the IEEE-RTS with changes in the required reserve, in the peak load and in the starting failure probability.

The research work in this thesis is focused on the application of the developed analytical and simulation programs to generating capacity adequacy evaluation. The

effect of unit derated states, unit state residence time distributions and the peaking load units on the system reliability are considered. The conclusions and techniques presented in this thesis should prove to be valuable in power system planning, expansion and operation.

REFERENCES

[1] R. Billinton, R.N. Allan, “Power System Reliability in Perspective”, IEE J. Electronics Power, 30(1984), pp. 231-236.

[2] Roy Billinton, Ronald N. Allan, “Reliability Evaluation of Power Systems” second edition, Plenum Press, New York, 1996.

[3] Roy Billinton, Wenyuan Li, “Reliability Assessment of Electric Power System Using Monte Carlo Methods”, Plenum Press, New York, 1994.

[4] Giuseppe Calabrese, “Generating Reserve Capacity Determined by the Probability Method”, AIEE Trans, vol. 66, pp. 1439-1450, Sept, 1947.

[5] John E. Propst, Daniel R. Doan,” Improvements in Modeling and Evaluation of Electrical Power System Reliability”, IEEE Trans on Industry Applications, vol. 37, no. 5, pp, 1413-1422, September/October 2001.

[6] Clark W. Gellings, Marek Samotyj, and Bill Howe, “The Future’s Smart Delivery System”, IEEE power & Energy Magazine, pp. 40-48, September/October 2004.

[7] Carmen L. T. Borges, Djalma M. Falcão, João Carlos O. Mello, and Albert C. G. Melo, “Composite Reliability Evaluation by Sequential Monte Carlo Simulation on Parallel and Distributed Processing Environments”, IEEE Trans on Power Systems, vol. 16, NO. 2, pp. 203-209, May 2001.

[8] Roy Billinton, Ronanld N. Allan, Luigi Salvaderi, “Applied Reliability Assessment in Electric Power Systems”, IEEE Press, New York, 1991.

[9] Nlma Amjady, Mehdi Ehsan, “Evaluation of Power Systems Reliability by an Artificial Neural Network”, IEEE Trans. on Power Systems, vol. 14, No. 1, pp. 287-292, February 1999.

[10] Roy Billinton, “Criteria Used by Canadian Utility in the Planning and Operation of Generating Capacity”, IEEE Trans. Power Syst. vol. 3, no. 4, pp. 1488-1493, November 1988.

[11] Roy Billinton, “Bibliography on the Application of Probability Methods in Power System Reliability Evaluation”, IEEE Trans. Power Apparatus Syst., vol. 91, no. 2, pp. 649-660, March/Apr. 1972.

[12] IEEE Subcommittee Report, “Bibliography on the Application of Probability Methods in Power System Reliability Evaluation 1971-1977”, IEEE Trans. Power Apparatus Syst., vol. PAS 97, no. 6, pp. 2235-2242, Nov./Dec. 1978.

[13] R.N. Allan, R. Billinton, S.H. Lee, “Bibliography on the Application of Probability Methods in Power System Reliability Evaluation 1977-1982”, IEEE Trans. Power Apparatus Syst., vol. PAS 103, no. 2, pp. 275-282, Feb. 1984.

[14] R.N. Allan, R. Billinton, S.M. Shahidehpour, C. Singh, “Bibliography on the Application of Probability Methods in Power System Reliability Evaluation 1982-1987”, IEEE Trans. Power Apparatus Syst., vol. 3, no. 4, pp. 1555-1564, Nov. 1988.

[15] R.N. Allan, R. Billinton, A.M. Breipohl, and C.H. Grigg, “Bibliography on the application of probability methods in power system reliability evaluation: 1987-1991”, IEEE Trans. Power Systems, vol. 9, no. 4, pp. 275-282, Feb. 1994.

[16] R.N. Allan, R. Billinton, A.M. Breipohl, and C.H. Grigg, “Bibliography on the application of probability methods in power system reliability evaluation: 1992-1996”, IEEE Trans. Power Systems, vol. 14, no. 1, pp. 51-57, Feb. 1999.

[17] Roy Billinton, Mahmud Fotuhi-Firuzabad, and Lina Bertling, “Bibliography on the application of probability methods in power system reliability evaluation: 1996-1999”, IEEE Trans. Power Systems, vol. 16, no. 4, pp. 595-602, Nov. 2001.

[18] R. C. Bansal, T. S. Bhatti, and D. P. Kothari, “Discussion of “Bibliography on the Application of Probability Methods in Power System Reliability Evaluation”, IEEE Trans. Power Systems, vol. 17, no. 3, pp. 924, Aug. 2002.

[19] C.J. Baldwin, D.P. Gaver, and C.H. Hoffman, “Mathematical Models for Use in the Simulation of Power Generation Outages I—Fundamental Considerations”, AIEE Trans. Power Apparatus Syst., vol. 78, pp. 1251-1258, Dec. 1959.

[20] L. Salvaderi and R. Billinton, “A Comparison between two fundamentally different approaches to composite system reliability evaluation”, IEEE Trans. Power Apparatus Syst., vol. PAS-104, no. 12, pp. 3486-3493, Dec. 1985.

[21] A. D. Patton, J.H. Blackstone, and N.J. Balu, “A Monte Carlo Simulation Approach to the Reliability Modeling of Generating Systems Recognizing Operating Considerations”, IEEE Trans. Power Systems, vol. 3. no. 3, pp. 1174-1180, Aug. 1988.

[22] R. Billinton, S. Kumar, N. Chowdhury, K. Chu, K. Debnath, L. Goel, et al. “A Reliability Test System for Educational Purposes – Basic Data,” IEEE Transaction on Power System, vol. 4, No. 3, pp. 1238-1244, August 1989.

[23] Reliability Test System Task Force of the IEEE Subcommittee on the Application of Probability Methods, “IEEE Reliability Test System,” IEEE Trans. on Power Apparatus and Systems, vol PAS-98 No. 6, pp. 2047-2054, Nov/Dec, 1979.

[24] Report of the IEEE Task Group on Models for Peaking Service Unit, “A Four State Model for Estimation of Outage Risk for Units in Peaking Service”, IEEE Trans. Power Apparatus System, vol. PAS-91, no. 2, pp. 618-627, Mar./Apr. 1972.

[25] “2003 Generating Equipment Statistics Annual Report, Equipment Reliability Information System”, Canadian Electricity Association, July 2004.

[26] Roy Billinton, and Ronald N. Allan, “Reliability Evaluation of Engineering Systems Concepts and Techniques”, Second Edition, Plenum Press, New York, 1992.
[27] Giuseppe Calabrese, “Generating Reserve Capacity Determined by the Probability Method”, AIEE Trans., vol. 66, pp. 1439-1450, Sept. 1947.
[28] J.D. Hall, R.J. Ringlee, and A. J. Wood, “Frequency and Duration Methods for Power System Reliability Calculations: I - Generation System Model”, IEEE Trans. Power Apparatus Syst., vol. PAS-87, no. 9, pp. 1787-1796, Sept, 1968.
[29] R.J. Ringlee and A. J. Wood, “Frequency and Duration Methods for Power System Reliability Calculations: II - Demand Model and Capacity Reserve Model”, IEEE Trans. Power Apparatus Syst., vol. PAS-87, no. 9, pp. 1787-1796, Sept, 1968.
[30] A.K. Ayoub, and A.D. Patton, “A Frequency and Duration Method for Generating Capacity System Reliability Evaluation”, IEEE Trans. Power Apparatus Syst., vol. PAS-95, no. 6, pp. 1929-1933, Nov./Dec. 1976.
[31] Roy Billinton, Chanan Singh, “Generating Capacity Reliability Evaluation in Interconnected Systems Using a Frequency and Duration Approach Part I., Mathematical Analysis”, IEEE Trans. Power Apparatus Syst., vol. PAS-90, no. 4, pp. 1646-1654, July/Aug. 1971.
[32] O. Bertoldi, L. Salvaderi, and S. Scalcino, “Monte Carlo Approach in Planning Studies: An Application to IEEE-RTS”, IEEE Trans. Power Syst., vol. 3, no. 3, pp. 1146-1154, Aug. 1988.
[33] Roy Billinton, and Jingdong Ge, “A Comparison of Four-State Generating Unit Reliability Models for Peaking Units”, IEEE Trans. Power Syst. vol. 19, No. 2, May 2004, pp. 763-768.
[34] D.O. Koval, and A.A. Chowdhury, “Generating peaking unit operating characteristics”, IEEE Trans. Industry Applications, vol. 30, Sept.-Oct. 1994, pp. 1309-1316.
[35] R. Billinton, and R. Ghajar, “Utilization of Monte Carlo Simulation in Generating Capacity Adequacy Evaluation”, Canadian Electrical Association, Power System Reliability Subsection, Power System Planning and Operation Section, Engineering and Operating Division, March 1987.

APPENDIX A. BASIC DATA FOR THE RBTS AND THE IEEE-RTS

Tables A.1 and A.2 present the generator data for the RBTS and the IEEE-RTS respectively.

Table A.1: Generator data for the RBTS

Unit Size (MW)	Type	No. of Units	MTTF (hr)	Failure Rate per Year	MTTR (hr)	Repair Rate per Year	Forced Outage Rate
5	Hydro	2	4380	2.0	45	198	0.010
10	Lignite	1	2190	4.0	45	196	0.020
20	Hydro	4	3650	2.4	55	157	0.015
20	Lignite	1	1752	5.0	45	195	0.025
40	Hydro	1	2920	3.0	60	147	0.020
40	Lignite	2	1460	6.0	45	194	0.030

Table A.2: Generator data for the IEEE-RTS

Unit Size (MW)	Type	No. of Units	MTTF (hr)	Failure Rate per Year	MTTR (hr)	Repair Rate per Year	Forced Outage Rate
12	Oil	5	2940	2.9796	60	146	0.02
20	Oil	4	450	19.4667	50	175.2	0.1
50	Hydro	6	1980	4.4242	20	438	0.01
76	Coal	4	1960	4.4694	40	219	0.02
100	Oil	3	1200	7.3000	50	175.2	0.04
155	Coal	4	960	9.1250	40	219	0.04
197	Oil	3	950	9.2211	50	175.2	0.05
350	Coal	1	1150	7.6174	100	87.6	0.08
400	Nuclear	2	1100	7.9636	150	58.4	0.12

The annual peak loads are 185 MW and 2850 MW for the RBTS and the IEEE-RTS respectively. Tables A.3 to A.5 present the normalized load profile for both the RBTS and the IEEE-RTS.

Table A.3: Weekly peak load in percent of annual peak

Week	Peak Load	Week	Peak Load	Week	Peak Load	Week	Peak Load
1	86.2	14	75.0	27	75.5	40	72.4
2	90.0	15	72.1	28	81.6	41	74.3
3	87.8	16	80.0	29	80.1	42	74.4
4	83.4	17	75.4	30	88.0	43	80.0
5	88.0	18	83.7	31	72.2	44	88.1
6	84.1	19	87.0	32	77.6	45	88.5
7	83.2	20	88.0	33	80.0	46	90.9
8	80.6	21	85.6	34	72.9	47	94.0
9	74.0	22	81.1	35	72.6	48	89.0
10	73.7	23	90.0	36	70.5	49	94.2
11	71.5	24	88.7	37	78.0	50	97.0
12	72.7	25	89.6	38	69.5	51	100.0
13	70.4	26	86.1	39	72.4	52	95.2

Table A.4: Daily peak load in percent of weekly peak

Day	Peak Load
Monday	93
Tuesday	100
Wednesday	98
Thursday	96
Friday	94
Saturday	77
Sunday	75

Table A.5: Hourly peak load in percent of daily peak

Hour	Winter weeks 1 -8 & 44 - 52		Summer weeks 18 -30		Spring/Fall weeks 9-17 & 31 - 43	
	Week Day	Week End	Week Day	Week End	Week Day	Week End
12-1 am	67	78	64	74	63	75
1--2	63	72	60	70	62	73
2--3	60	68	58	66	60	69
3--4	59	66	56	65	58	66
4--5	59	64	56	64	59	65
5--6	60	65	58	62	65	65
6--7	74	66	64	62	72	68
7--8	86	70	76	66	85	74
8--9	95	80	87	81	95	83
9--10	96	88	95	86	99	89
10--11	96	90	99	91	100	92
11-noon	95	91	100	93	99	94
Noon-1pm	95	90	99	93	93	91
1--2	95	88	100	92	92	90
2--3	93	87	100	91	90	90
3--4	94	87	97	91	88	86
4--5	99	91	96	92	90	85
5--6	100	100	96	94	92	88
6--7	100	99	93	95	96	92
7--8	96	97	92	95	98	100
8--9	91	94	92	100	96	97
9--10	83	92	93	93	90	95
10--11	73	87	87	88	80	90
11--12	63	81	72	80	70	85

APPENDIX B. FLOW CHARTS FOR THE ANALYTICAL PROGRAM

The basic block diagram for the analytical program is shown in Figure 2.8. The processes to form the COPT and calculate reliability indices are shown in the following.

The flow chart to form the COPT is shown in Figure B.1.

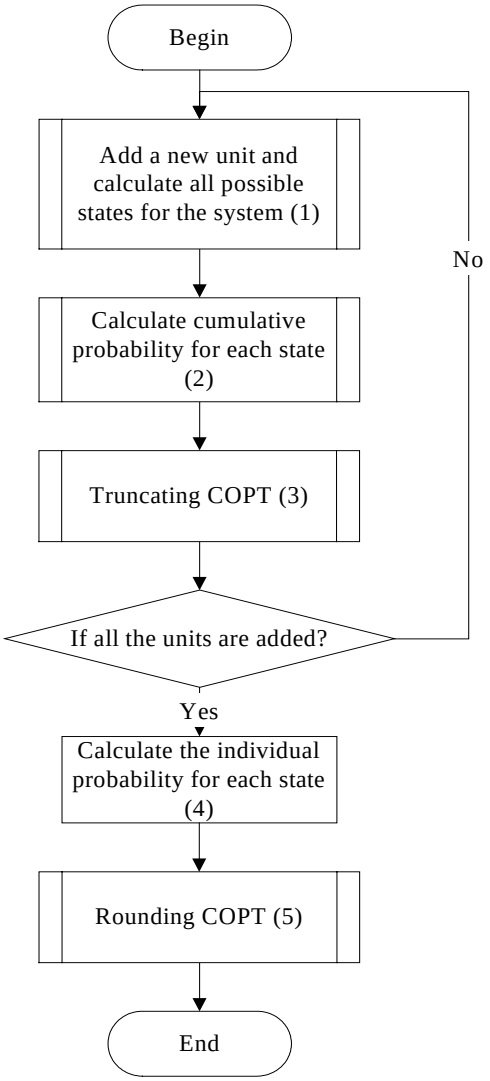

Figure B.1: Form COPT

Steps (1), (2), (3) and (4) in Figure B.1 are shown in detail as follows.

Step (1): All possible states for the system after a unit is added are calculated as shown in Figure B.2.

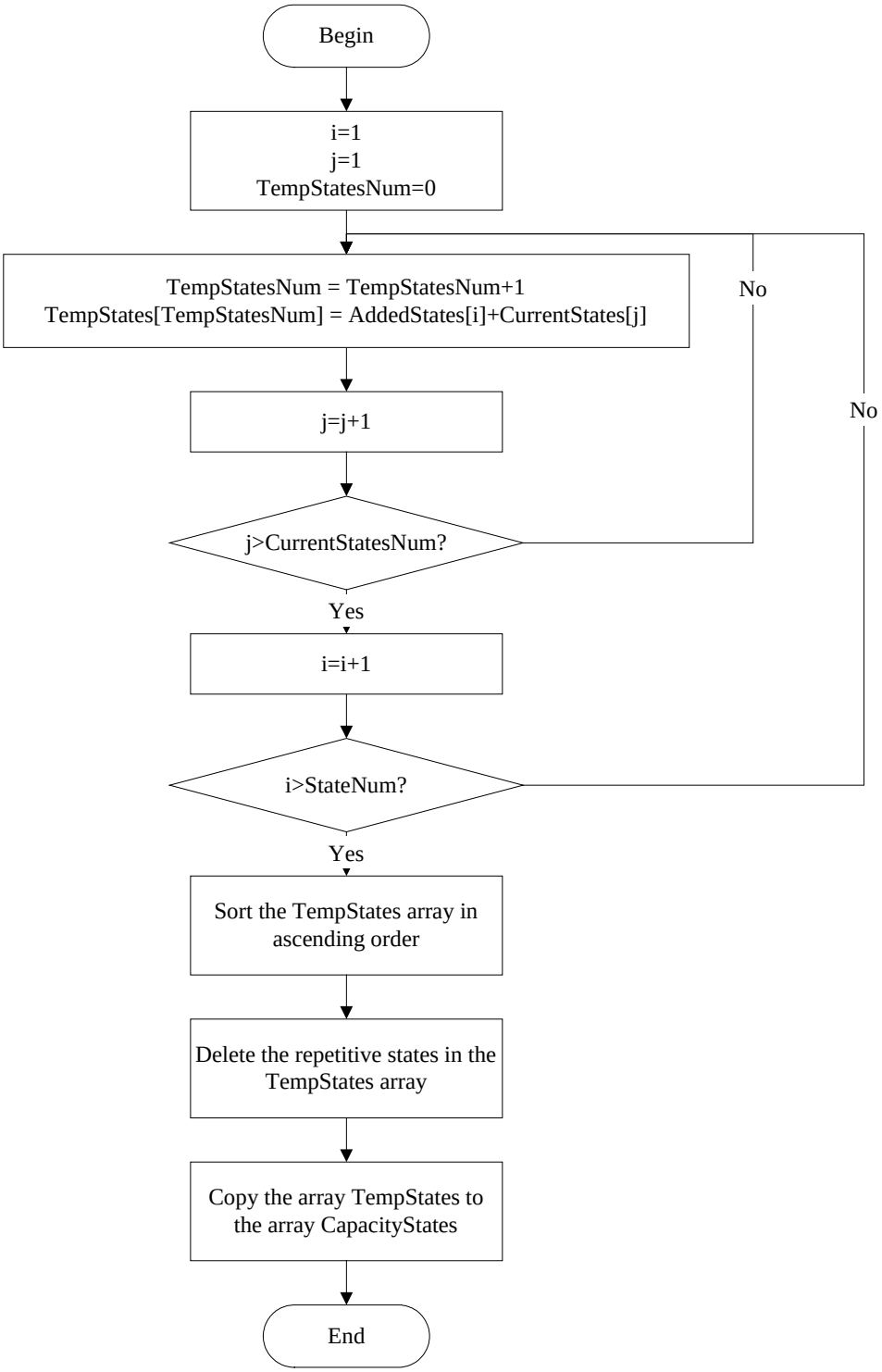

Figure B.2: Calculate all possible states after a unit is added

The variables used in Figure B.2 are described as follows.

TempStatesNum: Number of states of the COPT after a unit is added.

TempStates: An array. TempStates[i] represents the capacity out of service of state i in the COPT after a unit is added.

AddedStates: An array. AddedStates[i] represents the capacity out of service of the added unit at state i.

CurrentStates: An array. CurrentState[i] represents the capacity out of service of state i in the COPT before the unit is added.

CapacityStates: An array. CapacityStates[i] represents the capacity out of service of state i in the COPT.

Step (2): The processes to calculate probability for each state are shown in Figure B. 3. The variables used in Figure B.3 are described as follows.

CapacityStatesNum: The total number of states after a unit is added.

GStatesNum: an array. GStatesNum[j] represents the number of states of the added unit i.

PrevCapacity: The capacity out of service of the current COPT minus the capacity out of service of the added unit at state DeratedN.

OldStates: An array. OldStats[i] represents the capacity out of service of state i in the COPT before the unit is added.

OldStatesNum: The total number of states of the COPT before the unit is added.

oldStatesProb: An array. oldStateProb[i] represents the probability of state i in the COPT before the unit is added.

CumuProb: An array. CumuProb[k] represents the cumulative probability of state k in the COPT.

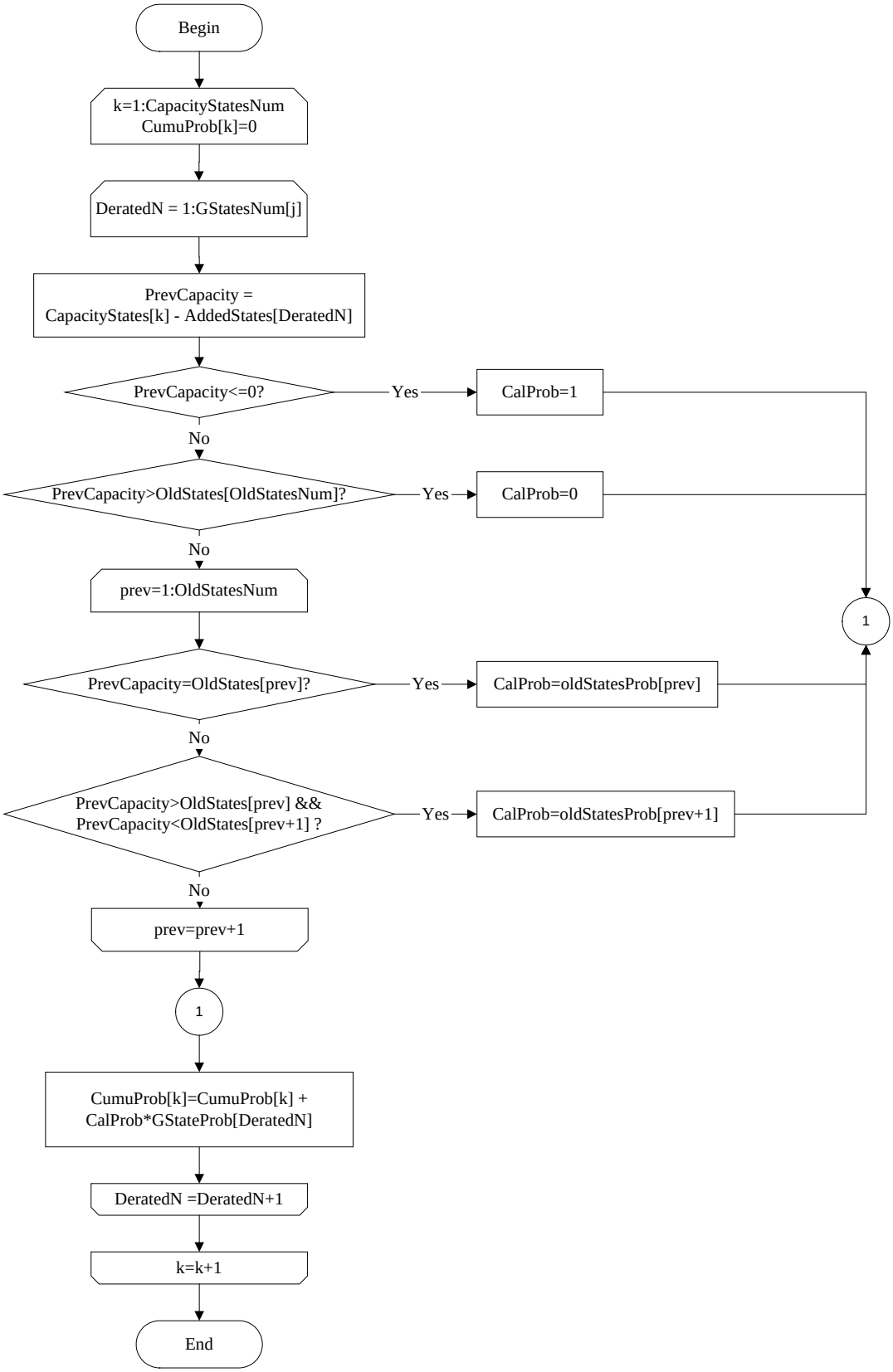

Figure B.3: Calculate cumulative probability for each state after a unit is added

Step (3): The processes to truncate the COPT after a unit is added are shown in Figure B.4.

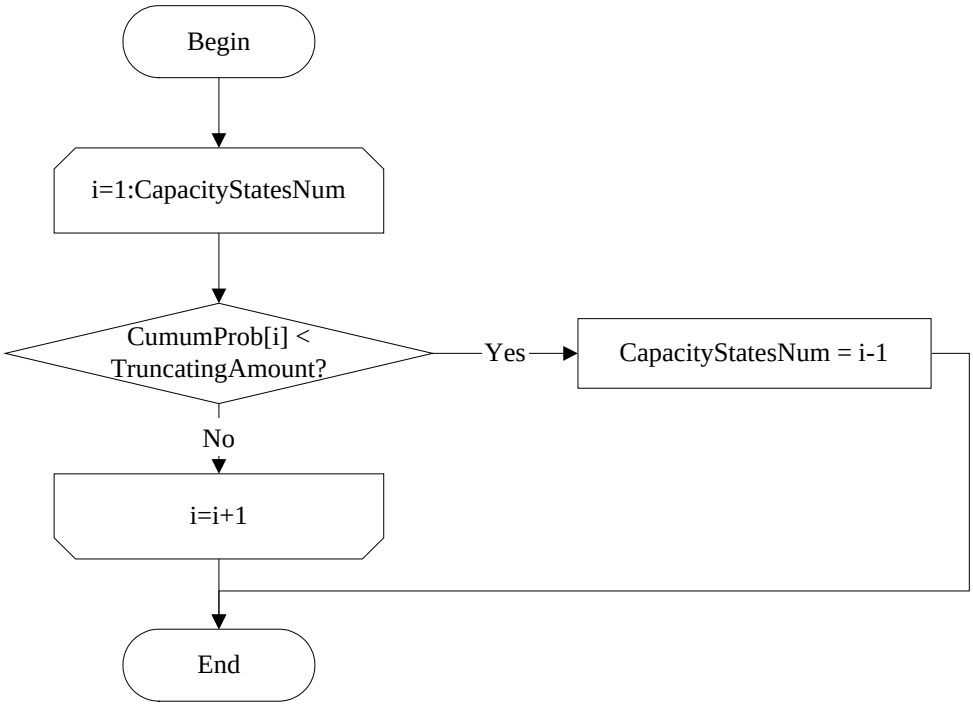

Figure B.4: Truncate the COPT after a unit is added

Step (4): The processes to calculate the individual probability for each state in the COPT after all units are added are shown in Figure B.5.

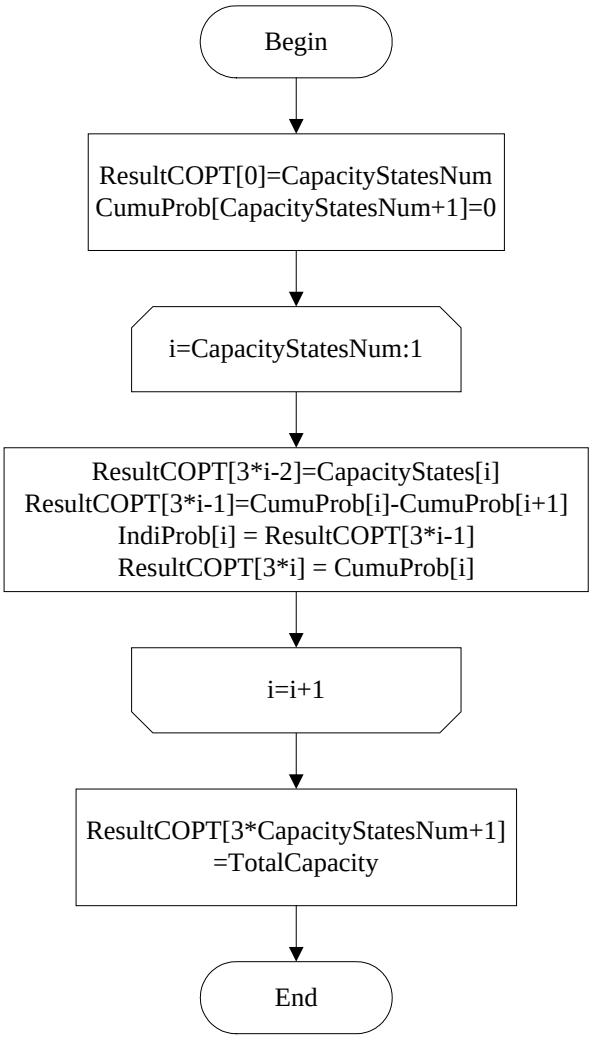

Figure B.5: Calculate individual probability for each state

The variables used in the process are described as follows.

ResultCOPT: An array to save all the COPT information.

ResultCOPT[0] represents the total number of states in the COPT.

ResultCOPT[3*i] represents the cumulative probability of state i in the COPT.

ResultCOPT[3*i-1]: represents the individual probability of state i in the COPT.

ResultCOPT[3*i-2]: represents the capacity out of service of state i in the COPT.

ResultCOPT[3*CapacityStatsNum+1]: represents the total capacity of the generating system.

IndivProb: An array. IndivProb[i] represents the individual probability of state i in the COPT.

Step (5): The processes to round the created COPT. A predefined process named GetRoundingProb is called in Step (5). The GetRoundingProb is used to calculate the individual probability of a state in the COPT according to the rounding increment. The flow chart for it is shown in Figure B.6. The flow chart for Step (5) are shown in Figure B.7.

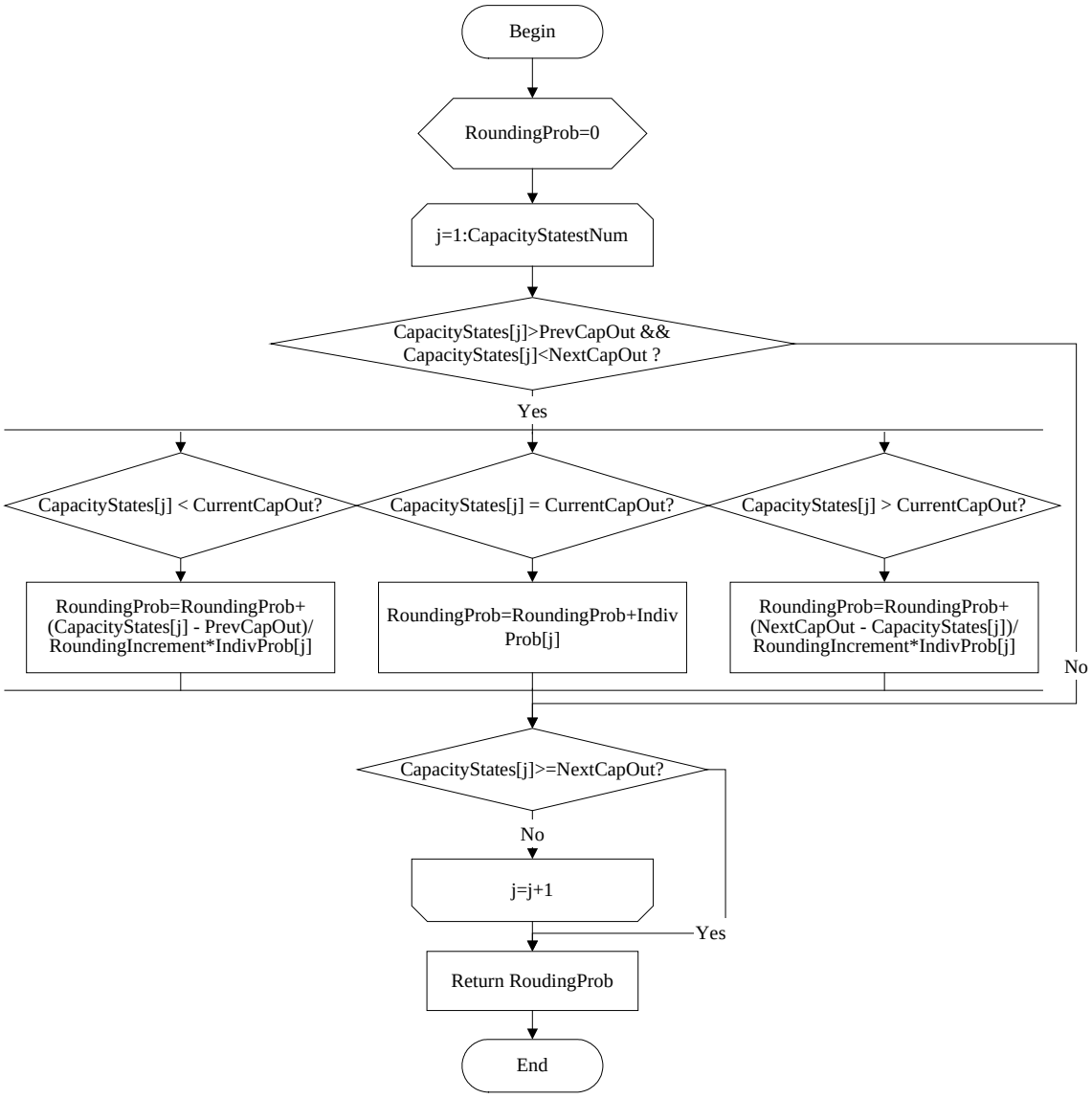

Figure B.6: The predefined process GetRoundingProb()

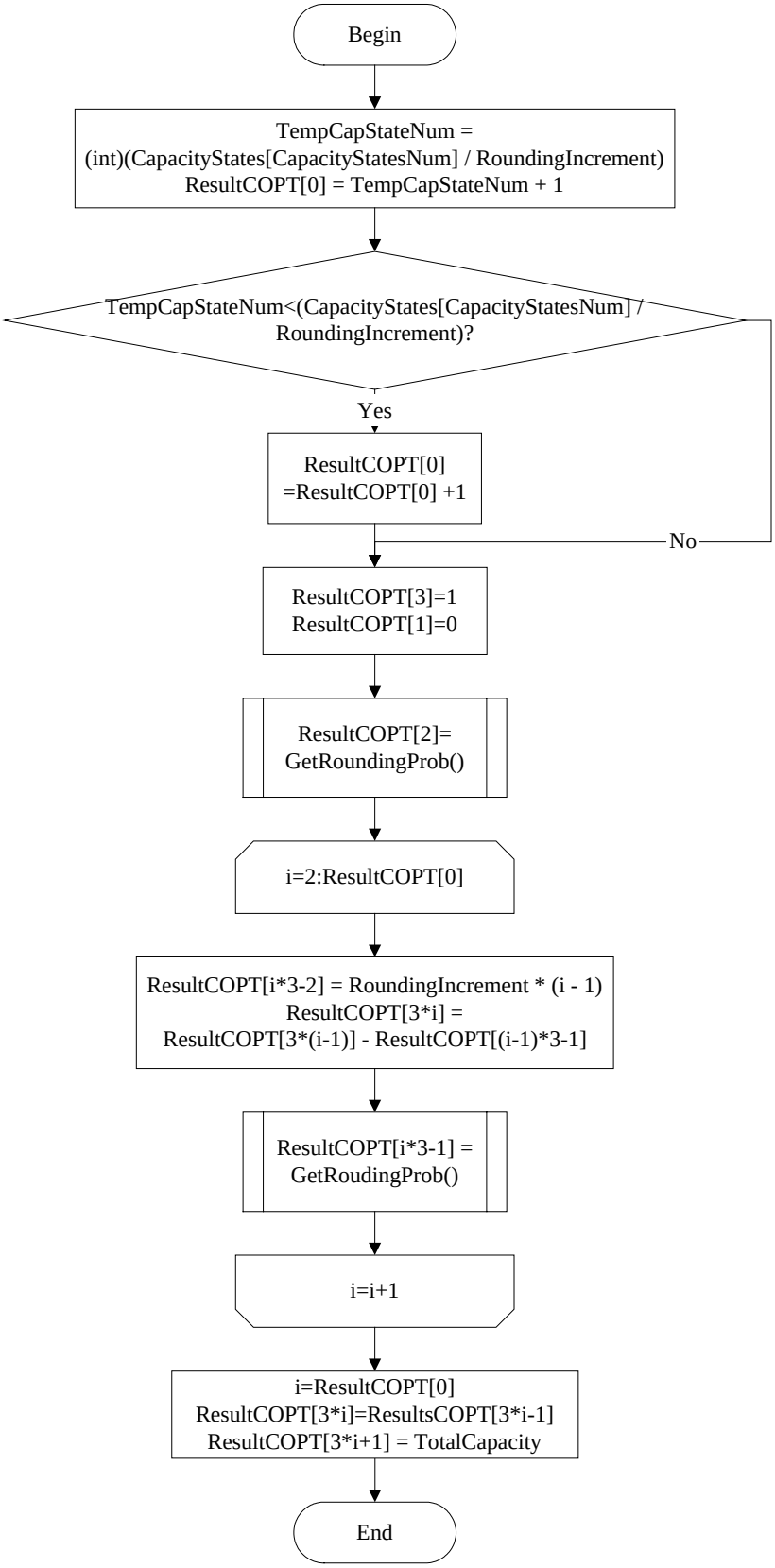

Figure B.7: Round the COPT

The variables used in Figures B.6 and B.7 are as follows.

RoundingProb: The individual probability for a rounding state.

CurrentCapOut: The capacity out of service for a rounding state.

RoundingIncrement: The increment of the rounding.

PrevCapOut: CurrentCapOut – RoundingIncrement.

NextCapOut: CurrentCapOut + RoundingIncrement.

The formed COPT is combined with the load data to calculate the reliability indices. The processes to calculate the reliability indices are shown in Figure B.8.

The variables used in this process are described as follows.

ResultLOLE: An array. ResultLOLE[i] represents the LOLE for the ith peak load.

ResultLOEE: An array. ResultLOEE[i] represents the LOEE for the ith peak load.

ResultLOLP: An array. ResultLOLP[i] represents the LOLP for the ith peak load.

LostEnergy: The energy that might lost at a peak load level.

TotalEnergy: The total energy that is required at a peak load level.

CurveType: The curve type of the load data. CurveType=1 represents straight line. CurveType=2 represents the discrete load points. CurveType=3 represents the multi-step load data.

LoadModel: LoadModel=1 represents constant load. LoadModel=2 represents daily peak load. LoadModel=3 represents hourly load.

LoadData: An array. LoadData[0] represents the number of load points. LoadData[1] represents the time period of the load data, the unit of which is year. LoadData[i+1] represents the ith load in percent of the peak load. If the load data are multi-step loads, LoadData[i+1+ LoadData[0]] represents the probability of this load level.

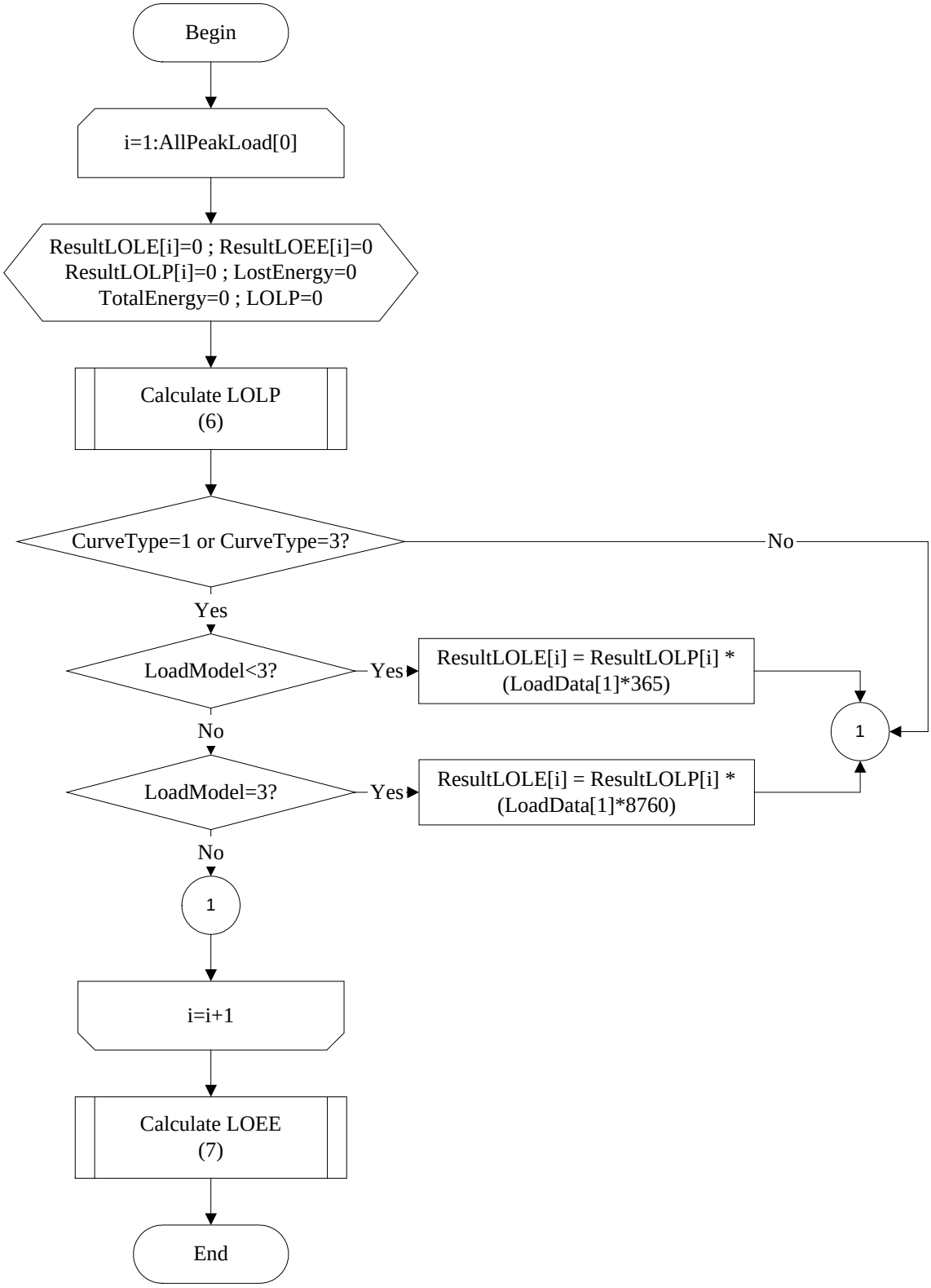

Figure B.8: Calculate reliability indices

Step (6): The processes to calculate the LOLP for a peak load level are shown in Figure B.9.

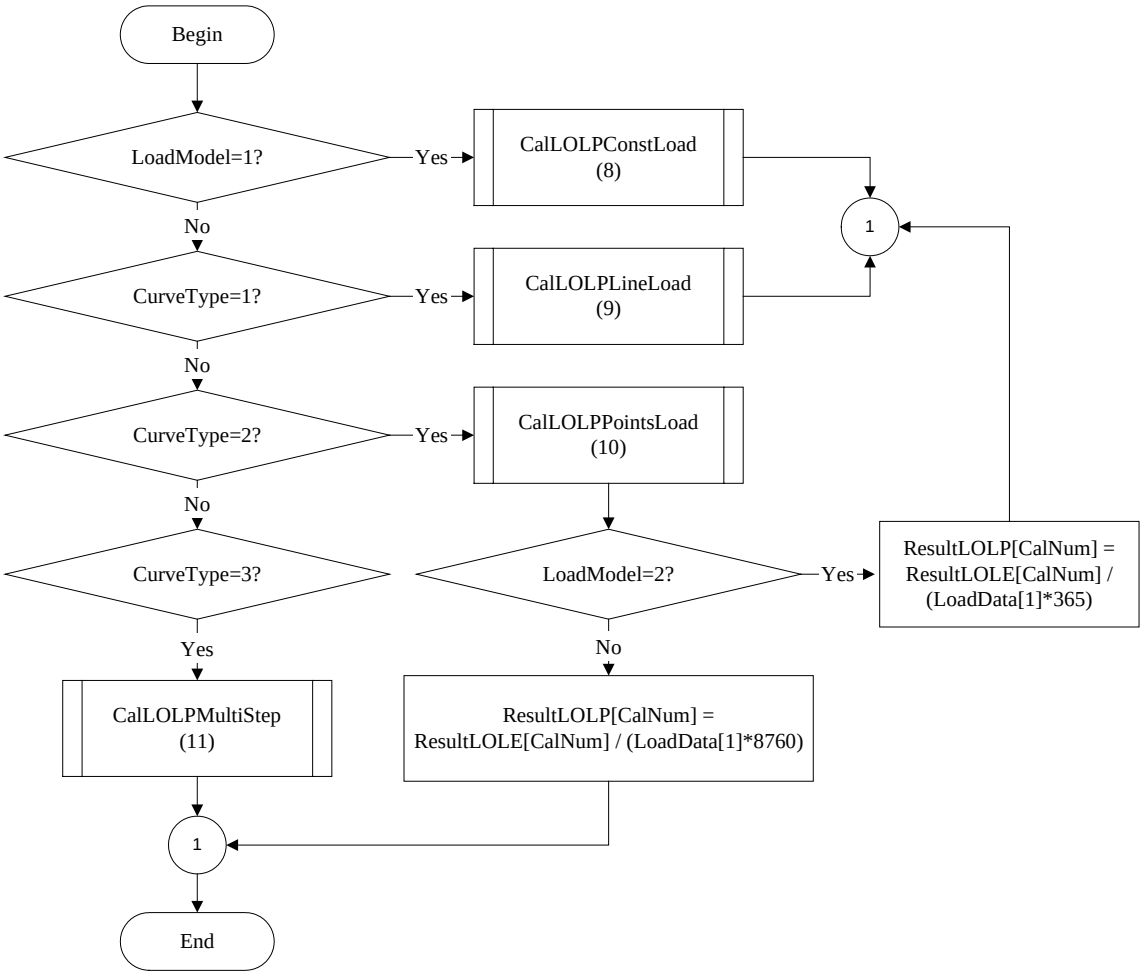

Figure B.9: Calculate the LOLP for a peak load level

In Figure B.9, the variable CalNum is the number of the peak load level.

Step (8): The processes to calculate the LOLP when the load is constant are shown in Figure B.10. The variables in Figure B.10 are described as follows.

StatesNum: Number of states of the COPT.

CapacityIn[i]: The capacity in service at state i in the COPT.

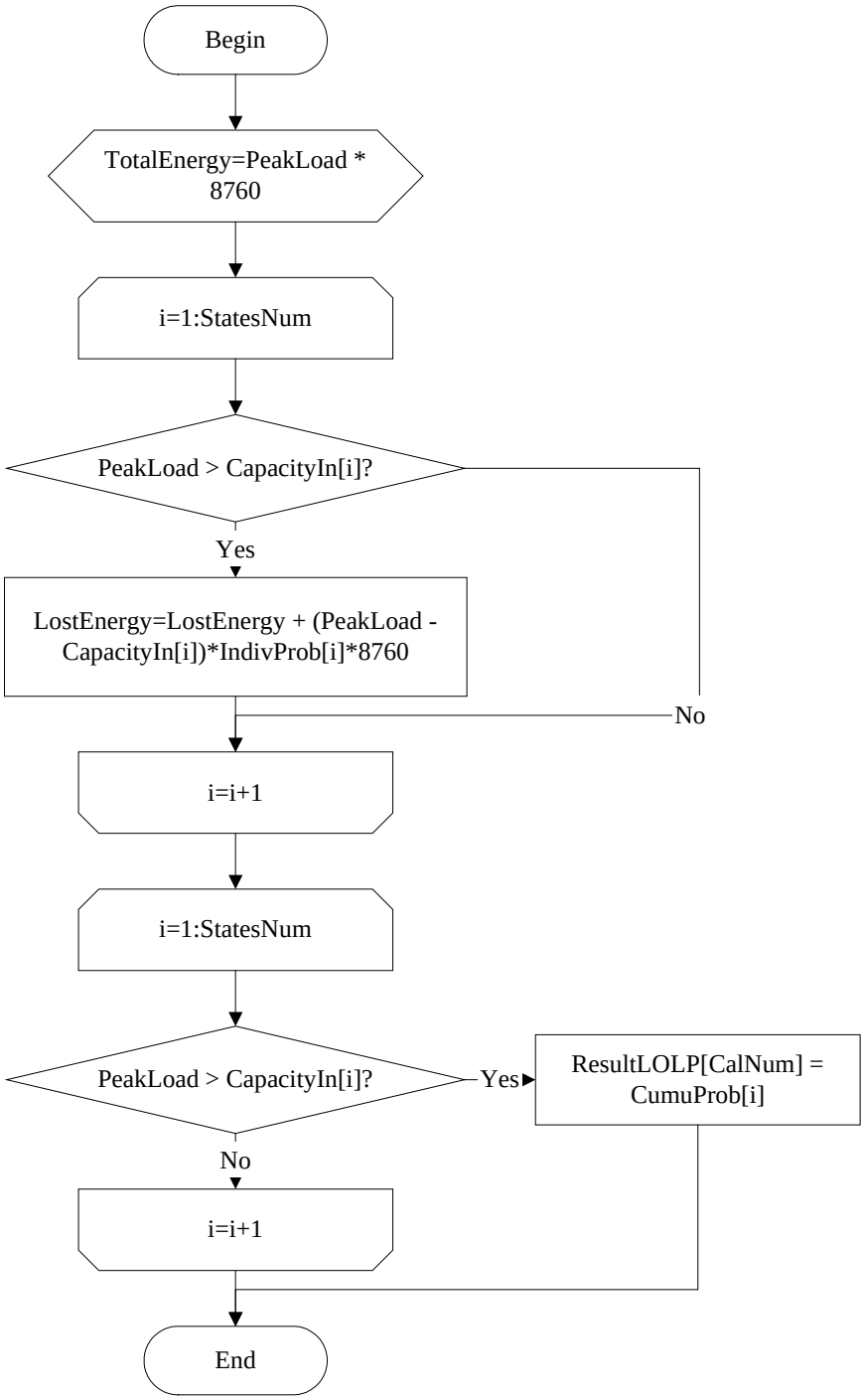

Figure B.10: Calculate the LOLP for constant load

Step (9): The processes to calculate the LOLP when the load is a straight line are shown in Figure B.11.

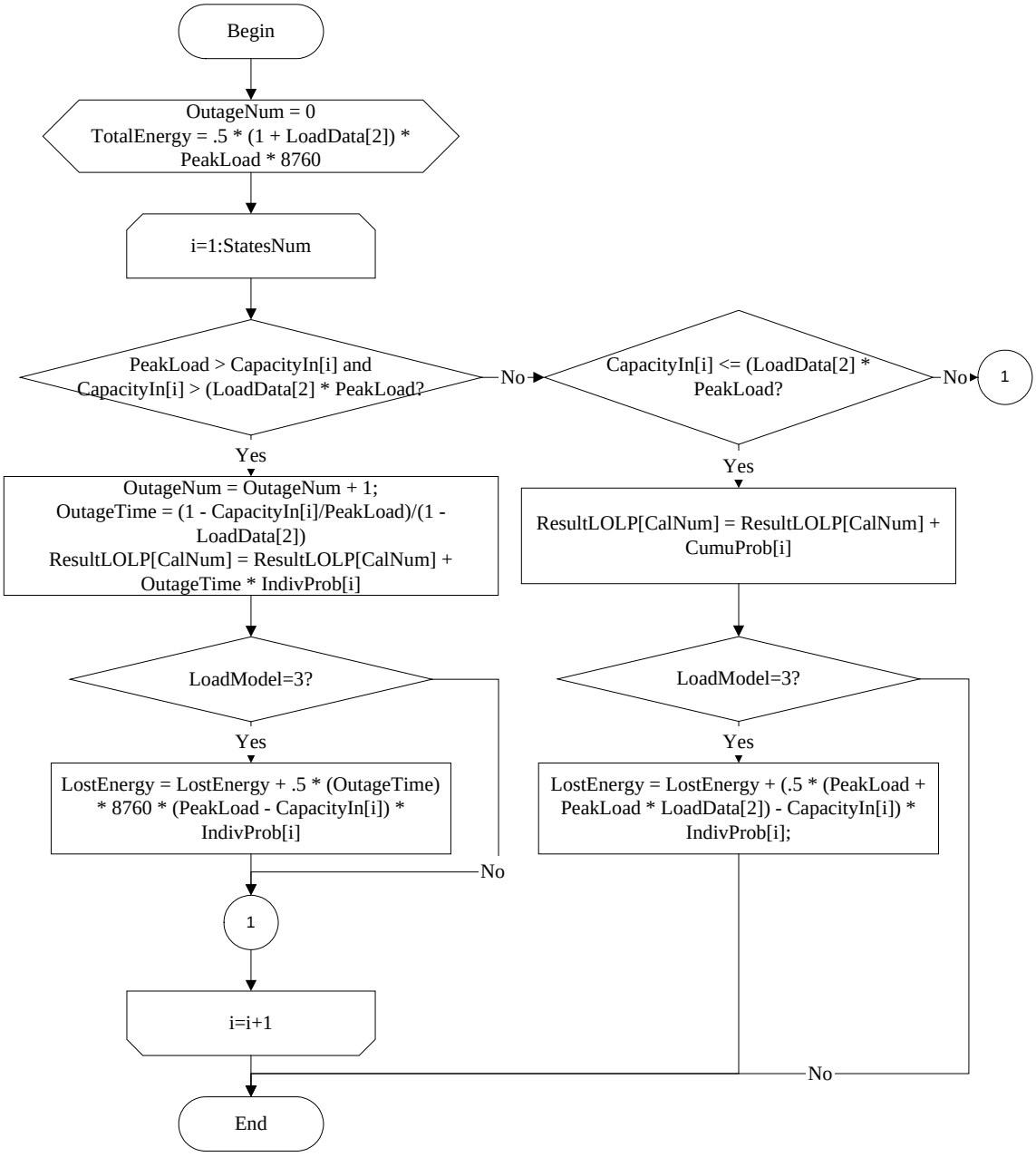

Figure B.11: Calculate the LOLP when load is a straight line

The variables used in Step (9) are described as follows.

OutageNum: The number of outages.

OutageTime: The outage duration when an outage occurs.

Step (10): The processes to calculate the LOLP when the load data are represented by discrete load points are shown in Figure B.12.

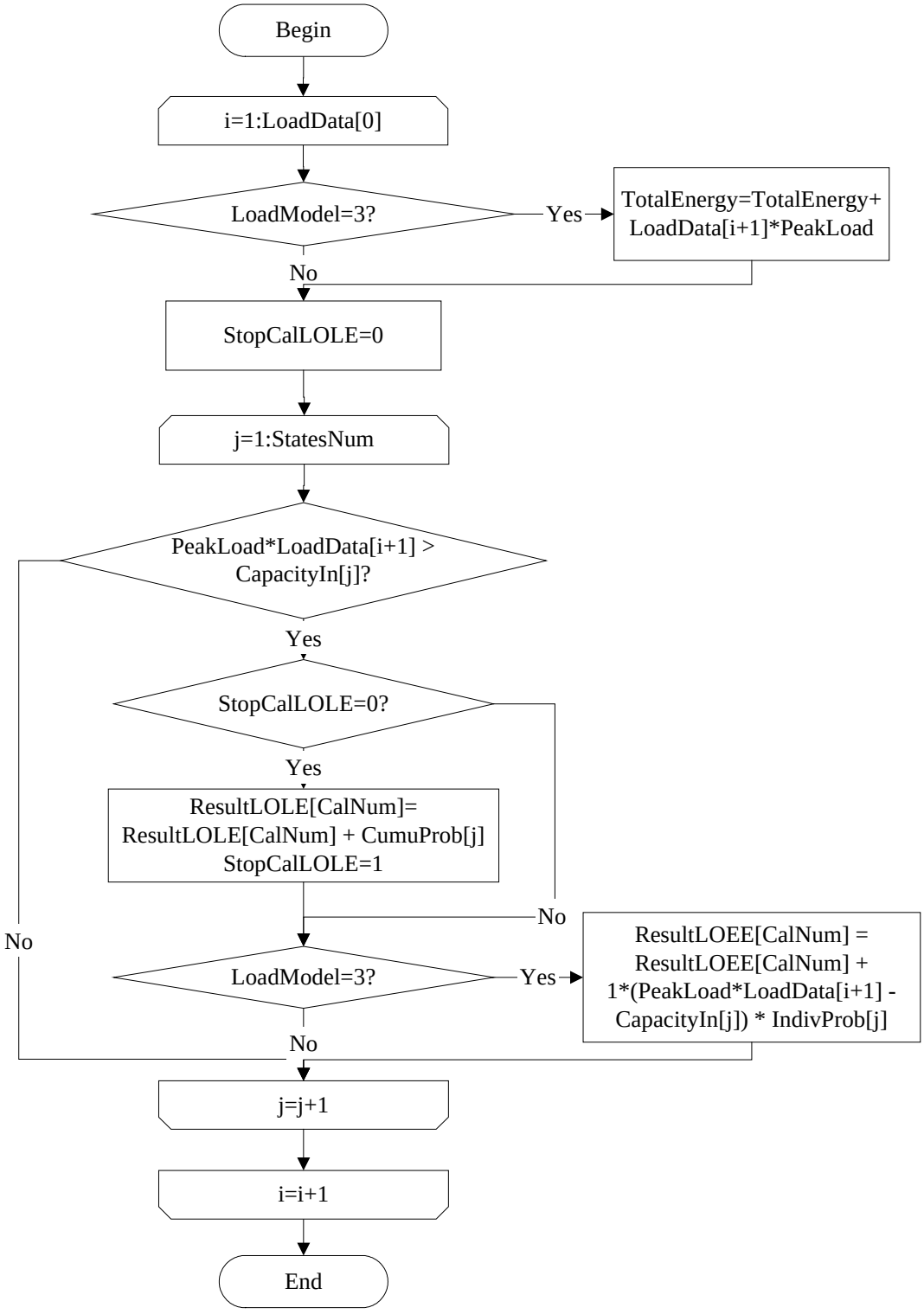

Figure B.12: Calculate the LOLP when load data are discrete points

Step (11): The processes to calculate the LOLP when the load is multi-step are shown in Figure B.13.

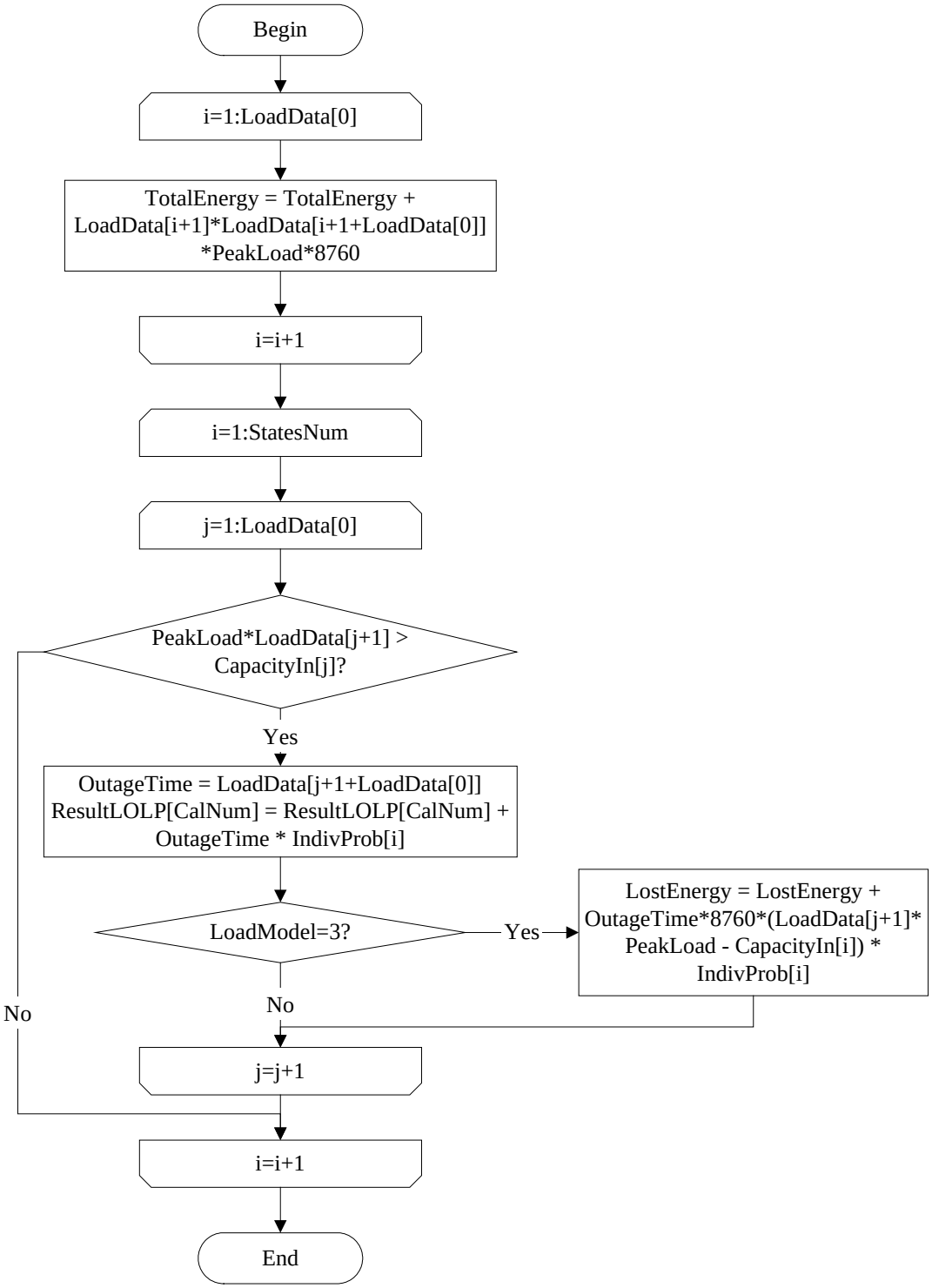

Figure B.13: Calculate the LOLP when load is multi-step

Step (7): The processes to calculate the LOEE are shown in Figure B.14.

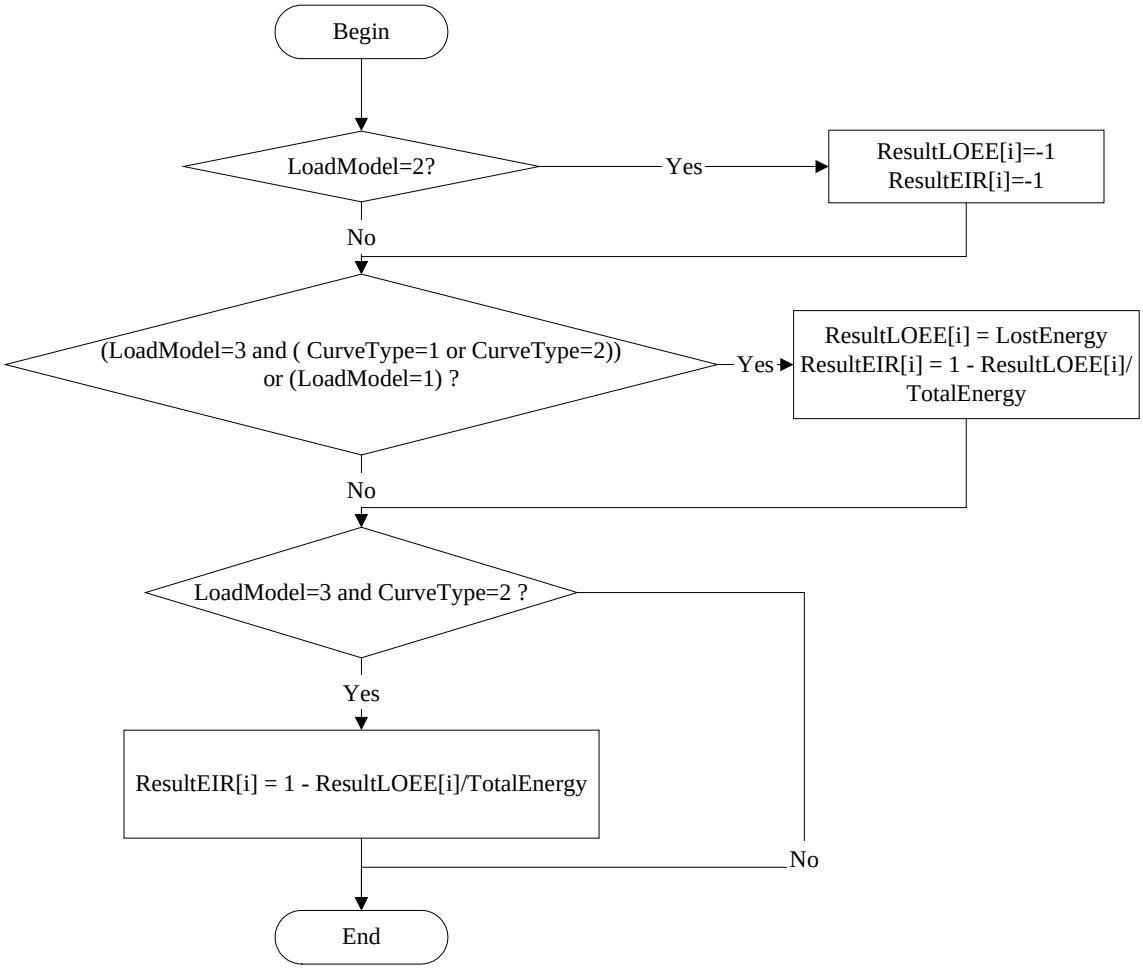

Figure B.14: Calculate the LOEE

The variables used in Figure B.14 are described as follows.

ResultEIR: An array. ResultEIR[i] represents the calculated EIR at peak load i.

APPENDIX C. FLOW CHARTS FOR THE SIMULATION PROGRAM

The basic block diagram for the simulation program is shown in Figure 2.14. The flow charts for all steps are shown in the following.

Step (1): The processes to simulate the base load unit operating histories are shown in Figure C.1. The variables used in this process are described in the following.

ChangeNum: It represents the number of changes for a unit in a given study period.

GChangeTime: An array. GchangeTime[i][0] represents the total number of changes of unit i in the study period. GchangeTime[i][j] represents the time that the generating unit i changes j times in a given study period.

CurGNum: It represents the number of the generating unit.

CurStateNum: represents the current state that the unit resides.

GState: An array. GState[i][j] represents the state of the generating unit i at the jth change.

TDuration: An array. TDuration[i][j] represents the generating unit i's duration at the jth change.

GStatesNum: An array. GStatesNum[i] represents the number of the states of the generating unit i.

CompPara: An array. CompPara[1] represents the transition rate between states for exponential distributed state. CompPara[2] and CompPara[3] represent the scale and the shape parameter of the Weibull distribution respectively.

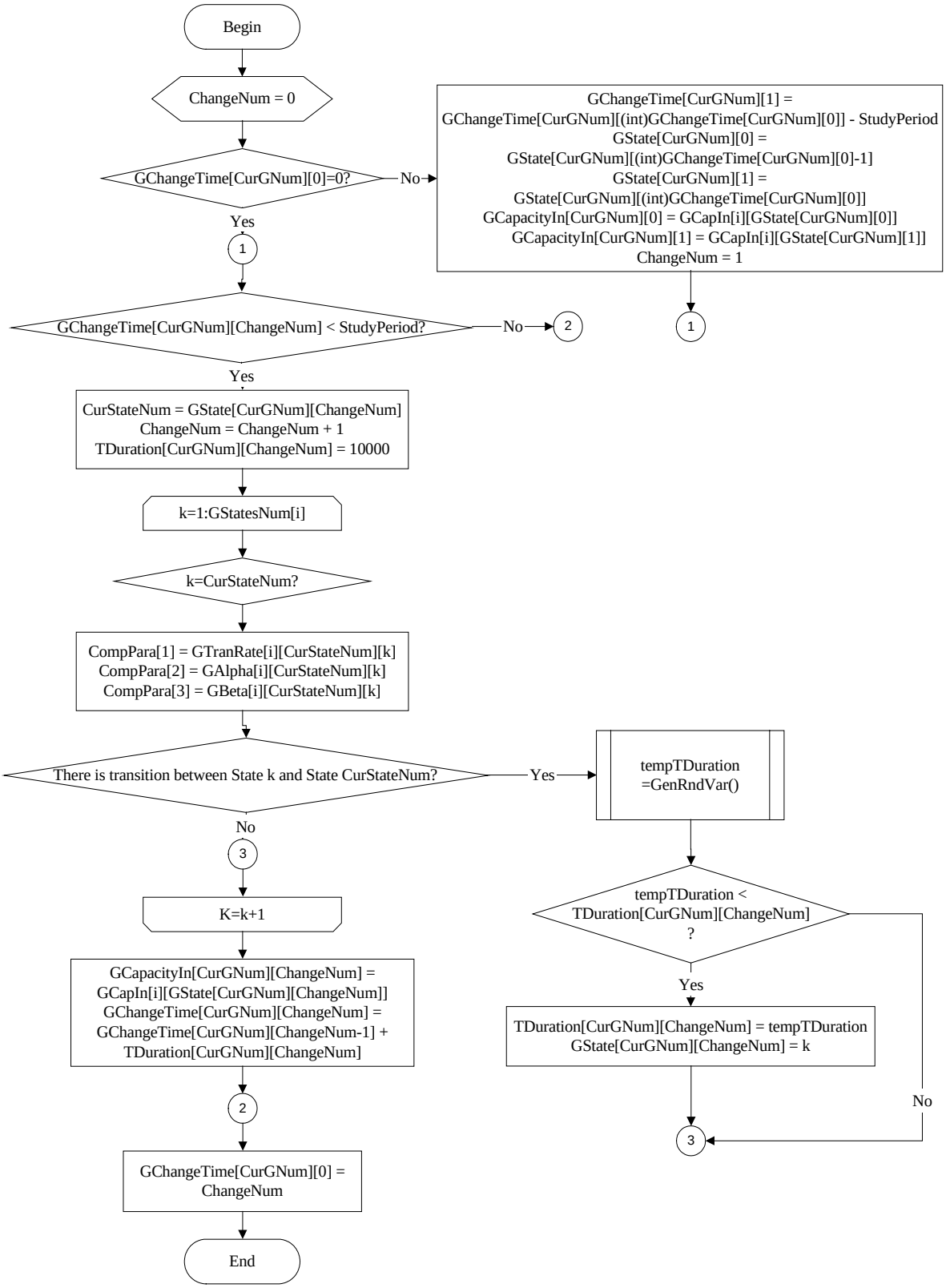

Figure C.1: Simulate base load unit operating histories for a study period

GCapacityIn: An array. GCapacity[i][j] represents the capacity in service of unit i at the jth change.

GCapIn: An array. GCapIn[i][j] represents the capacity in service of the unit group i at state j.

GenRndVar() in Step (1) is a predefined process to calculate the unit duration at a state and is shown in Figure C.2.

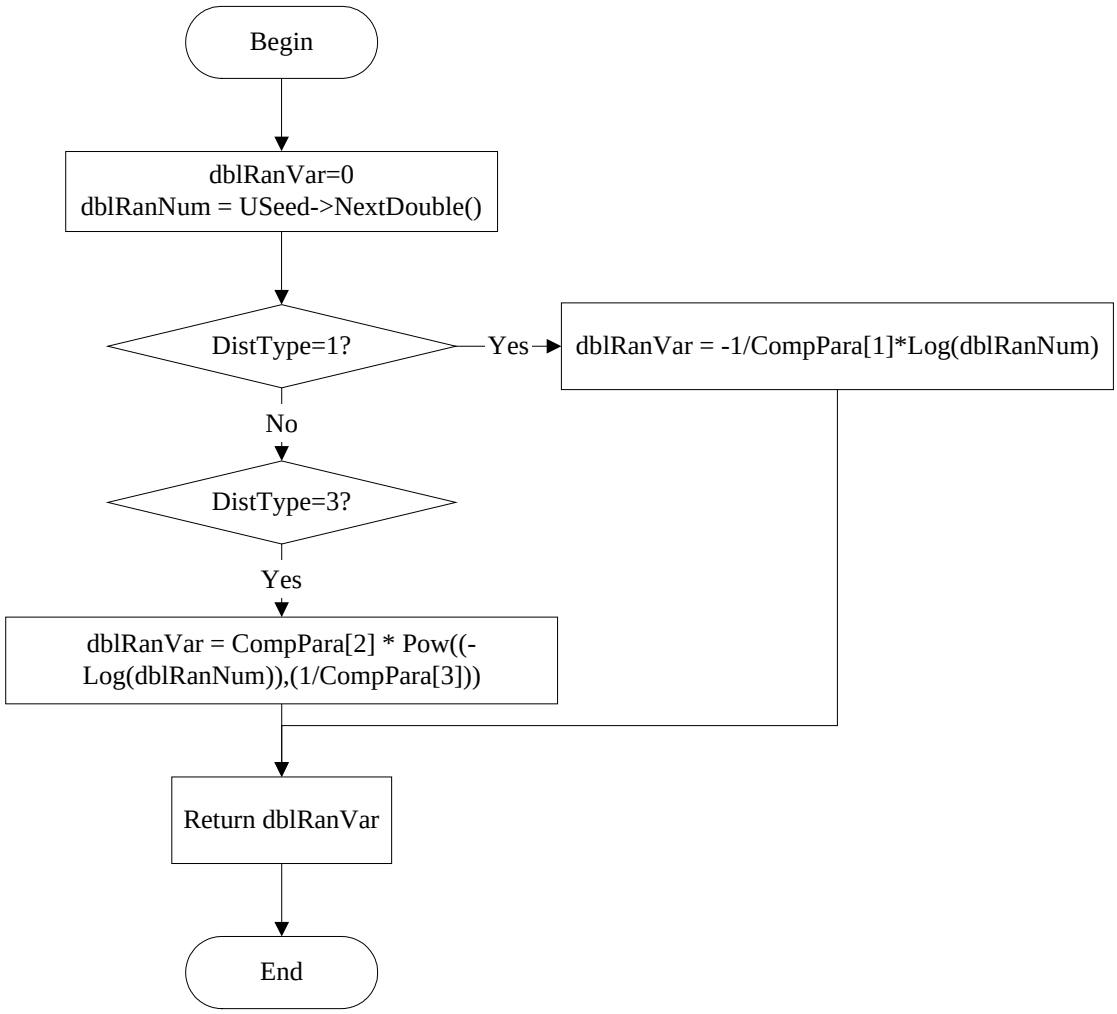

Figure C.2: The predefined process GenRndVar()

The variables used in this process are described in the following:

dblRanNum: a uniformly distributed random number between [0,1].

dblRanVar: The random variate produced from the dblRanNum according to the distribution type.

Step (2): The processes to calculate base load unit available capacity are shown in Figure C. 3.

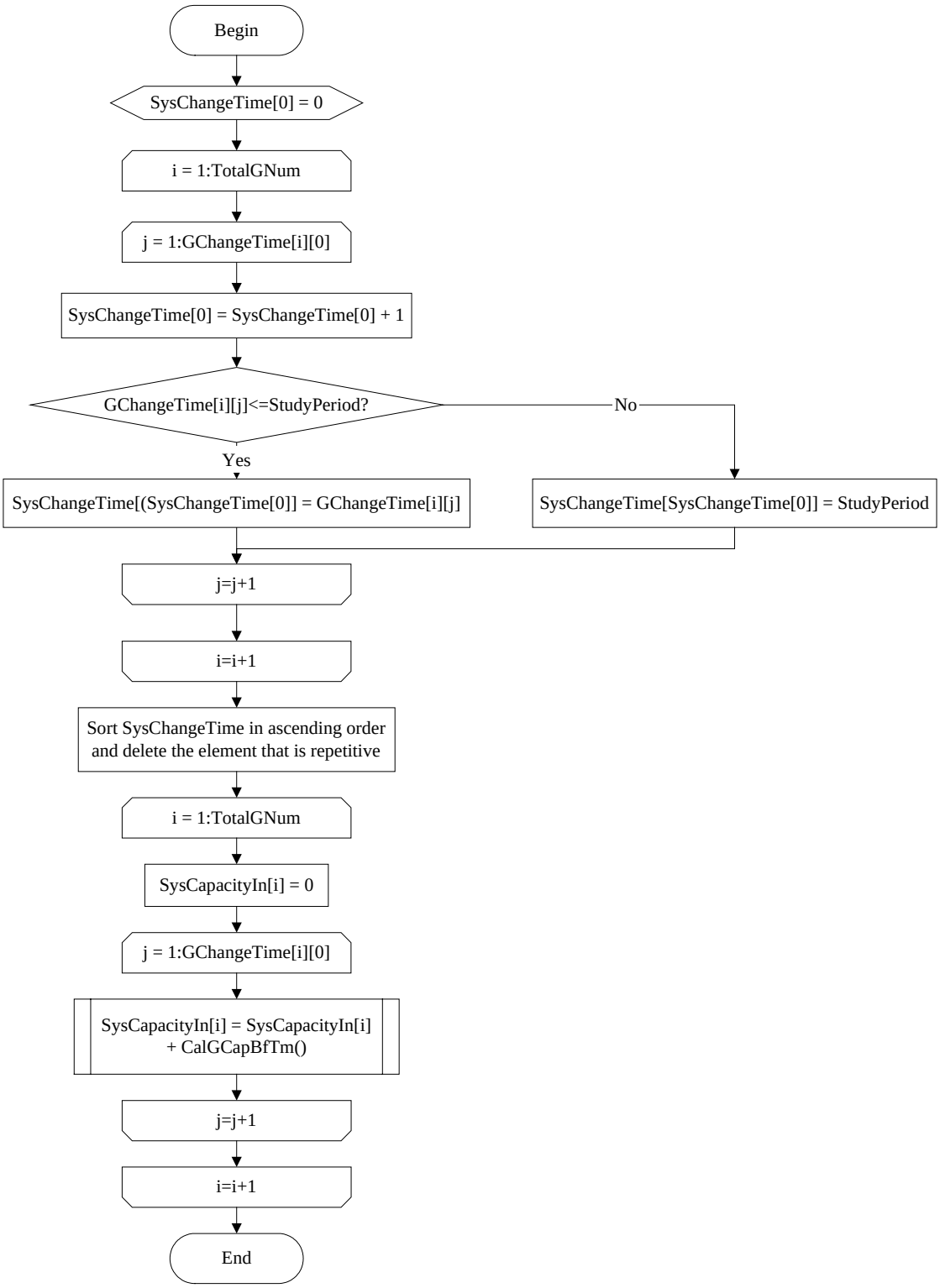

Figure C.3: Calculate base load unit available capacity

The variables used in Step (2) are described in the following.

SysChangeTime: An array. SysChangeTime[0] represents the number of changes of the system capacity in the study period. SysChangeTime[i] represents the time when the system capacity changes.

TotalGNum: Total number of base load units.

SysCapacityIn: An array. SysCapacityIn[i] represents the system available capacity at change i.

The predefined process CalGCapBfTm() in Step (2) is to calculate the capacity in service of the unit GNum has during the interval before ChaningTime. The process is shown in Figure C.4. The variables are described as follows.

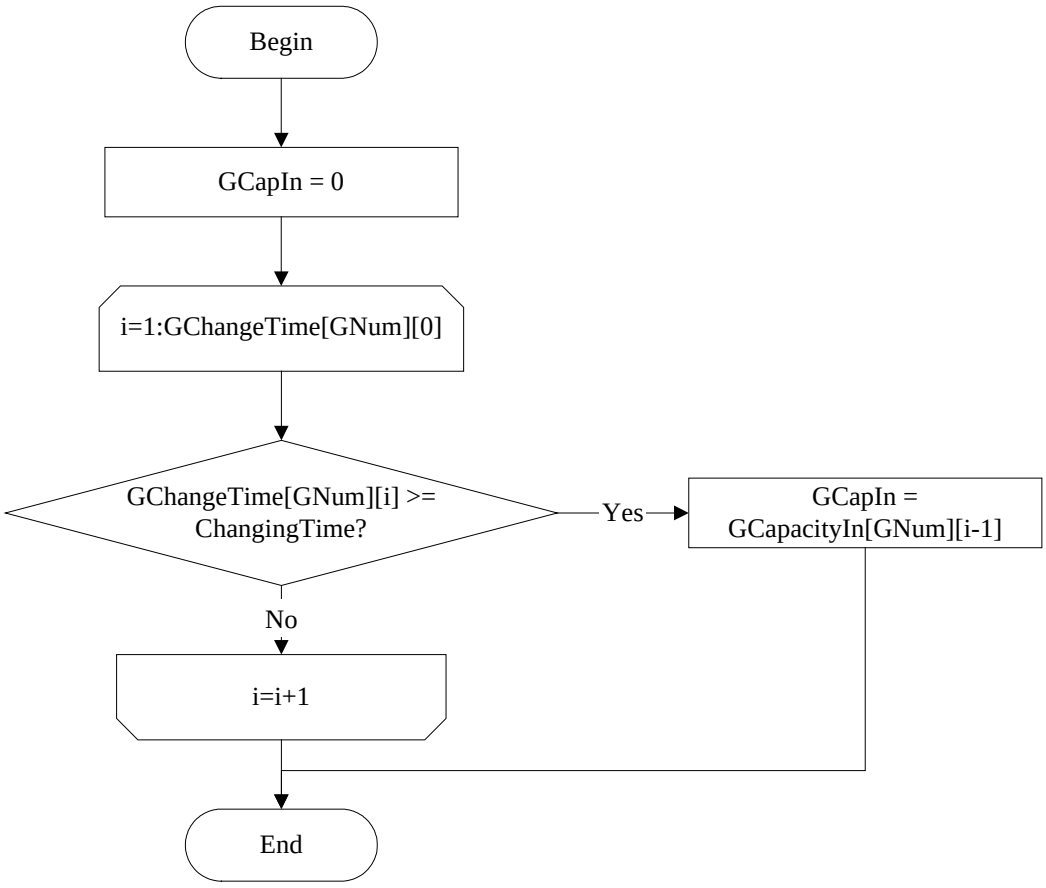

Figure C.4: The predefined process CalGCapBfTm()

GCapIn: represents the capacity in service of unit GNum.

GNum: represent the number of the unit.

Step (3): The processes to calculate base load unit capacity margin are shown in Figure C.5.

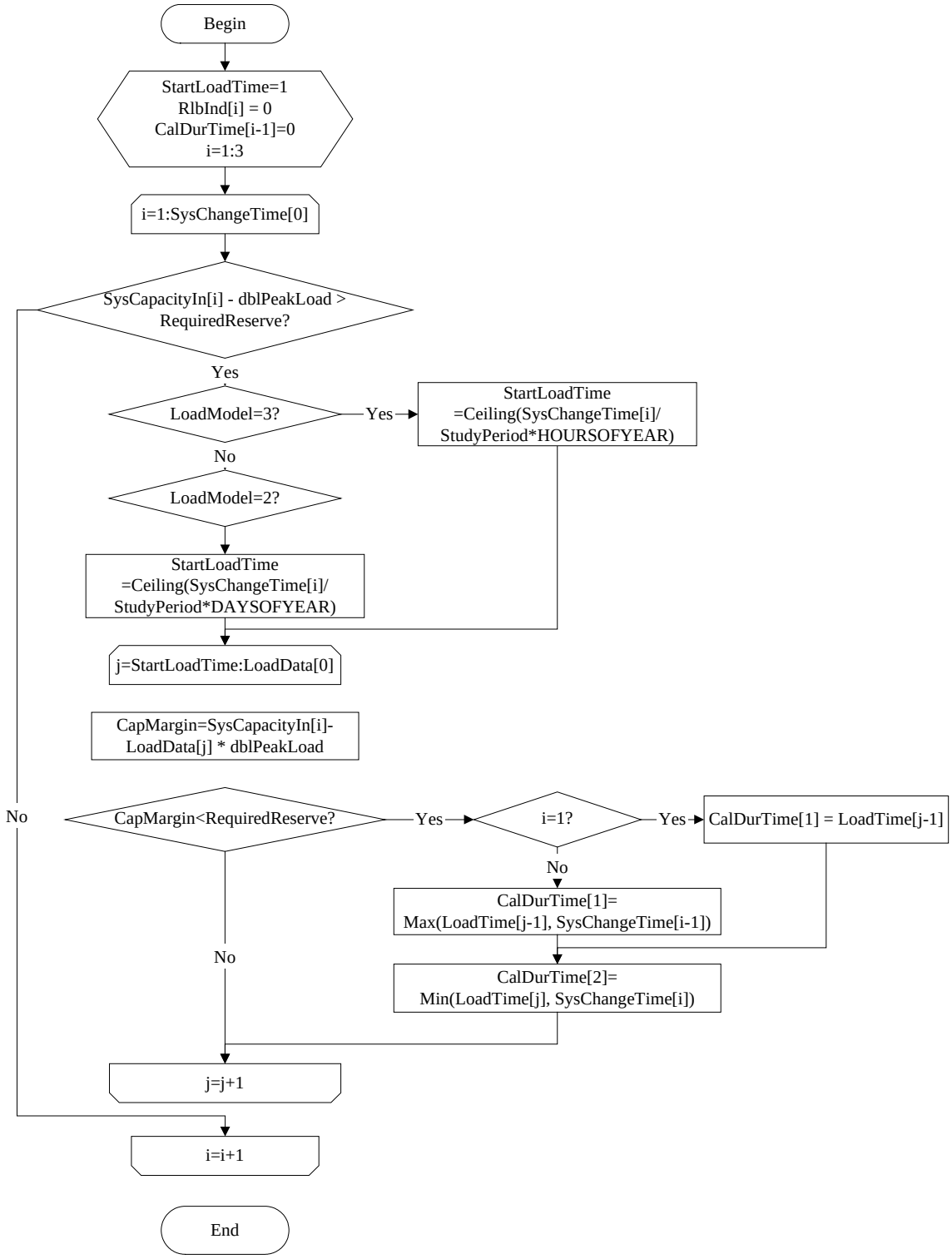

Figure C.5: Calculate base load unit capacity margin

The variables used in this process are described as follows.

StartLoadTime: The number of the load time interval.

RlbInd: An array. RlbInd[i] gives the value of LOLE, LOEE and LOLF for one study period when i is equal to 1, 2 and 3 repectively.

CalDurTime: An array. CalDurTime[1] represents the start time of the time interval when the load exceeds the available base load unit capacity. CalDurTime[2] represents the end time of the time interval when the load exceeds the available base load unit capacity. CalDurTime[3] represents the number of change in the base load unit capacity. CalDurTime[4] represents the number of change in the load data.

dblPeakLoad: System peak load.

RequiredReserve: Required reserve.

LoadModel: LoadModel=2 represents the daily peaks. LoadModel=3 represents the hourly load values.

StudyPeriod: The study period for the system in years.

HOURSOFYEAR represents the hours in a year.

DAYSOFYEAR represents the days in a year.

LoadData: An array. LoadData[0] represents the number of load points. LoadData[i] represents the load in percent of the peak load of the ith point.

CapMargin: CapMargin represents the base load unit capacity margin.

Step (4): The processes to calculate the total capacity margin are shown in Figure C.6. The variables used in this step are described in the following.

TotalPeakLoadNum: The total number of peaking load units.

CalPLUcapBtwn(): The predefined process to calculate the available peaking load unit capacity in the time interval [CalDurTime[1], CalDurTime[2]].

NewChangeDuration: An array. NewChangeDuration[0] represents the number of change in the total capacity during the time interval [CalDurTime[1], CalDurTime[2]]. NewChangeDuration[i] represents the duration of the ith change.

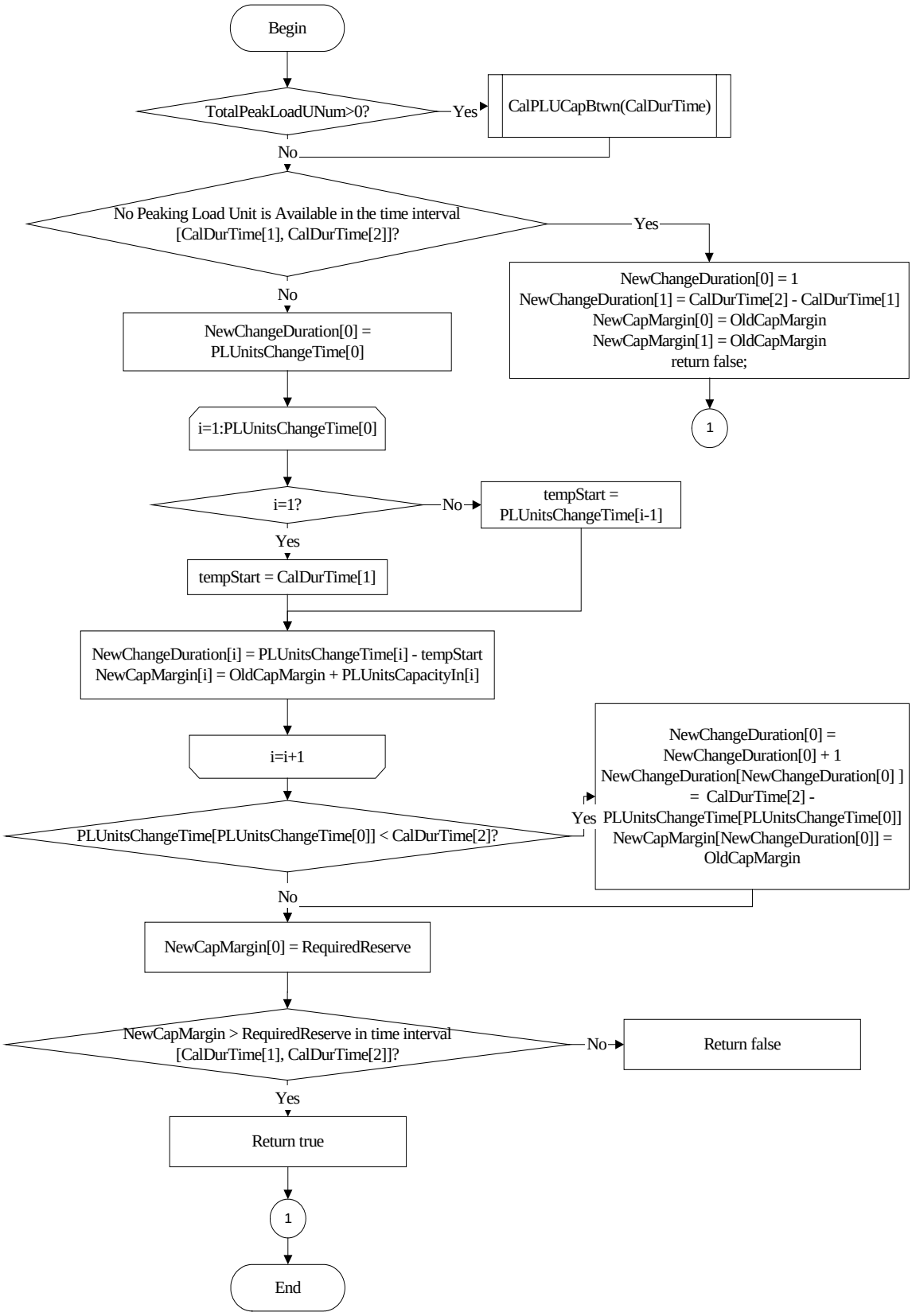

Figure C.6: Calculate total capacity margin

NewCapMargin: An array. NewCapMargin[i] represents the total capacity margin at the ith change in the total capacity.

OldCapMargin: OldCapMargin represents the base load unit capacity margin.

PLUnitsChangeTime: An array. PLUnitsChangeTime[0] represents the number of change in the available peaking unit capacity in the study period. PLUnitsChangeTime[i] represents the peaking load unit capacity at the ith change.

PLUnitsCapacityIn: An array. PLUnitsCapacityIn[i] represents the available peaking load unit capacity at the ith change.

The return value is false in this process means that the total capacity margin is less than the required reserve.

The predefined process CalPLUcapBtwn() are shown in Figure C.7. The variables used in this process are described as follows.

CurChangeNum: An array. CurChangeNum[i] represents the number of changes of the peaking load unit i at the current time.

CurGNum: The number of the peaking load unit.

CalGCapAtChange() is a predefined process to calculate the peaking load unit available capacity at the ith change.

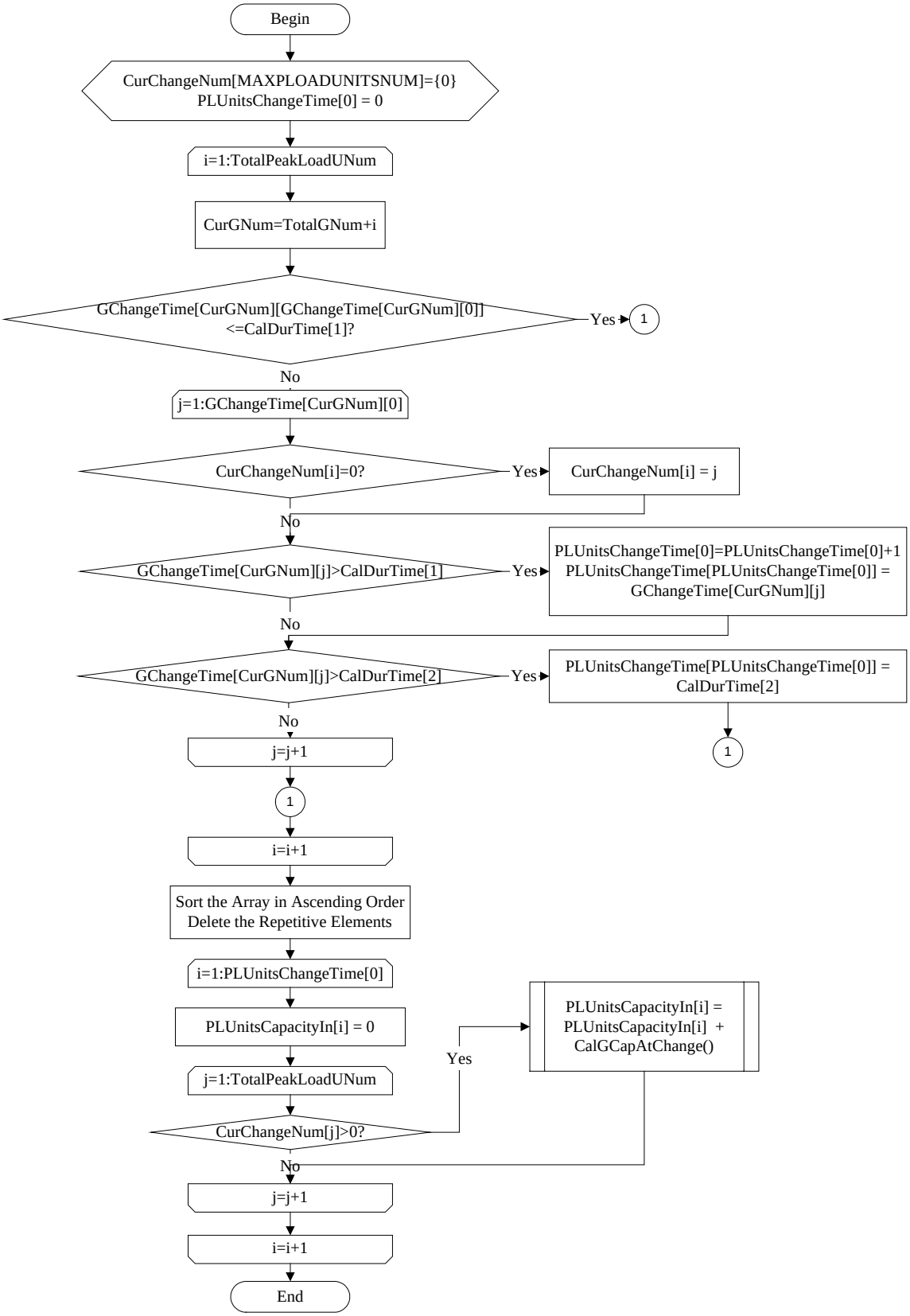

Figure C.7: The predefined process CalPLUcapBtwn()

The process of CalGCapAtChange() are shown in Figure C. 8. The variables used in this process are described as follows.

GCapIn: The peaking unit capacity during a certain change time.

GNum: The number of the peaking load unit.

ChangingTime: The time when the peaking load unit state changes.

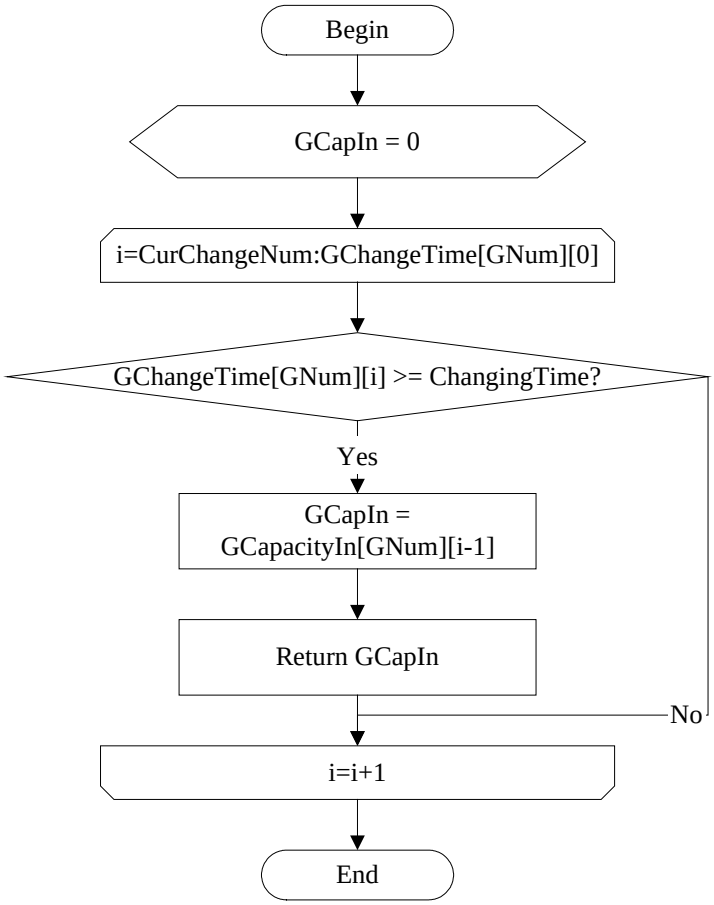

Figure C.8: The predefined process CalGCapAtChange()

Step (5): The processes to simulate the peaking load units are shown in Figure 5.2.

Step (7): The processes to determine the peaking load units to be started are shown in Figure C.9. The variables used are:

CurPLUNum: The number of the current peaking load unit.

SPLUnitsList: An array. SPLUnitsList[0] represents the number of the peaking load units that are selected to be started. SPLUnitsList[i] represents the number of the selected peaking load unit.

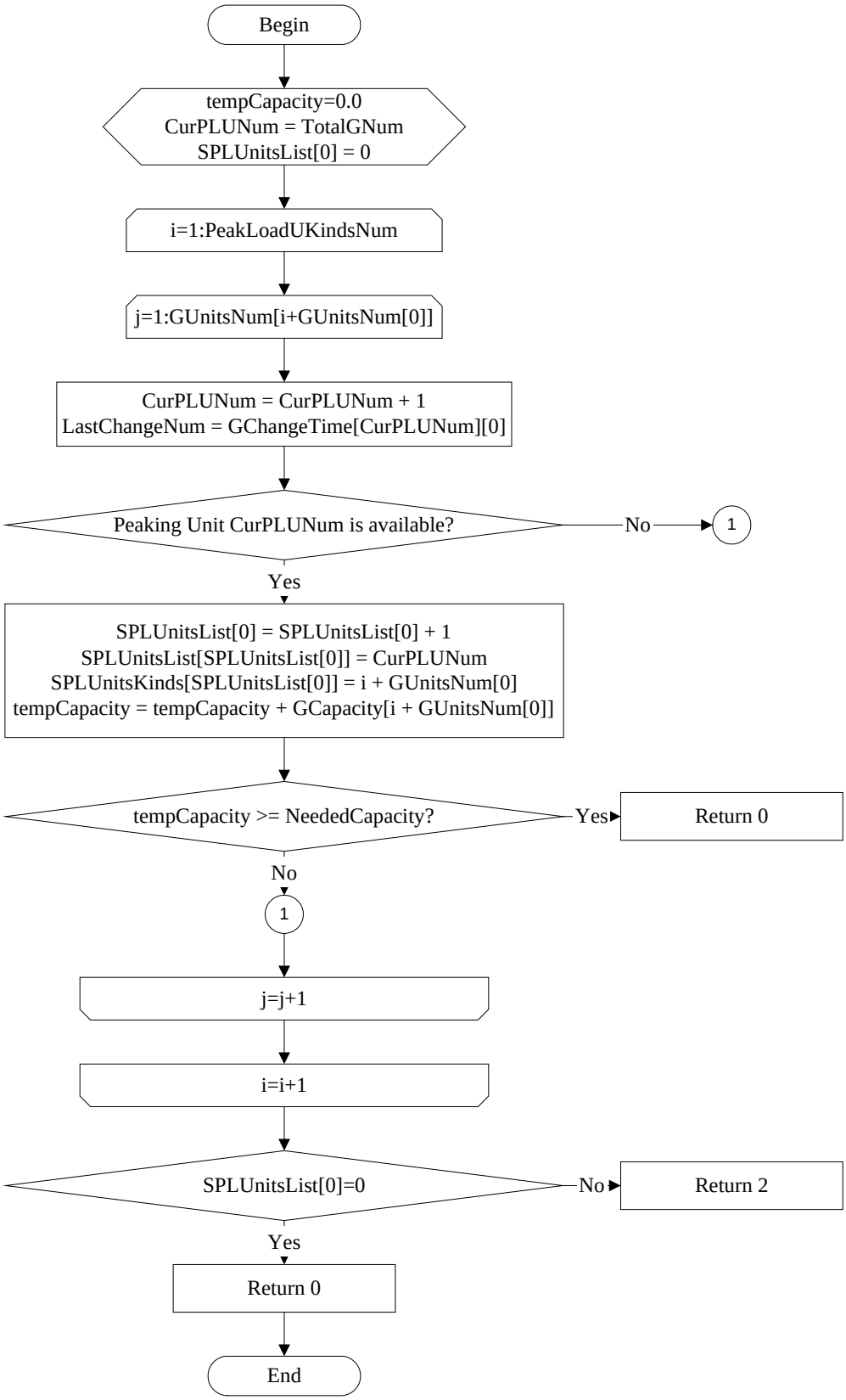

Figure C.9: Determine the peaking load units to be started

SPLUnitsKinds: An array. SPLUnitsKinds[i] is the number of group that the unit belongs to.

GUnitsNum[0]: The number of base load unit groups.

Step (8): The processes to calculate the in-need time for the selected peaking load units are shown in Figure C.10.

The variables used in Step (8) are described as follows.

dblInNeedTime: An array. dblInNeedTime[1] represents the start time of the in-need time. dblInNeedTime[1] represents the end time of the in-need time.

RecordedLoadTime: The number of load change when the total capacity margin is larger than the required reserve.

RecordedSysTime: The number of system change when the total capacity margin is larger than the required reserve.

OrgDurTime: An array. OrgDurTime[1] and OrgDurTime[2] represent the start and end time respectively when the load exceeds the base load unit capacity.

Step (9): The processes to simulate the selected peaking load units for the calculated in-need time are shown in Figure C.11.

The variable PLUNum is the number of the peaking load unit.

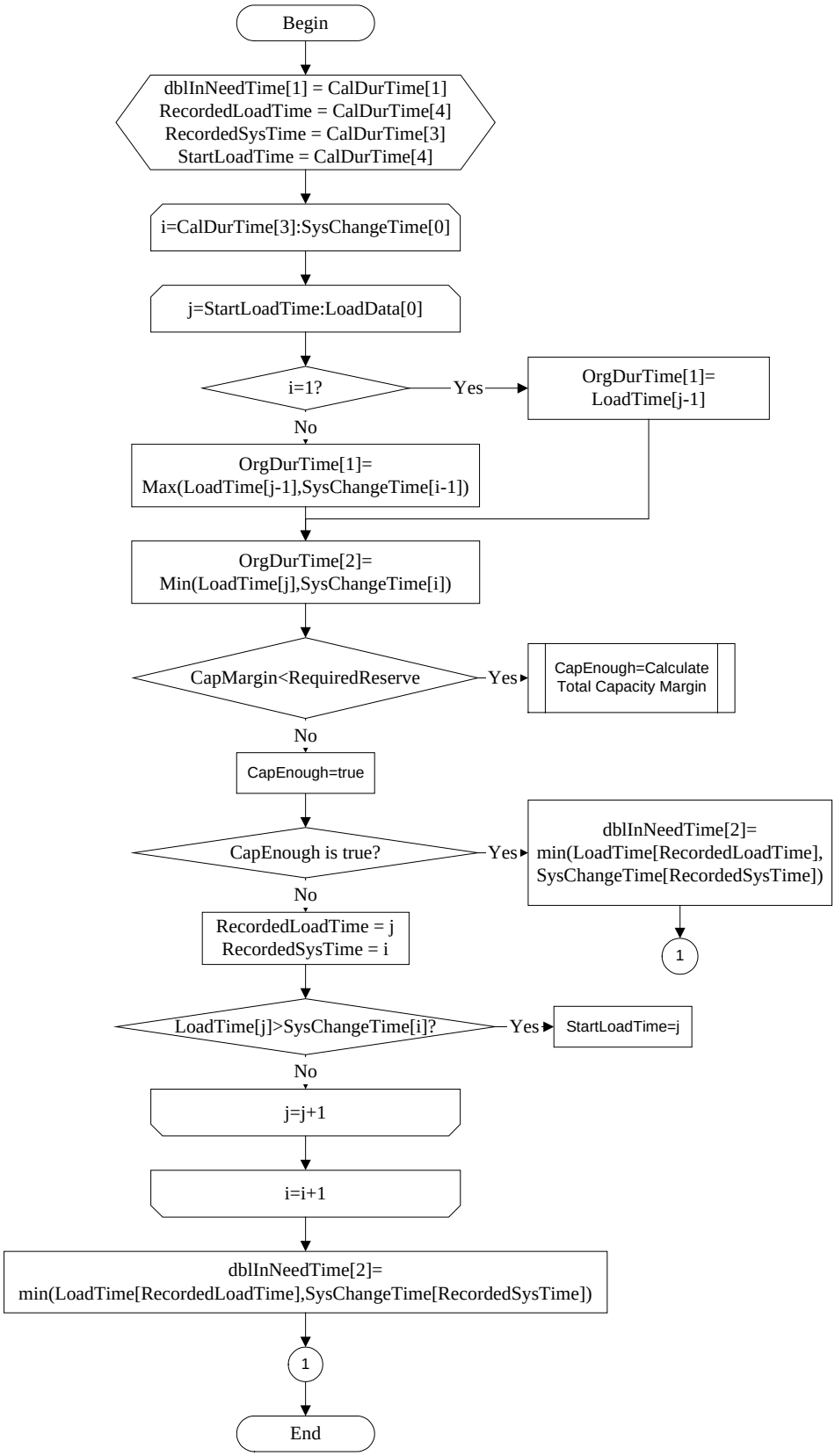

Figure C.10: Calculate in-need time for the selected peaking load units

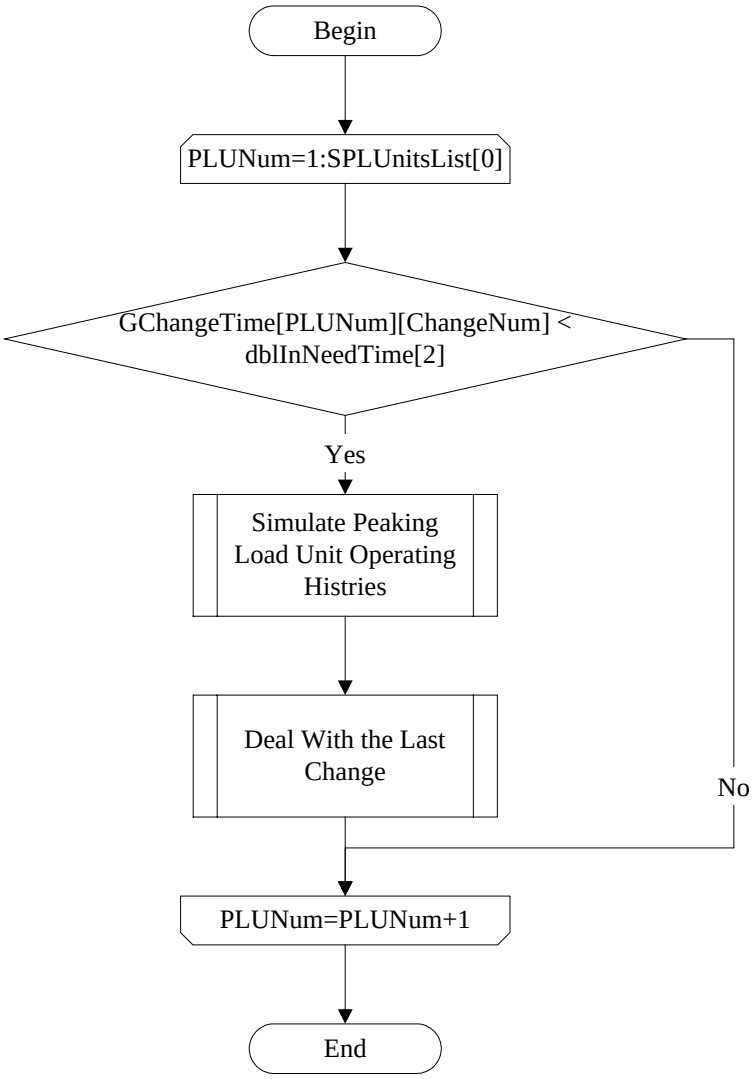

Figure C.11: Simulate the selected peaking load units for the calculated in-need time

The predefined process to simulate the peaking load unit operating histories is shown in Figure C.12. The variables used in Figure C.12 are described as follows.

PLUTDuration: An array that deposits the peaking load unit state residence times, number of startups and number of outages.

CurStateNum: The current state of the peaking load unit.

ChangeNum: The number of change in the state for the peaking load unit.

StartingFProb: The generated random number to represent the starting failure of the peaking load unit. If it is larger than the starting failure probability then the peaking load unit is started successfully.

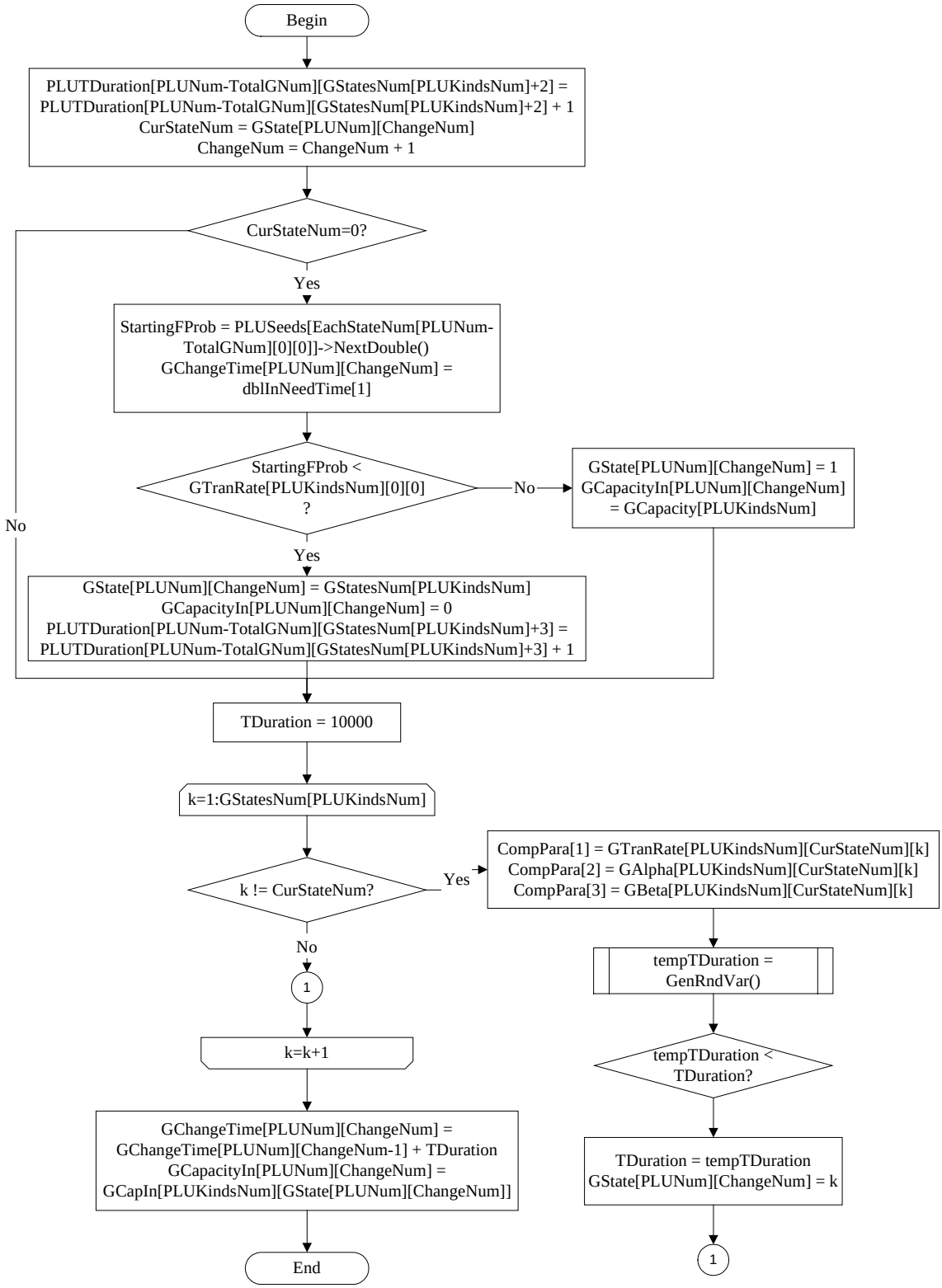

Figure C.12: Simulate peaking load unit operating histories

PLUSeeds: The random seeds that can produce uniformly distributed random

number for the peaking load units.

GTranRate: Deposit the transition rates between states for the peaking load unit. GTranRate[i][0][0] represents the starting failure probability of the peaking load unit group i. GTranRate[i][j][k] represents the transition rates of peaking load unit group i between states j and k.

TDuration: The duration of the peaking load unit residing at the new state.

The predefined process GenRndVar() in Figure C.12 is shown in Figure C.2.

The predefined process to deal with the last change of the peaking load unit is shown in Figure C.13.

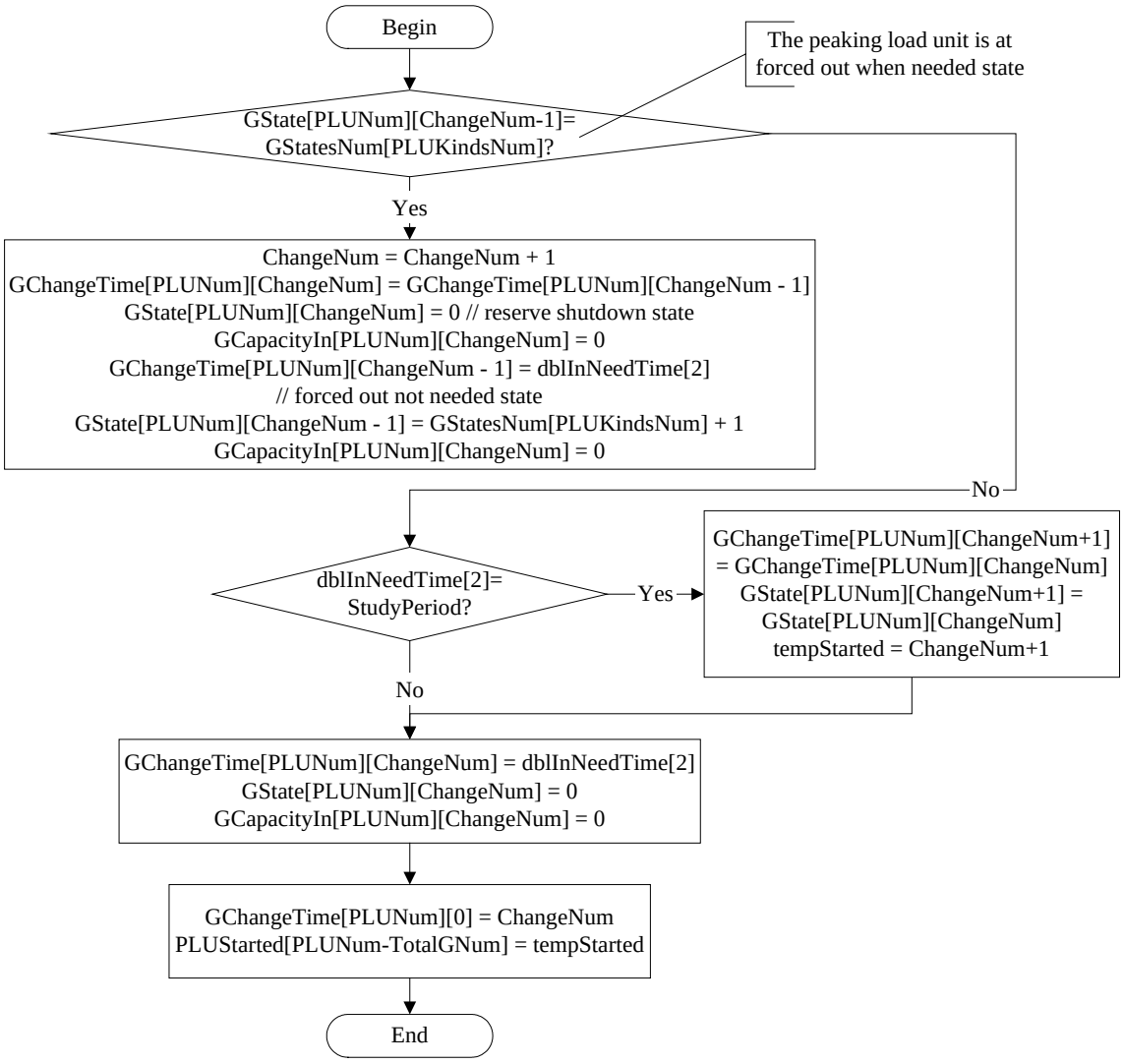

Figure C.13: Deal with the last change of the peaking load unit

Step (6): The processes to calculate reliability indices are shown in Figure C.14.

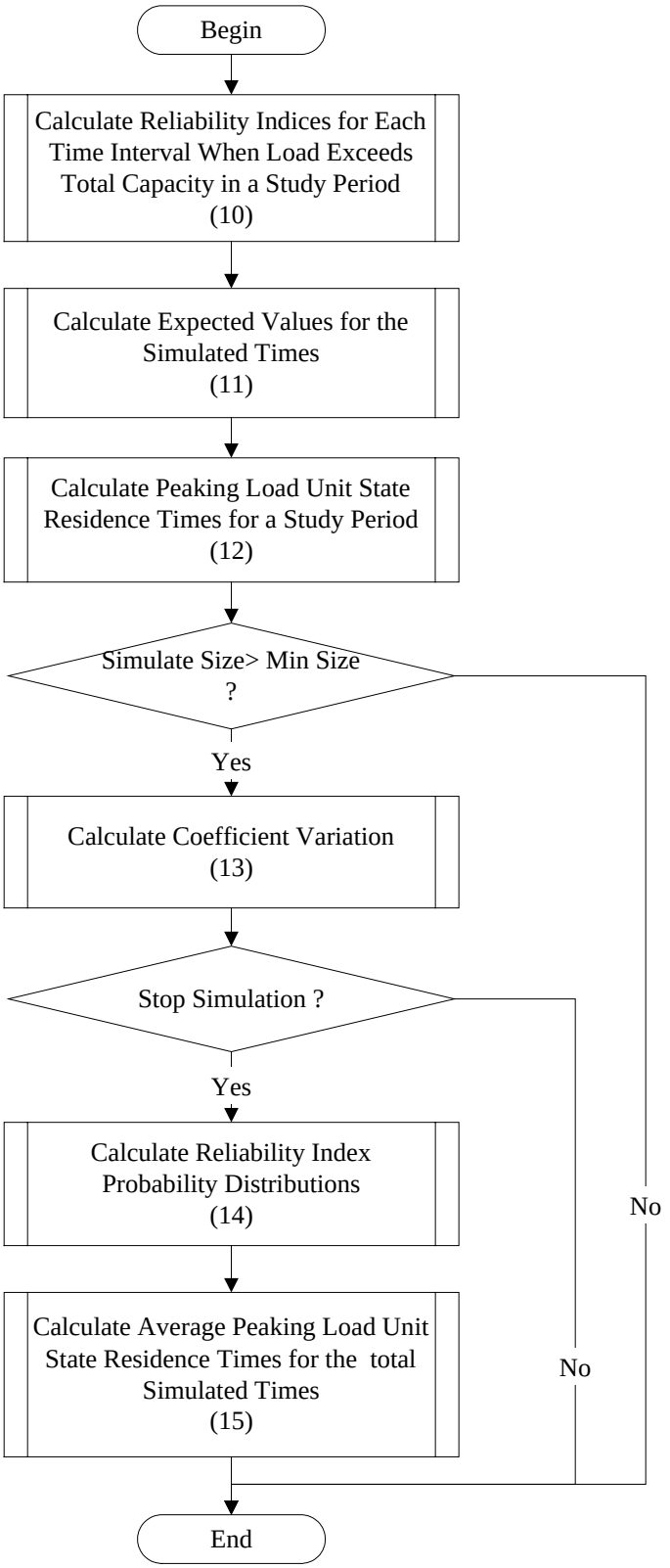

Figure C.14: Calculate reliability indices

Step (10): The processes to calculate reliability indices for each time interval when load exceeds the total available capacity in a study period are shown in Figure C.15.

Step (11): The processes to calculate expected values of the reliability indices for the simulated times are shown in Figure C.16. The variables used in this step are described as follows.

LOLE: An array. LOLE[0] is the total loss of load in the simulated times. LOLE[i] is the loss of load in the ith study period.

LOEE: An array. LOEE[0] is the total loss of energy in the simulated times. LOEE[i] is the loss of energy in the ith study period.

LOLF: An array. LOLF[0] is the total loss of load frequency in the simulated times. LOLF[i] is the loss of load frequency in the ith study period.

DOI: An array. DOI[0] is the expected duration per interruption in the simulated times. DOI[i] is the duration per interruption for the ith study period.

ENSI: An array. ENSI[0] is the expected energy not supplied per interruption in the simulated times. ENSI[i] is the energy not supplied per interruption for the ith study period.

LCI: An array. LCI[0] is the expected load curtailed per interruption in the simulated times. LCI[i] is the load curtailed per interruption for the ith study period.

SmpTimes: Sampling times.

OutLOLE: An array. OutLOLE[i] represents the LOLE for peak load i.

OutLOEE: An array. OutLOEE[i] represents the LOEE for peak load i.

OutLOLF: An array. OutLOLF[i] represents the LOLF for peak load i.

OutDOI: An array. OutDOI[i] represents the DOI for peak load i.

OutENSI: An array. OutENSI[i] represents the ENSI for peak load i.

OutLCI: An array. OutLCI[i] represents the LCI for peak load i.

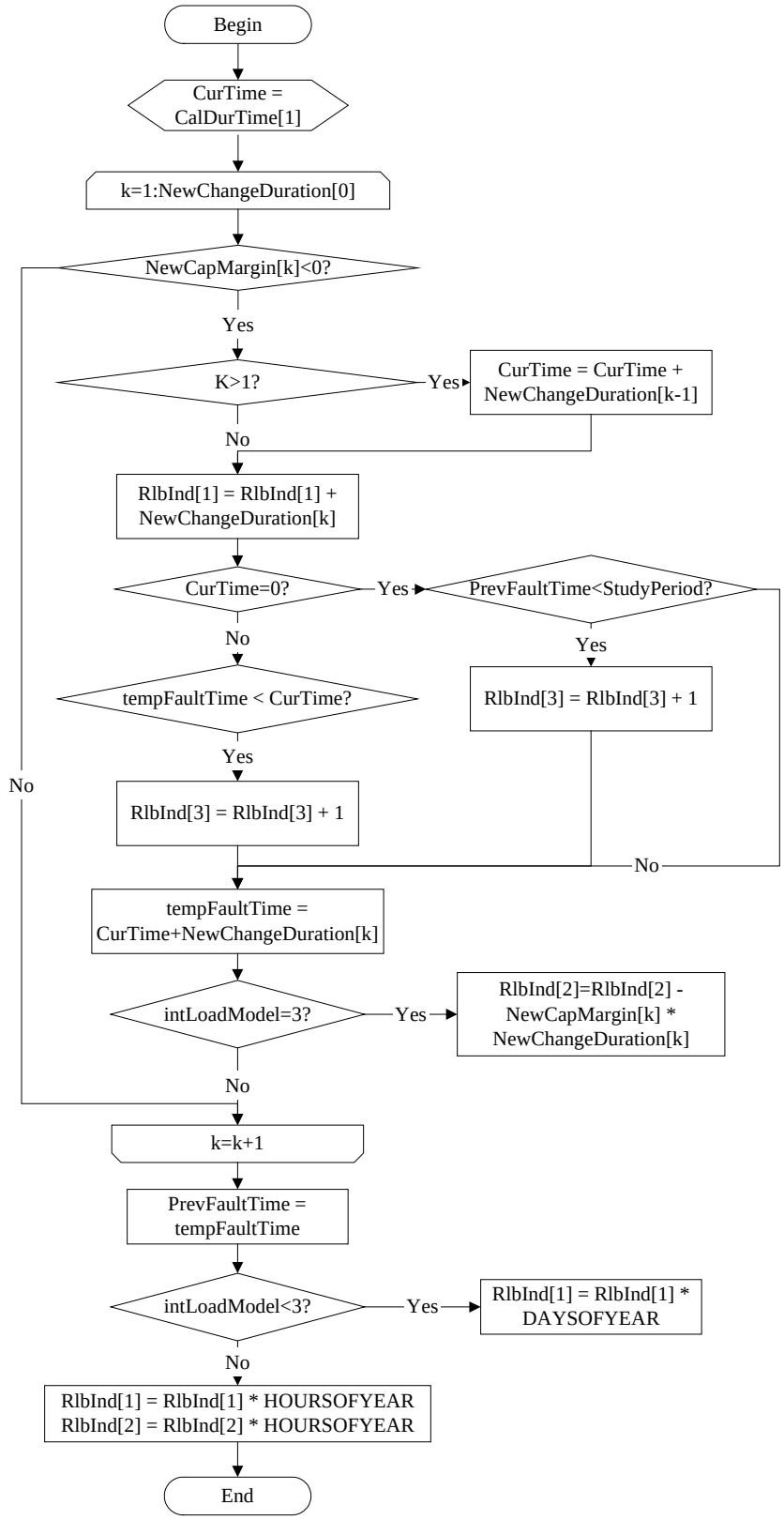

Figure C.15: Calculate reliability indices for each time interval when the load exceeds the available capacity in a study period

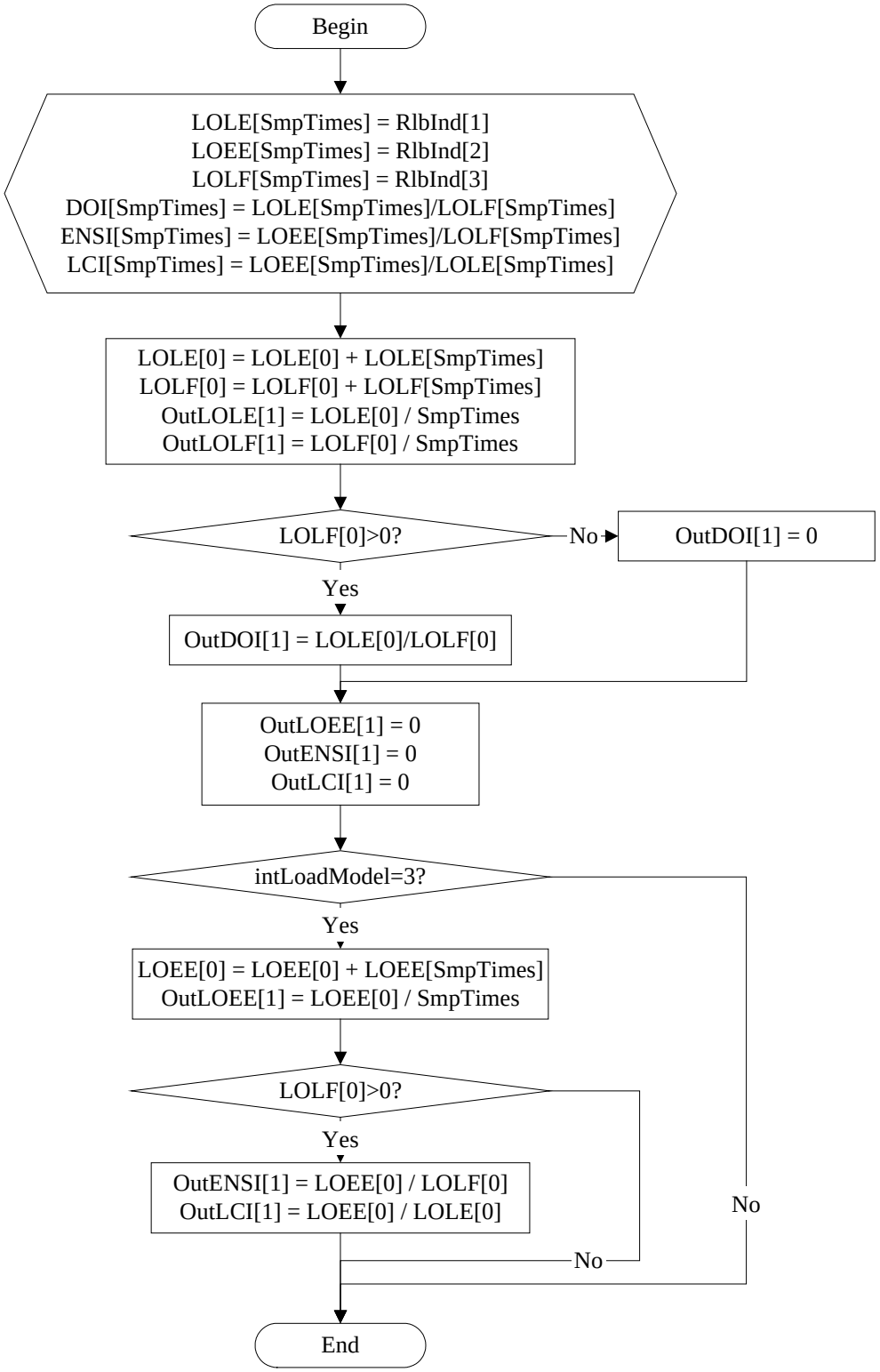

Figure C.16: Calculate expected values of reliability indices

Step (12): The processes to calculate peaking load unit state residence times for a study period are shown in Figure C. 17.

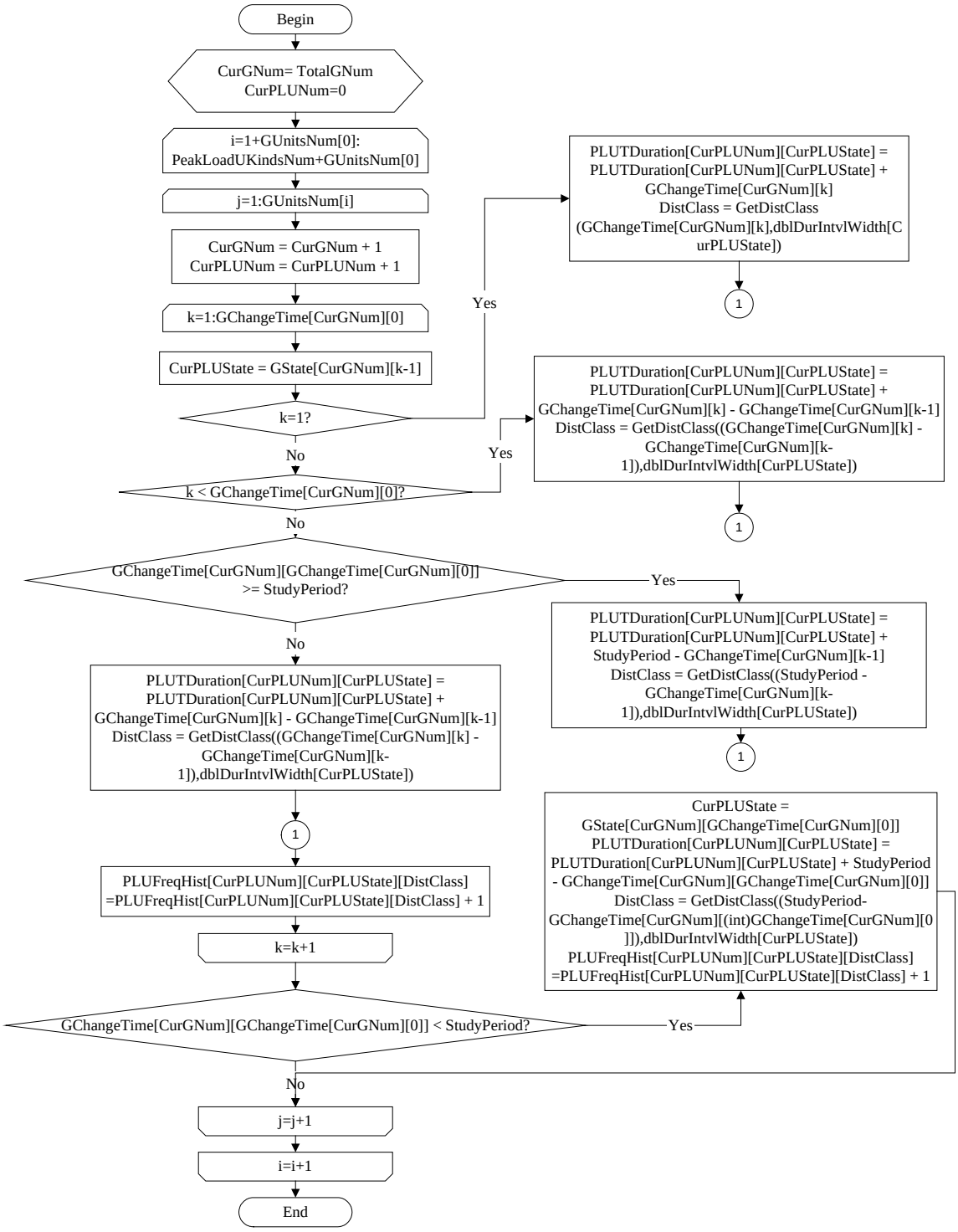

Figure C.17: Calculate peaking load unit state residence times for a study period

Step (13): The processes to calculate coefficient of variation are shown in Figure C.18.

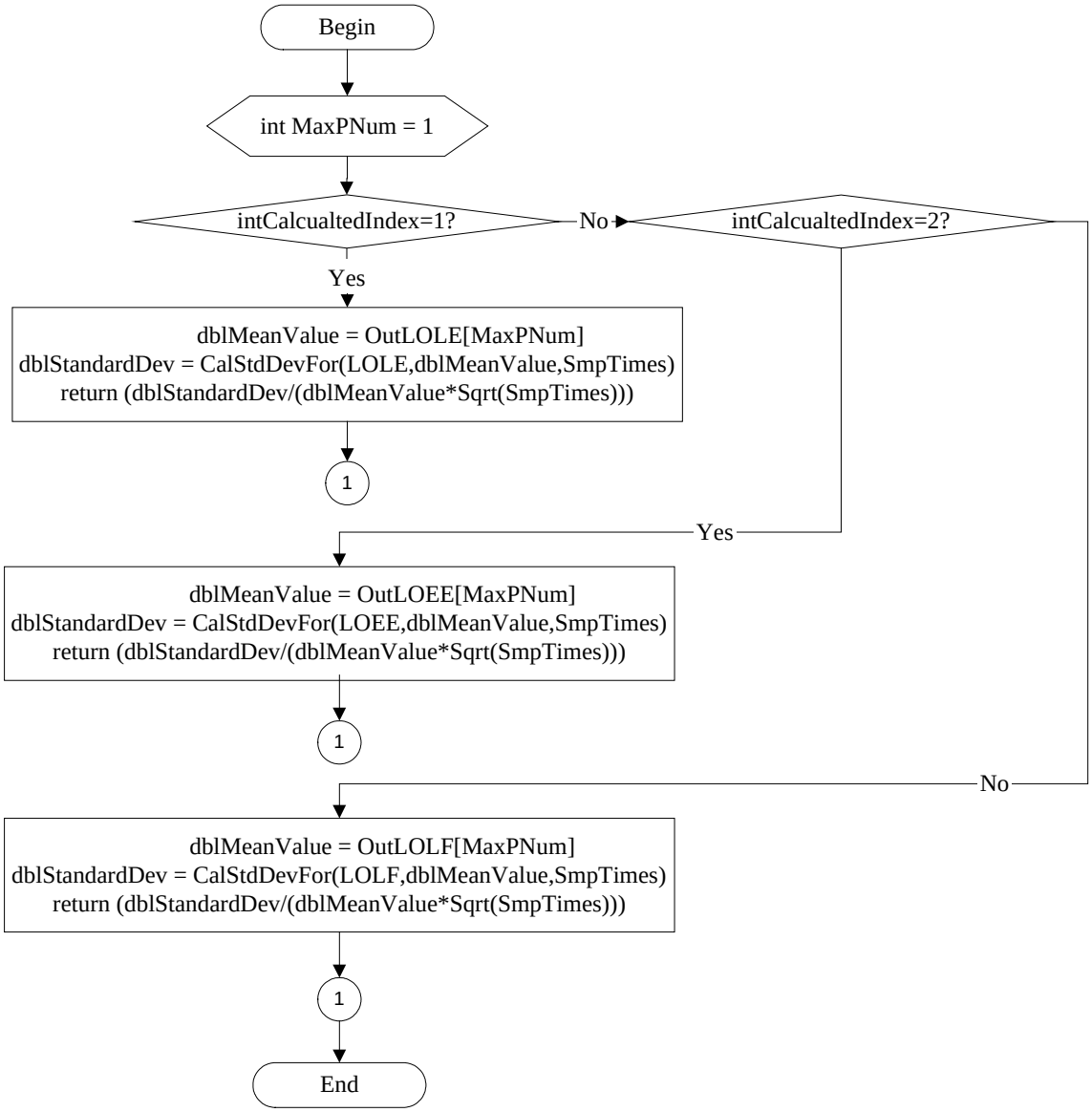

Figure C.18: Calculate the Coefficient Variation

The variables in Figure C.18 are as follows.

intCalculatedIndex=1,2 and 3 represent that the coefficient variation is calculated using the index of LOLE, LOEE and LOLF respectively.

dblMeanValue: Mean value of the index.

dblStandardDev: Standard deviation of the index.

Step (14): The processed to calculate reliability index probability distributions are

shown in Figure C.19.

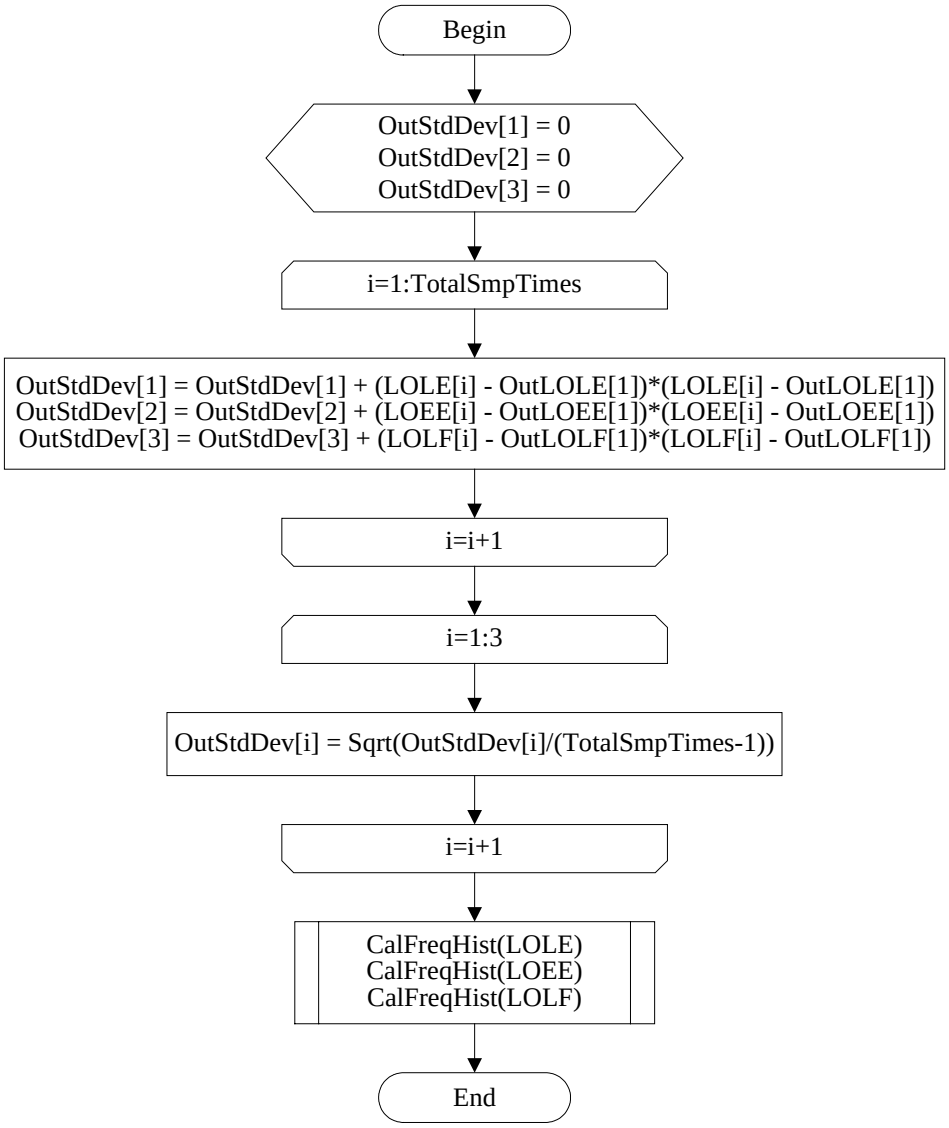

Figure C.19: Calculate reliability index probability distributions

The variables used in Step (14) are as follows.

OutStdDev: An array. OutStdDev[1], OutStdDev[2] and OutStdDev[3] represent the standard deviation of the LOLE, LOEE and LOLF respectively.

TotalSmpTimes: Total sampling times.

CalFreqHist() is a predefined process. The flow chart for this process is shown in Figure C.20.

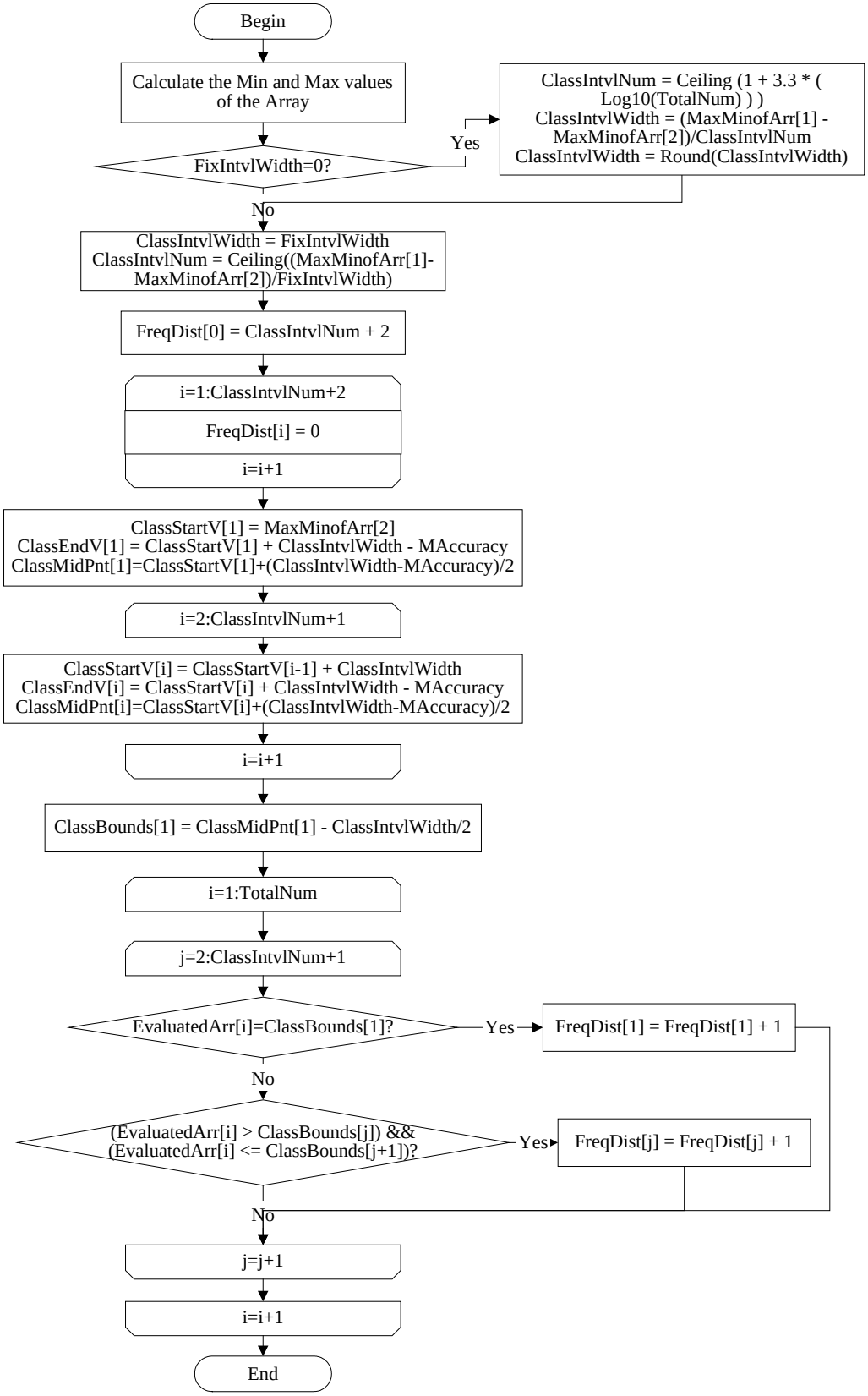

Figure C.20: The predefined process CalFreqHist()

The variables used in Figure C.20 are as follows.

FixedIntvlWidth: Fixed interval width. FixedIntvlWidth=0 means that the interval width are not fixed. FixedIntvlWidth>0 means that the interval width is equal to this value.

ClassIntvlNum: The number of class intervals.

ClassIntvlWidth: The width of the class intervals.

MaxMinofArr[1]: The min value of the array elements.

MaxMinofArr[2]: The max value of the array elements.

FreqDist: An array. FreqDist[0] is the number of class intervals of the array. FreqDist[i] represents the frequency of the class interval i.

MAccuracy: Measurement accuracy.

ClassStartV: An array. ClassStartV[i] is the starting value of the class interval i.

ClassEndV: An array. ClassEndV[i] is the end value of the class interval i.

ClassMidPnt: An array. ClassMidPnt[i] is the mid-value of the class interval i.

TotalNum: Total number of observations.

EvaluatedArr: The array to be evaluated.

Step (15): The Processes to calculate average peaking load unit state residence times for the total simulation times are shown in Figure C.21.

The variables used in Step (15) are as follows.

TotalBLGKindNum: The number of the base load unit groups.

TotalPeakLoadUNum: Total number of the peaking load units.

PeakLoadUKindsNum: The number of the peaking load unit groups.

CurPLGNum: The number of the current peaking load unit.

CurGTotalStatesNum: The number of states of the current peaking load unit.

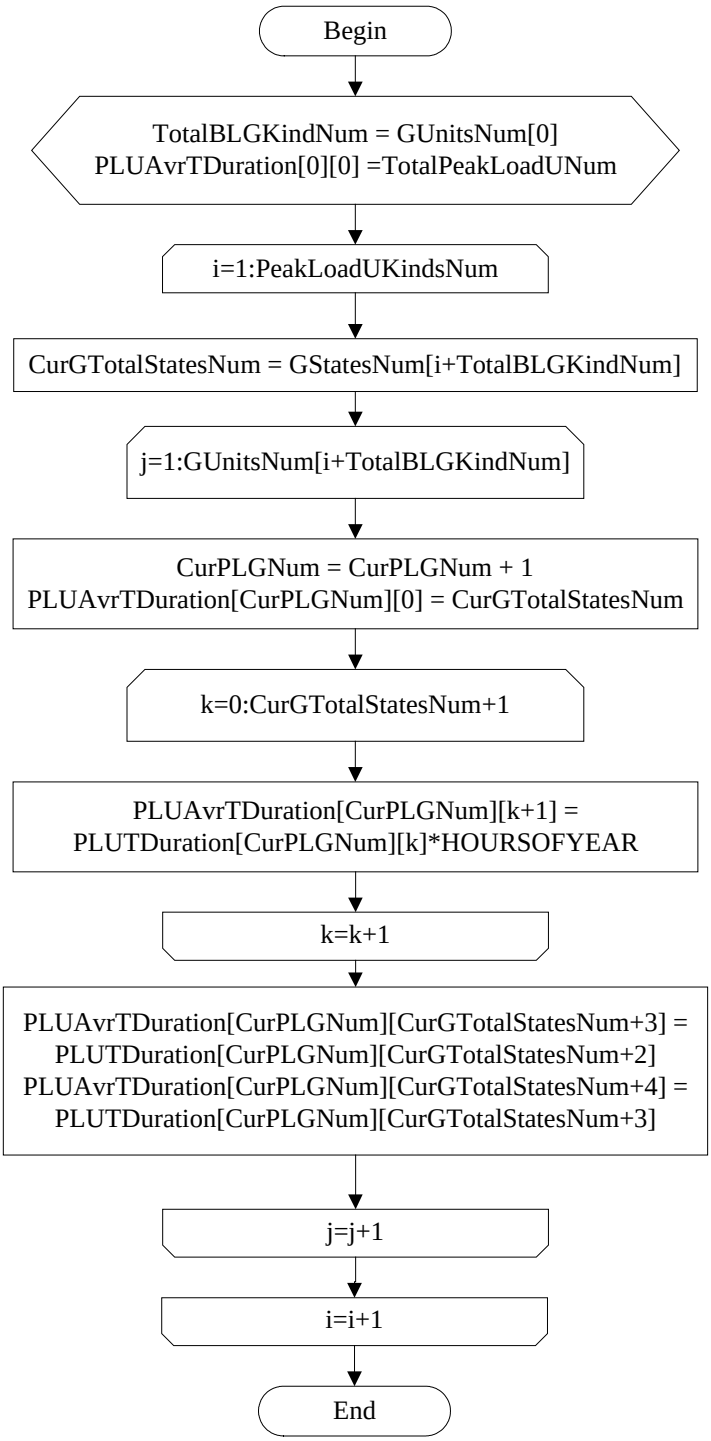

Figure C.21: Calculate average peaking load unit state residence times

APPENDIX D. THE RELIABILITY INDICES FROM THE ANALYTICAL AND SIMULATION PROGRAMS

Table D.1 shows the RBTS reliability indices for the three load models obtained using the analytical program.

Table D.1: Reliability indices using the analytical program

Reliability Index	Constant Load	Daily Peak Loads	Hourly Loads
LOLE (days/yr)	3.0447	0.1469	-
LOLE (hrs/yr)	73.0728	-	1.0919
LOEE (MWh/yr)	823.2555	-	9.8613

Table D.2 shows the RBTS reliability indices for the three load models using the simulation program. The sampling time in this case is 100,000 years and the coefficient of variation is less than 1%.

Table D.2: Reliability indices using the simulation program

Reliability Index	Constant Load	Daily Peak Loads	Hourly Loads
LOLE (days/yr)	3.0258	0.1496	-
LOLE (hrs/yr)	72.6183	-	1.0901
LOEE (MWh/yr)	816.8147	-	9.9268
LOLF (Occ/yr)	2.8309	0.2171	0.2290